CONCEPT STUDY ON MAN-PACK

EARTH STATION ANTENNA

FOR MUSAT

Submitted By

S.H. Lim and W.F. Weir
Andrew Antenna Company Limited
606 Beech Street
Whitby, Ontario
Canada
7 February 1978.

ANDREW S.O. 22194

Prepared under D.S.S. Contract No. OPC76-00091

for

Communications Research Centre
Shirley Bay
Ottawa, Ontario
Canada

TABLE OF CONTENT

TABLE OF CONTENT

ABSTRACT

Presented are results of a concept study for a lightweight, man-portable earth station antenna (ESA) for the proposed Multi-Purpose UHF Satellite (MUSAT). The requirement is for a circularly polarized antenna with a gain of 13 dBic at both the receive (274-290 MHz) and transmit (370-400 MHz) frequency bands. Fifteen different antenna configurations were evaluated. The most promising was found to be a new co-axial helix antenna developed during the study. This consists of two helical coils placed concentric to each other. Experimental results presented show that the new co-axial helix antenna has a better bandwidth performance than a uniform helix. In addition, experimental results for uniform helix and short back-fire (SBF) antenna designs are presented. Full mechanical design details, including cost analysis, are given for the co-axial helix and SBF antennas. Multipath effects on the circularly polarized ESA are analyzed and computed results are presented as a series of graphs. References and a literature survey are included.

IDENTIFIERS

Earth Station Antennas, Co-axial helix, non-uniform helix, helical, short back-fire, UHF, parabolic antennas, Yagi, circular polarization, multipath, ground reflection, lightweight, portable, MUSAT.

1.0 INTRODUCTION

This report represents the results of a concept study of man-pack earth station antennas (ESA) suitable for use with the proposed Multi-Purpose UHF Satellite (MUSAT). System requirements call for a circularly polarized antenna with a 13 dBic gain at the receive (274-290 MHz) and transmit (370-400 MHz.) bands. The antenna must be suitable for use anywhere in Canada including places accessible only on foot. It must therefore be a lightweight man-portable unit that can be quickly deployed on an unprepared site. A preliminary study of several antennas was carried out to choose the most suitable antenna types capable of meeting the mechanical and electrical requirements given in section 2.

A study of different antenna types (some antenna types include several different configurations) is reported in section 3. It was found that the most promising antenna configurations were (a) the short back-fire (SBF) antenna, (b) a new co-axial helix configuration and (c) a separate receive and transmit helix configuration. The SBF antenna feed consists of radiator (such as dipole) and a circular reflector. This is mounted within a reflector cavity. Section 5 provides the results of a study to optimize the performance of a SBF model antenna. The co-axial helix is a new helix antenna configuration that was proposed and developed in the course of this study. The experimental study of a scale model which is reported in section 6, shows that the co-axial helix is comparable in length to a conventional uniform helix and has a better bandwidth performance. It is shown in section 3 that a single conventional helix cannot meet the gain specification over the receive and transmit bands so that two separate helixes were required. An optimized version of the separate receive and transmit helix configuration is described in section 7.

A detail mechanical study (including drawings of proposed full scale antennas) was carried out for the SBF antenna and the co-axial helix antenna. The results are included in sections 5 and 6.

A study of the effect of multipath propagation on the antenna system performance is given in Appendix I. Appendix II gives details of a cost study of the proposed configurations.

2.0 DESIGN OBJECTIVE

The electrical and mechanical design objectives for the antenna system are set out in sections 2.1 and 2.2 respectively. Both the mechanical and electrical requirements were studied and reviewed with the design authority in the course of this study. This led to modifications of the original specifications which are noted in sections 2.1 and 2.2. One such modification was the reduction in transmit gain from 17 dBic to 13 dBic minimum when the study showed that all possible high gain antenna configurations would result in an unacceptably heavy antenna. The higher transmit gain configurations were included in this report although they were not considered in the final selection. A complete review of all system configurations was carried out after the change in the gain specifications.

2.1 ELECTRICAL SPECIFICATION AND REQUIREMENTS

The following is a summary of the electrical specification for the antenna.

Frequency	Receive 274-290 MHz
	Transmit 370-400 MHz
Gain	274-290 MHz - 13 dBic min.
	14 dBic desirable
	370-400 MHz - 13 dBic min.
Polarization	Receive - RHC
	Transmit - RHC
Axial Ratio	2 dB max.
VSWR	1.5:1 max.
Input Impedance	50 Ohms

2.1.1 ORIGINAL GAIN SPECIFICATION

The gain requirement was originally set at:

274 MHz - 13 dBic
290 Mhz - 13.7 dBic
370 Mhz - 16 dBic
400 Mhz - 17 dBic

2.1.1 ORIGINAL GAIN SPECIFICATION (Cont'd)

The transmit band requirement proved difficult to meet in a single broadband antenna. Some of the configurations described in the sections that follow were studied in an attempt to meet this higher transmit gain requirement. Since the MUSAT system studies showed that the higher transmit gain could be relaxed the specifications were revised to that shown in section 2.1 .

2.2 MECHANICAL SPECIFICATION AND REQUIREMENTS

The following is a summary of the mechanical specification for the antenna.

Weight - 30 pounds maximum.
Configuration - designed for back packing by one person.
Packaged Size - 37 inches long by 13 inches wide maximum.
Operating Temperature - $+50^{o}C$ to $-50^{o}C$.
Operating Wind - 60 mph.
Elevation Adjustment - 0^{o} to 40^{o} above horizon.
Assembly and Disassembly - See paragraph 2.2.3.

2.2.1 WEIGHT VS. RUGGEDNESS

Ref: Minutes of Progress Meeting of 19 July '77

The required gain of the antenna results in an assembled structure with at least one dimension equal to or exceeding six feet. It is desirable that the disassembled structure be comfortably carried by one person on foot over long distances which means a maximum weight of 25 to 30 pounds. It is further desired that the structure be fit for rugged field use without mechanical failure.

These requirements are mutually contradicting and compromise is necessary. The design authority dictated that weight be of prime importance.

The resulting designs therefore are slightly less rugged than the designer would prefer. Relatively careful field handling will be necessary to preclude mechanical failure.

2.2.2 PACKAGING FOR CARRYING

Ref: Minutes of Progress Meeting of 8 June '77.

It was agreed that in addition to a weight restriction it was necessary to restrict the size of the dissassembled package in order to meet the objective of comfortable portability over long distances by one person.

The design authority's opinion was that such a package could not exceed 37 inches in length by 13 inches in width.

2.2.3 ASSEMBLY, DISASSEMBLY & FITTNESS FOR USE

The following design features are considered desirable: -

1. Tools should not be required for assembly or disassembly.
2. Assembly and disassembly should be possibly by a person wearing winter mittens.
3. There should be a minimum number of loose parts.
4. Corrosion-proof material should be used and corrosion producing dissimilar metals should not be in contact.
5. No part of the antenna should collect and retain water.
6. Assembly, disassembly and operation should be possible in temperatures ranging from +50 to -50^{o}C.

2.2.3 ASSEMBLY, DISASSEMBLY & FITTNESS FOR USE (Cont'd)

7. Assembly and dissassembly should be easily carried out by one person in a minimum time.
8. Design details such as close fitting telescoping tubes which will jam when sandy or dirty should be avoided.

2.2.4 WIND LOAD AND ASSEMBLED STABILITY

Anchoring a man-pack antenna (for which there can be no prepared foundation) so that it will not be blown over by high winds is a major problem. Ground conditions at the assembly site could be ice, rock, gravel, hard clay, sand, soft soil or marsh. A complete array of stakes, screw anchors and other possible ground attachment devices could account for more bulk and weight than the antenna itself.

It is therefore necessary to design for minimum profile area to minimize the forces applied by the wind. It is also advantageous to keep the center of the wind force as close to the ground as possible but this must be compromised with gain loss due to multipath effects as outlined in Appendix I.

It is proposed that the best solutions to the anchoring problem are as follows:-

a) Three ropes for guying the antenna to local firm objects should be part of the antenna package.
b) A container or platform to hold local material (rocks, earth etc.) would add weight to the assembly tending to prevent it from blowing over.
c) Other necessary equipment (such as batteries) could be integrated with the mount to hold it down.

3.0 REVIEW OF POSSIBLE CANDIDATE ANTENNA SYSTEMS

Many different antenna configurations can in theory be considered. In order to limit the scope of the study, the candidate antenna systems given below were chosen for the initial investigation.

a) Helical Antennas
b) Short Back-Fire Antennas
c) Parabolic Antennas
d) Yagi Antennas
e) Composite Helical/Yagi Arrays
f) Log Periodic Antennas
g) Active Antennas
h) Surface Arrays

Many other possible antenna systems have been excluded mainly because they cannot meet the weight or portability requirements. As an example, pyramidal or conical horns were excluded because they are difficult to collapse for packing although they can be light-weight. The subsections that follow describe briefly the different candidate antennas considered.

3.1 HELICAL ANTENNAS

The axial-mode helical antenna was described by Kraus (23) (24) in 1947 when he presented experimental results and an analysis of its operation. This work was later extended by various other authors (1) (12) (26) (38). The axial-mode Helical antenna (see Figure 3.1.1) is a relatively simple antenna. It consists of a conductor wound in the form of a helix. It can be fed at one end via an unbalance transmission line. A reflector or alternatively a cavity is placed at the fed end to improve its directivity and pattern.

The helical antenna has found wide application because it is relatively simple to fabricate and can be optimized for high gain. It can also have a good VSWR over a wide band when properly matched. Due to its helical structure fields produced are circularly polarized. Thus unlike many of the other configurations considered no special polarizer or provision for circular polarization is required.

3.1 HELICAL ANTENNAS (Cont'd)

Maclean and Konyoumjian (26) and more recently King and Wong (21) (37) have shown experimentally that the simple gain equations as given by Kraus have validity only over a limited range of frequency. It was shown that the bandwidth is limited. The higher the gain required the narrower the bandwidth. Based on the above, it can be shown that it is very difficult to achieve 13 dBi gain over a 1:1.45 bandwidth ratio (MUSAT requirements).

Experimental results for a single helix are presented in section 7.0. These show that a single uniform helix can be designed to give good performance over either the receive or transmit band.

Thus, an antenna covering both bands would require the use of two helixes, one optimized for receive band and the other optimized for the transmit band. Such a configuration is discussed in detail in section 7.

Another alternative would be to use a broadband helix. To cover both bands the uniform helix would have to be modified. One such modified helix, the non-uniform helix of Wong and King (36), is described in section 3.1.4. A new configuration, the co-axial helix, is discussed in section 3.1.5.

3.1.1 BI-HELIX

A bi-helix is shown in figure 3.1.2. This consists of two single helixes fed with equal power and phase. The beamwidth remains the same as that for the single helix in the plane perpendicular to that containing the two helical axes. The beamwidth in the plane containing the helical axes is narrower than that of a single helix. It is however dependent on the spacing in wavelengths between the helixes. This frequency-dependence makes it difficult to optimize in a dual-band system if the frequency separation is too great. The boresight gain of such arrays is given by:

$$G_a = 10 \log_{10} n_e + G_e \quad \text{dB} \quad -(3.1.1)$$

where G_a = boresight gain of array in dBi
n_e = no. of elements in the array.
G_e = gain of each array element.

The gain of a bi-helix would therefore in theory be 3 dB above that for each individual helix. In practice, the gain is always slightly lower due to many factors such as coupling between antennas, imperfect phasing, additional

3.1.1 BI-HELIX (Cont'd)

feeder and divider loss. This additional loss can vary from 0.3 to 1.0 dB.

This system,as well as that for the tri-helix (3.1.2) and quad-helix (3.1.3), were originally proposed to satisfy the original high transmit gain requirement (17 dBi). Study on these were terminated when the transmit gain requirement was lowered to 13 dBi, since helical arrays are no longer necessary for the revised gain requirement.

3.1.2 TRI-HELIX

This is similar to the bi-helix except that 3 individual helixes are fed with equal power and phase. The theoretical gain over a single helix is 4.77 dB (see equation 3.1.1). As in the bi-helix it is slightly lower in practice.

Unlike the bi and quad-helix, the tri-helix does not have an axis of symmetry. The most common form of the tri-helix is the one shown in figure 3.1.3. Here the patterns from 0^{o} to 120^{o} is repeated in the regions 120^{o}-240^{o} and 240^{o}-360^{o}. By a proper choice of spacing between the helixes it is possible to ensure that the beamwidth stays fairly constant from 0-360^{o}. The near-in sidelobe structure however varies over this range. Johnson and Haas (11) give examples of how the pattern varies over the complete range in their report on a tri-helix.

3.1.3 QUAD-HELIX

The quad-helix configuration is perhaps the most popular where high gain is required. From equation 3.1.1 the gain over a single helix is 6 dB. In practice a gain of 5 dB above that for each individual element can easily be achieved.

The pattern of a quad-helix is more circularly symmetrical than either the bi-helix or the tri-helix. Figure 3.1.4 shows a quad-helix. The dimensions are those given by Kraus (24) who also gave details of its performance.

3.1.4 THE NON-UNIFORM HELIX

Wong and King (20) (21) (36) have recently described a new helix configuration which has a better bandwidth than the uniform helix. Figure 3.1.5 shows a non-uniform helix which exceeds the 13 dB gain specification over both the receive and

3.1.4 THE NON-UNIFORM HELIX (Cont'd)

transmit bands. It is essentially two uniform helixes connected together by a tapered section. No exact theory for its operation has been given by the authors. Figure 3.1.6 shows the measured gain vs. frequency for the helix of figure 3.1.5. These results are based on data from the references given above.

It can be seen that the non-uniform helix does in fact provide good gain over the receive and transmit bands (> 13.5 dBic). However, its one disadvantage is that its overall length is 151 inches. This makes it very difficult to support and deploy for a light-weight and portable earth station antenna.

It should be noted that the non-uniform helix is a significant development in the field of broad band circularly polarized antennas. It should find many future applications at higher frequencies or in systems where weight and size are not as critical as in the application being studied.

3.1.5 THE CO-AXIAL HELIX

The co-axial helix is proposed as a means of solving the problem of long overall length inherent in the non-uniform helix. Instead of two helical elements connected in series the co-axial helix has the two helical elements placed concentric to each other (figure 3.1.7). Because they are concentric the helixes couple very strongly. This coupling and the way the helixes are excited determines the phase and amplitude of the current distribution in each helix. It was found experimentally that it was possible to arrange this distribution to enhance the bandwidth of the helix. A detail analysis of the operation of the co-axial helix will not at present be given. A rough physical analogy may be drawn with the operation of a broadband Yagi antenna. This consists of a reflector, a driven element (or elements) and directors. It is possible to broadband a Yagi by tuning the directors for the high end of the band and the reflectors for the low end of the band. The inner helix can be regarded as an element whose current distribution is tuned to enhance the performance at the high end of the band. The co-axial helix configuration is described in detail in section 6.1.
Preliminary experimental results for this antenna are presented in section 6.0. These show that a co-axial helix can be made shorter than a non-uniform helix and it also has a larger bandwidth than the conventional helix.

3.1.5 THE CO-AXIAL HELIX (Cont'd)

Insofar as can be determined by a survey of the literature, this is the first time such a system is proposed and experimentally verified.

3.2 THE SHORT BACK-FIRE ANTENNA

The short back-fire antenna was first proposed by Ehrenspeck (8) in 1965 as a compact antenna capable of good efficiency. As shown in figure 3.2.1, it consists of a dipole radiator placed between two reflectors. The larger reflector is in the form of a cavity whose rim plays an important part in enhancing the gain of the system. It should be noted that while Ehrenspeck's original communication showed this rim, its importance was not generally recognized until more recently. Many of the earlier analysis of the antenna (14) (25) (29), as well as Ehrenspeck's original patent (6), do not show or consider the rim at all. The effect of the rim was described in various reports (10) (13) (7) and fully described in a paper by Ehrenspeck (7) in 1974. This paper also shows clearly for the first time that the short back-fire (SBF) antenna can have high efficiency over a very broad frequency band.

A great deal of interest was generated after the appearance of this paper as it indicates the possibility of a new class of broadband antennas. However, since this interest is relatively recent not many antenna systems using the SBF concept have been designed and built. It is expected that the SBF antenna will be applied to many future antenna requirements in the frequency range of 200 to 2000 MHz.

For any circular radiating aperture the gain is given by

$$G = \eta \left(\frac{\pi D}{\lambda}\right)^2 \quad - (3.2.1)$$

where D = aperture diameter

λ = wavelength

η = overall efficiency

The overall efficiency η is a measure of the performance of a reflector antenna. It is typically 55% for a parabolic antenna and 80-95% for very large reflectors which have specially shaped surfaces. Figure 3.2.1 shows a curve gain vs frequency plotted using data from Ehrenspeck's paper (7), for a SBF reflector of 83" diameter.

3.2 THE SHORT BACK-FIRE ANTENNA (Cont'd)

It can be seen that a gain of more than 13.5 dBi is possible over both the receive and transmit bands.

Some important points should be noted about this curve. First, some parts of the gain curve shown imply an efficiency of over 100%. This is only because of the rim which acts to some extent as a secondary radiator. The effect of this is to increase the actual radiating aperture so that it is larger than the physical aperture. This difference in actual and physical radiating aperture accounts for the high efficiency possible with the SBF antenna.

It can be seen that the receive and transmit bands lie on either side of the main gain peak of the curve. The data published are for a given optimization and by no means the best possible for this application. It should be possible to improve the gain in both bands by optimizing for a broader gain peak curve. However, the curve is shown to illustrate the fact that a SBF antenna design is feasible based on published data. It should be noted that figure 3.2.1 gives directive gain. This is obtained by pattern integration and does not include feed losses. Most of the actual applications reported so far for the SBF antenna take advantage of its good gain and pattern.. They are generally narrow band applications. For the MUSAT antenna,which is a wideband application, it is essential that a system design be based on an actual experimental study.

3.3 PARABOLIC ANTENNAS

The paraboloid reflector which is inherently broadband is used extensively for dual-band applications at microwave frequencies. For this application the only practical configuration is a true paraboloid with the feed at the focus. For such an antenna the gain is also given by equation 3.2.1.
The efficiency η is now given by

$$\eta = \eta_{ap} x (1-L_{sp}) x (1-L_{oL}) x (1-L_r) x (1-L_f) \quad (3.3.1)$$

where

η_{ap} = aperture or illumination efficiency

L_{sp} = Spillover Loss

L_d = Loss due to diffraction effects at the reflector

L_r = Loss due the reflector surface. This consists of r.m.s. error losses and losses due to leakage through a mesh reflector

L_f = Feed and feeder losses

L_r and L_f can be kept reasonably small for this requirement. So the main sources of losses are spillover losses (L_{sp}) and diffraction losses (L_d).

The main difficulty, however, is to obtain a high aperture efficiency using a simple feed without introducing unacceptably high spillover losses.

The geometry of the system is shown in figure 3.3.1. The ray OA leaves the focus O and is reflected at A so that AB is parallel to the axis. OA thus represents a spherical wave with its phase centre at O and AB a plane wave with a wave front perpendicular to the axis.
The reflector surface must be such that Snell's law of reflection is obeyed.

3.3 PARABOLIC ANTENNAS (Cont'd)

i.e. $$\frac{dr}{d\beta} = r \tan\left(\frac{\beta}{2}\right) \qquad (3.3.2)$$

On integrating, putting r = a (the focal length) and for = o;

$$r = a \sec^2 \frac{\beta}{2} \qquad (3.3.3)$$

which is the equation of the reflector.

The aperture distribution $F_a(x)$ can be found by equating the power flow through a solid angle formed by rotating r and the power flow through the corresponding aperture ring of width dx and radius x.

$$2\pi F_a(x)\, x\,dx = F(\beta) - 2\pi c \sin\beta \, d\beta$$

where c is a constant and $F(\beta)$ is the feed pattern function.

Giving

$$F_a(x) \propto \frac{F(\beta) \sin\beta}{x} \times \frac{d\beta}{dx}$$

as $$x = r \sin\beta = 2a \tan\left(\frac{\beta}{2}\right)$$

and $$\frac{dx}{d\beta} = 2a \sec^2\left(\frac{\beta}{2}\right)$$

$$F_a(x) \propto F(\beta) \cos^4\left(\frac{\beta}{2}\right) \qquad (3.3.4)$$

For uniform aperture illumination

$$F(\beta) = \sec^4\left(\frac{\beta}{2}\right) \qquad (3.3.5)$$

It can be seen from equation 3.3.4 that F(x) decreases with respect to $F(\beta)$ as β increases. This space attenuation shown in figure 3.3.2 is very pronounced for deep dishes. However, for shallow dishes with β up to about 30^0 it is quite small. Thus from the point of view of illumination efficiency a shallow dish is much better than a deep dish. However, shallow dishes must have the feed mounted much further from the aperture and may be rejected because of mechanical considerations.

3.3 PARABOLIC ANTENNAS (Cont'd)

Thus for maximum aperture efficiency the feed pattern should be kept as uniform as possible. On the other hand feed energy outside the illuminated region decreases the spillover efficiency. This spillover loss should therefore be kept as low as possible. In practice the overall efficiency is highest when the edge taper (ie. the amplitude of the field at the edge of the illuminated region relative to the boresight amplitude), is about -10 to -12 dB. It is thus necessary in a dual-band design to ensure that the 10 dB beamwidth of the feed changes as little as possible over the two bands. Typical overall parabolic efficiencies obtainable are in the range of 50-60%. This efficiency is however for dishes where the reflector size is large in terms of wavelength. Where this is not true, an additional loss due to diffraction effects (L_{of}) must be taken into account. As an example calculations of the diffraction fields indicate a loss of 10% to 15% for a six-wavelength diameter reflector.

A typical 6' paraboloid (such as the Andrew No. 34810-1) has an efficiency of 40% at 390 MHz. Therefore to produce a 13 dBi gain at 274 MHz. would require a paraboloid of 8' diameter (assuming a gain 40% efficiency).

It can thus be seen that a parabolic reflector antenna has to be larger than an equivalent SBF reflector discussed in the previous section. Since the construction of a parabolid surface is more difficult than that for a SBF cavity it is concluded that the parabolid dish has no advantage over an equivalent SBF reflector for this application.

3.4 YAGI ANTENNAS

Yagi antennas are widely used for UHF frequencies. The exact analysis of Yagi antennas with more than three elements is difficult. However, a great deal of experimental data and analysis is available and have presented by various authors (3) (33) (35) (39). The Yagi antennas have two important advantages. They are lightweight and have elements that can be stored in a compact package.

3.4 YAGI ANTENNAS (Cont'd)

However, they also have two serious disadvantages:

a) The need for a cross-Yagi.

b) Narrow bandwidth. The requirement for circular polarization means that a cross-Yagi arrangement (see figure 3.4.1) must be used.

This can be regarded as two separate linearly polarized Yagis. For circular polarization, the two linearly polarized Yagis are fed with equal power with a 90^{o} phase difference between them. The impedance of the dipole is reduced from its free space value of about 70 Ohms to about 20 to 50 Ohms by coupling between the elements of the same Yagi. In contrast there is very little coupling from one Yagi to the other. The 90^{o} phase lag to one Yagi can be produced by feeding it via an additional 90^{o} line length. However, unless the feeder line has the same impedance on the antenna terminals it would act as a 1/4 wavelength impedance transformer. This would mean that the antennas no longer have the same impedance at the power divider and would no longer be fed with equal powers. Alternatively a 90^{o} hybrid can be used to provide the 90^{o} phase shift and equal power division. A circularly polarized Yagi thus has double the elements of a linearly polarized Yagi and also needs a much more complex feeder network.

A Yagi antenna can be typically optimized over a 10% bandwidth (within 1 dB.). Figure 3.4.2 shows the performance expected from a 10-element Yagi optimized for the received band. It can be seen that the antenna can only be used over one band. To cover both bands would require an array with separate and transmit antennas (see section 3.4.1 which follows) or a broadband Yagi (section 3.4.2).

3.4.1 YAGI ARRAYS

Figure 3.4.3 is a design curve for gain vs number of elements for a typical Yagi antenna with an element spacing of 0.34λ. It can be seen that for a gain of 13 dBi a 10-element Yagi can be used. This would have a typical performance shown in figure 3.4.2. By the use of separate receive and transmit Yagis it would become possible to meet the system

3.4.1 YAGI ARRAYS (Cont'd)

requirements. Figure 3.4.4 shows the dimensions of two 11-element Yagis that can be used to produce 13 dBi at both the transmit and receive bands. A reduction in overall lengths may be possible if the director spacing is reduced from the 0.34λ assumed. However, such a reduction would have to be experimentally verified. This configuration was rejected because the size of the receive Yagi antenna would make it difficult to support and deploy. Due to the need for two separate Yagis the weight requirement would also be exceeded.

The original gain requirement of 16-17 dBi in the transmit band would require a Yagi antenna of about 18'-22' long. This is clearly impractical to implement. In this case a 4-antenna broadside array can be used instead. The design of such arrays have been described in section 3.1.3. Using a similar procedure it was shown that the individual antenna in the quad-Yagi array must have a gain of 11 dBi.

This calls for a 6-element Yagi. The receive band would be covered by a single Yagi placed at the centre of the quad-Yagi array. The system dimensions calculated for such a setup are shown in figure 3.4.5.

3.4.2 BROADBAND YAGI ANTENNAS

Many commercially available Yagi antennas are designed using broadband techniques to enable the antenna to cover a wider frequency band. The references given should be consulted for a detail description of the many techniques used. A few of the techniques will be briefly discussed here with reference to the design criteria.

The reason that a conventional Yagi array is narrow band is because the director elements are tuned to the design frequency. As the frequency increases the elements become too long and no longer resonate.

A capacitive reactance can be added at the base of each director to decrease the effective length. However, there is no passive network which has an increasing capacitive reactance for increasing frequency. One solution would be to use an active network with such a characteristic. Such an active antenna is described in section 3.7.

3.4.2 BROADBAND YAGI ANTENNAS (Cont'd)

A fairly recent development is the "Tri-linear" director of Kluge (22) which is reported to be resonant over a much broader band than a conventional director. This consists of three flat in-line elements connected together by an insulator.

It performs as a single 1/2λ element at the low end and three 1/2 λ element at the high end of a 1:1.5 frequency band. It would be suitable for this application (receive;transmit = 1:1.45). Unfortunately, very little design or performance information was given by the author as this was developed for a commercial application. It is therefore impossible to properly evaluate the performance of such directors at this stage.

One common broadband method used is to design the directors to resonate at the high end of the band and design the reflector to resonate at the low end of the band. The driven elements (more than one may be used since this improves the bandwidth) are designed for the middle of the band. Using such a method it would be possible to design an antenna to cover both the receive and transmit bands. However, a 10-element Yagi that covers 274-400 MHz would only have a gain of 8-10 dBi. It would be difficult to achieve 13 dBi gain with a single antenna of reasonable size. Thus for 13 dBi gain a two or three Yagi array would be needed. This would therefore not offer any significant improvement over the separate receive/transmit array described in 3.4.1.

Another approach is to have a wide band driven element (or elements) and separate directors for both transmit and receive bands. The directors have to be very carefully located and interleaved for good performance. The problem of obtaining 13 dBi gain is similar to the previous case.

3.5 COMPOSITE HELICAL/YAGI ARRAY

This composite array was proposed as one solution when a transmit gain of 16 to 17 dBic was required. The array is shown in figure 3.5.1. This consists of a quad-Yagi array (similar to that described in section 3.4.2) designed for a transmit gain of 16-17 dBic. Instead of a single cross-Yagi for the receive band a uniform helix is used. The helix is smaller in size than a comparable Yagi antenna. For 13 dBic transmit and receive gains this configuration would no longer be considered since the quad-Yagi array is only necessary for high gain.

3.6 LOG PERIODIC ANTENNA

A log periodic antenna has a structure which is designed so that its electrical properties vary with the logarithm of the operating frequency. If variations within an octave can be kept small the antenna is broadband since variations repeat over each octave. Such antennas have been described by various authors (5) (15) (16) (17).

A circularly polarized log periodic antenna configuration would consist of two linearly polarized log periodic antennas placed orthogonally to each other. This antenna like most log periodic antennas, has low gain (8-10 dBic) since radiation takes place only from a region of about one wavelength in size. An array of log periodic elements is necessary for an increase in gain. Experimental results show that the half power beamwidth of a log periodic array is given approximately by

$$\theta_{3dB} = \frac{4D}{D/\lambda}$$

when θ_{3dB} = half-power beam width
D = equivalent broadside aperture
λ = wavelength

Deschamps (17)describes a 6-element H-plane array with a gain of over 16 dBic. For a linearly polarized antenna of 13 dBic an array of 4 elements with D/λ = 1.5 can be used. For circular polarization 8 elements would be required. It can be seen that a circularly polarized log periodic array would have no advantage over either a helix or Yagi configuration. This conclusion

3.6 LOG PERIODIC ANTENNA (Cont'd)

is not surprising since the main advantage of a log periodic antenna (operation over several octave bands) is not required for the MUSAT application where operation is only required over a 1:1.45 band ratio.

3.7 ACTIVE ANTENNAS

All the antennas considered in the previous sections are passive devices and their behaviour at different frequencies are limited by the frequency characteristics of the passive elements. It is possible to overcome this limitation by the use of active, non-linear solid state devices as part of a radiating structure. Antennas containing such radiating elements are called active antennas. The advantage of such antennas is that they can be designed to have a better match over a broader frequency band than an equivalent passive antenna.

One of the earlier applications of active antennas has been as receive-only HF and VHF antennas. Many such antennas are commercially available and have been used individually as a broadband antenna or as part of a large antenna array. A typical HF antenna (3$\frac{1}{4}$) can operate from 2 to 32 MHz with a maximum VSWR of 1.5. Its electronic gain varies from -7 dB to +20 dB over the same frequency range. A review of the various techniques used for active antennas together with descriptions of different antenna configurations have been given by Murphy et. al. (28). An example of what can be achieved with such antennas is the active Yagi antenna described by them (28). The antenna was designed to operate from 600 to 900 MHz. However, for convenience of comparison, the dimension of a model scaled for the MUSAT operating band is given in Table 3.7.1.

TABLE 3.7.1 ACTIVE YAGI ANTENNA

Overall length	-	35.44"
Dipole Length	-	23.06"
Reflector Length	-	21.38"
Director Length	-	18.56"
Director Spacing	-	6.75"
No. of Elements	-	6
Min. gain at 274-290 MHz	-	10.2 dBi
Min. gain at 370-400 MHz	-	9.7 dBi

The gain of the active Yagi antenna varies between 9.7 to 11.2 dBi between 274-400 MHz. This compares favourably with a typical 6-element Yagi

3.7 ACTIVE ANTENNAS (Cont'd)

(see figure 3.4.3) which has a gain of about 11 dBic. It may therefore be possible by increasing the number of elements to design an active Yagi antenna with the required 13 dBi gain. However, such a design is beyond the scope of this concept study. It was therefore decided by the design authority that further investigation of active antennas would be the subject of a separate study.

The advantage of active antennas for this application is the possible development of a light-weight and compact antenna. The disadvantages include possible high development cost and high antenna cost. Another likely problem is in the design of an active antenna capable of transmitting the relatively high peak power called for by the Musat specification.

3.8 SURFACE ARRAYS

If it is possible to control the phase and amplitude of the field at any given antenna aperture surface, the shape and direction of the antenna beam can be regulated. Such control can be used to achieve high aperture efficiency, to steer the beam and to null out interference. One way of achieving control of aperture phase and amplitude is with the use of a surface array. This consists of a group of radiating elements placed on a given surface.

Surface arrays find wide application as microwave phased array antennas. However, only surface arrays suitable for the Musat application will be considered here. The most attractive configuration would be a printed circuit planar array made up of radiating elements excited by a feed/power-divider network. The antenna could be divided into a series of identical modules which could easily be disassembled and stuck together into a compact package for transport. To be feasible at UHF frequencies, the antenna must be designed to be as thin as possible in terms of electrical wavelengths.

An example of what can be achieved with a thin antenna is the 5 GHz. 4x4 planar array described by Munson and Sandford (27). The equivalent dimensions of the array for the Musat receive band (282 MHz) would be 90"x90"x0.7". Each radiating element is 16" square so that if each element is formed as a module the elements can be stacked together for transport to form a

3.8 SURFACE ARRAYS (Cont'd)

package of size 16"x16"x11". The antenna has a maximum gain of 14 dBi and is designed as a phase array with a maximum steering angle of 60^{o}. An array with no scan capability can be optimized to reduce the size further.

Such surface arrays have a future potential as a cheap, light-weight and high performance antenna for the Musat application. Because of their relatively large size, the material used for UHF surface arrays present a problem in terms of cost and weight. Development of a suitable low cost, light-weight and perhaps, even low wind resistance stripline medium for UHF is essential. One possible medium would be some form of honeycomb sandwich such as that recently developed by Keeping and Sureau (19). A 1/4" thick sheet was reported to have a material cost of $3.50 per square foot. The design and successful development of a surface array suitable for the Musat application is beyond the scope of this concept study. Surface arrays are therefore ruled out as a possible antenna configuration since development cost would be too high.

4.0 CONSIDERATIONS IN THE SELECTION OF THREE CANDIDATE ANTENNAS

The advantages and disadvantages of each candidate antenna system have been included in the description of each antenna system reviewed in section 3. For convenience a summary of the main advantages and disadvantages has been included in Table 4.1. It indicates the reasons why the three most promising configurations were chosen. The three configurations are:

1) Short back-fire antenna.
2) Co-axial Helix
3) Separate receive and transmit helix

Many of the configurations were rejected because they have disadvantages that are difficult to overcome. The remaining of those rejected do not have such serious disadvantages. However, they have been shown to be electrically or mechanically less attractive than the chosen configurations. Each of the configurations chosen offer the possibility that they can be compact, light weight and collapsible. Also they can meet the electrical requirements.

TABLE 4.1 COMPARISON OF CANDIDATE ANTENNAS

ANTENNA TYPE	ADVANTAGES	DISADVANTAGES	COMMENTS
A Helix Antenna	1) Circular Polarization 2) Easily Collapsible 3) Small Reflector 4) Lightweight and low cost	5) Special modification need to cover both bands at once.	These general characteristics apply to all group A antennas.
A(i) Separate helix for receive and transmit	1) as in A(1)-(4) 2) 13 dBic gain possible	3) Two helixes required. 4) Mounting more complex than single helix	Chosen for further study because of (1)-(2)
A(ii) Bi-Helix	1) as in A(1)-(4) 2) Higher gain than A (i)	3) Cannot operate over both bands	Ruled out for this application by (3)
A(iii) Tri-Helix	1) as in A(1)-(4) 2) High gain possible	3) Cannot operate over both bands	Ruled out because of (3). Also (2) not required.
A(iv) Quad-Helix	1) As in A(1)-(4) 2) High gain possible	3) Cannot operate over both bands.	Ruled out because of (3). Also (2) not required.
A(v) Non-Uniform Helix	1) as A(1)-(4). 2) Can operate over both bands 3) 13 dBic gain possible	4) Too long mechanically	Dropped in favour of A(vi)
A(vi) Co-axial Helix.	1) as A(1)-(4) 2) Can operate over both bands. 3) Gain higher in receive than transmit. 4) 13 dBic may be possible	5) Co-axial structure more complicated than single helix.	Chosen because of (1) to (4)

TABLE 4.1 COMPARISON OF CANDIDATE ANTENNAS

ANTENNA TYPE	ADVANTAGES	DISADVANTAGES	COMMENTS
B. Short-Back-Fire Antenna	1) High Efficiency (>60%). 2) Broadband. 3) Lightweight. 4) Reflector can be folded.	5) Reflector large and expensive to build.	Chosen because of (1)-(4).
C.Parabolic Antenna	1) Broadband. 2) Lightweight 3) Reflector can be folded.	4) Reflector even larger than B. 5) Low efficiency (< 40%)	Dropped in favour of B.
D. Yagi Antenna	1) Easily collapsible 2) Lightweight and low cost. 3) 13 dBic gain possible	4) Cross Yagi required. 5) Matching and phasing network required. 6) Narrow Band.	Ruled out because of (4)-(6).
D(i) Yagi Arrays	1) As D(1)-(3). 2) Higher gain than D possible.	3) as D(4)-(6).	Ruled out by (3).
D(ii) Broadband Yagi Antenna	1) as D(1)-(2)	2) As D(4)-(5). 3) Gain only < 10 dBi for reasonable size.	Ruled out by (2) and (3)
E. Composite Helical/ Yagi Array	1) High gain possible.	2) As D(4)-(5). 3) Size and weight too large.	Ruled out by (2) and (3) also (1) not needed.
F. Log periodic Antenna	1) as D(1)-(2)	2) Array required for 13 dBic. 3) Array too heavy and complex.	Ruled out because of (2) and (3).
G. Active Antennas	1) Broadband possible. 2) Compact size and lightweight.	3) Development cost too high. 4) Transmit power may be limited.	Ruled out by (3).

TABLE 4.1 COMPARISON OF CANDIDATE ANTENNAS

ANTENNA TYPE	ADVANTAGES	DISADVANTAGES	COMMENTS
H. Surface Arrays	1) High Efficiency. 2) Compact size possible.	3) Development cost too high. 4) Present state-of-art antenna too expensive.	Ruled out by (3) and (4).

5.0 SHORT BACK-FIRE ANTENNA DESIGN

The short back-fire (SBF) antenna was chosen for this design study because it is the most promising of all reflector antenna configurations studied. Most of the successful applications described for this antenna have been over a relatively narrow frequency band. The Musat requirement however calls for operation over a much broader band. This study therefore concentrates on examining the performance of the SBF antenna over the Musat receive and transmit bands. Methods of matching the antenna over a wide frequency band is another area where little have been published. This problem is studied in section 5.2.

5.1 ANTENNA PERFORMANCE AND CHARACTERISTICS - SBF ANTENNA

The performance of the SBF antenna has been described in section 3.2 which also showed the directive gain against frequency characteristic for one such antenna. The results obtained in section 5.2 show a behaviour similar to that described in section 3.2. The antennas described are linearly polarized. However, instead of a single dipole, a cross-dipole feed can be used to obtain circular polarization. The characteristic of such a circularly polarized antenna should be similar to that for a linearly polarized antenna. It was decided that the initial optimization should be carried out using a single dipole since such an arrangement is much easier to fabricate in a scale model. This is sufficient to predict the pattern performance of the antenna. The design of a matching and phasing network suitable for cross-dipole feed can be implemented when a full scale antenna is built.

A cross-dipole is not necessarily the only or the best feed for a circularly polarized SBF antenna. Another possibility is a spiral antenna in place of the cross dipole. Section 5.2 describes measurements made on an equiangular spiral designed for use in a S.B.F. antenna.

5.2 MEASUREMENT AND RESULTS - SBF ANTENNA

Experimental measurements on the SBF antenna configuration were carried out using a scale model. Scale models were also used to derive experimental data on both the co-axial helix (section 6) and the uniform helix (section 7). This approach was taken because for this study, scale models have many advantages. The small size of a model means that it can be constructed very quickly and inexpensively. This is an important point in a parametric study which may require more than one model.

5.2 MEASUREMENT AND RESULTS - SBF ANTENNA (Cont'd)

For this study the scale models are mounted by means of a low reflection support on a rotator placed about 20 feet above the ground. The source antennas are placed at the same height on a tower about 20 feet away. Because the operating frequency of the models lie in the 1.5-2.7 GHz range it is possible to use standard microwave measurement techniques. Thus, microwave absorbers are used where necessary to reduce reflection. Also standard gain horns with gains comparable to that of the model antennas can be used to derive the gains of the experimental antennas.

The scale model used for the experimental measurements is shown in figure 5.2.1 The radiating element is a slot-fed dipole. The cavity is made in two parts so that the cavity depth is adjustable. The model is designed so that every parameter, including the dipole arm length, is adjustable.

The results presented here are measurements made on antennas given in table 5.2.1. For convenience the equivalent dimensions for a full scale antenna are given.

TABLE 5.2.1 SBF ANTENNA PARAMETERS
(all dimensions in inches)

Antenna	Dipole Length	Cavity Diameter	Cavity Depth	Secondary Reflector Diameter	Matching Slot Depth	Dipole Height	Secondary Reflector Spacing
	L_d	M	D	Z	S	Y	P
A	23.6	74.3	18.6	18.6	9.3	9.3	9.3
B	19.0	72.3	16.4	-	9.9	8.0	-
C	19.0	72.3	19.7	-	9.9	8.0	-
D	19.0	72.3	26.3	-	9.9	8.0	-
E	19.0	72.3	26.3	18.1	9.9	8.0	16.4
F	19.0	72.3	26.3	18.1	9.9	8.0	13.1
G	19.0	72.3	26.3	18.1	9.9	10.0	9.2

5.2 MEASUREMENT AND RESULTS - SBF ANTENNA (Cont'd)

The various dimensions in the table are defined by figure 5.2.2. For all the patterns shown, data in the title refer to those for an equivalent full scale antenna.

Figures 5.2.3 to 5.2.11 show the behaviour of antenna A (see table 5.2.1) where the dipole is placed half-way between the two reflecting surfaces. The cavity depth is adjusted so that the rim edge is in the same plane as the secondary reflector. The performance for this antenna is similar to that described in section 3.2 (figure 3.2.1). From 203 to 227 MHz (figures 5.2.3 to 5.2.5) the antenna has a low backlobe and almost equal E and H-plane patterns. At 274 MHz (figures 5.2.6) the E-plane has become narrow and two distinct lst sidelobes are present. The H-plane has also begun to narrow though no sidelobes are visible. As the frequency increases (figures 5.2.7 to 5.2.8) the E-plane sidelobe level decreases while the value of the H-plane beamwidth approaches that of the E-plane. At 324 MHz the E and H plane beamwidths are almost equal and the sidelobes and backlobes are both very small. This point represents the main peak in the gain-frequency characteristic. The gain falls beyond this point (figures 5.2.7 to 5.2.11) as the sidelobe levels begin to increase. For the first time the H-plane's first sidelobe becomes visible. At 400 MHz the sidelobes have become fairly high (H-plane = -10 dB and E-plane = -15 dB). Figure 5.2.12 shows the way beamwidth and sidelobe levels vary over the complete frequency range of antenna A.

The effect of the secondary reflector on sidelobe levels is illustrated in figures 5.2.13 and 5.2.14. Figure 5.2.13 is the pattern of antenna A at 312 MHz showing that sidelobe levels are generally below -25 dB (one E-plane sidelobe was -18 dB). Figure 5.2.14 is also a pattern of antenna A at the same frequency except the 18.5" diameter secondary reflector is now replaced by one of 20.2" diameter. The sidelobe levels have risen to about -15 dB.

The effect of a cavity on a single dipole (without a secondary reflector) at 274 MHz can be seen in figures 5.2.5 to 5.2.17. Here the cavity depths is increased from 16.4" to 26.3". The resultant change in beamwidth is shown in table 5.2.2 below.

TABLE 5.2.2 CHANGE IN BEAMWIDTH WITH CAVITY DEPTH AT 274 MHz

Antenna	Cavity Depth	3 dB Beamwidth H-Plane	E-Plane
B	16.4"	42^{o}	50^{o}
C	19.7"	38^{o}	47^{o}
D	26.3"	35.5^{o}	41.5^{o}

Figures 5.2.17 to 5.2.20 show the behaviour of antenna D over both the Musat receive and transmit frequency bands. It can be seen that the beamwidth is much broader over the transmit band. Corresponding patterns for antenna B and C, not included here, are similar to figures 5.2.19 and 5.2.20.

The effect of the secondary reflector is illustrated by patterns for antenna E(figures 5.2.21 to 5.2.24) which is antenna D with the addition of a secondary reflector. Table 5.2.3 compares the beamwidth and sidelobe levels of antennas D and E.

TABLE 5.2.3 COMPARISON OF SYSTEM PERFORMANCE WITH (ANTENNA E) AND WITHOUT (ANTENNA D) A SECONDARY REFLECTOR

Frequency (MHz)	Antenna	3 dB Beamwidth H-Plane	E-Plane	1st Sidelobe Level H-Plane	E-Plane
274	D	35.5^{o}	42^{o}	-19.5 dB	-
	E	43.5^{o}	35^{o}	-	-15.5 dB
290	D	32^{o}	39^{o}	-13 dB	-
	E	35^{o}	36.5	-16 dB	-16 dB
370	D	33^{o}	40^{o}	-2.8dB	-
	E	21.5^{o}	33^{o}	-7.8 dB	-
392	D	40^{o}	50^{o}	-2.5 dB	-
	E	19^{o}	53^{o}	-4.3 dB	-10.2 dB

It can be seen that the effect of the secondary reflector is to improve the beamwidth and sidelobe performance of the antenna. The effect is most pronounced in the Musat transmit band.

5.2 MEASUREMENT AND RESULTS - SBF ANTENNA (Cont'd)

While antenna E is an improvement on antenna D its performance at the transmit band is still poor. Figures 5.2.25 to 5.2.32 show how performance at the transmit frequency band was improved by a reduction in the secondary reflector to dipole-feed distance. This distance was reduced from 16.4" (antenna E) to 13" (antenna F) and finally to 10" (antenna G). The drastic improvement at the transmit band can be seen by comparing antenna G (figures 5.2.31 and 5.2.32) with antenna E (figures 5.2.23 and 5.2.24). Of the three, antenna G has the best performance and can be used as a basis for further optimization.

No gains have been measured on the antennas described above since it proved impossible to match the antennas over both receive and transmit bands simultaneously. This is partly because the dipole used cannot be made resonant over the receive and transmit bands.. An attempt to use a circular disc sleeve dipole in place of the simple dipole was unsuccessful. No conclusion regarding the possibility of matching a dipole feed over both bands should be drawn from the above. Techniques do exist for resonating a dipole over two bands. Special matching networks can also be designed to broadband an antenna.

It was decided instead to replace the inherently narrow band dipole with a broadband radiating element. A printed circuit version of an equiangular spiral antenna shown in figure 5.2.33 was constructed. A spiral is not only broadband, it also provides the circular polarization required for the full scale antenna. The spiral and secondary reflector were supported by a feeder network fabricated from semi-rigid co-axial cables. A half wavelength co-axial balun provided a balance feed for the spiral. Figure 5.2.34 shows a plot of return loss against frequency characteristic measured on the model feed alone. Except for one sharp dip the curve is fairly smooth showing an average return loss of about 12 dB. Such a constant mismatch can generally be eliminated by an impedance transformation network. The results confirm that the equiangular spiral has a broad impedance bandwidth. Figure 5.2.35 shows the effect of placing the feed within the antenna. The antenna parameters shown were those optimized for good return loss performance. It can be seen that the antenna has a very strong effect on the feed impedance. It can therefore be concluded that further design effort must be devoted to matching the SBF antenna before a full scale version can be built.

5.2 MEASUREMENT AND RESULTS - SBF ANTENNA (Cont'd)

Unfortunately, all design efforts on the SBF antenna had to terminate at this stage in favour of the co-axial helix study.

5.3 MECHANICAL DESIGN - SHORT BACK-FIRE ANTENNA

5.3.1 DESCRIPTION

The mechanical design of the short back-fire antenna is depicted by drawing WSK430. The primary structure is thin wall aluminum tubing which gives a high strength-weight ratio. The rather large area of reflector surface is a knitted wire cloth which is very flexible for folding, opaque to RF energy at UHF frequencies, and almost transparent to wind forces.

The knitted wire cloth is fabricated from monel wire .004 to .005 inches in diameter. Monel is a high strength,extremely ductile, corrosion-proof alloy containing approximately 2/3 nickel and 1/3 copper. One pound of this cloth covers an area of 40 square feet.

The assembly folds like an umbrella into a package half a diameter (36 inches) in length as shown on drawing WSK430.

Tripod legs, feed assembly, and azimuth elevation adjustment unit would be strapped to this and the entire package would be fastened to a standard backpack frame.

5.3.2 WEIGHT - SHORT BACK-FIRE ANTENNA

The weight of this design is as follows: -

a) Tripod	3.1 lbs
b) Feed system and coaxial cable	6.4
c) Wire cloth	1.7
d) Antenna frame	5.2
e) Az-el adjustment unit	4.3
f) Backpack and miscellaneous	7.3
	28.0 lbs.

5.3.3 WINDLOAD - SHORT BACK-FIRE ANTENNA

In a 60 mph wind at zero degrees elevation angle the wind load would be 85 lbs.
This load could be easily carried by guy ropes.

5.3.3 WINDLOAD -SHORT BACK-FIRE ANTENNA (Cont'd)

In the absence of guy ropes, the uplift on one tripod leg would be 149 lbs.

6.0 A NEW CO-AXIAL HELIX DESIGN

The co-axial helix configuration is a new design that resulted from the study. It was developed to meet the requirement for a compact broad-band helix that can cover both the Musat receive and transmit frequencies. It consists of two helical coils, wound in the same sense, placed concentric to each other. In the models developed, both coils have the same number of turns and pitch distance. The ratio of outer to inner coil diameter is approximately 2:1. This is the most promising of all the antenna configurations studied. It is mechanically compact and cost studies indicate that it is significantly cheaper than a S.B.F. antenna.

The scope of this concept study of antenna types does not permit a detail optimization investigation and analysis of this new configuration. Such an investigation would form part of a developmental study of the antenna to be initiated at the conclusion of this one. The results presented in the subsections that follow can therefore be regarded as representing the first phase of a complete study of this antenna. They indicate that the co-axial helix can be developed as a broadband circularly polarized antenna.

6.1 PERFORMANCE AND CHARACTERISTIC - CO-AXIAL HELIX

A helical configuration has many advantages for a Musat man-pack antenna.The required circularly polarized fields are produced without any special polarizers by a helix. The helix is relatively easy to match over the entire receive and transmit bands. The ease with which it can be collapsed into a compact package is another important advantage. For these reasons helix configurations were extensively studied for this project.

Like the non-uniform helix the co-axial helix can be regarded as a modification of the uniform helix. It is therefore necessary to relate its performance to that for the uniform helix. The characteristic of the uniform helix which is described fully in Section 7 will be briefly summarized.

Figure 7.1.1 shows the gain frequency characteristic for uniform helixes. A gain peak occurs when the circumference in wavelength (C_λ) is 1.1 to 1.15. Operation beyond the gain peak is only possible over a limited range since the gain falls rapidly and the axial ratio becomes large. In the region

6.1 PERFORMANCE AND CHARACTERISTIC - CO-AXIAL HELIX (Cont'd)

before the peak the gain-slope is more gradual and the axial ratio is generally less than 2 dB. The gain slope is such that for a 10 turn helix the gain over the transmit band would be over 13 dBic, while the receive band gain would only be about 9.3 dBic. If the gain-slope remains constant it would be possible, by increasing the number of turns, to boost the receive band gain to 13 dBic. Unfortunately, the gain slope becomes steeper as the number of turns increases (ie. the helix becomes more narrow-band). It is in fact not possible to boost the receive gain beyond about 11 dBic.

A modification to improve the bandwidth therefore involves altering the gain-frequency characteristic described above. One way of doing this is the non-uniform helix described in section 3.1.4. This consists essentially of a uniform helix which has a smaller diameter uniform helix attached to its end.

The smaller helix is approximately 20% smaller in diameter than the larger helix. Figure 3.1.6 shows how the frequency range of the helix has been extended by the presence of a second peak. Considering the diameter of the larger helix the first gain peak corresponds approximately to that expected for an equivalent uniform helix since it occurs at $C_\lambda = 1.19$. The second peak occurs at $C_\lambda = 1.4$, a region where the equivalent uniform helix would give very poor results. It would therefore appear that the presence of the second smaller diameter helix serves to extend the frequency range of the antenna beyond $C_\lambda = 1.2$.

Results presented in section 6.2 show that the co-axial helix differs from both the uniform and non-uniform helix. Like the non-uniform helix the frequency range is extended by the presence of another gain peak. However, unlike the non-uniform helix, the first gain peak occurs at $C_\lambda = 0.93$ ($C_\lambda = 1.1$ for uniform and non-uniform helixes). This shows clearly the coupling effect of the inner helix. The second gain peak occurs close to where a corresponding single helix would be expected to have its peak.

The relative size of a co-axial helix can be obtained by comparing the size of the outer helix to a uniform helix giving approximately the same peak gain. This assumes that helixes of the same mechanical size is compared. Table 6.1.1 shows a comparison of the dimensions of the co-axial helix measured in section 6.2(see table 6.2.1) to the receive band unfform helix design of section 7.2 (see table 7.2.1.).

TABLE 6.1.1 COMPARISON BETWEEN CO-AXIAL HELIX AND UNIFORM HELIX

	Co-Axial Helix (Outer Helix Dimensions)	Uniform Helix (Receive Band Helix)
Helix diameter	11.85"	15.65"
Helix length	88"	83"
No. of Turns	14	7
Pitch Distance	6.3"	11.86"
Pitch Angle	9.6^0	13.9^0

It can be seen that the overall length of both helix is almost the same. The diameter of the co-axial helix is only 75% that of the uniform helix. This indicates the effect of the inner helix (discussed in the preceding paragraph) which shows up physically as a reduction in outer helix diameter. The pitch angle of the co-axial helix has been reduced by about 3^0 to 4^0 in comparison to that for a normal uniform helix design. It is interesting to note that the non-uniform helix is also designed with a low pitch angle (10.6^0). The number of turns and pitch distance are fixed by the choice of helix diameter, length and pitch angle.

The way that the co-axial helix differs from the uniform and non-uniform helixes is summarized in table 6.2.1.

TABLE 6.1.2 COMPARISON OF THE CHARACTERISTICS OF HELIXES

	Co-Axial Helix (1) (Outer Helix)	Non-Uniform Helix (2) (Larger Helix)	Uniform Helix (1) (Receive Band)
1st Gain Peak (in C_λ)	0.93	1.19	1.15
2nd Gain Peak (in C_λ)	1.21	1.40	none
Diameter	11.85"	14.03"	15.65"
Length	88"	151"	83"

Note:

(1) The uniform helix and co-axial helix are the same as that of table 6.2.1.
(2) The non-uniform helix is that of King and Wong (20). It should be noted that while the frequency range is approximately the same the gain of this helix is higher than the others. Caution is therefore required in comparing parameters of this helix (in particular the length) with the other helixes.

6.2 RESULTS FOR THE CO-AXIAL HELIX

Figure 6.2.1 gives details of the 1:4.75 scale model of the co-axial helix configuration. The helical coils for both the inner and outer helixes were made from solid copper wire of diameters shown. Each helical coil was fabricated on a lathe by winding the wire on to a cylindrical former whose diameter corresponds to the inner diameter required for the helix. By feeding the wire on to the former at the specified pitch angle, the correct helical pitch distance is automatically maintained. The resultant helical coil is of the correct shape but would distort if it is not supported along its length. The support is provided by a 1/8" thick sheet of Rexolite 2200. This has a series of holes spaced at the pitch distance. (see figure 6.2.1). The helical coils is then threaded into the Rexolite sheet until every turn is supported at two points. The resultant helix is reasonably rigid mechanically (except in high winds). Rexolite 2200 was chosen because it has good mechanical and electrical properties. It has a dielectric constant of 2.6 and loss tangent of 0.001 at 2 GHz. This is important since the presence of dielectric material close to the helical coils would lead to field perturbations and losses. The mounting method adopted ensures that very little dielectric material lies close to the helical coil. By using a dielectric that has both low loss as well as low relative permittivity the effect of the support can be kept small.

Figures 6.2.2 to 6.2.26 are radiation patterns taken using the co-axial helix model. The cavity diameter and frequency included in the titles refer for convenience to a full scale version of the co-axial antenna. Each pattern also has a data block where the actual model dimensions and frequency are recorded. A S.B.F. antenna was used as the source antenna over the frequency range of 1200 to 1600 MHz. (253 to 338 MHz. for full scale). For frequencies above this range a small WR430 horn was used as the source. In the discussion that follows, reference will always be made to the full scale dimensions and associated frequencies. Figure 6.2.21 shows the orientation of the source. The electric field is vertical at 0^{o} and horizontal at 90^{o}. Patterns are generally taken at 0^{o} and 90^{o} and for convenience these are marked H and E. This corresponds to the H-plane and E-plane patterns for linearly polarized antennas. In addition to the patterns, the source is also rotated through 360^{o} with the co-axial helix at the boresight position. The resultant vertical line gives the axial ratio of the antenna on boresight. For each frequency the

6.2 RESULTS FOR THE CO-AXIAL HELIX (Cont'd)

system gains are kept constant so that it is possible to compare the 0 and 90^{o} patterns as well as the axial ratio plot.

Figures 6.2.2 to 6.2.10 show patterns for the co-axial helix where all the turns are uniform. The reflector cavity used was 20" in diameter and 4 3/4" deep. Figures 6.2.2 and 6.2.3 (frequency = 274 and 295 MHz) indicate the performance over the receive band. It can be seen that over the receive band the main beam and first sidelobe is well defined. The axial ratio is below the specified 2 dB and the sidelobe and backlobe are all below -10 dB. The patterns are similar in nature to that obtained with a single helix (see section 7.2) showing that the helix is operating in the axial mode. Figures 6.2.4 to 6.2.10 (frequencies = 364 to 395 MHz) show the performance of the helix in the transmit frequency band. The main beam is still well defined at the centre of the band. However, at the band edges the main beam is beginning to deteriorate. The sidelobes are higher than those in the receive band. The axial ratio is also much worse, being about 4 to 5 dB at the band edges.

To improve the sidelobe performance of the system the cavity diameter was increased to 22" (the depth remains at 4 3/4"). Figures 6.2.11 to 6.2.16 show the improvement achieved. As an example comparison can be made between figures 6.2.2 and 6.2.11 which show the helix operating at 274 MHz. It can be seen that the backlobe region of the helix has been reduced by the use of a large cavity. The effect on the E-plane is greater than that for the H-plane. The main beam however has remained constant. This is generally true for the receive and transmit bands. However, the effect on the transmit band is less. This is to be expected since the effect of increasing the cavity size is more pronounced at the lower receive frequency where the cavity is smaller in terms of wavelength.

To improve the axial ratio the last two turns of the outer helix were tapered. Figures 6.2.17 to 6.2.25 show the effect of tapering the outer helix. Figures 6.2.17 and 6.2.18 show that the axial ratio has now been improved to 1 dB over the receive band. A similar improvement is also evident in the transmit frequency band, (figures 6.2.19 to 6.2.25) where the axial ratio measured is now within 2 dB except at 369 MHz. (Figure 6.2.19) where it is 2.5 dB. In addition to the improvement in axial ratio the backlobe has also been

6.2 RESULTS FOR THE CO-AXIAL HELIX (Cont'd)

improved over the entire transmit band. It can be concluded that tapering the end of the co-axial helix not only improves the axial ratio but also enables it to radiate much more strongly in the forward direction. Figures 6.2.21 and 6.2.22 together show the effect of rotating the source antenna polarization at the middle of the transmit band (385 MHz). This is equivalent to rotating the co-axial helix to take pattern cuts through different planes passing through the axis. The source is generally rotated in preference to the test antenna because it is much more simple to achieve mechanically. Remote control of source antenna orientation is normal on most pattern ranges. Figures 6.2.23 to 6.2.25 show the effect of rotating the source at 395 MHz. It can be seen that at both 385 and 395 MHz. the axial ratio remains reasonably constant within most of the main beam. Figure 6.2.26 shows that it is possible to match the co-axial helix over both bands.
Table 6.2.1 show the gains measured on the co-axial helix (22" cavity diameter with end two turns tapered). The gains are obtained with the gain by comparison method using standard gain horns.

TABLE 6.2.1 CO-AXIAL HELIX GAIN

Frequency (MHz)		Circumference (C_λ)		Gain
Full Scale Helix	Model Helix	Outer Helix	Inner Helix	(dBic)
253	1200	0.80	0.34	11.4
274	1300	0.86	0.36	13.0
295	1400	0.93	0.40	13.7
316	1500	1.00	0.42	13.5
385	1825	1.21	0.52	12.2

The results presented do not by any means represent an optimized version of the co-axial helix. They do however, show that the concept of the co-axial helix is a very promising one that deserves further study.

6.3 MECHANICAL DESIGN - COAXIAL HELIX ANTENNA

6.3.1 DESCRIPTION

The mechanical design of the coaxial helix antenna is depicted by drawing WSK 439.

The deployable helical elements are made by winding an aluminum tube on a mandrel of the desired diameter. The tube is wound in the packed or stowed configuration and then slit longitudinally to remove torsional stiffness while retaining bending stiffness about all axes. This results in a deployable helical element which does not require as many support points as a cross section with less bending stiffness. Fewer support points mean fewer parts, lower cost, and quicker assembly and dissassembly.

It is planned to try an aluminum support boom initially and change to fiberglass if necessary for electrical performance reasons.

The frame of a standard backpack is to be incorporated into the reflector at the fed end of the antenna and permanently attached to the helixes.

Tripod legs, guy ropes, azel adjustment mechanism and support boom would be strapped to the backpack adjacent to the helices in the packed configuration.

6.3.2 WEIGHT-COAXIAL HELIX ANTENNA

The weight of this design is as follows: -

a)	Tripod	3.1 lbs
b)	Inner helix	2.8
c)	Outer helix	5.0
d)	Boom and Helix supports	5.0
e)	Az-el adjustment unit	4.3
f)	Backpack and miscellaneous	7.3
	TOTAL	26.8 lbs.

6.3.3 WINDLOAD COAXIAL HELIX ANTENNA

In a 60 mph wind the windload of this design would be 60 lbs. If this load was not carried by guy ropes, the uplift on one tripod leg would be 105 lbs.

7.0 SEPARATE RECEIVE AND TRANSMIT HELIX

This configuration, unlike the previous broadband helix, uses the helix as a narrow-band antenna. Each band is covered by a separate helix. Thus, instead of the common feeder cable, there would be a separate receive and transmit feeds. Because of the separate helixes, it is very easy to optimize each band for any specified gain. It is, however, considered to be more complex mechanically than the co-axial helix. Design effort on this configuration was terminated in favour of the co-axial helix.

7.1 ANTENNA PERFORMANCE AND CHARACTERISTIC

Kraus (24)gives the gain of a helix as being approximately

$$G \simeq K_G C_\lambda^2 \frac{ns}{\lambda} \qquad - 7.1.1$$

where λ = free space wavelength

s = pitch of the helix

c_λ = circumference in wavelength

n = number of turns

K_G = Gain factor = 15

This formula is based on an approximate relationship between directive gain and the 3 dB beamwidth of a pattern. While this relationship holds well for large microwave antennas errors are introduced when the sidelobe levels are too high or when the axial ratio of an antenna becomes large.

Thus in practice the gain against frequency behaviour of helixes are more complex than would be implied by equation 7.1.1. A design of a helix should therefore be based on actual measured gains. In this regard, one of the most significant reports to appear is the very recently published report of King and Wong (21)on the uniform helix. This presents the results of actual measurements on helixes of different lengths. This report was received only after the experimental and design phase of this project was completed. Data from this report would have made the experimental optimization of this study much easier.

A presentation of all the results and conclusions of King and Wong (21), will not be attempted here. However, a few aspects of the report which are of direct interest to this study are discussed below.

7.1 ANTENNA PERFORMANCE AND CHARACTERISTIC (Cont'd)

King and Wong (21) present results for a fixed length uniform helix (30.8" long and 4.3" diameter) with pitch angles from 12.5° to 14.5° (n = 8.5 to 10). They give the empirically derived expression for the peak gain for such helixes as: -

$$G_p = 8.3 \left(\frac{\pi D}{\lambda_p}\right)^{\sqrt{n+2} - 1} \left(\frac{ns}{\lambda_p}\right) \quad 0.8 \left[\frac{\tan 12.5^\circ}{\tan \alpha}\right]^{\sqrt{n}/2}$$

- 7.1.2

where

n and s are as previously defined

λ_p = wavelength at peak gain

α = pitch angle

D = diameter of the helix

They also conclude that the gain frequency characteristics measured are in general agreement with equation 7.1.1 for $C_\lambda < 1.1$. However, instead of the gain factor (K_G) of 15 given by Kraus they found that K_G varies from 4.2 to 7.7 for a C_λ range of 0.8 to 1.2. They presented experimental data which indicate that the gain slope depends on antenna length and is approximately proportional to $f^{\sqrt{n}}$ (in equation 7.1.1 the gain slopeis f^3).

The experimental optimization carried out for this project showed that it is not possible for a single helix to have a gain of 13 dBic at both the receive and transmit bands. This is confirmed by results given by King and Wong. One of the most important results presented by them is a plot of gain against frequency (as well as C_λ) for helixes of 5 to 35 turns. This is reproduced here as figure 7.1.1. It can be seen that the greater the number of turns of a given helix the narrower its frequency bandwidth.
This graph can be used to consider the design of a uniform helix for the Musat frequencies since a C_λ scale is included as an alternative to the actual frequency scale. It is therefore necessary to determine the actual position and extent of the Musat receive and transmit bands in terms of C_λ. It can be seen from the graph that C_λ for the receive band should be as large as possible since gain increases with C_λ . Since the transmit and receive bands have a fix relationship this in practice means the choice of as large a C_λ for the transmit band as possible. The top end of the transmit band

7.1 ANTENNA PERFORMANCE AND CHARACTERISTIC (Cont'd)

cannot however be greater than $C_\lambda = 1.2$. This is because gain generally falls off beyond this point and the axial ratio deteriorates badly. This gives $C_\lambda = 1.11$ to 1.20 for the transmit band and $C_\lambda = 0.82$ to 0.87 for the receive band. Figure 7.1.1 differs from the original of King and Wong in that these two bands have been added to it. It can be seen that for helixes of 10 to 22 turns a transmit gain of > 13 dBic can be achieved. However, the corresponding receive gain varies from about 9.3 to 11.0 dBic. The best compromise that can be managed for a single uniform helix would be perhaps one of 12 turns. Figure 7.1.1 shows that this gives a transmit gain of 13.5 dBic and a receive gain of 9.6 dBic. However, since the receive gain specification is fixed at an absolute 13 dBic min. this compromise helix would not be acceptable.

A better solution using the uniform helix would be to have separate receive and transmit helixes. It is then possible to optimize each helix by operating each within the peak region of the gain curve. For equal gain in the receive and transmit bands it is only necessary to optimize experimentally a uniform helix for the transmit band. The receive helix can be obtained using a 1:1.45 scale. This is the approach taken here since it meets the minimum gain requirements.

An alternative approach would be to design the receive band helix for the 13 dBic specification. Mechanically it should be permissable to allow the transmit helix to be as long as the receive helix since they are mounted side by side. If this is the case, it is possible to have more turns in the transmit helix. The transmit helix would then be optimized for maximum gain with the mechanical lengths as a constrain. This would produce a receive helix of 13 dBic gain and a transmit helix of higher gain ($\simeq$14.5 dBic).

7.2 MEASUREMENTS AND RESULTS

Scale models of a uniform helix were used to obtain experimental data required to optimize a single helix for 13 dBic gain. The final optimized 1:5 scale model is shown in figure 7.2.2. It consists of a helical coil of copper wire supported by a sheet of 1/8" thick Rexolite 2200. This arrangement gives good mechanical support with little perturbation of the antenna fields. The Rexolite is chosen because it has good rigidity and low loss. The

cavity dimensions shown are the smallest possible for good gain and patterns.

Figure 7.2.3 to Figure 7.2.10 show measured field patterns of the helix model from 1615 to 2300 MHz. (323 to 460 MHz. full scale for transmit frequency). The frequencies shown in the titles are the full scale frequencies. The patterns were those taken in the course of the optimization. The output signal level of the test generator varied with frequency, and strong winds vibrating the helix introduced some ripples in figures 7.2.9 and 7.2.10. Since this phase of the project was terminated it was not possible to repeat the patterns under more ideal conditions.

Figure 7.2.11 shows a sweep frequency plot of the return loss of the helix.

The gain of the helix was measured using a gain by comparison method. The gains were compared to that of a WR430 standard gain horn. Figure 7.2.12 shows a plot of the gain vs frequency for the antenna. This shows that the gain is 13.0 dBic over the transmit band. The results obtained can also be applied to the receive band. Here a scaling factor of 1:6.9 has to be applied. The full scale dimensions for the final recommended configuration are shown in table 7.2.1.

TABLE 7.2.1 FULL SCALE HELIX DIMENSIONS

PARAMETERS	RECEIVE HELIX	TRANSMIT HELIX
1. Number of turns	7	7
2. Helix pitch	11.86"	8.60"
3. Overall length	83"	60.2"
4. Helix Diameter	15.65"	11.05"
5. Cavity Diameter	29.3"	21.25"
6. Cavity Depth	6.9"	5.0"
7. Design Frequency (MHz)	274-290	370-400
8. Minimum Gain	13 dBic	13 dBic

No mechanical design is given for this configuration since the co-axial helix design was chosen instead. The helixces should be separated by at least 40 inches between their axial centres.

8.0 EVALUATION OF CANDIDATE ANTENNA SYSTEMS

A complete mechanical design and cost analysis were carried out on two of the three antenna designs given in sections 5 to 7. This section evaluates the three systems and summarizes the reasons for selecting the co-axial helix and SBF antennas for detail mechanical study. Design details and experimental measurements on the three candidate antennas have been given in preceding sections and will not be repeated here. Similarly, the advantages and disadvantages of individual designs have been covered already.

From the mechanical design point of view, the coaxial helix and uniform helix antennas are very similar. The design of a lightweight cavity and a collapsible helical coil for each configuration are almost the same. Thus design factors affecting the weight, package dimensions and construction for one design can be used to estimate those for the other. It was decided that only the more promising helical configuration be selected for a full mechanical design since only one design will ultimately be chosen.

The coaxial helix design described in section 6 is therefore compared with the uniform helix design of section 7. A comparison of the two designs is given in table 8.1 below.

Table 8.1 Comparison between Co-axial and Uniform Helix Antenna Design

	Co-axial Helix Antenna		Uniform Receive/Transmit Helix Antenna	
	Outer	Inner	Receive	Transmit
Length	88"	88"	83"	60.2"
Diameter	11.86"	5.0"	15.65"	11.05"
No. of Turns	14	14	7	7
Cavity Diameter	22"		29.3"	21.25"
Cavity Depth	4.75"		6.9"	5.0"

It can be seen that the outer helix of the co-axial helix antenna is comparable in size to the receive uniform helix. Similarly the inner helix and the transmit helix are also comparable. However, the coaxial helix needs only one cavity while the uniform helixes require two. In addition, the coaxial helix needs only one set of support members for both helixes while two sets of support members are required for the two helixes. Finally,

because the uniform helixes must be mounted separately the ground mount must be more complex and heavier. The only advantage the uniform helixes antenna has over the coaxial helix antenna is that it can meet the Musat gain requirement over both frequency bands. The present coaxial helix design can meet the gain requirement in the receive frequency band but not in the transmit frequency band. However, it is hoped that further optimization of the coaxial helix antenna will improve the gain in the transmit band.

From the above considerations, the coaxial helix antenna configuration is chosen in preference to the uniform separate receive/transmit helix antenna. The SBF antenna was chosen as the second antenna for the detail mechanical study. The design of the SBF antenna differs radically from the coaxial helix design and is therefore not comparable mechanically. It is however possible to consider the relative cost and weight of the two designs. The weight specification calls for an antenna of 25 to 30 lbs. Both the coaxial helix and SBF antennas are able to satisfy this requirement (28.8 and 28 lbs. respectively). A detail analysis of the cost is given in appendix II. The simplified breakdown of cost given in table 8.2 below shows how the difference in design affect the cost.

Table 8.2 Comparison of Unit Cost (for Qty. 100) between the Co-axial Helix and SBF Antenna

	Co-axial Helix Ant.	SBF Antenna
Tripod	$ 300.00	$ 220.00
Reflector	160.00	1000.00
Feed	440.00	220.00
Total	900.00	1440.00

It can be seen that the cost of the co-axial helix antenna at $900 is significantly cheaper than that for the SBF antenna at $1440.00 This is due mainly to the high cost of the reflector in the SBF antenna. The reflector is expensive because of its size and the difficulty inherent in fabricating the foldable mesh surface.

9.0 SYSTEM DETAILS OF RECOMMENDED ANTENNAS

The antenna details given below represent the results of the studies carried out on the coaxial and SBF antennas. The data given are representive of what an actual full size optimized antenna would be. However, since further optimization studies are required for both systems the details of an actual production antenna may differ to some extent from those shown below.

9.1 CO-AXIAL HELIX ANTENNA SYSTEM DETAILS

Drawing WSK 439 shows design details of the co-axial helix and includes all dimensions. The major system parameters are summarized in table 9.1 below.

Table 9.1 Co-axial Helix Antenna Design

Outer Helix	-	
Diameter	-	11.9"
Length	-	7'3"
No. of turns	-	14
Inner Helix		
Diameter	-	5.0"
Length	-	7'3"
No. of turns	-	14
Cavity		
Width	-	23½"
Length	-	23½"
Depth	-	4 3/4"
Total Antenna Weight	-	28.8 lbs.
Total selling price/unit (for qty. 100)	-	900.00
PACKAGE SIZE	-	33"x24"x11"

9.2 SHORT BACK-FIRE ANTENNA SYSTEM DETAILS

Drawing WSK 430 shows the design details of the SBF antenna and includes all dimensions. The major system parameters are summarized in table 9.2 below.

Table 9.2 Short Back-Fire Antenna Design

Cavity		
Depth	-	26"
Diameter	-	72"
Secondary Reflector		
Diameter	-	18"
Height above Cavity	-	20"
Dipole		
Length	-	18"
Height above Cavity	-	10"
Total weight of antenna	-	28 lbs.
Total Selling price/unit (for Qty. 100)	-	$1400.00
Package Size	-	37"x13" diameter

10.0 CONCLUSION

The objective of this study was to evaluate all possible antenna configurations for an antenna suitable for use as part of a portable ground station for the proposed Multi-Purpose UHF Satellite. The main requirement is for a circularly polarized antenna with 13 dBic gain over the receive band (274-290 MHz) and the transmit band (370-400 MHz) which are widely separated. Mechanically the antenna has to be lightweight (< 30 lbs) and be capable of being packed into a man-portable package.

The review of fifteen possible candidate antennas showed that only a few configurations can meet the MUSAT requirements. The three most promising configurations were found to be a new co-axial helix antenna developed during the study contract, a SBF antenna and an antenna using separate receive/transmit uniform helixes.
Experimental results obtained for each of the three configurations indicate that they are all potentially capable of meeting the electrical requirements. However, the limited time span of the project did not allow the development of optimized versions of each configuration. Based on the electrical measurements, detail mechanical designs were developed for the coaxial helix and the SBF antennas. These designs showed that each of the antenna configurations is capable of meeting the weight and portability requirements. However, it was also shown that the SBF antenna was more complex mechanically. This is reflected in the higher price estimated for the SBF antenna at $1,400. compared to the co-axial helix antenna at $900.

The co-axial helix antenna is therefore the preferred antenna from the mechanical point of view.

The co-axial helix antenna which is a new configuration was proposed and developed to overcome the short comings found in the existing configurations studied. Because of the limited time span and scope of the study, it did not prove possible to fully develop. However, results obtained so far indicate that it is capable of operating over both receive and transmit frequency bands. They also indicate that the co-axial helix is potentially the best choice for the MUSAT application. Once the

10.0 CONCLUSION (Cont'd)

antenna configuration is fully developed it should also find applications in many other UHF antenna systems. It is therefore recommended that the coaxial helix antenna be further developed to produce an antenna suitable for the MUSAT application.

11.0 References: -

1. Angelakos, D.J. and Kajfez, D. - "Modifications on the Axial-Mode Helical Antenna, "Proc. IEEE, Vol. 55, No. 4, April 1967; pp. 558-559.

2. Bailey, A.B. - "TV and Other Receiving Antenna," John Francis Rider, Publisher, Inc., New York, 1950.

3. Bojsen, J.H., et. al. - "Maximum gain of Yagi-Uda Arrays", Electron. Lett., vol. 7, pp. 531 - 532, Sept. 1971.

4. Breetz, L.D. - "A Circularly Polarized Yagi Antenna System for NTS-1 and NTS-2 Ground Stations" - Naval Research Lab. Washington.

5. Du Hamel, R.H., and Berry, E.G. - "Logarithmically Periodic Antenna Arrays", IRE Wescon Convetion Record, 1958, Part I, pages 161-177.

6. Ehrenspeck, H.W. - "Short-Backfire Antenna", U.S. Patent, No. 3438043, Apr. 1969 U.S. Patent No. 3508278, Apr. 1970.

7. Ehrenspeck, H.W. - "A New Class of Medium Size High-Efficiency Reflector Antennas" - IEEE Trans. AP-22, PP. 329-332, Mar. 1974.

8. Ehrenspeck, H.W., "The Short-Backfire Antenna", Proc IEEE Vol. 53, Aug. 1965, pp. 1138-1140.

9. Fishenden, R.M. and Wiblin, E.R. - "Design of Yagi Aerials", Proc. IEE (London), pt. III, vol. 96, p. 5, 1949.

10. Gibson, G.A., et. al. - "Analysis of the Short-Backfire Antenna, AP-S Symposium 1976, pp.229-232.

11. Haas, H.W. and Johnson, G.E. - "A ground based right circularly polarized tri-helix telemetry antenna array", New Mexico University Report NASA C70711,1963.

12. Harris, E.F. - "Helical Beam Antenna Performance", - Comm. Eng. July-Aug. 1953.

13. Hartmann, G.K. and Engelhardt, W. - "Dispersion Measurements of One-Element Shor Backfire (SBF) Antennas", IEEE Trans Antennas Propagation, Vol. AP-23, Mar 1975, pp. 289-293.

14. Hong, M.H. et. al. - "Radiation fields of open-cavity radiators and a backfire antenna," IEEE Trans Antennas Propagation, vol. AP-18, Nov. 1970 pp.813-815.

15. Isbell, D.E., "Log Periodic Dipole Arrays", IRE Transactions on Antennas and Propagation, May 1960, pages 260-267.

16. Isbell, D.E. - "A Log-Periodic Reflector Feed", Proc. IRE, pp. 1152, June,1959.

17. Jasik, H. - "Antenna Engineering Handbook"McGraw-Hill, New York.

18. Johnson, E.O. and Kalor, R.F. - "Practical TV Antennas for UHF", RCA Victor Division, Home Instrument Dept., Advanced Development Section, Camden, N.J.

19. Keeping, K.J. and Sureau, J.C. - "Low Cost Stripline Medium and its Application", AP-S Symposium 1977, pg. 96-99.

20. King, H.E. and Wong, J.L. - 240-400 MHz. Antenna System for the Fleetsatcom Satellites" - AP-S Symposium 1977, pp.349-352.

21. King H.E. and Wong, J.L. - "Characteristics of 5 to 35 - Turn Uniform Helical Antennas". Nerospace Corp, Samso-TR-77-200, 1977.

22. Kluge, J.E. - "Advanced Antenna Design and an Ultralow-Noise Preamplifier Extend UHF Viewing Area" - IEEE Trans. BC-23, pp. 17-22, March 1977.

23. Kraus, J.D. - "The Helical Antenna", Proc. IRE, vol 37, no. 3, pp. 263-272, March, 1949.

24. Kraus, J.D. - "Antennas", McGraw-Hill Book Co., 1950; Ch. 7

25. Loh, S.C. and Leung, W.L. - "The radiation field of the short-backfire antenna", Radio & Electronk Engr. vol. 39, 1970, no. 198-200.

26. MacLean, T.S. and Kouyoumjian, R.G. - "The Bandwidth of Helical Antennas," IRE Transactions on Antennas and Propagation, Vol. AP-7, Special Supplement, December 1959, pp. S379-S386.

27. Munson, R.E. and Sandford, G.G. - "Microstrip Phased Array Developed for 5 GHz. Application", AP-S Symposium 1977 pg. 72-75.

28. Murphy, E. et.al. - "Integrated Radiator Techniques Study", Rome Air Development Centre, RADC-TR-66-651, 1967.

29. Patel, D.C., "Directivity of Short Back-fire Antenna", Proc. IEEE Vol. 118, pp. 1550-1552", Short Backfire antenna far-field radiation pattern", Int'l J. Electron, Vol. 30, 1971, pp. 185-187.

30. Picguenard, A. - "Radio Wave Propagation", MacMillan Press Limited, 1974.

31. Reed, H.R. and Russell, C.M. - "Ultra High Frequency Propagation", - John Wiley Inc. 1953.

32. Reid, P.G. - "The Gain of an Idealized Yagi Array", J. IEE (London), pt. IIIA, vol. 93, p. 564-1946.

33. Shen, L.C. - "Directivity and bandwidth of single-band and double-band Yagi arrays", IEEE Trans. Antennas Propagat. (Commun.), vol. AP-20, pp.778-780 II, Nov. 1972.

34. Snyder, R.E. - "Receiving System Design using Active Antennas" - Adams-Russell Co. Application Note. No. 1 February 1974.

35. Uda, S. and Mushiake, Y. - Yagi-Uda Antenna", chaps. 7, 8 Sasaki Printing and Publishing Co. Ltd., Sendai, Japan, 1954.

36. Wong, J.L. and King, H.E. - "Broadband Quasi-Taper Helical Antennas", The Aerospace Corporation, Electronics Research Laboratory, Technical report

37. Wong, J.L. and King, H.E. - "A Technique for broadband gain-pattern synthesis of Helical Antnnas", AP-S Symposium 1977, pp. 234-237.

38. Wong, J.Y. and Loh, S.C. - "Radiation Field of An Elliptical Helical Antenna", IRE Trans. AP-7., pp. 46-52 January 1959.

39. Yagi, H. - "Beam Transmission of Ultra Short Waves," Proc. IRE, vol. 16, pp. 715-741, June, 1928.

APPENDIX I EFFECTS OF MULTIPATH ON FINAL ANTENNA SYSTEMS

A1.1 REVIEW OF MULTIPATH EFFECTS

Only a very brief review of multipath effects on the antenna will be given here since a detail treatment of the subject is given in standard texts such as Reed (31).

Figure A1.1 showsthe three main sources of multipath signals that can arrive at the antenna. The multipath signals can either add or subtract from the direct signal depending on the relative phase. This variation in signal strength and the way it affects the output of the antenna is the main factor of multipath propagation considered here. To determine completely the effect of multipath at any site requires the use of a combination of ray theory, wave or diffraction theory as well as actual measurements.

One multipath source is reflection from a reflecting object such as a building. The interfering signal can be strong if the object is a good reflector and is placed such that a reflected ray arrives at the antenna (see figure A1.1). Moving the antenna away from such a reflected ray is one method of minimizing the effect. If this is not possible, the effect of such obstructions can be calculated for a fixed site using a method similar to that given in Section A1.2.

When a ray illuminates an irregular object Snell's law of reflection no longer applies. As shown in figure A1.1 the energy is scattered in all directions. Some of this diffraction field arrives at the antenna as a multipath signal. However, unless there are many such scatterers close to the antenna the fields would be small compared with the direct field.

The third source of multipath is ground reflection which is generally significant for UHF antennas. Unlike reflection from obstructions the reflection cannot be reduced by moving the antenna horizontally if the ground is flat and level. However, it is possible to maximize signal strength by moving the antenna vertically.

A prediction of signal strength expected for different antenna heights can be used to select the optimum height for the antenna. This Appendix describes a method that can be used for such a prediction. The model used assumes plane

A1.1 REVIEW OF MULTIPATH EFFECTS (Cont'd)

wave reflection from the ground. It assumes that the wave arriving from the source is a plane wave (ie. rays are parallel with no divergence). This is true for signals from a satellite. It also assumes a flat (as opposed to a spherical) ground. This is again true since the actual point of reflection is only a maximum of 15'-20' away.

For plane wave reflection the minimum grazing angle, ψ_{min}, must be

$$\psi_{min} = \left(\frac{\lambda}{\frac{8\pi a}{3}} \right)^{1/3}$$

where

a = terrestrial radius, and

λ = free space wavelength.

At the receive frequency, ψ_{min} is approximately 0.17^{o}. Since the lowest grazing angle is 5^{o}, reflection theory applies.

Plane wave reflection assumes a smooth surface which may not be true in practice. The test used to determine the required surface smoothness is the Rayleigh criterion. This gives the maximum allowable height of obstacles as

$$h_{max} = \frac{\lambda}{16 \sin \psi} \quad \text{where}$$

ψ is the grazing angle. It is shown in Section A1.3 that the lowest grazing angle of 5^{o} is also the most critical with regards to reflection. This gives h_{max} = 30" and 22" at the receive and transmit bands respectively. For surface roughness greater than the above plane wave reflection no longer applies. The reflected energy becomes more diffused. This however means that the multipath signal becomes weaker and hence it has less effect on the intrinsic antenna gain.

Of the three modes of multipath reviewed only the ground reflection ray can be analyzed in a systematic way. Since the sites on which the antenna will be used are random, only the ground reflection effects will be considered here. This however covers the majority of the cases for this antenna since the requirement is only for a reasonably clear ground 15 to 20 feet in front of the antenna. Reflections from large obstructions further away can usually be avoided by sitting the antenna away from signal nulls caused by such reflections.

A1.1 REVIEW OF MULTIPATH EFFECTS (Cont'd)

Results presented in section A1.3, which are based on the model described in section A1.2, are therefore useful in predicting multipath effects for the antenna system.

A1.2 SYSTEM MODEL

This section describes the model used to calculate the effect of ground reflection on the circularly polarized antenna described in this report. It is necessary to predict the magnitude and phase of a ray reflected from the ground. Figure A1.2 shows the way a ray representing the signal from a distant source is reflected and refracted at a dielectric/air interface. The magnitude of the reflected ray is given for horizontal polarization by: -

$$|R_h| e^{j\phi_h} = \frac{\sin\psi - \sqrt{n^2 - \cos^2\psi}}{\sin\psi + \sqrt{(n^2 - \cos^2\psi)}} \quad \text{- A1.1}$$

and for vertical polarization by:

$$|R_V| e^{j\phi_V} = \frac{n^2 \sin\psi - \sqrt{n^2 - \cos^2\psi}}{n^2 \sin\psi + \sqrt{(n^2 - \cos^2\psi)}} \quad \text{- A1.2}$$

R_h = magnitude of the reflection coefficient for vertical polarization

R_V = magnitude of the reflection coefficient for horizontal polarization.

ϕ_h = phase of reflected ray for horizontal polarization

ϕ_v = phase of reflected ray for vertical polarization

ψ = glazing angle

n is the refractive index of the ground which is complex and can be calculated by

$$n^2 = \epsilon_r - j\,60\,\sigma\lambda \quad \text{- A1.3}$$

ϵ_r = relative permittivity of the ground

σ = conductance of the ground

λ = free space wavelength

The values of ϵ_r and σ vary greatly with ground conditions as well as frequencies. Typical values for UHF frequencies are shown in table A1.1 below.

TABLE A1.1 TYPICAL VALUES FOR ϵ_r AND σ

Material	ϵ_r	σ (mho-m/sq. m)
Sea water	80	3 - 5
Fresh water	80	10^{-2} - 10^{-3}
Marsh land	5 - 30	10^{-1} - 10^{-3}
Dry land	2 - 5	10^{-4} - 10^{-5}
Average land	15	0.028

Actual values used in the calculations (shown in each graph) are typical values for the frequency.

Figure A1.4 and A1.5 show both the magnitude and phase of the reflected ray calculated using A1.1 and A1.2 for average soil at the receive and transmit frequency.

The way a signal is received from a satellite by an earth station antenna is shown in figure A1.3. Here it is assumed that the antenna is placed at a height h and receives a direct ray at angle θ as well as a reflected ray as shown.

It can be shown that the difference in path length is $2h \sin \theta$. The reflected ray is given by $E_d R e^{j\phi}$. The direct ray is received on the boresight of the antenna. However the reflected ray is received at an angle of 2θ so that its magnitude is less. The amplitude and phase of the resultant is given by

$$\text{Amplitude } E^2 = E_x^2 + E_y^2 \quad \text{A1.4}$$

$$\text{Phase } \beta = \tan^{-1}\left(\frac{E_y}{E_x}\right) \quad \text{A1.5}$$

where

$E_x = E_d \left(1 + R \cos (2h \sin \theta + \phi) \times F(2\theta) \right)$

$E_y = E_d R \sin (2h \sin \theta + \phi) \times F(2\theta)$

$F(2\theta)$ = pattern factor of the antenna at angle 2θ

R and ϕ are obtained from either equation A1.1 or A1.2 (horizontal or vertical)

The circularly polarized incoming wave can be resolved into two equal components one vertical and the other horizontal. They differ in time phase by 90^0. Each of these components can be treated separately. By using equations A1.4 and A1.5 the resultant vertical and horizontal components (E_v, β_v, E_h and β_h) can be obtained.

This can be recombined into an elliptically polarized wave with axial ratio and tilt angle given by

$$\text{Axial Ratio AR} = \sqrt{\frac{-\gamma + (\gamma^2 - 4)^{1/2}}{2}} \quad - \quad \text{A1.6}$$

$$\text{Tilt Angle } \tau = \tfrac{1}{2} \tan^{-1} \left[\frac{2 E_v E_h \cos (90 + \phi_v - \phi_h)}{E_v^2 - E_h^2} \right] \quad - \quad \text{A1.7}$$

$$\text{where} \qquad \gamma = -\frac{(E_v/E_h)^2 + 2\cos^2(90+\phi_v-\phi_h) + (E_h/E_v)^2}{\sin^2 (90 + \phi_v - \phi_h)}$$

If the antenna has perfect circularity then the power transferred would be a constant depending only on AR and τ. However in general the antenna is elliptically polarized with an axial ratio and tilt angle of AR_a and τ_a. The power transferred is then variable depending on the relationship of τ_a and τ as well as AR_a and AR. It can be shown that the maximum and minimum power transferred is given by: -

$$P_{\substack{max \\ min}} = \frac{(AR+1)^2(AR_a+1)^2 + (AR-1)^2(AR_a-1)^2 \pm 2(AR^2-1)(AR_a^2 - 1)}{4(AR^2+1)\,(AR_a^2+1)} \quad - \text{A1.8}$$

A computer model based on equations A1.1 to A1.8 was developed to analyse the effect of multipath reflections. Results obtained using this model are given in Section A1.3.

A1.3 COMPUTED RESULTS

Presented below are results computed for the antenna system using the model of section A1.2 and typical measured patterns for the antenna. Figures A1.4 and A1.5 show the way the amplitude and phase vary for vertical and horizontal polarizations at the receive frequency for the case of average soil. That for the transmit frequency is almost identical.

Figures A1.6 - A1.9 are plots showing variation of antenna output power against the height of the antenna above the ground. The power output shown is relative to that of the antenna in free space. Thus the dotted OdBic line represents the power output of the antenna when all reflection and ground effects are eliminated. Values on the curves to the left of this OdB line indicate that the ground reflection signal is cancelling some of the direct signal. All curves represent the minimum power transfer for a receive antenna with an axial ratio of 2 dB. The maximum power transfer curves (ie when the major axes of both polarization elipses coincide) are generally 0.2 to 1.5 dBic higher.

Figures A1.6 and A1.7 give antenna outputs for average soil at the receive and transmit frequencies respectively. At each frequency curves are given for antenna elevation angles of 5^{o}, 10^{o}, 15^{o} and 20^{o}. Values for higher elevation angles are calculated but are not plotted since their variations about the OdB line are small. From figures A1.6 and A1.7 it is possible to select the best compromise height for the antenna which is 1.2m (or $\triangleq$ 4 ft.). For this height the worst case receive-loss of 0.3 dB occurs for the 5^{o} elevation angle. That for the transmit frequency is 0.8 dB at 20^{o} elevation angle. The chosen antenna height is also a convenient one for antenna elevation and azimuth adjustments. Furthermore this height places the antenna at about 1 wavelength above the ground so that the ground effect on antenna free-space impedance is small.

Figures A1.8 and A1.9 show the effect of types of ground at antenna elevation angles of 5^{o} and 15^{o} respectively. It can be seen that the variation for almost all ground types are small. Thus the curves for average ground is representive. The only exception is sea water at 5^{o} elevation angle where the signal loss is 2.6 dBic. Fortunately most water surfaces encountered in Canada are fresh water. However, in an application where sea water is present it would be advisable to increase the antenna height to 1.6 m.

S.H. Lim
Andrew Antenna Company Limited
10 January 1978.

APPENDIX II COST ESTIMATES

Results of a cost study of the proposed short back-fire and co-axial helix antennas are presented below. The study is based on data contained in drawings WSK430 (short back-fire antenna) and WSK 439 (co-axial helix). Table A2.1 gives the estimated selling price for both configurations. This includes all production cost and tooling but does not include development engineering cost.

TABLE A2.1 TOTAL ESTIMATED UNIT COST

	Co-axial Helix Ant.		S.B.F. Antenna	
	Qty 25	Qty 100	Qty 25	Qty 100
a) Material/unit	137.55	137.55	588.55	343.86
b) Labour/unit	718.06	671.57	1,175.18	960.99
c) Tooling/unit	359.39	89.85	228.60	138.84
Total Selling Price /unit	1,215.00	898.97	1,992.33	1,443.69

A detail breakdown of cost is given in tables A2.2 and A2.3.

TABLE A2.2 DETAIL COST BREAKDOWN FOR S.B.F. ANTENNA

	Qty 25	Qty 100
Tripod: Material/unit	$ 59.43	$ 59.43
Labour/unit	175.99	144.34
Total Tooling	2,037.75	2,037.75
Reflector: Material/unit	422.60	236.19
Labour/unit	823.20	653.78
Total Tooling	3,028.84	11,198.36
Feed: Material/unit	106.52	48.24
Labour/unit	175.99	162.87
Total Tooling	648.38	648.38

TABLE A2.3 DETAIL COST BREAKDOWN FOR COAXIAL HELIX ANTENNA

		Qty 25	Qty 100
Tripod:	Material/unit	$ 77.19	$ 77.19
	Labour/unit	200.69	188.34
	Total Tooling	3,797.63	3,797.63
Reflector:	Material/unit	16.21	16.21
	Labour/unit	143.57	134.31
	Total Tooling	741.00	741.00
Feed:	Material/Unit	44.15	44.15
	Labour/Unit	373.80	348.92
	Total Tooling	4,446.00	4,446.00

APPENDIX III SURVEY OF EXISTING WORK

A3.1 EXISTING ANTENNA SYSTEMS

As part of the concept study, a survey of existing antenna systems that may meet the MUSAT specifications was carried out. This included an on-line search of the United States National Technical Information Service (NTIS) data base which consists of bibliographic citations of Federally-sponsored reports dating from 1964. Revelant citations obtained as a result of the search is presented in section A3.2. The citations show that design information does exist for some of the antenna configurations considered in the study. However, none of the citations describe an antenna system with performance close to that required by the MUSAT specification. This would indicate that the present study does not duplicate any past United States Government-sponsored research. A parallel survey of the revelant technical journals and manufacturers literature confirms that no existing antenna can meet all the MUSAT requirements.

The only existing antenna system which comes close to meeting the MUSAT requirements is the non-uniform helix of Wong and King which is described in section 3.1.4. This antenna can meet all the MUSAT electrical specifications. However, since it is 151" long it would be difficult to implement a design that can meet the weight and portability requirements. The review of all candidate antennas (Section 3) describes many other existing antenna systems which are revelant to this study. These include the SBF antenna of Ehrenspeck (Section 3.2), the tri-linear antenna of Kluge (Section 3.4.2), the active Yagi of Murphy (Section 3.7) and the planar array of Munson and Sandford (Section 3.8).

A3.2 LITERATURE SURVEY

LIST OF REVELENT CITATIONS FROM AN NTIS SEARCH (MARCH 1977)

Bartlett, H.E., Lewis, B.L., Pietsch, L and Collins, G.W. - 'Study of Special Beamshaping Antennas' - Radiation Inc., Melbourne, Fla.

Bolam, P.F. & Dutton, E.J. - 'Service Test of Selected Lightweight Avionic Equipment (SLAE)' - Army Aviation Test Board Fort Rucker, Ala.

Bothe, H - 'Short Helical Antennas with Exact Circular Polarization Behavior by a Conducting Disc at the End of the Helix' - Brunswick University (West Germany) - Deutsche Forschungs.

Coleman, R.J., Graf, E.R. & Roberts, S.B. - 'A Proposal for a Circularly Polarized Tracking Antenna and Its Evaluation Technical Report No. 1' - Auburn Univ., Ala.

Dudgeon, J.E. - 'Phased Array Antenna Matching Simulation and Optimization of a Planar Phased Array of Circular Waveguide Elements' - Alabama Univ.

Ehrenspeck, H.W. - 'High-Gain UHF Backfire Antenna for Communications, Telemetry, and Radio Astronomy' - Air Force Cambridge Research Labs.

Finneran, R.J. - 'Anna IB Satellite Data for Days 115 through 122' - Johns Hopkins Univ.

Goebel, W. - 'Utilization of Simple Omnidirectional VHF Antennas on Board of ships for Satellite Reception by Eliminating the Multipath Effects through a Diversity System' - Deutsche Forschungs - Und Versuchsanstalt Fuer Luft-Und Raumfahrt, Oberpfaffenhofen (West Germany).

Gohlke, C. & Lerner, T. - 'AN/TRC-104 (XW-1) Lightweight Troposcatter Radio Set' - Bell Aerosystems Co.

Goodwin, R.C. - 'A Study of Tactical Communications Problems' - Laboratory for Electronics Inc. Boston.

Gouillon, R. & Ringenback, G. - 'The A.C.H. Short Helical Antenna and its Applications' - Office National D Etudes et de Recherches Aerospatiales, Paris (France).

Graf, E.R. - 'Receiver Antennas for Application in a Television Broadcast Relay System' - Auburn Univ. Ala.

Harrison, M.G. & Kajfez, D. - 'Experimental Investigation of the Tripole Antenna' -Mississippi Univ.

Herman, J.E., Rhee, S.B., Rasswejen, G.G., Simanyi, A.I. - 'Study and Investigation of a UHF-VHF Antenna' - Radiation Lab Univ. of Michigan.

Lemson, P.H. - 'Broadband Modified Turnstile Antenna Patent Application' -National Aeronautics and Space Administration.

Maillowx, R.J. & Van Atta, L.C. - 'A Circularly Polarized Antenna' - National Aeronautics and Space Administration.

New Mexico State Univesity - 'A Ground based right circularly polarized Tri-Helix Telemetry Antenna Array for the 225 to 250 MC/SEC Frequency Band' - New Mexico State Univ., University Park.

Pietsch, L., Moseley, R.E., Livingston, M.L. & Schopke, E.N. - 'Lightweight Antenna Techniques' - Radiation, Inc., Melbourne

Steyskal, H. - 'An Experimental Study of Coupling Effects in a Planar Array Antenna' - Research Inst. of National Defence, Stockholm (Sweden).

Strom, J.A. & Ehrenspeck, H.W. - 'An SBF Array for Reception of Atmospheric Noise' - Air Force Cambridge Research Labs.

Thomas, B.M. - 'The Log-Periodic Aerial for Measurements of Circular Polarization -Commonwealth Scientific and Industrial Research Organization Sydney (Australia).

Uryniak, A.J. -'Test and Evaluation Report on Log-Periodic Antenna Group' - Rome Air Development Centre.

Wheeler, W.R. & Schepler, K.L.-' Research in New Types of Antenna Systems for The Frequency Range 450-1150 Mc - Denver Research Inst. Colo.

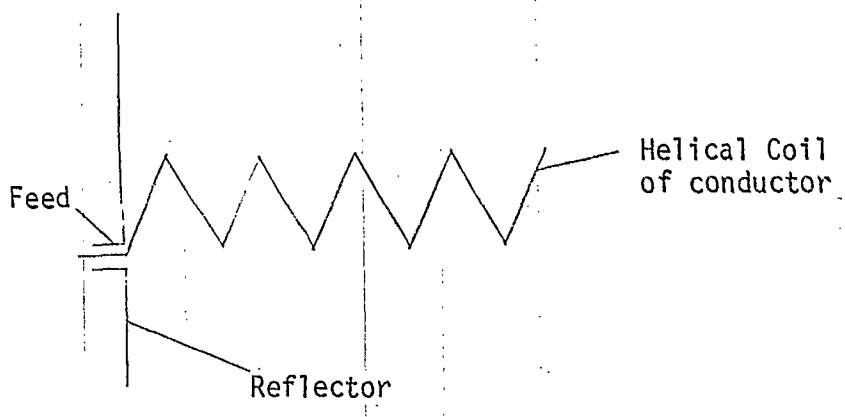

FIGURE 3.1.1 AXIAL-MODE HELIX

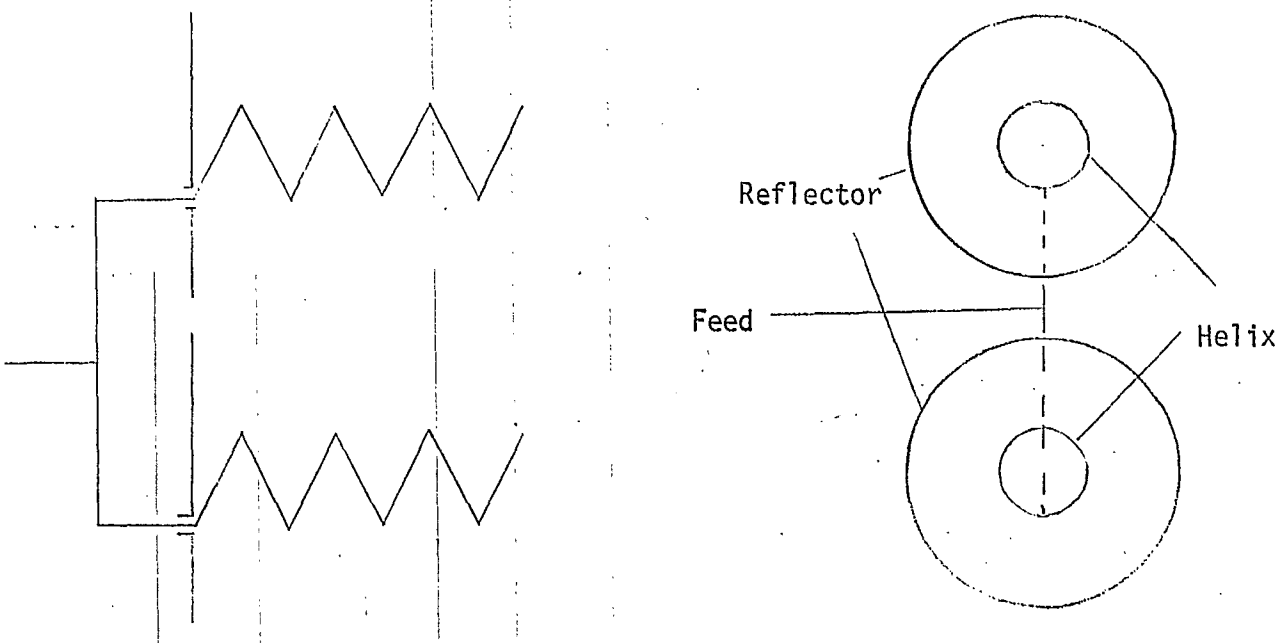

FIGURE 3.1.2 BI-HELIX

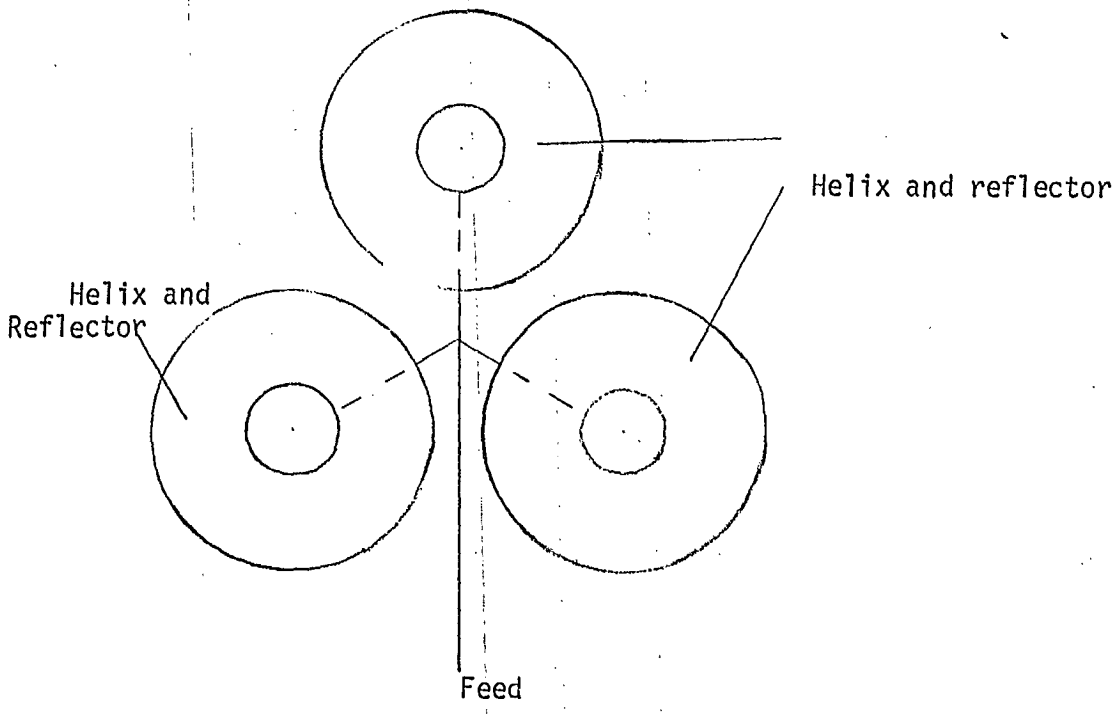

FIGURE 3.1.3 TRI-HELIX.

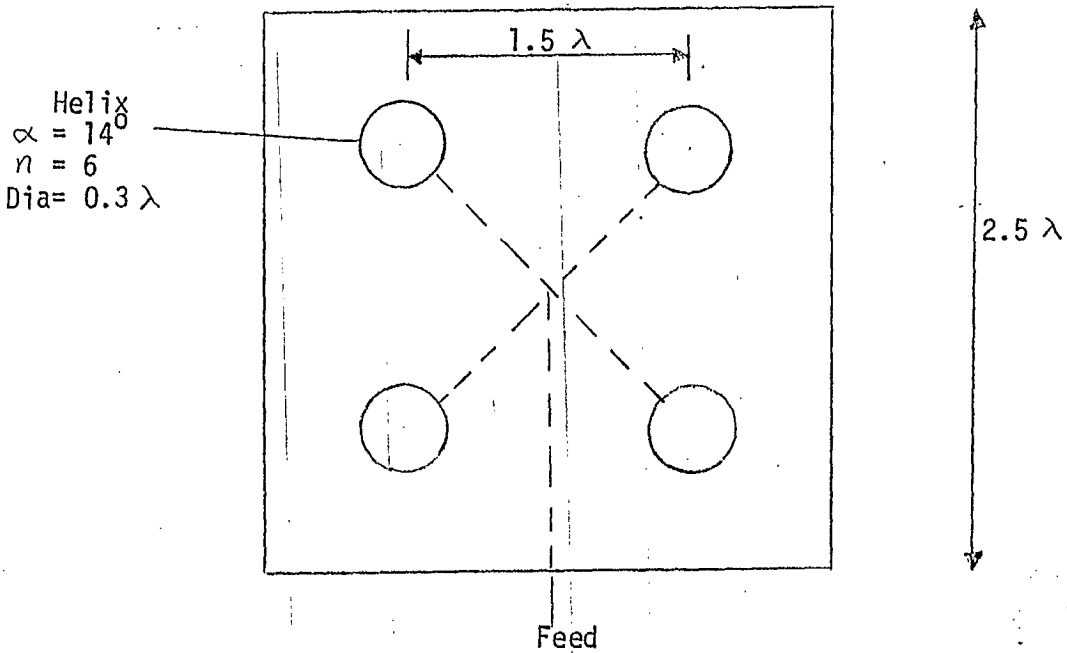

FIGURE 3.1.4 QUAD HELIX

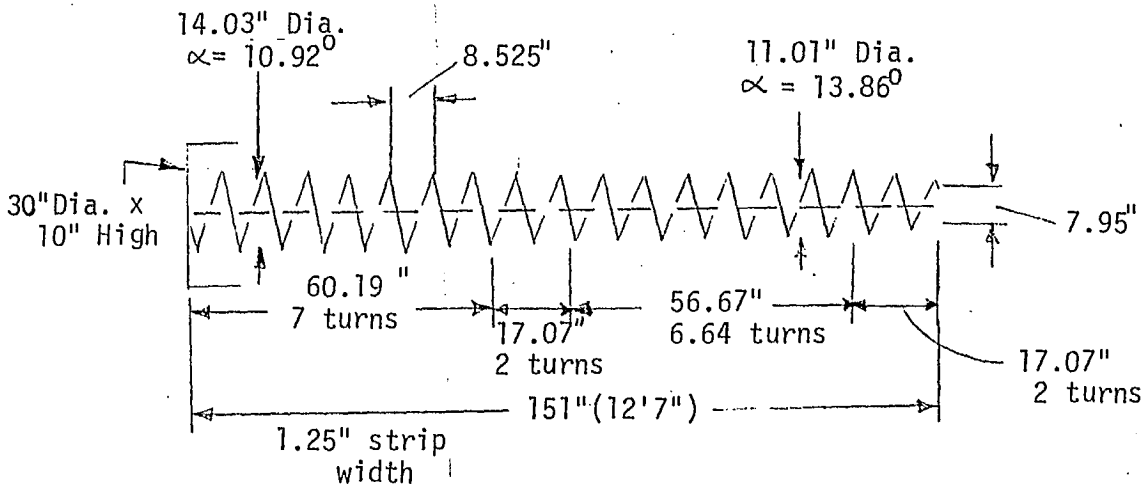

FIGURE 3.1.5 NON-UNIFORM HELIX

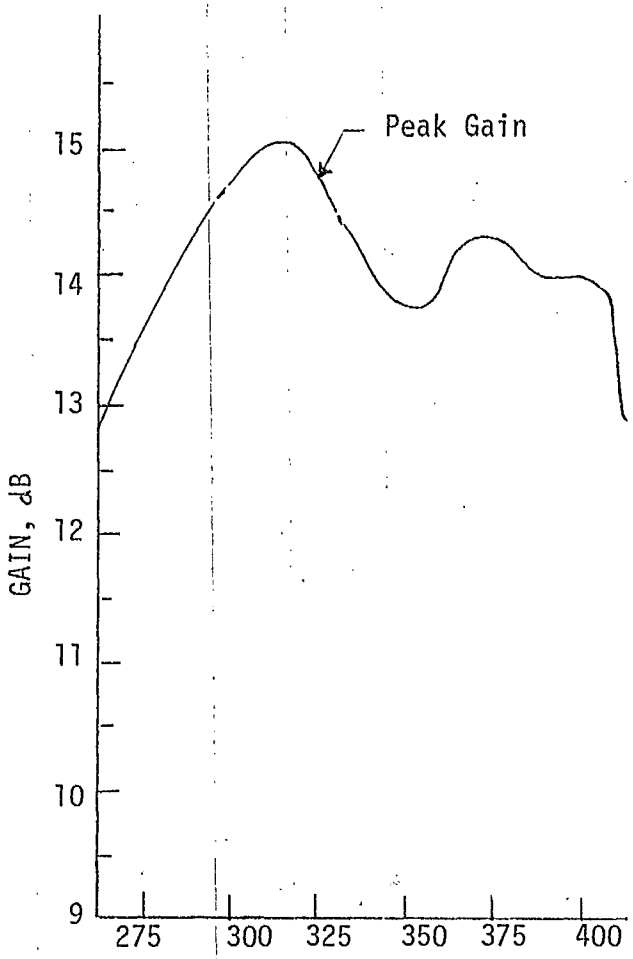

FIGURE 3.1.6 GAIN OF NON-UNIFORM HELIX

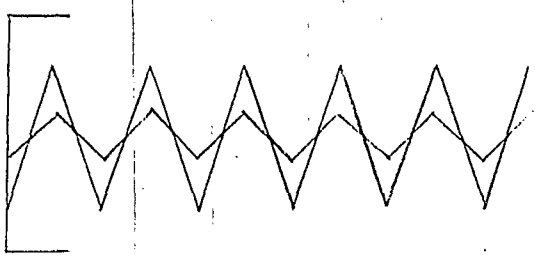

FIGURE 3.1.7 CO-AXIAL HELIX

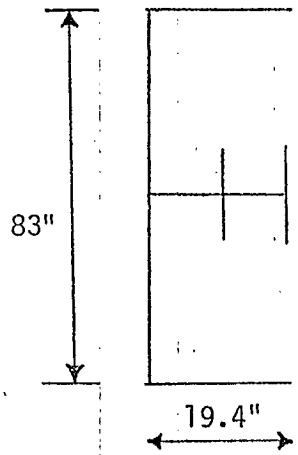

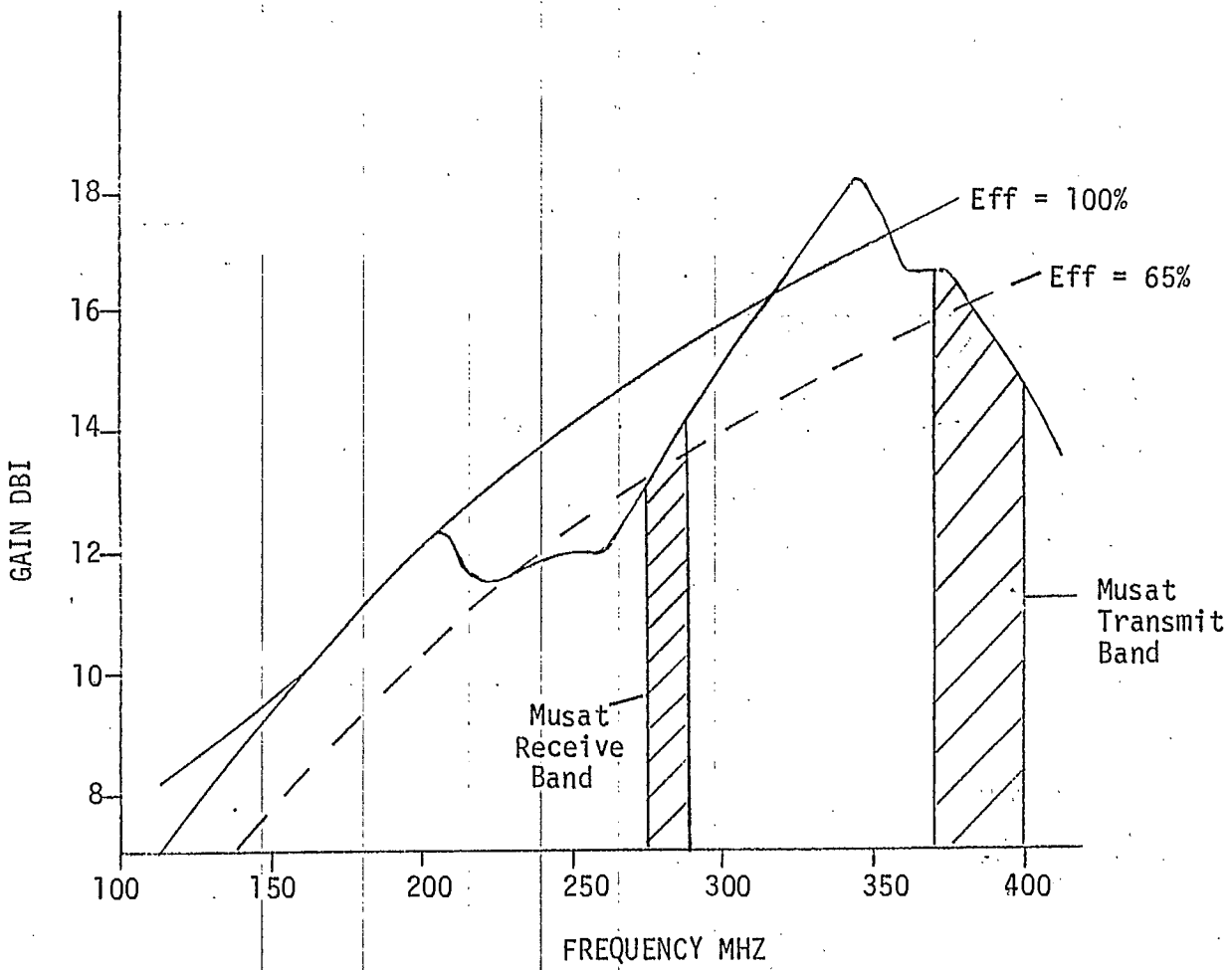

FIGURE 3.2.1 DIRECTIVE GAIN AGAINST FREQUENCY FOR S.B.F. ANTENNA

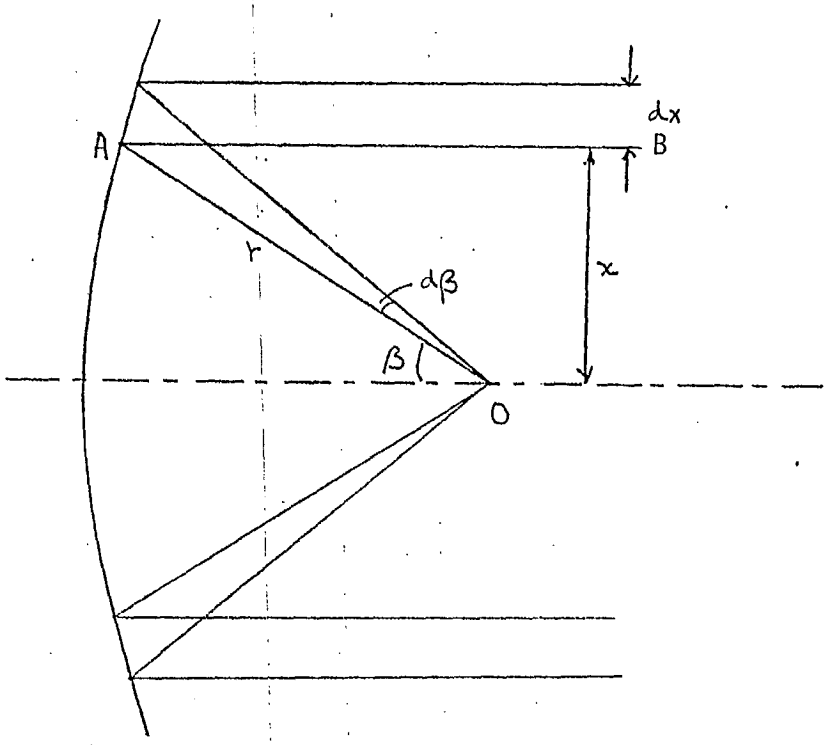

Fig. 3.3.1 Geometry for a prime focus paraboloid.

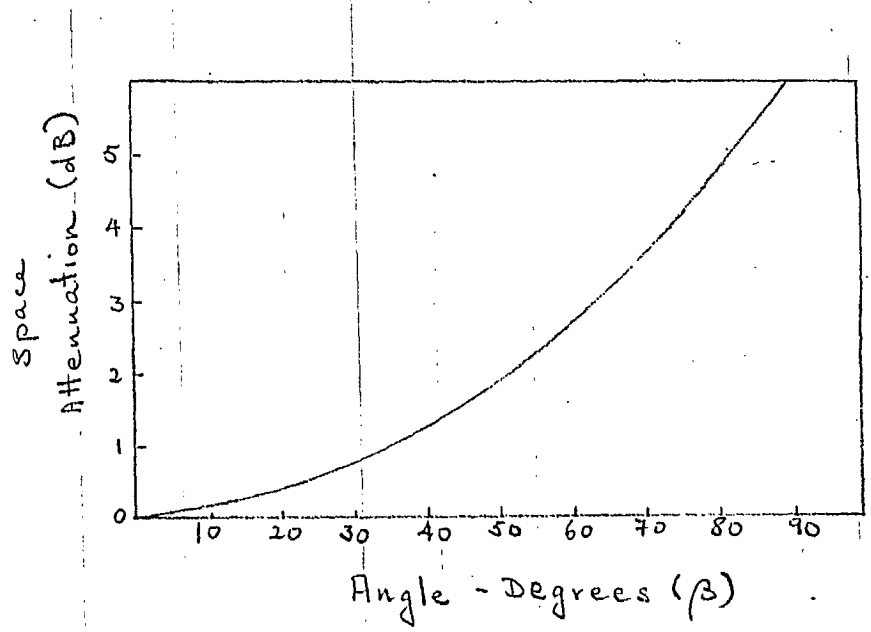

Fig. 3.3.2 Space attenuation vs feed angle for a prime feed paraboloid.

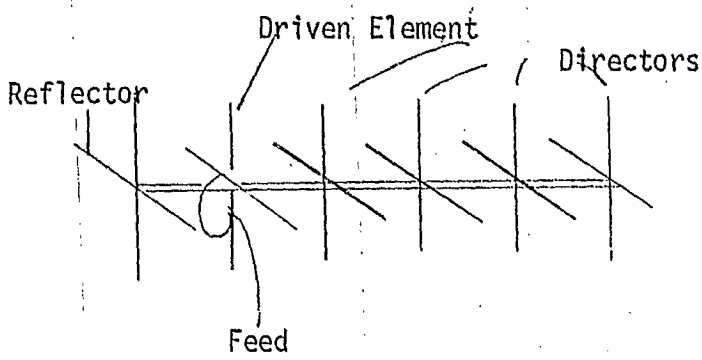

FIGURE 3.4.1 CROSS-YAGI FOR CIRCULAR POLARIZATION

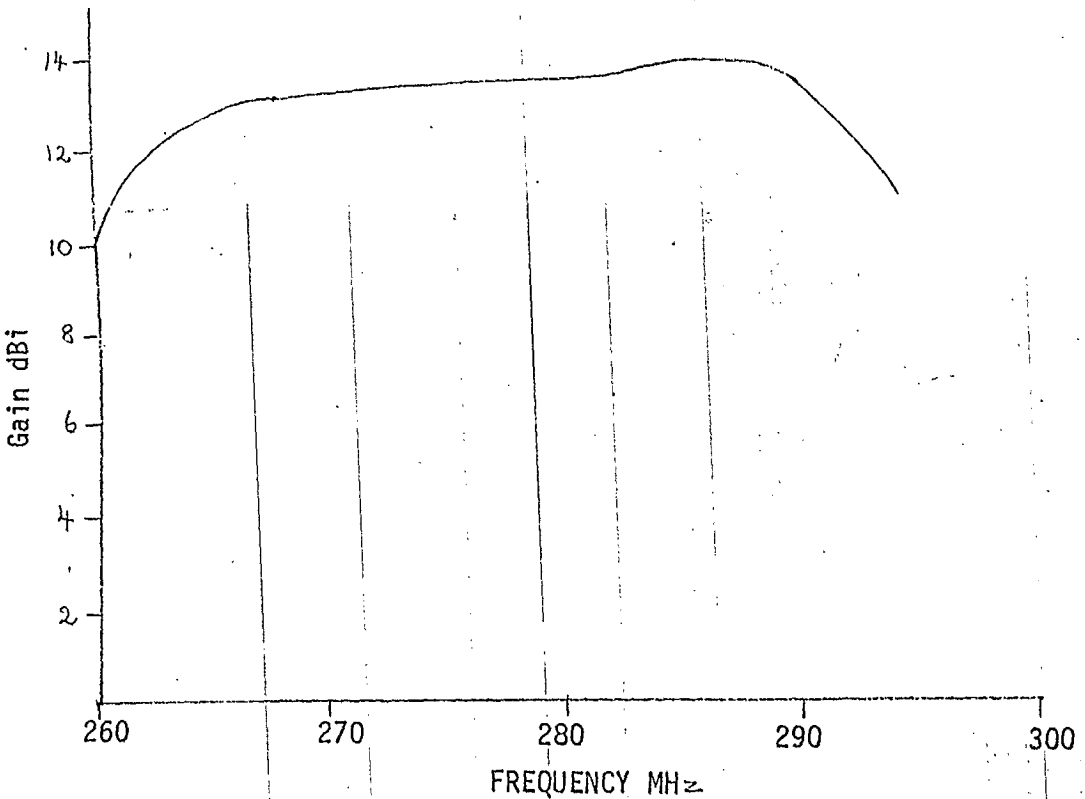

FIGURE 3.4.2 GAIN VS FREQUENCY FOR A 10-ELEMENT YAGI

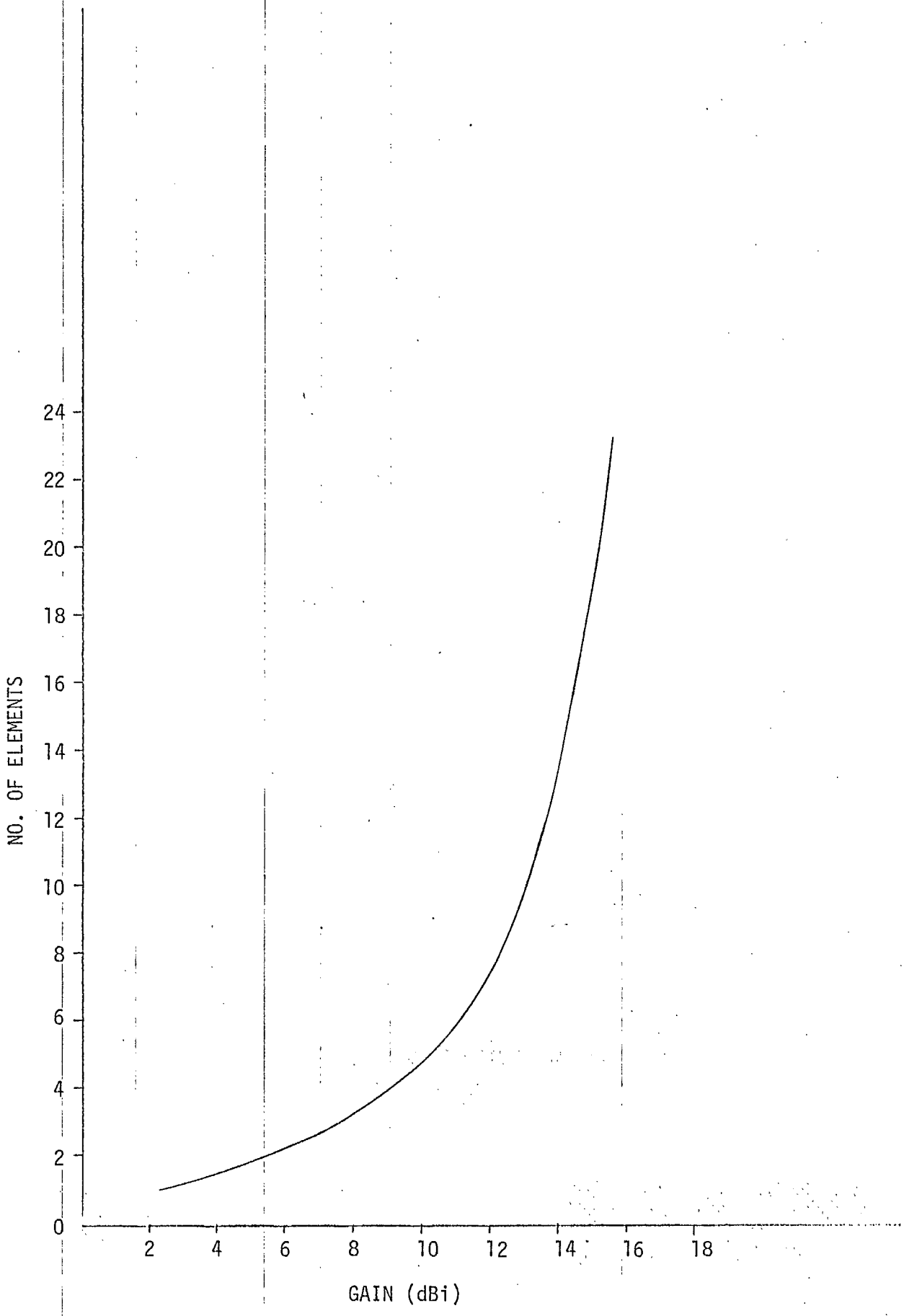

FIGURE 3.4.3 GAIN VS NO. OF ELEMENTS FOR TYPICAL YAGI ANTENNAS

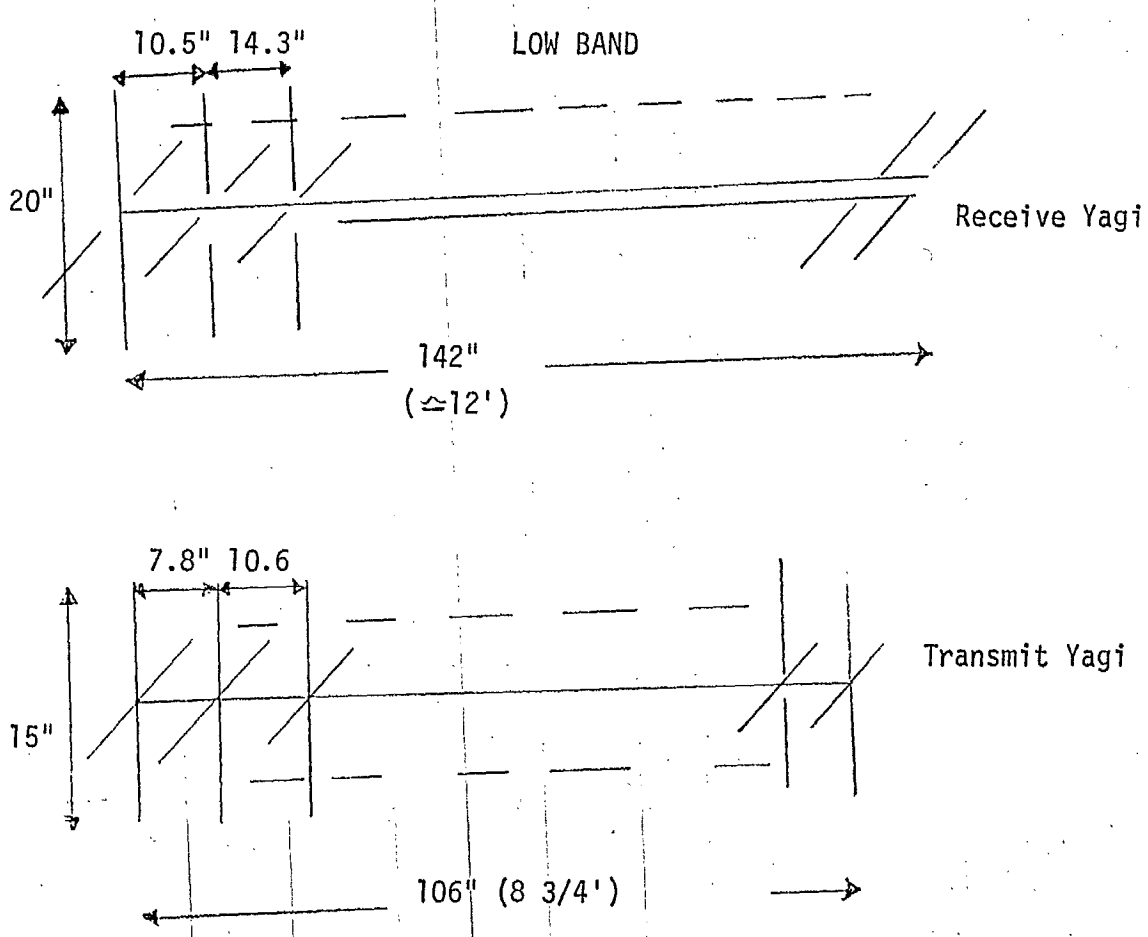

FIGURE 3.4.4 ARRAY OF RECEIVE AND TRANSMIT CROSS-YAGI ANTENNAS

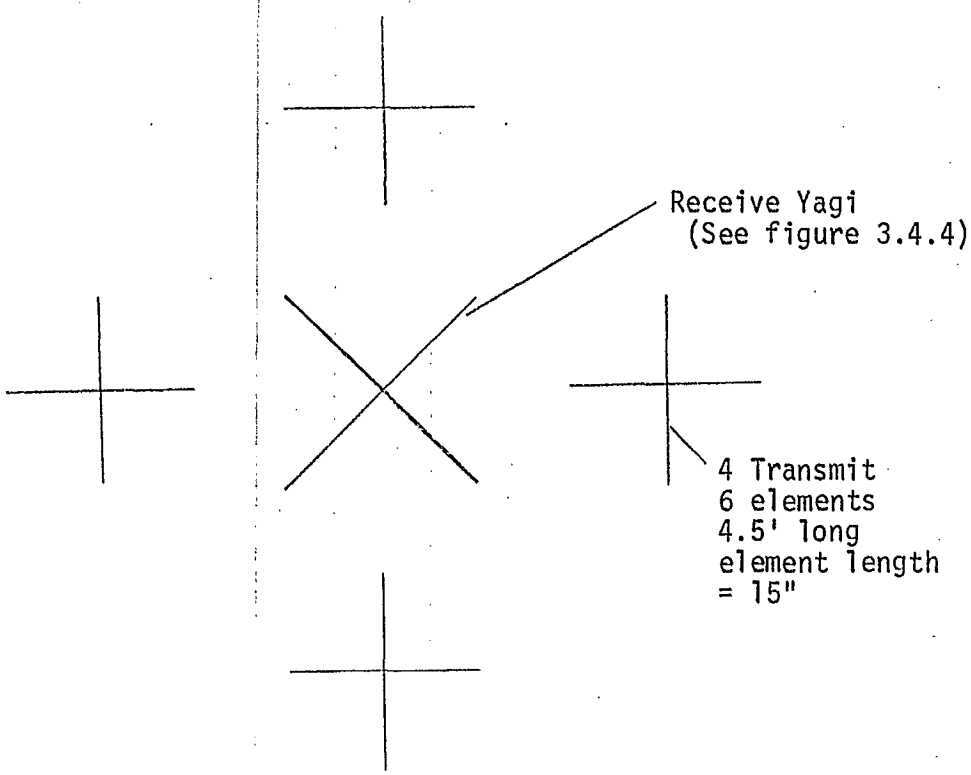

FIGURE 3.4.5 HIGH GAIN TRANSMIT ARRAY WITH RECEIVE YAGI

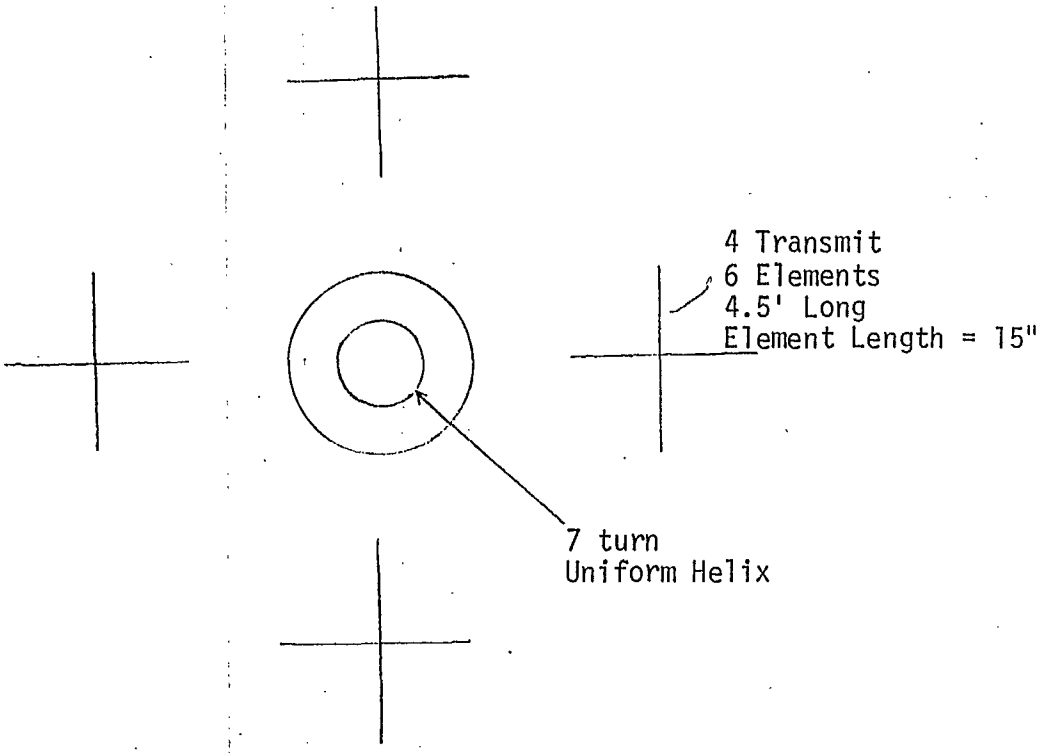

FIGURE 3.5.1 COMPOSITE HELICAL/YAGI ARRAY

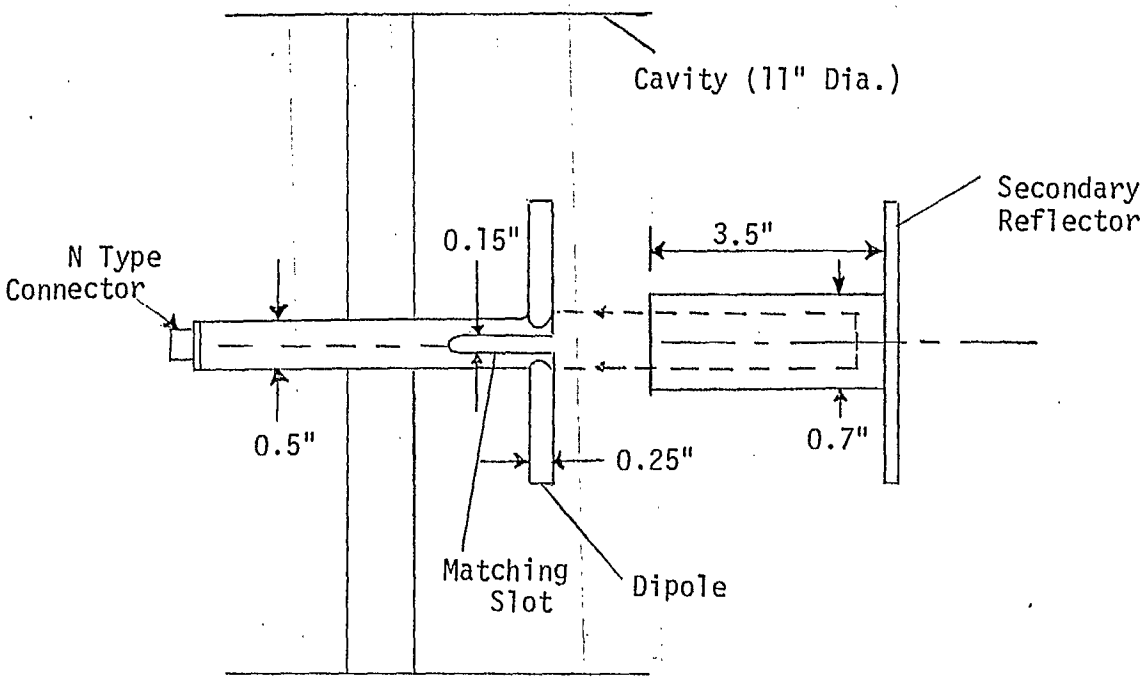

FIGURE 5.2.1 SBF ANTENNA MODEL

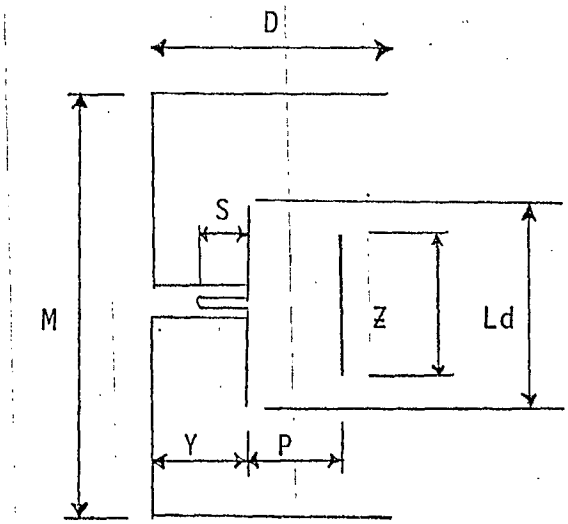

FIGURE 5.2.2 SBF ANTENNA DIMENSIONS

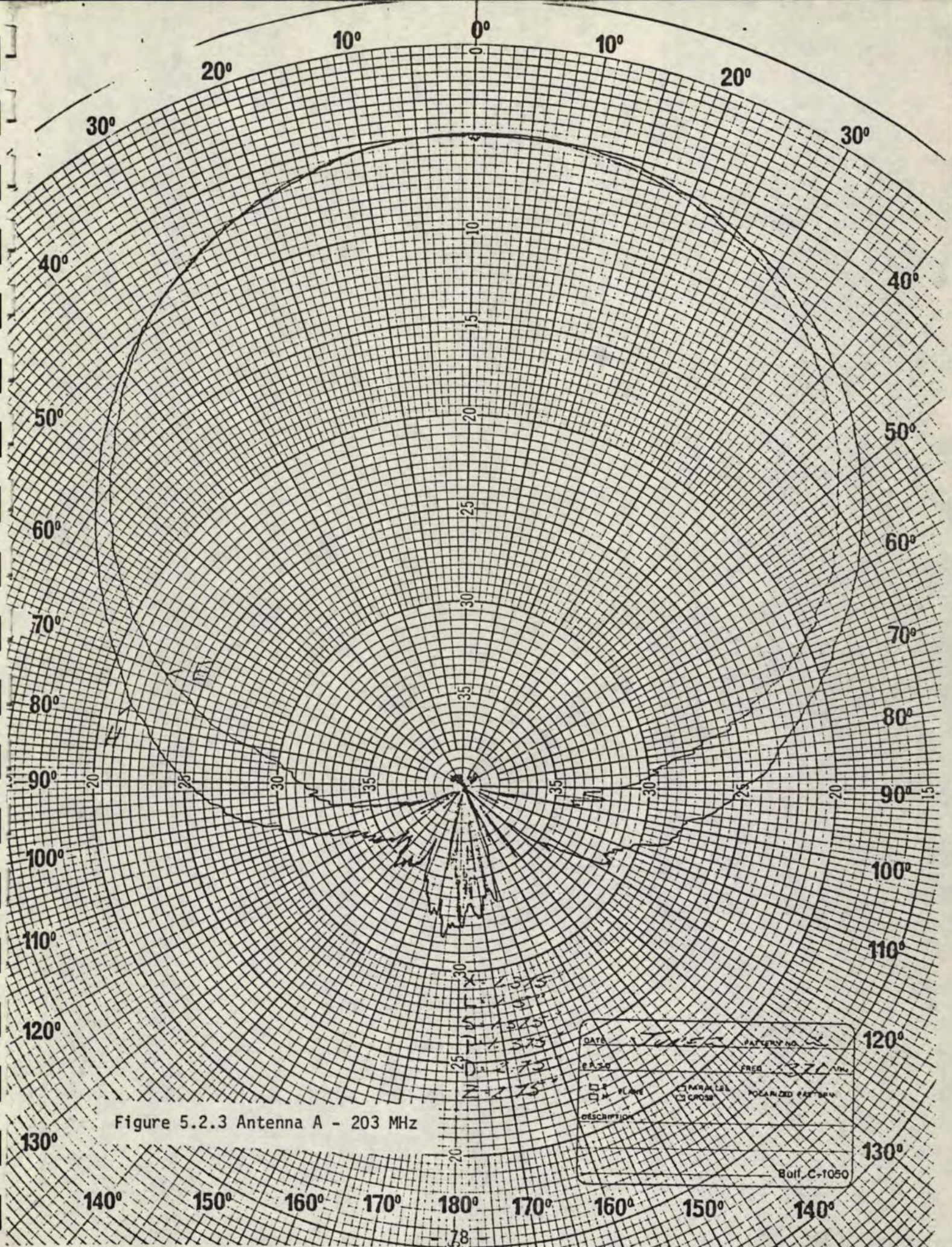

Figure 5.2.3 Antenna A - 203 MHz

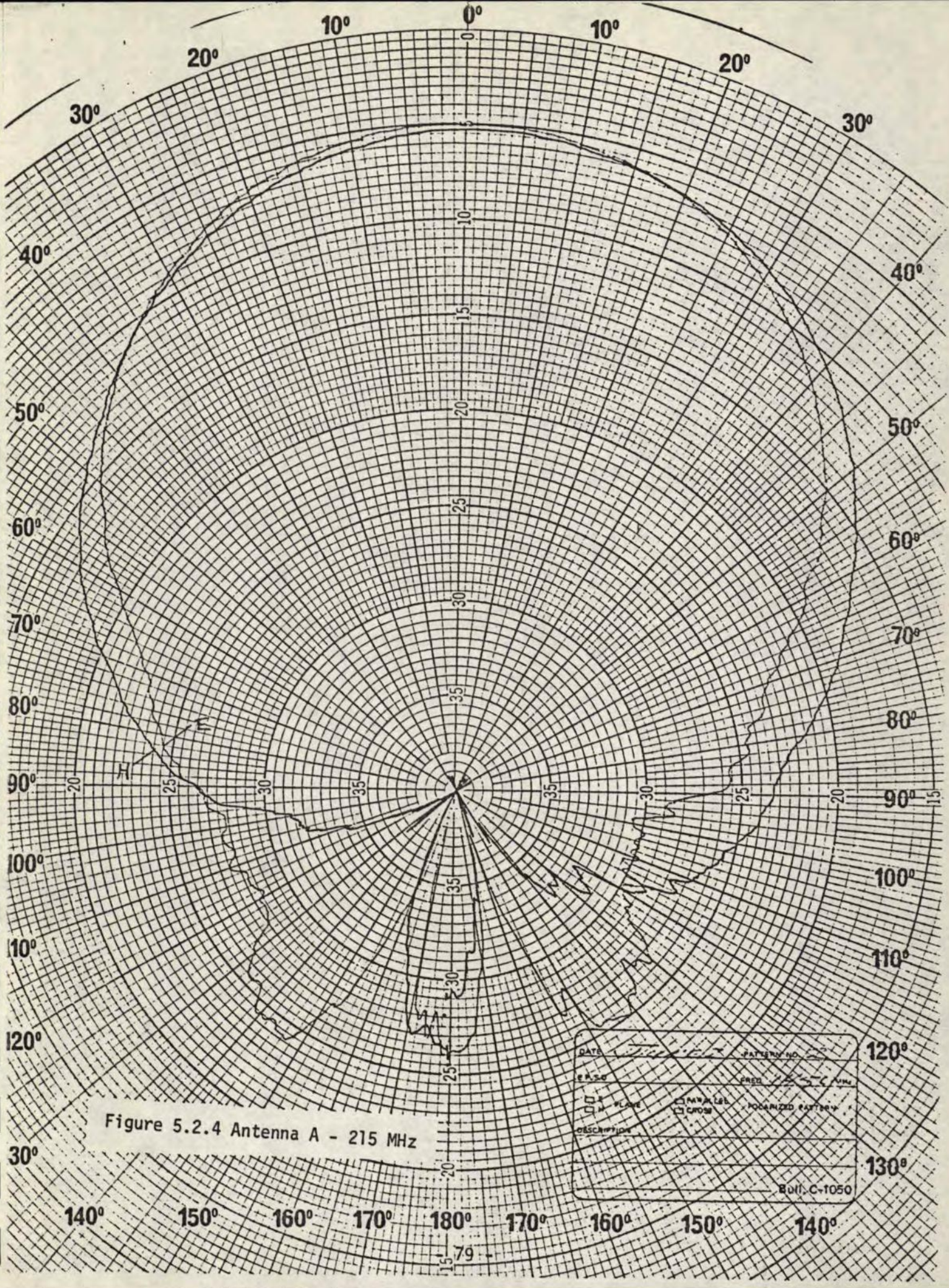

Figure 5.2.4 Antenna A - 215 MHz

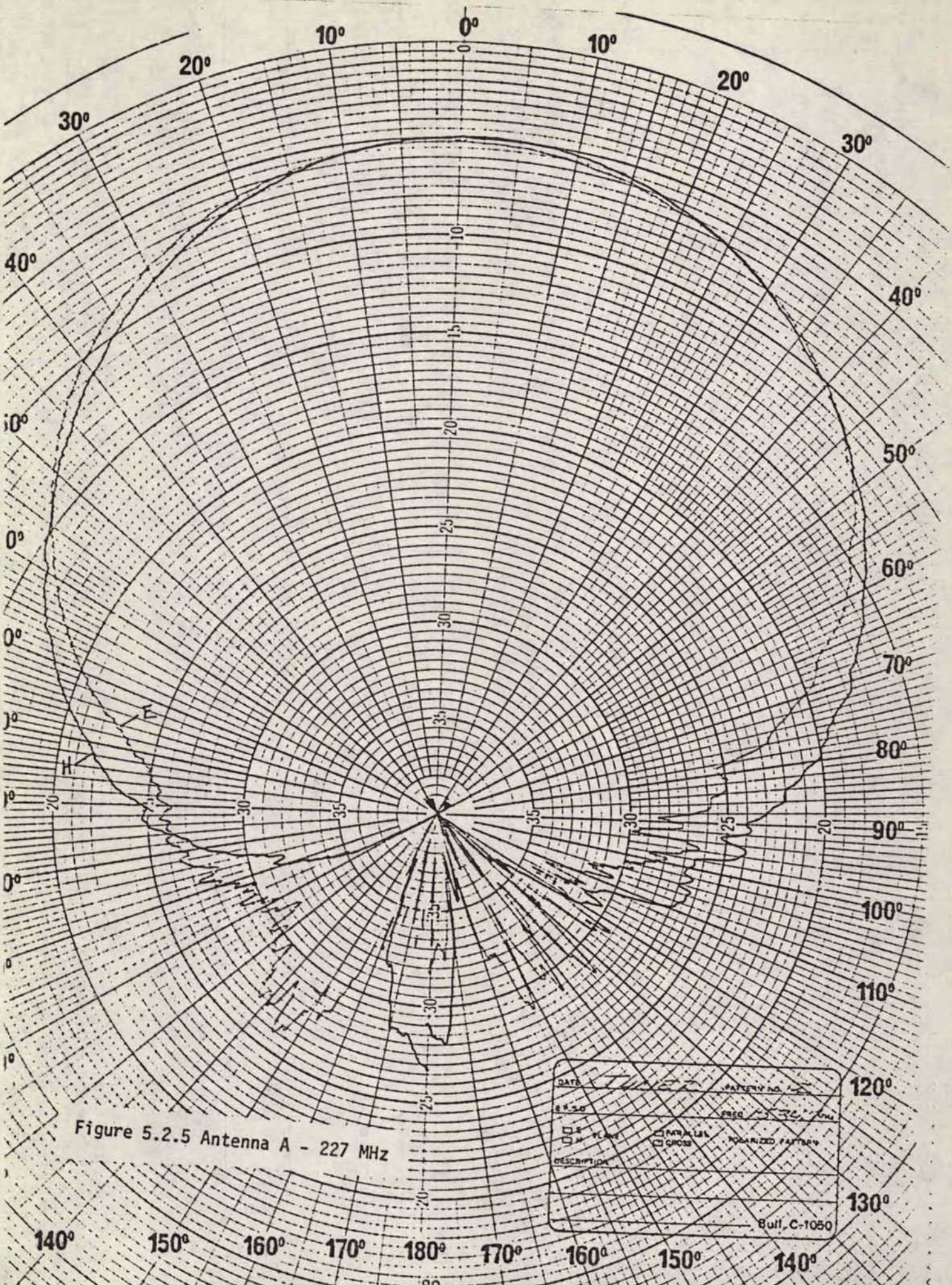

Figure 5.2.5 Antenna A - 227 MHz

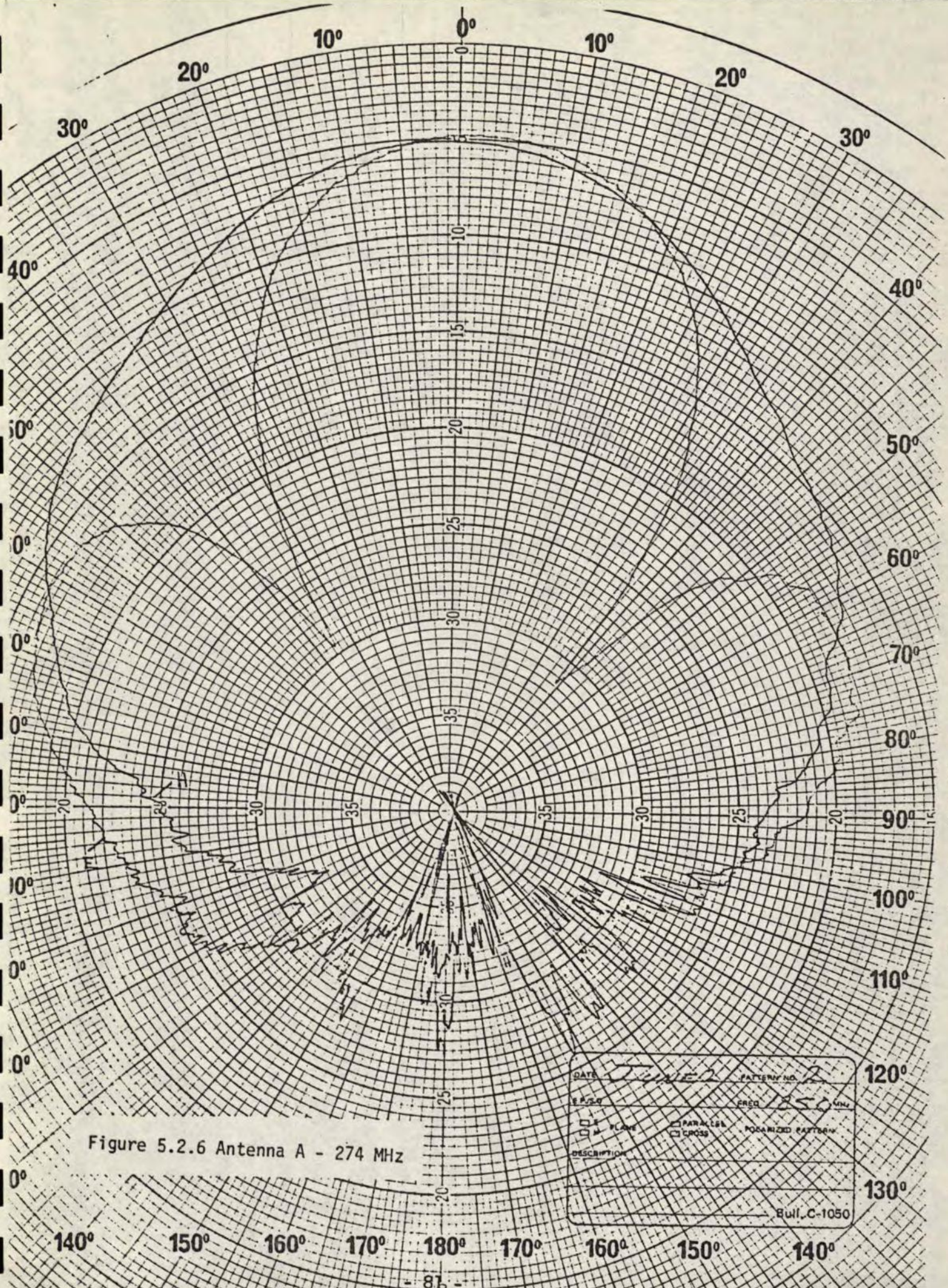

Figure 5.2.6 Antenna A - 274 MHz

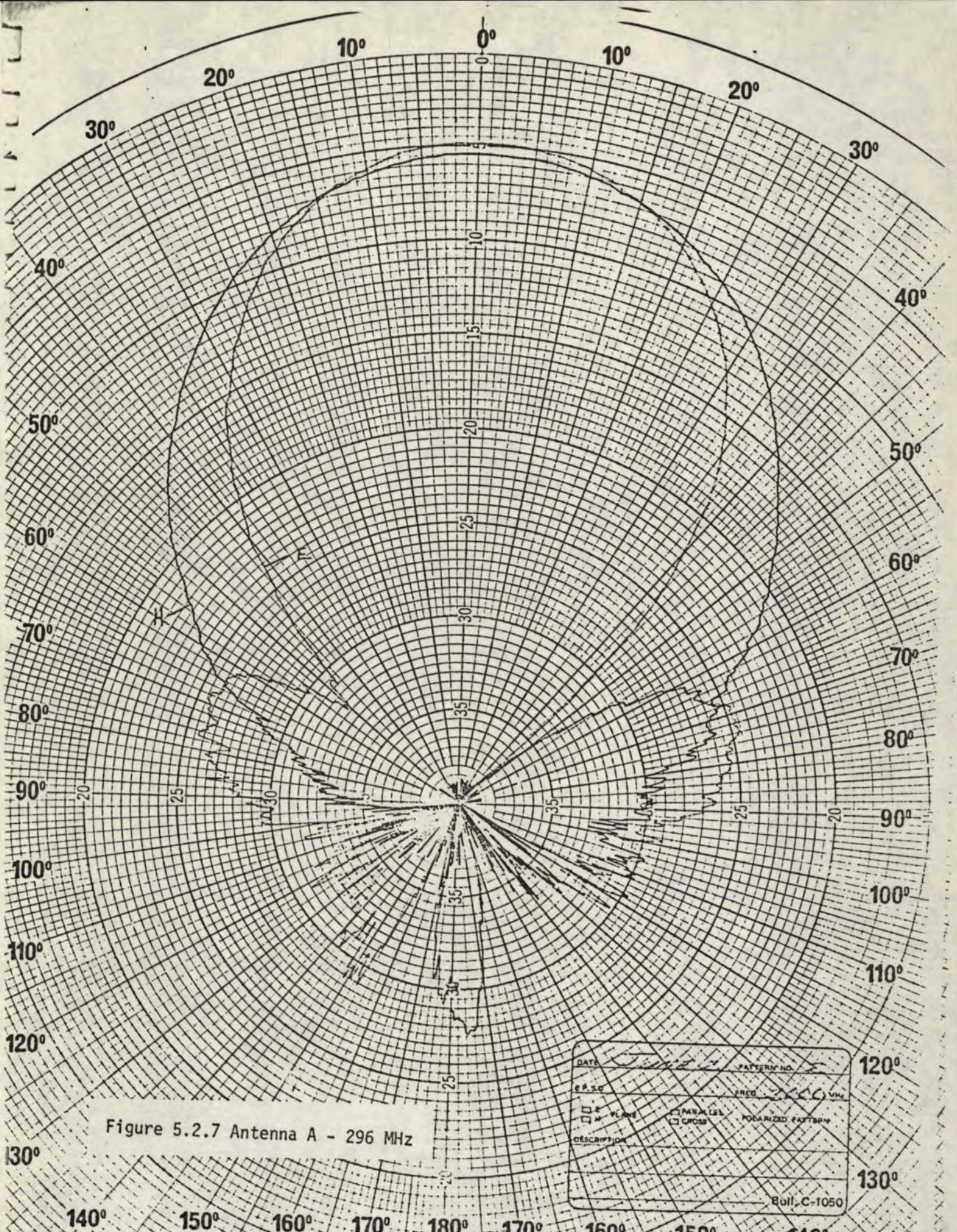

Figure 5.2.7 Antenna A - 296 MHz

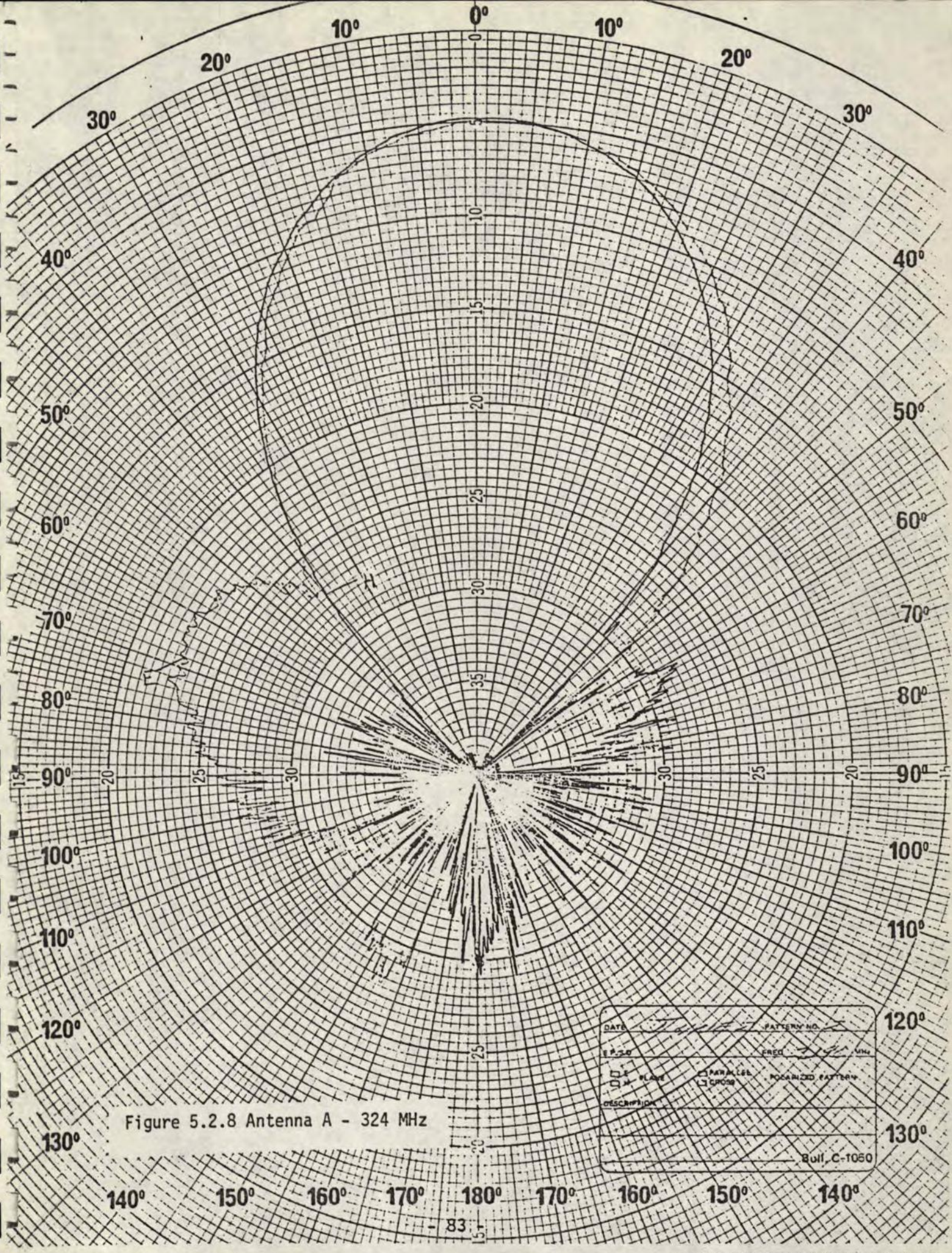

Figure 5.2.8 Antenna A - 324 MHz

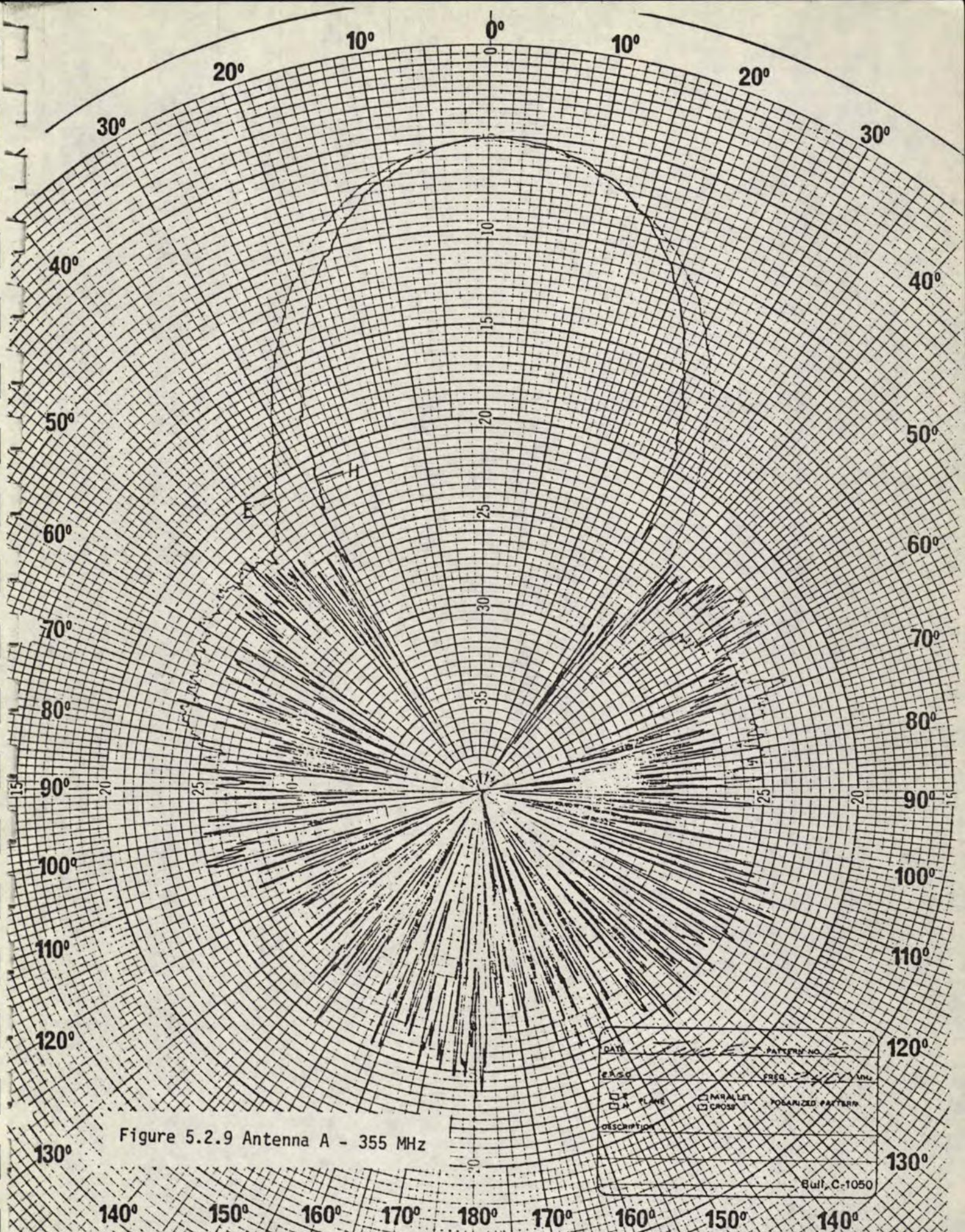

Figure 5.2.9 Antenna A - 355 MHz

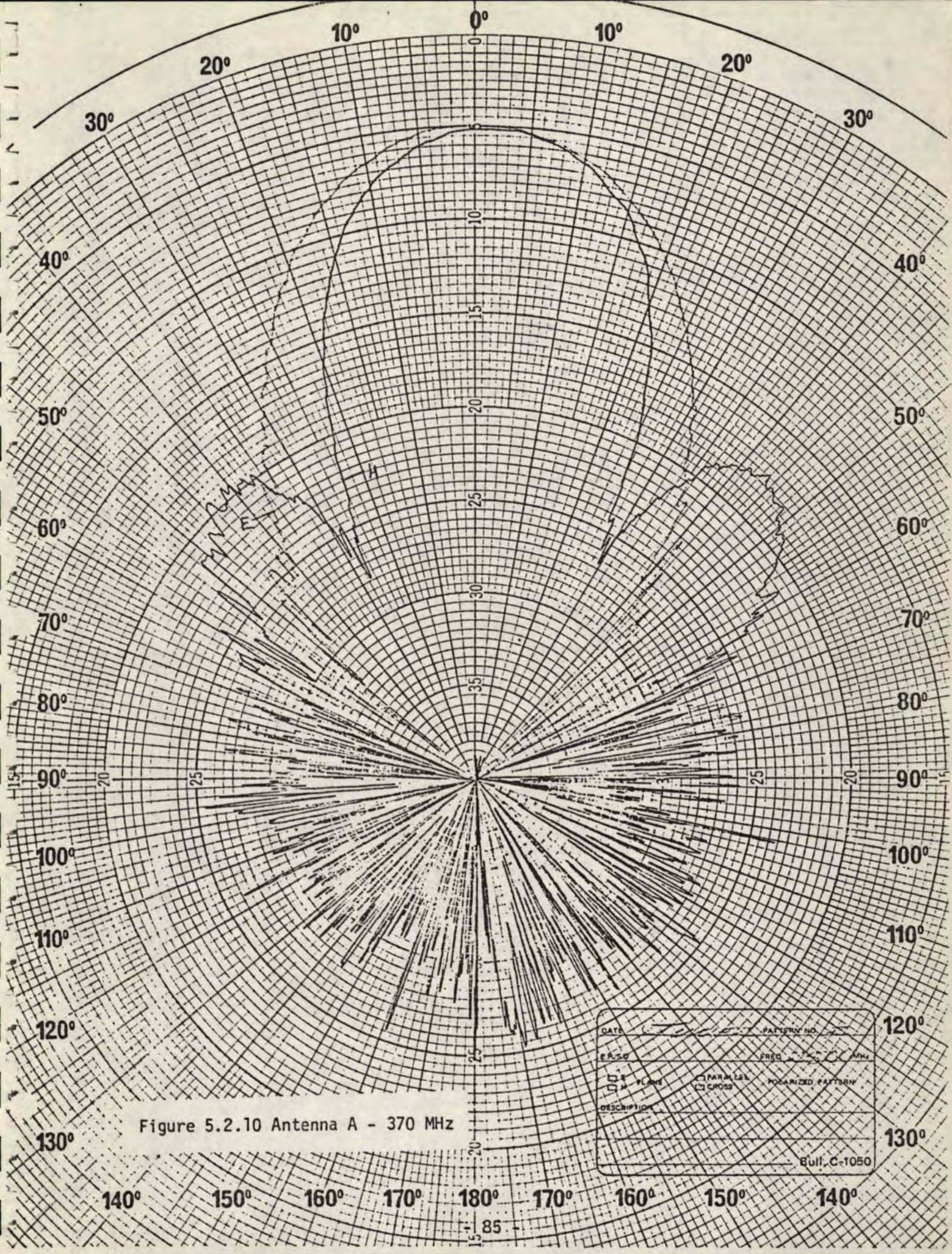

Figure 5.2.10 Antenna A - 370 MHz

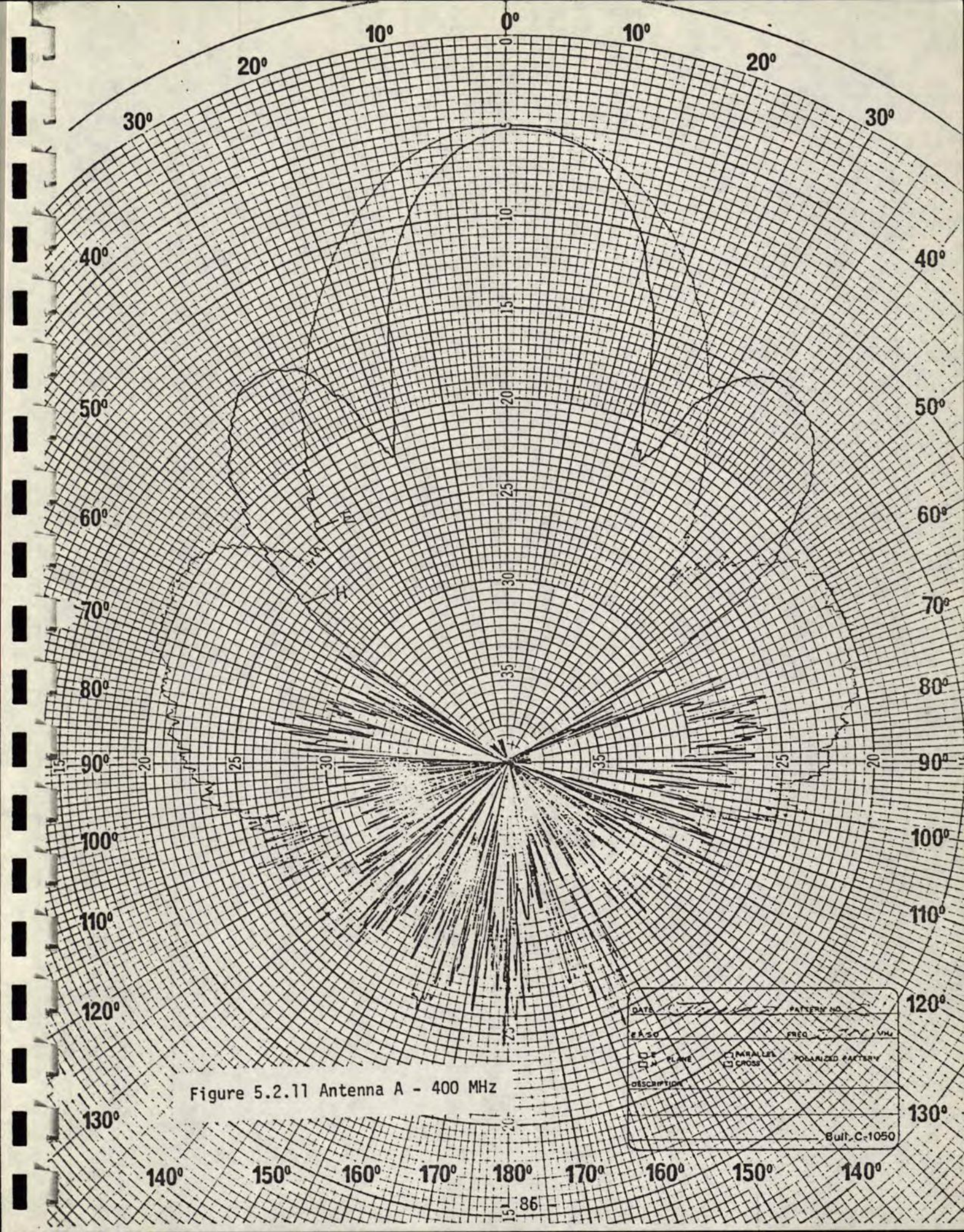

Figure 5.2.11 Antenna A - 400 MHz

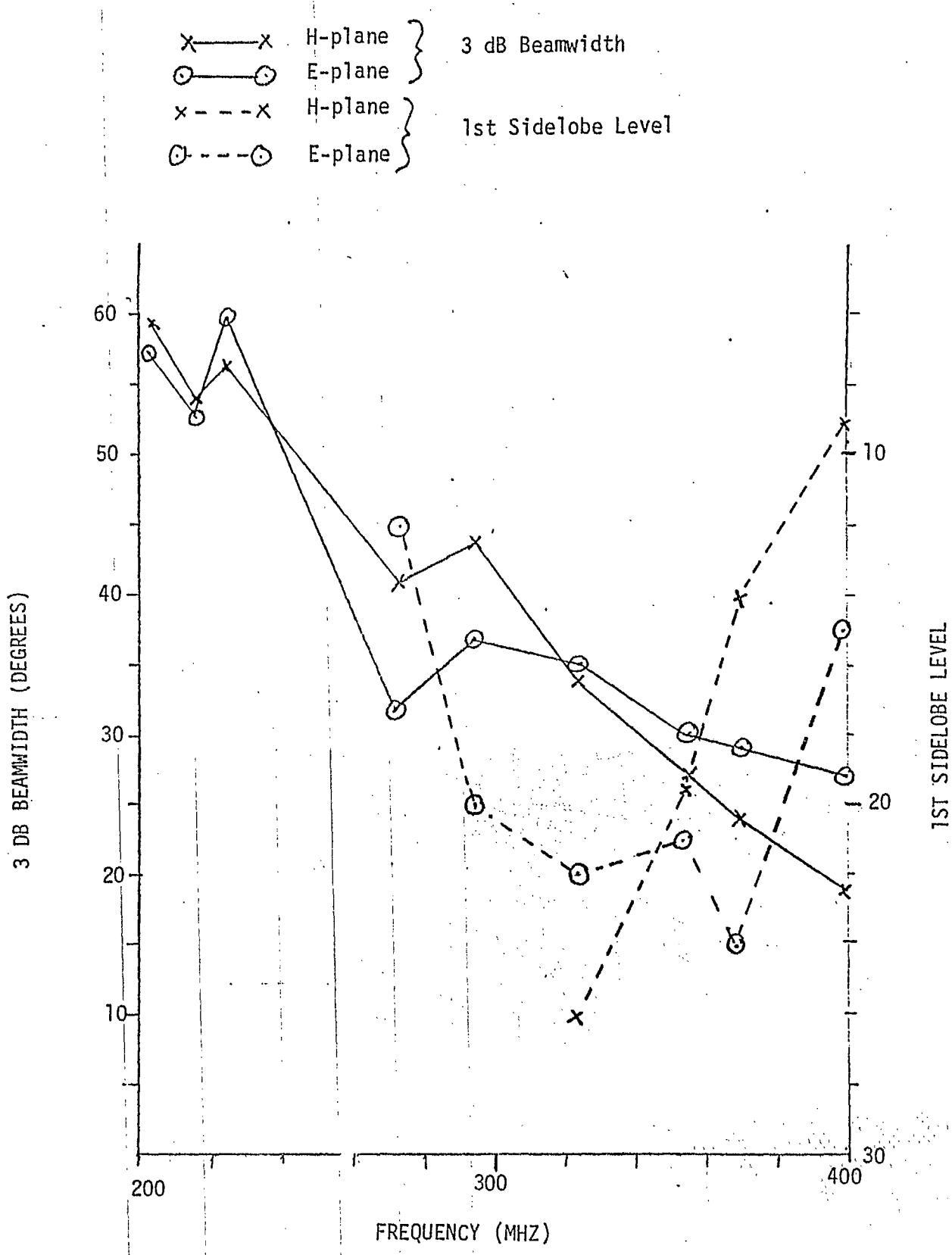

FIGURE 5.2.12 3 DB BEAMWIDTH AND 1ST SIDELOBE LEVEL VS FREQUENCY FOR ANTENNA A

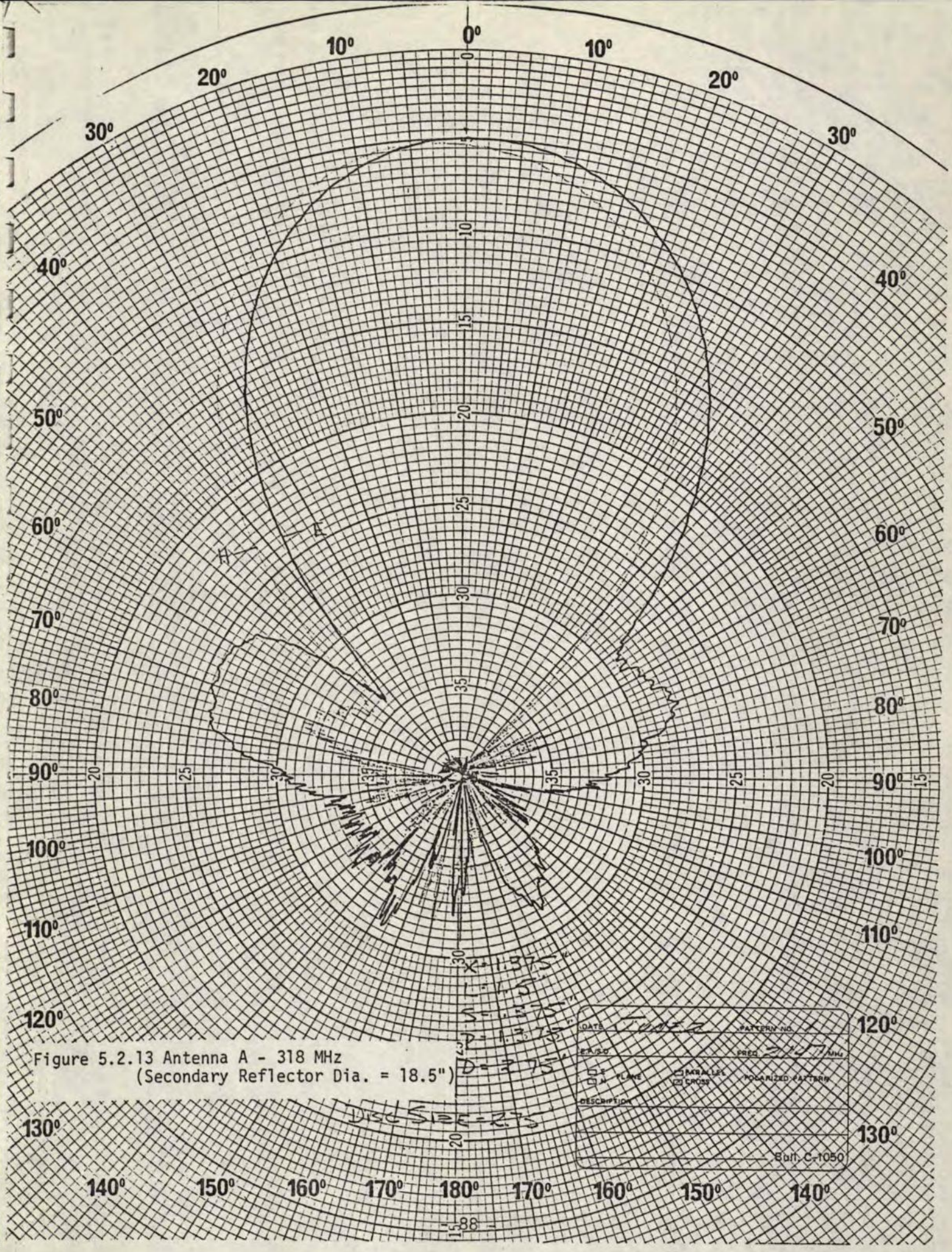

Figure 5.2.13 Antenna A - 318 MHz
(Secondary Reflector Dia. = 18.5")

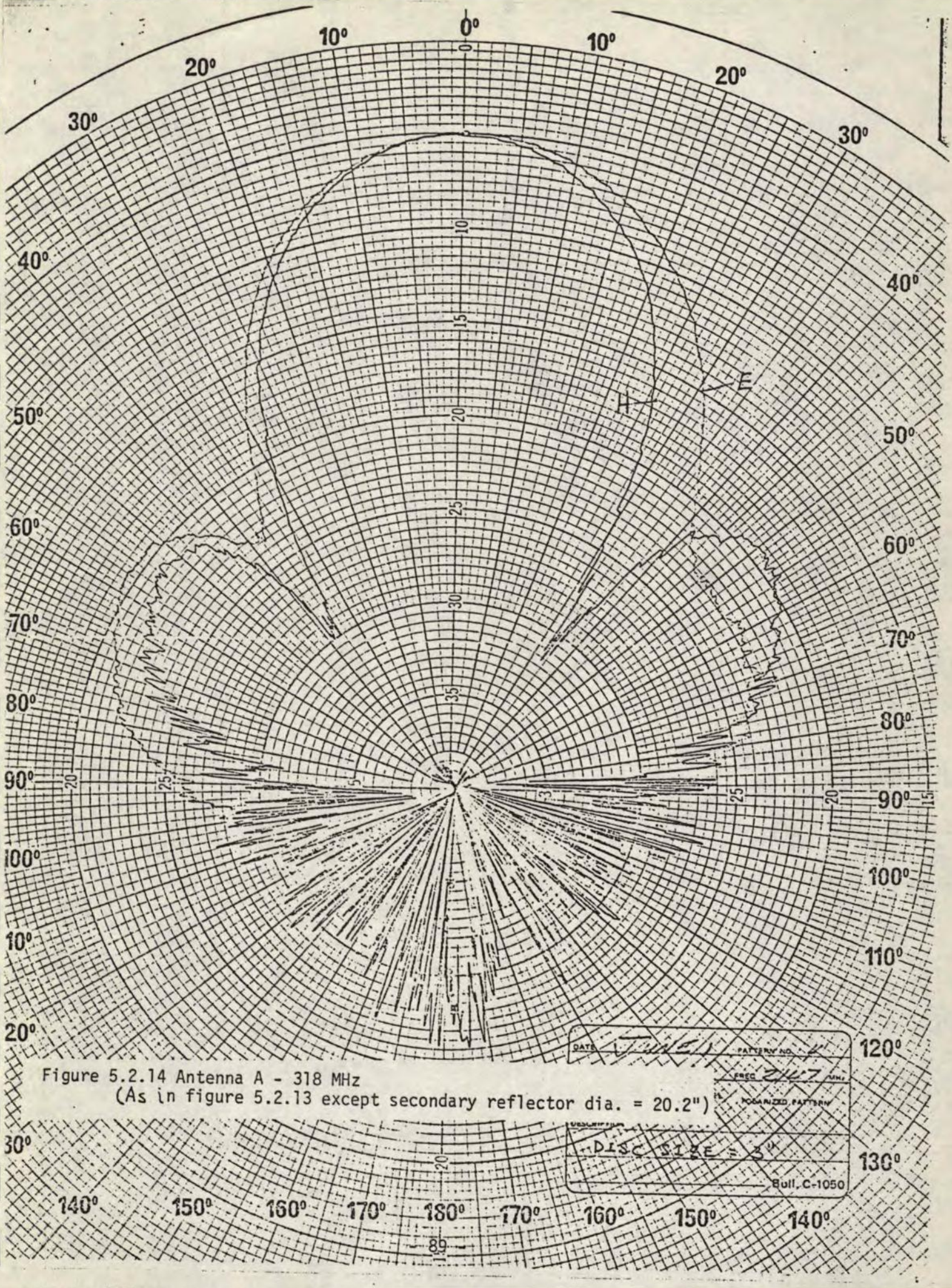

Figure 5.2.14 Antenna A - 318 MHz
(As in figure 5.2.13 except secondary reflector dia. = 20.2")

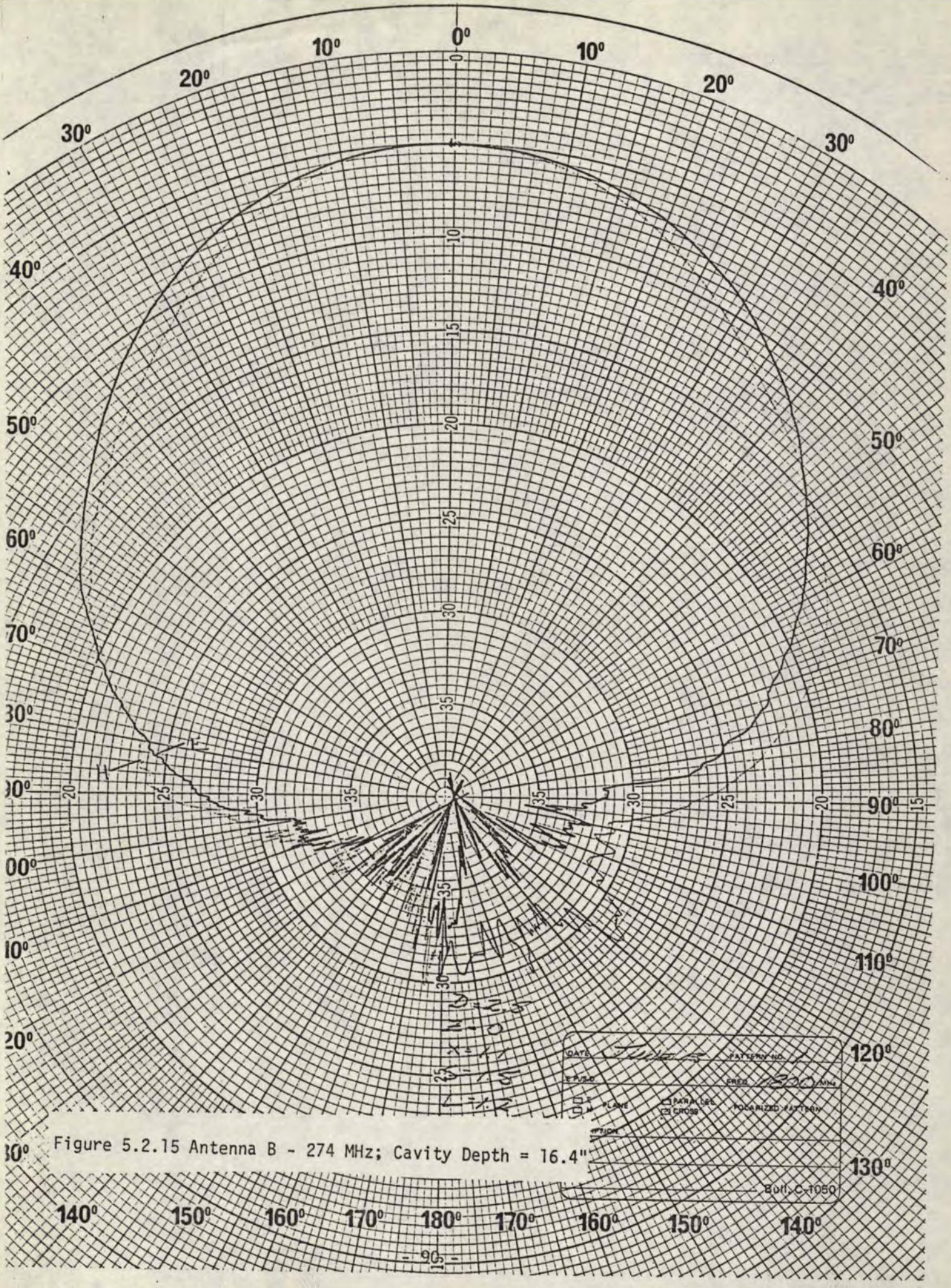

Figure 5.2.15 Antenna B - 274 MHz; Cavity Depth = 16.4"

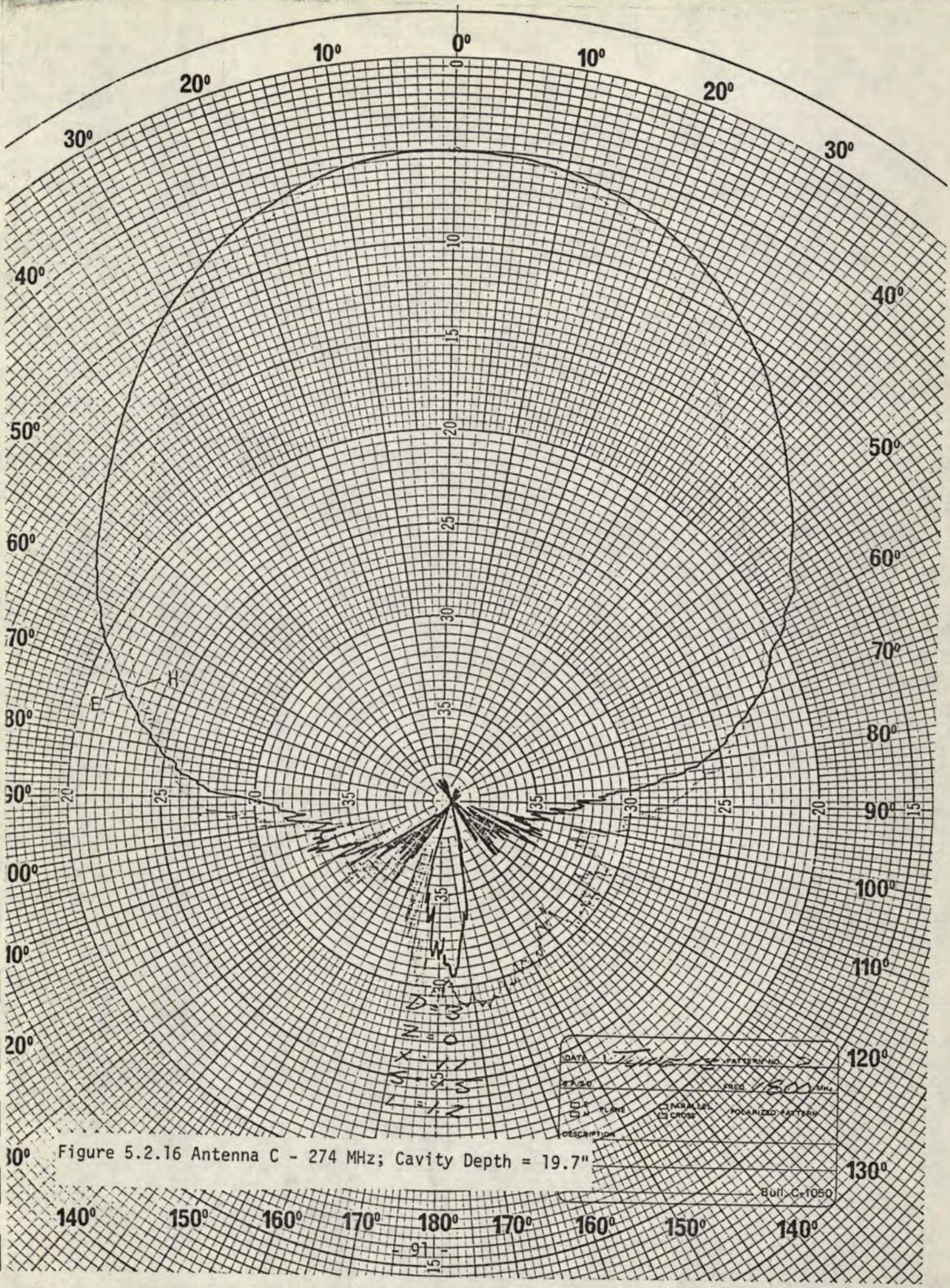

Figure 5.2.16 Antenna C - 274 MHz; Cavity Depth = 19.7"

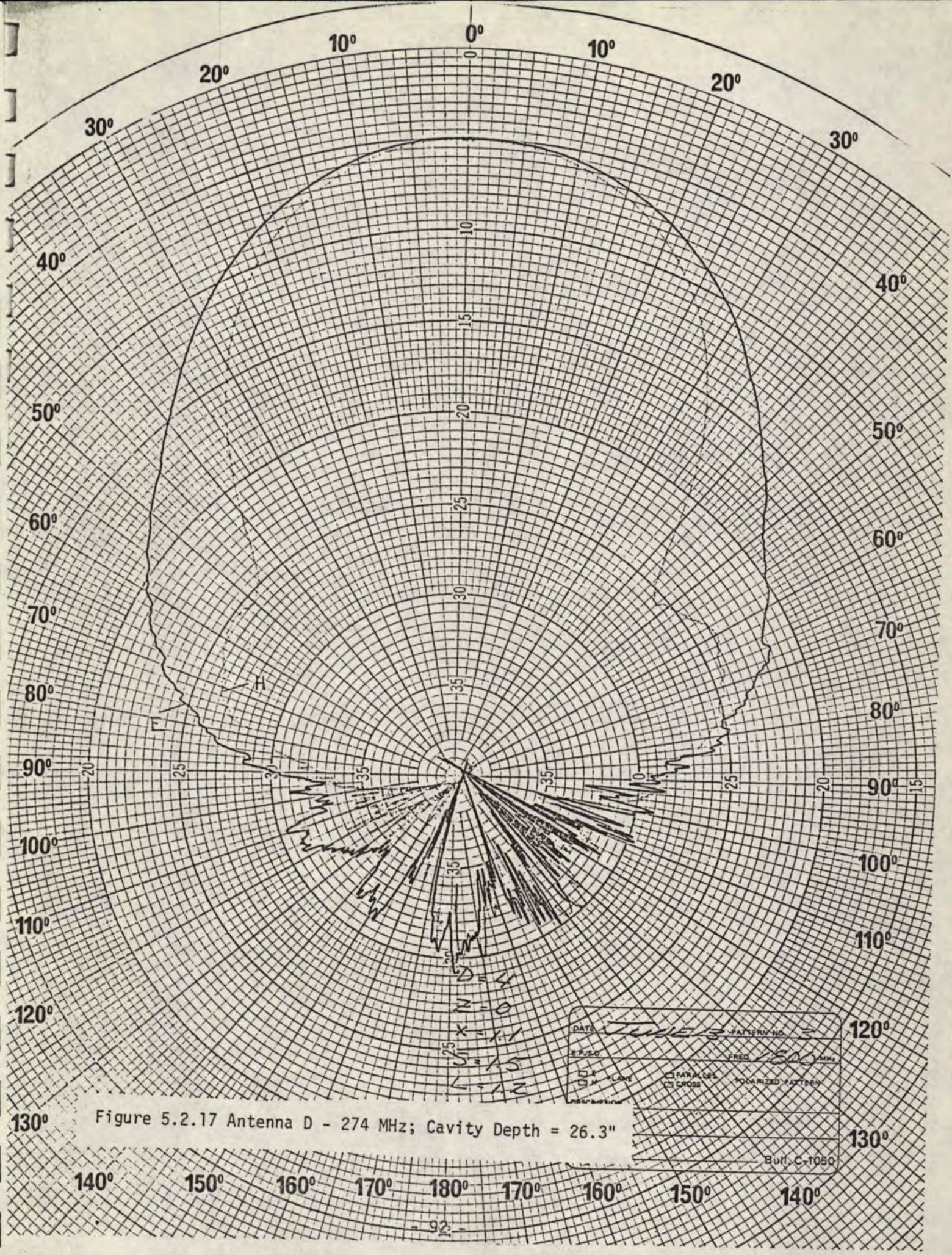

Figure 5.2.17 Antenna D - 274 MHz; Cavity Depth = 26.3"

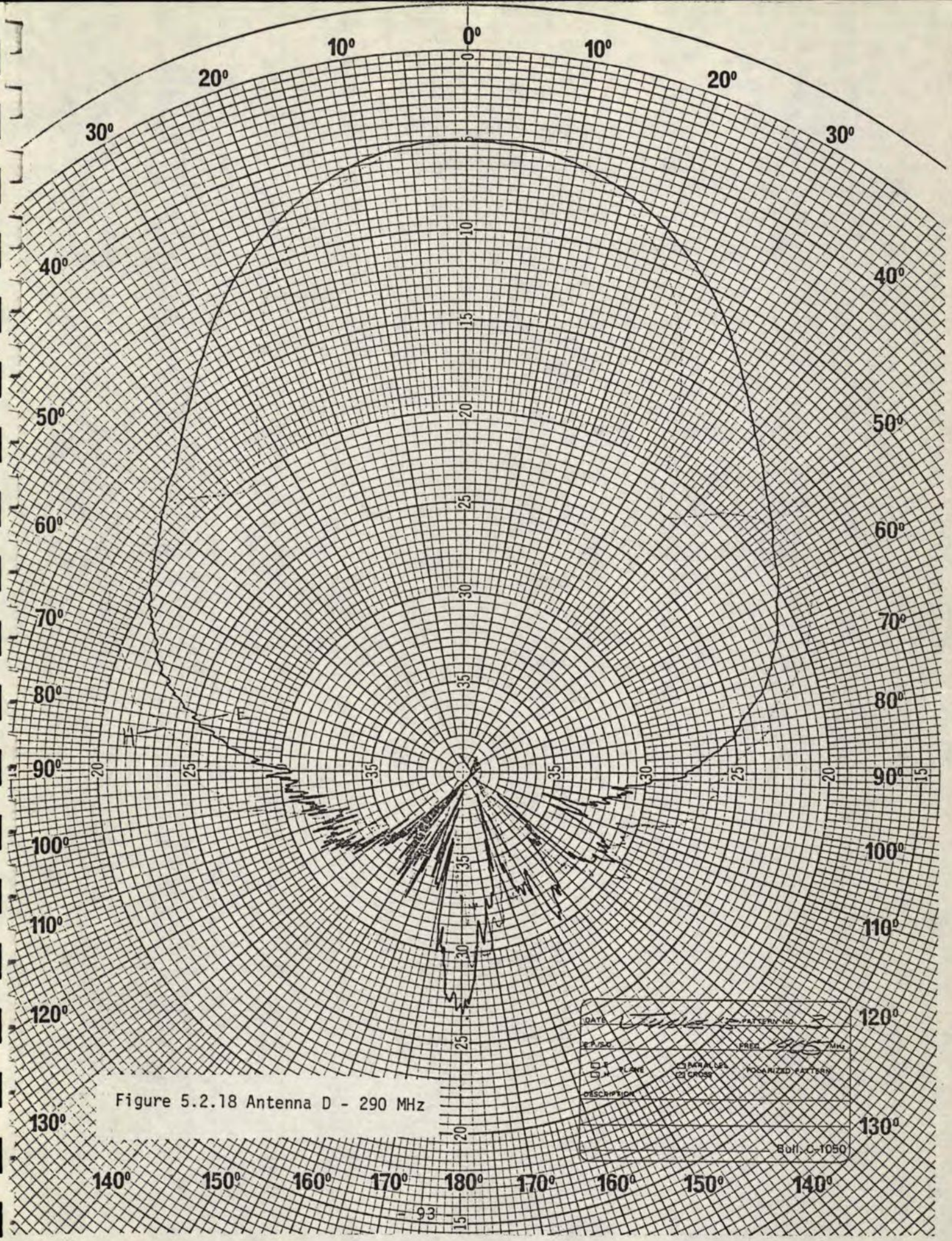

Figure 5.2.18 Antenna D - 290 MHz

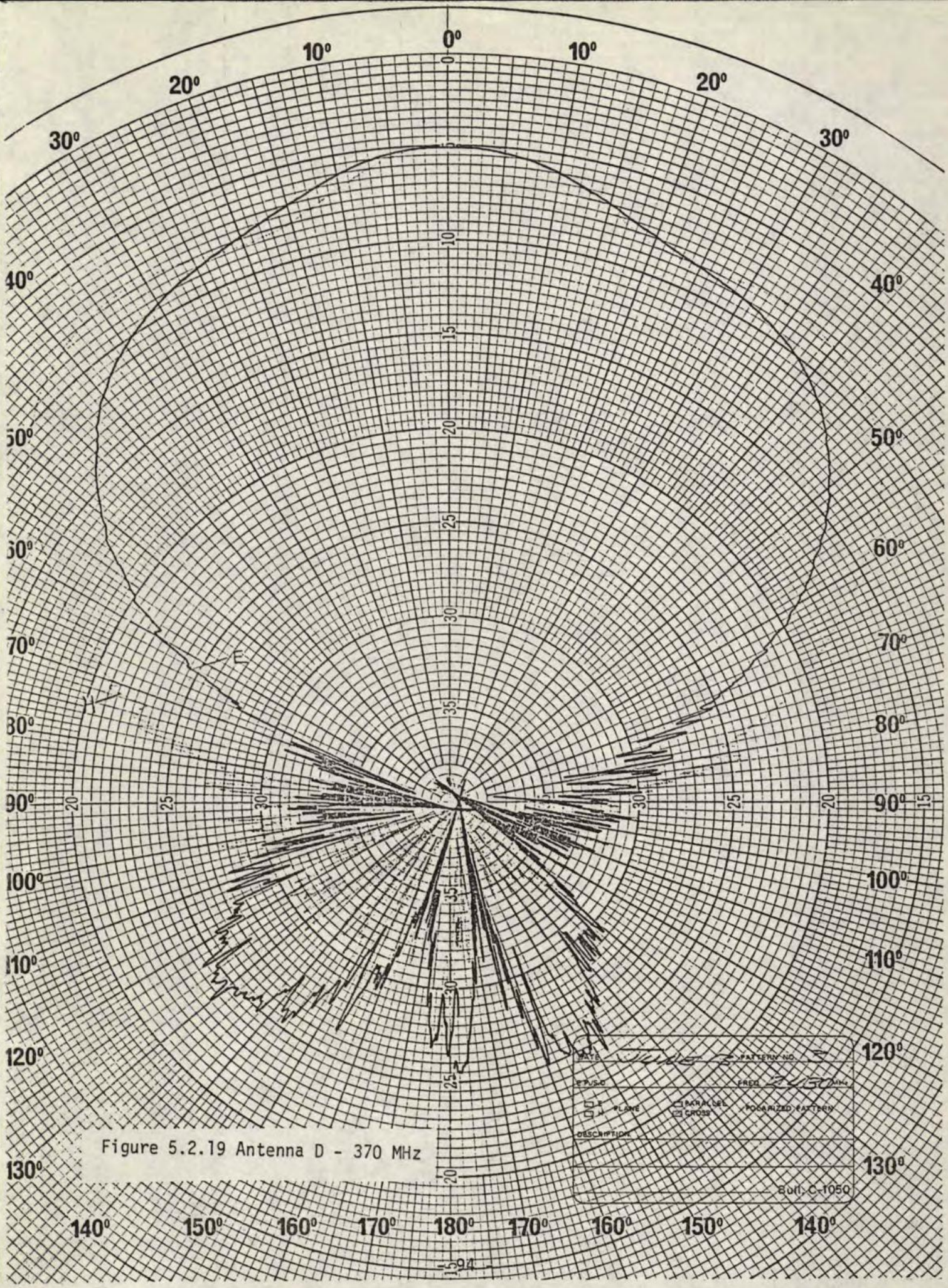

Figure 5.2.19 Antenna D - 370 MHz

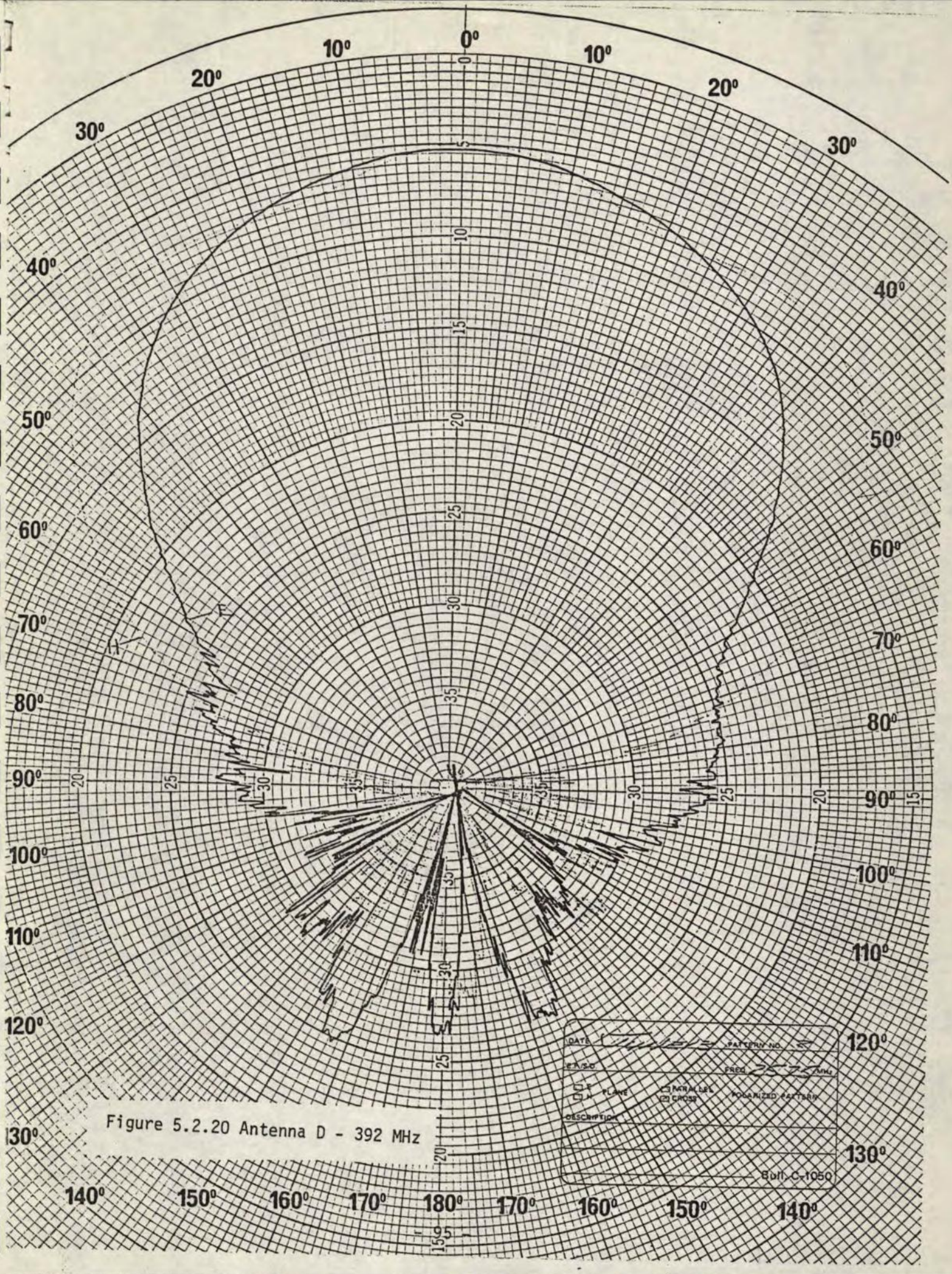

Figure 5.2.20 Antenna D - 392 MHz

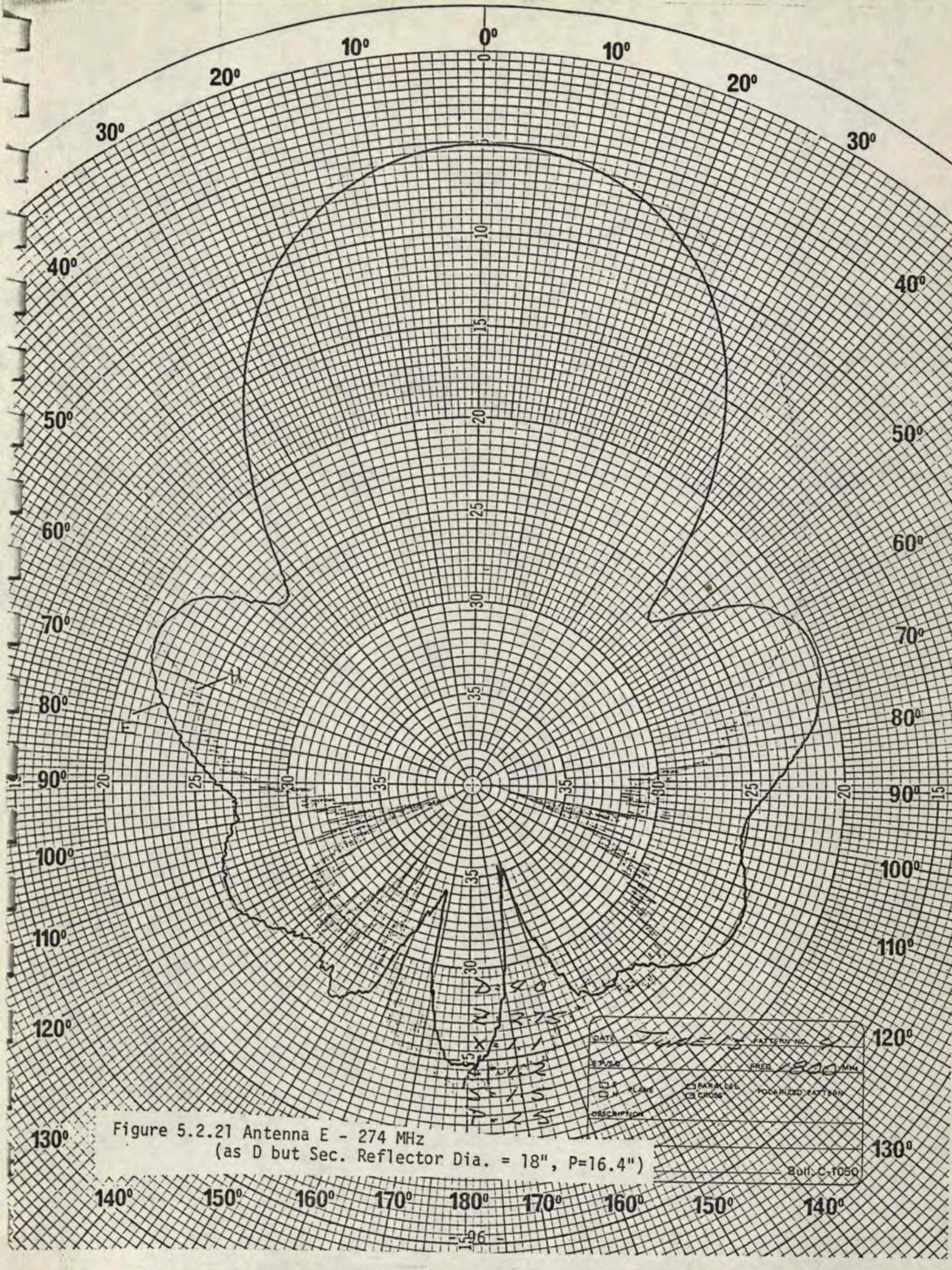

Figure 5.2.21 Antenna E - 274 MHz
(as D but Sec. Reflector Dia. = 18", P=16.4")

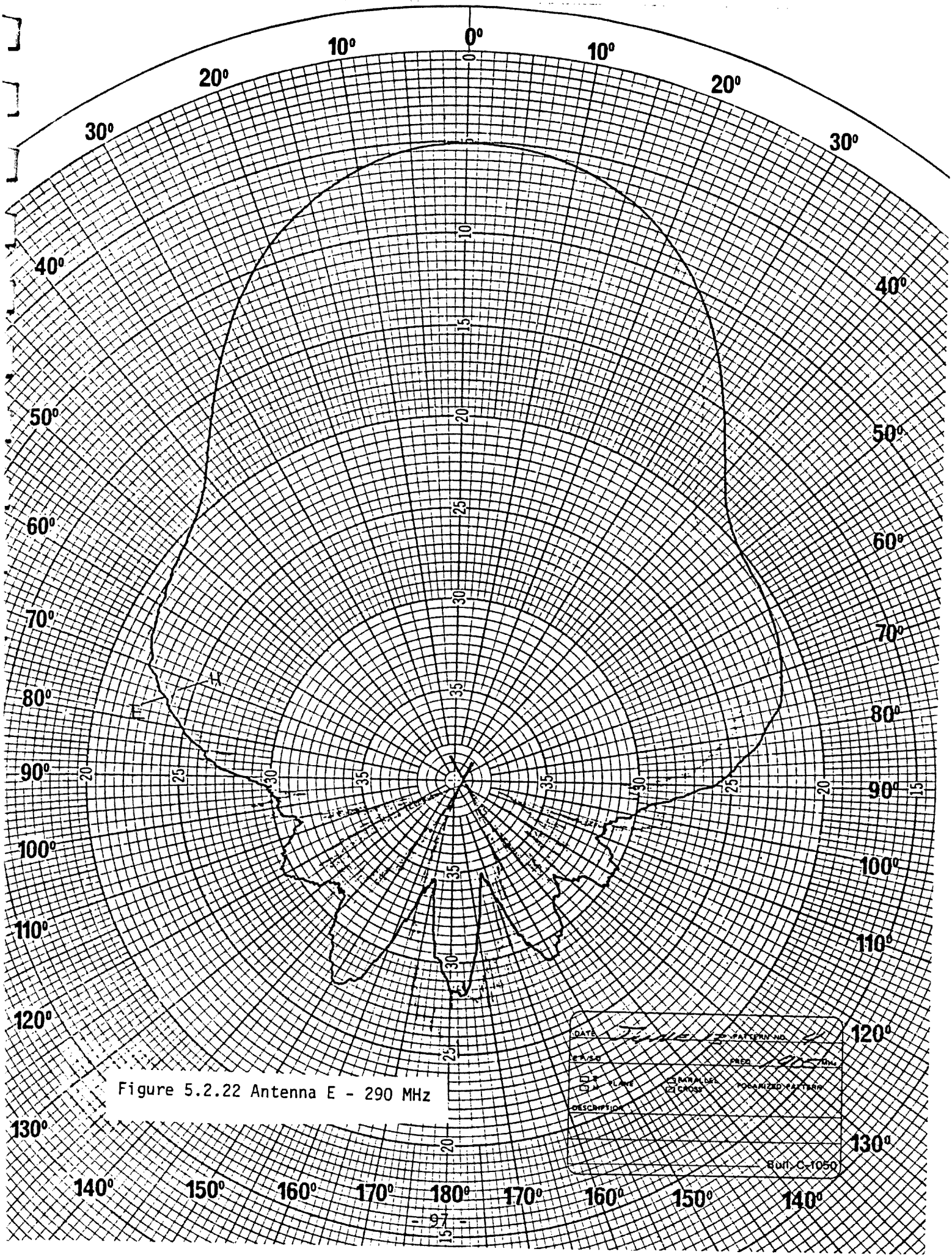

Figure 5.2.22 Antenna E - 290 MHz

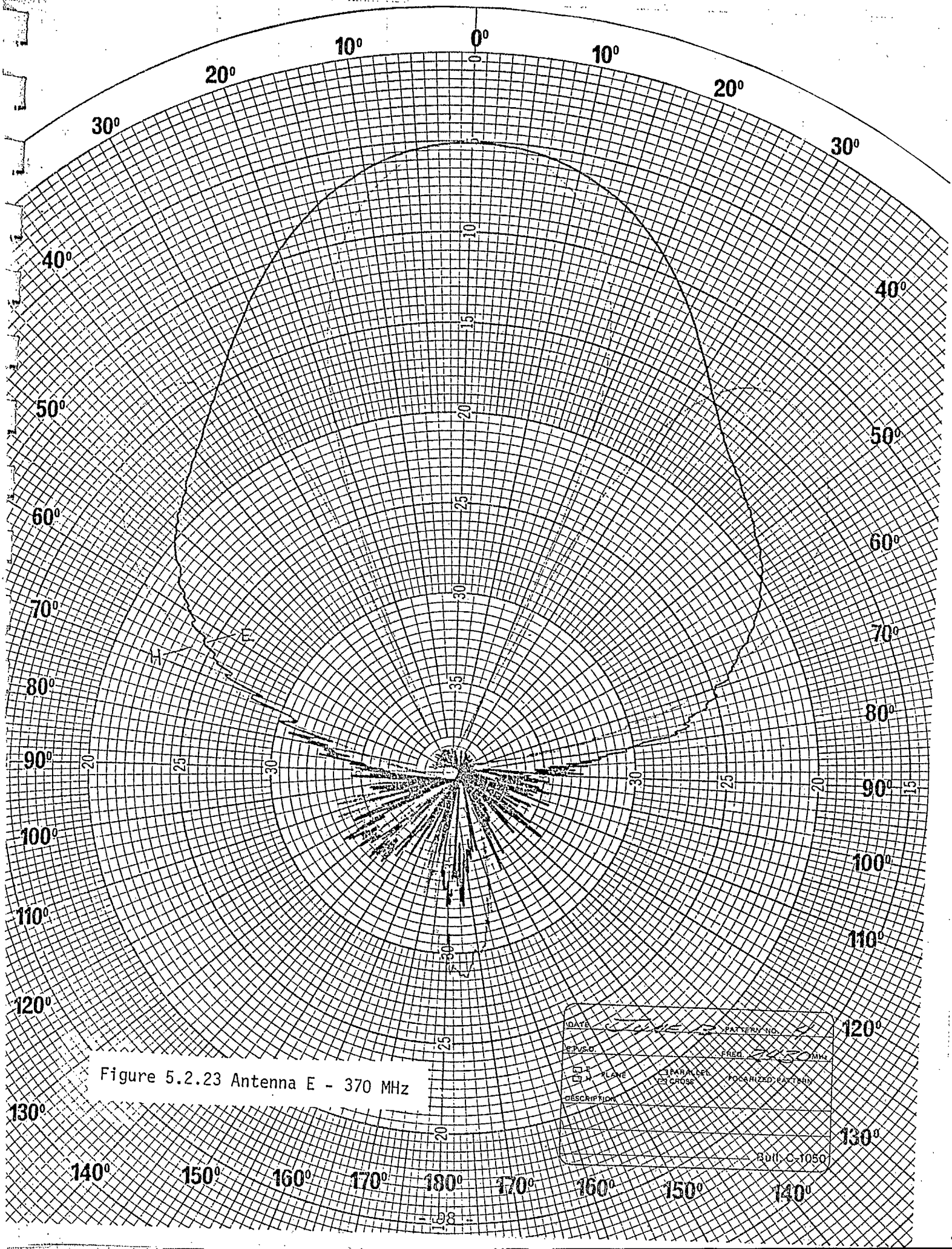

Figure 5.2.23 Antenna E - 370 MHz

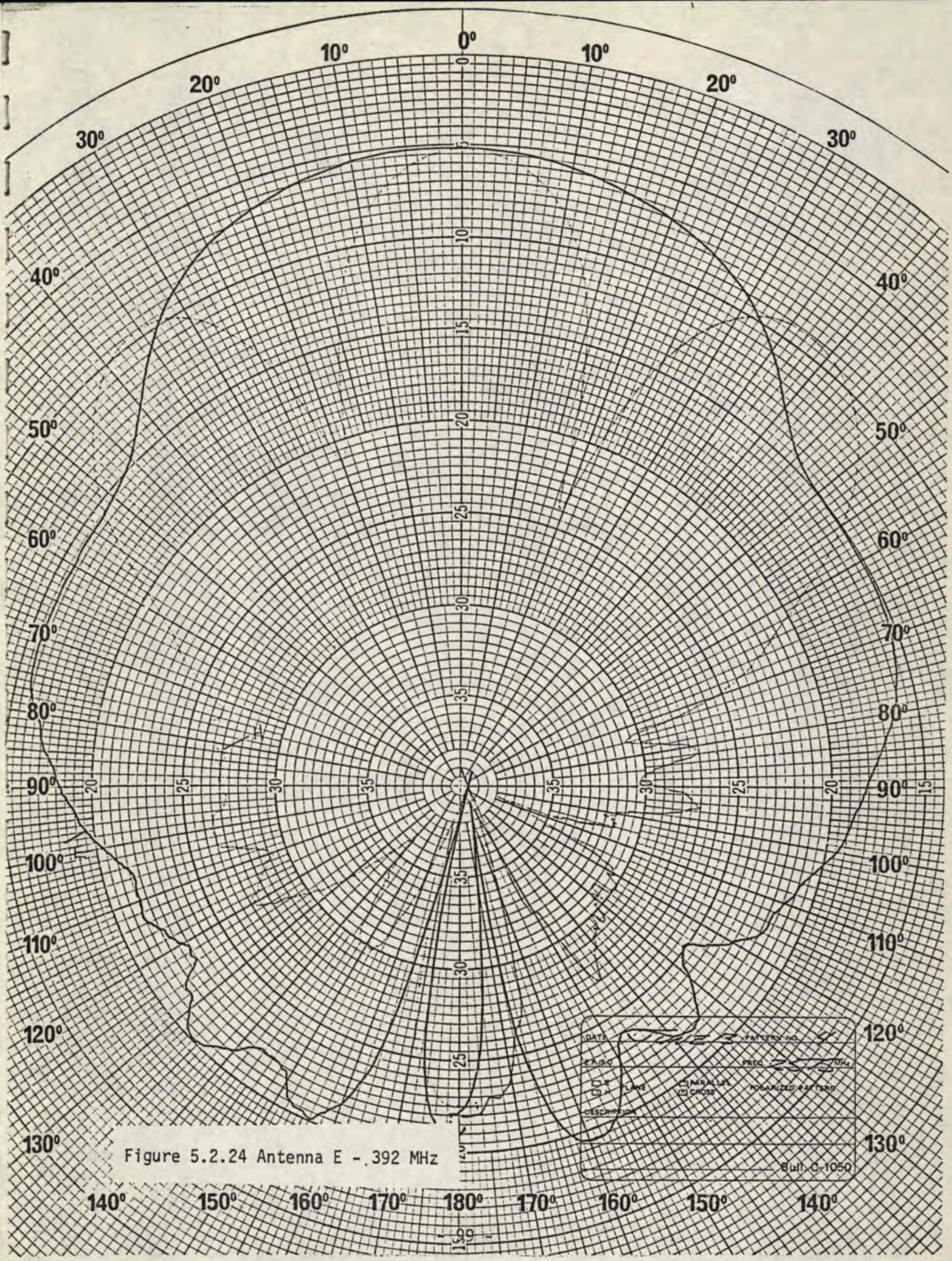

Figure 5.2.24 Antenna E - .392 MHz

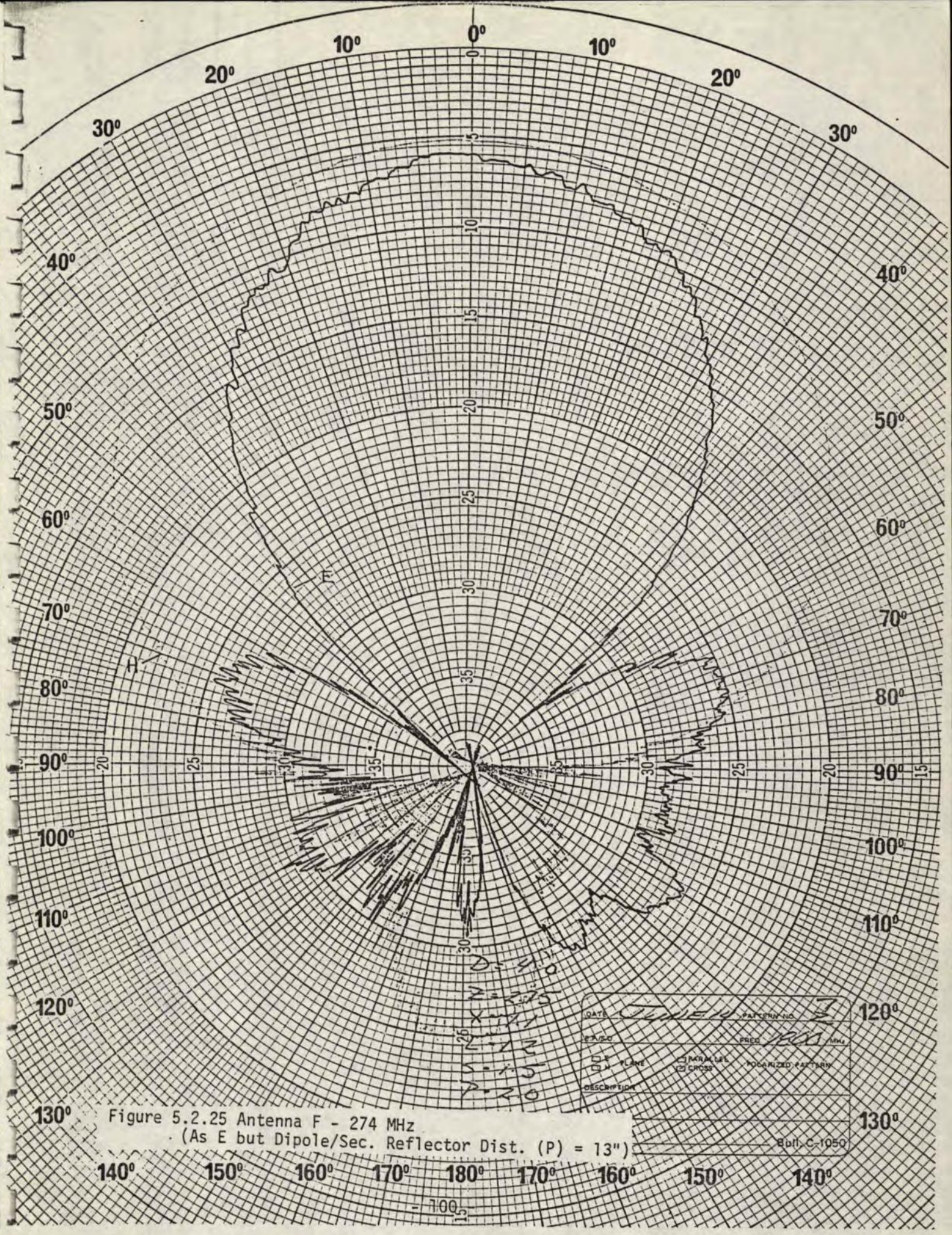

Figure 5.2.25 Antenna F - 274 MHz
(As E but Dipole/Sec. Reflector Dist. (P) = 13")

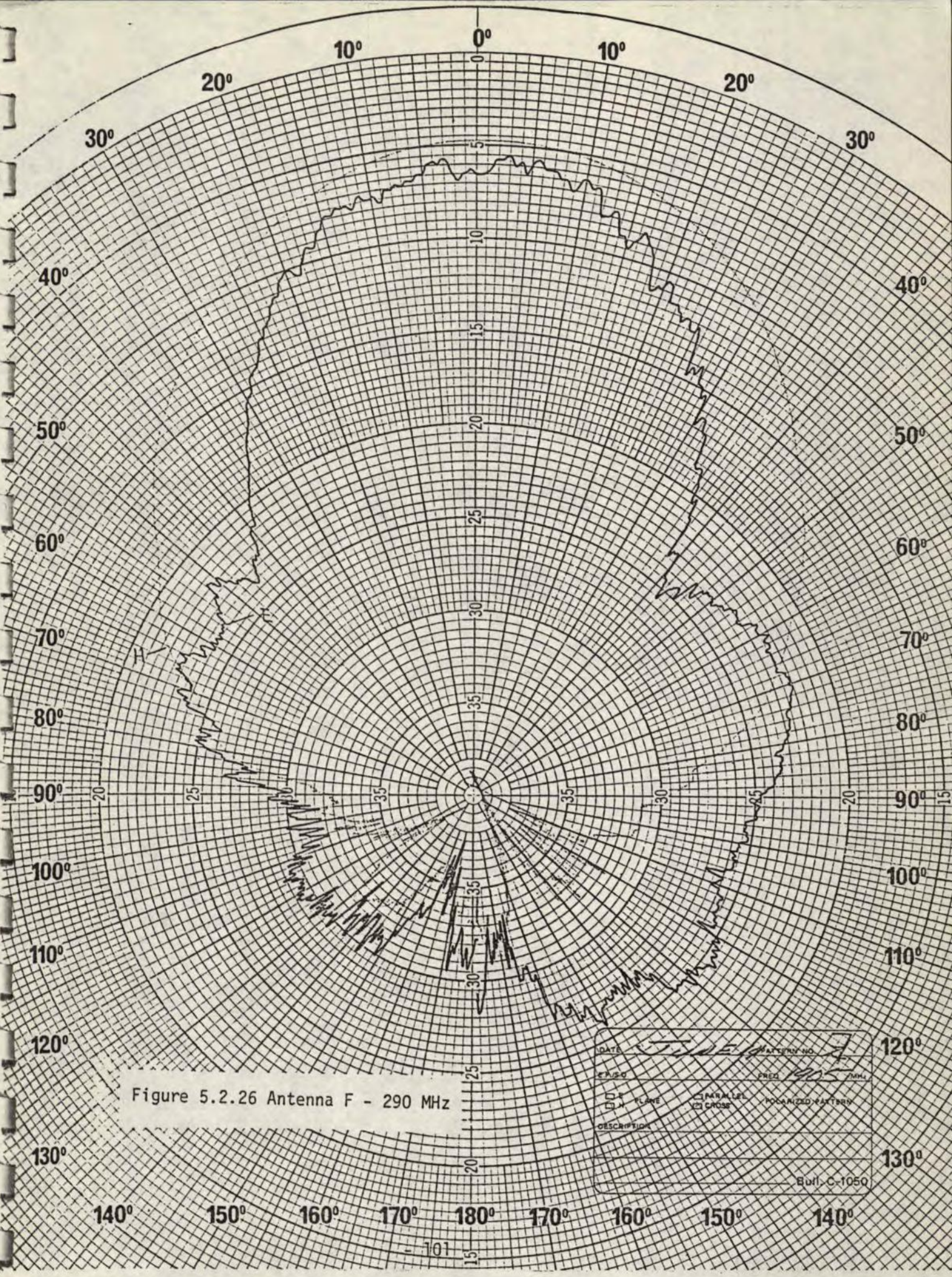

Figure 5.2.26 Antenna F - 290 MHz

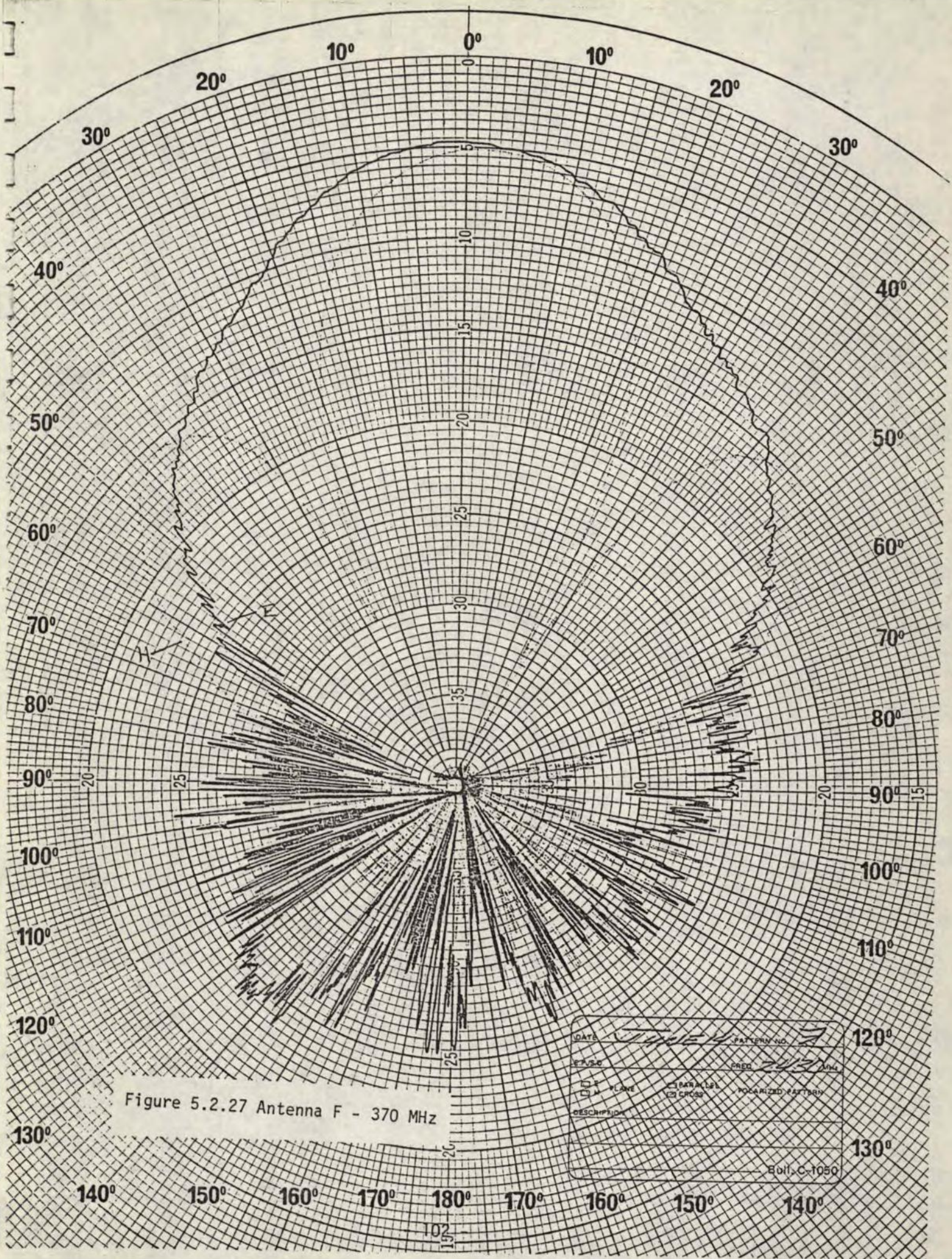

Figure 5.2.27 Antenna F - 370 MHz

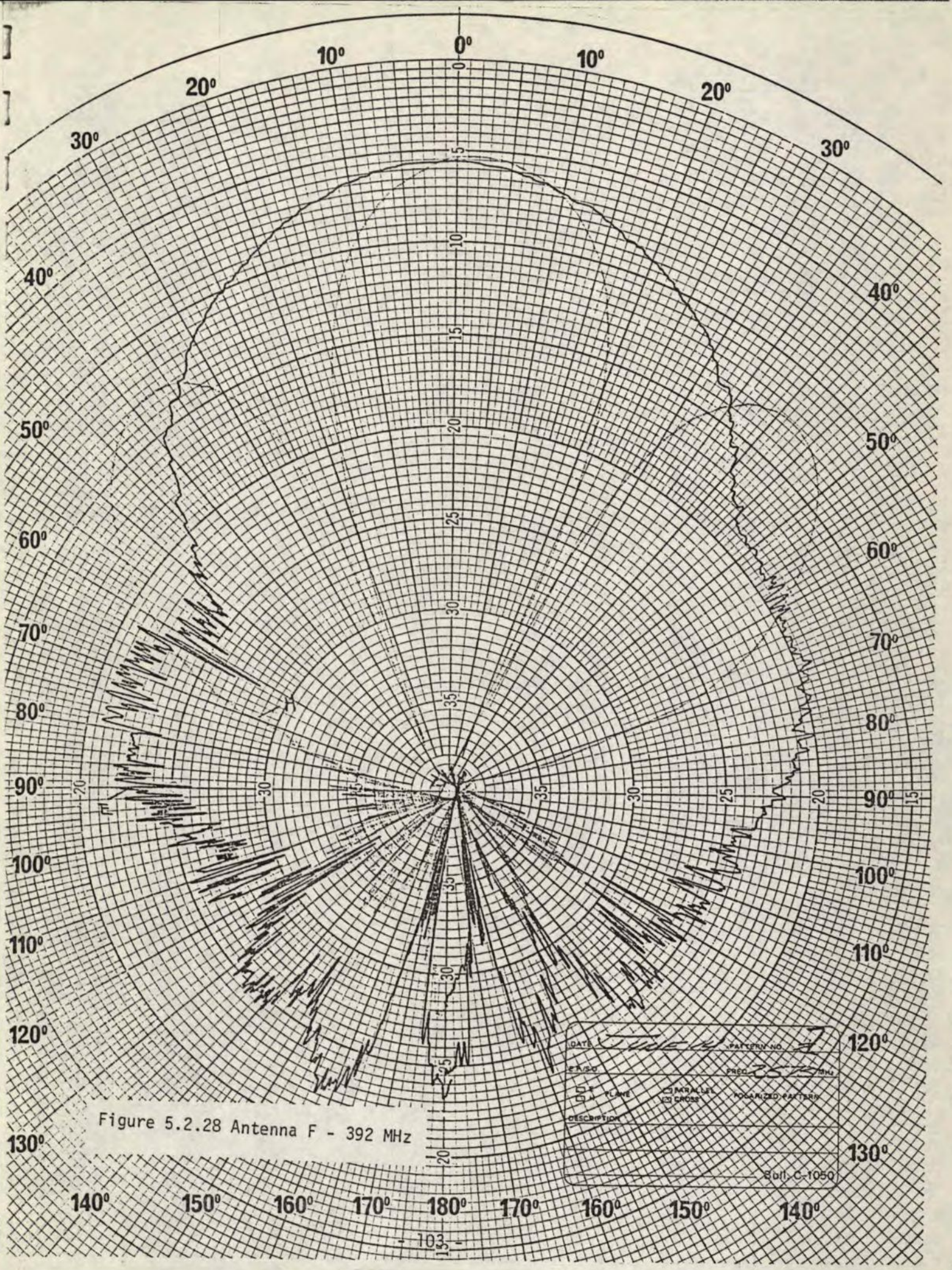

Figure 5.2.28 Antenna F - 392 MHz

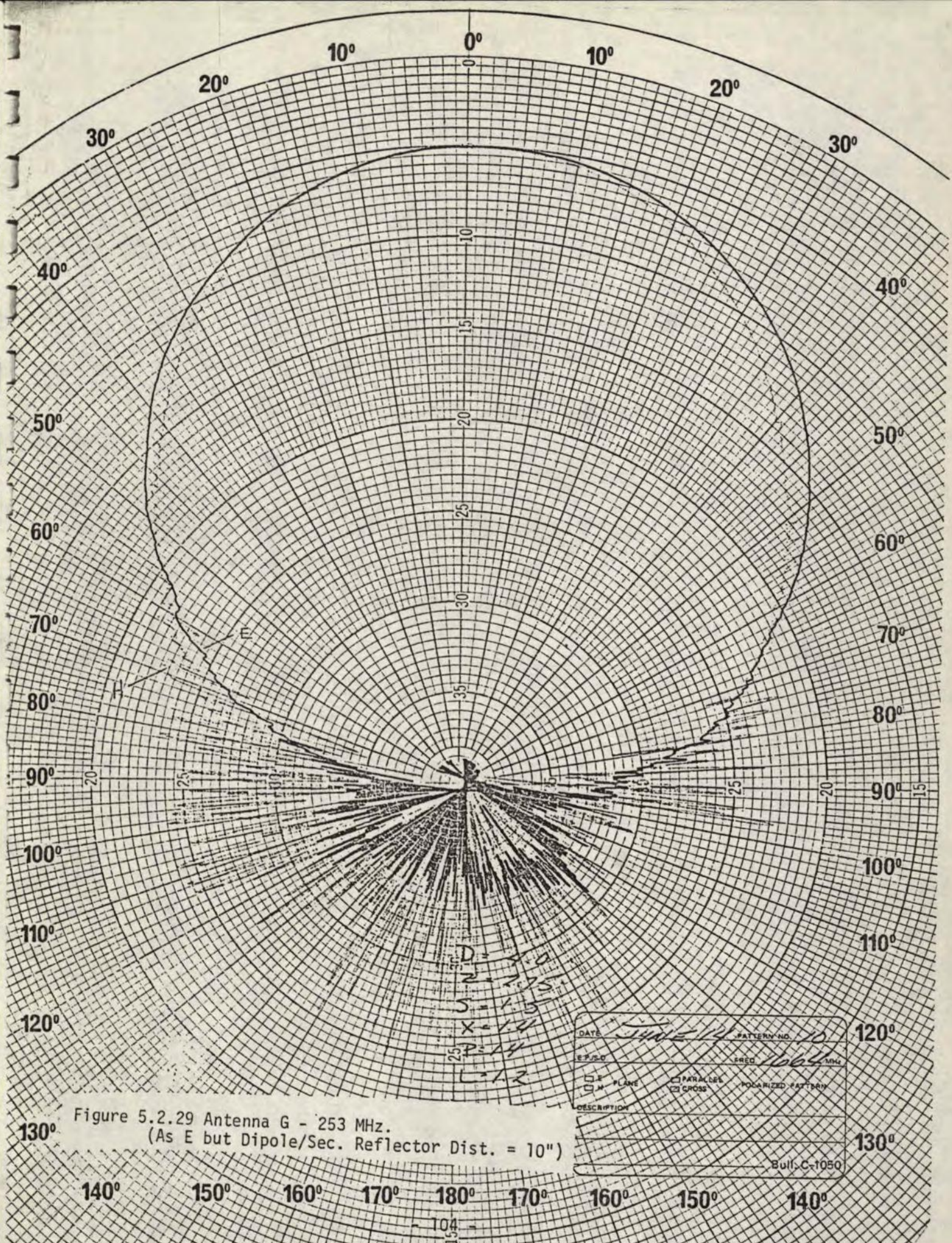

Figure 5.2.29 Antenna G - 253 MHz.
(As E but Dipole/Sec. Reflector Dist. = 10")

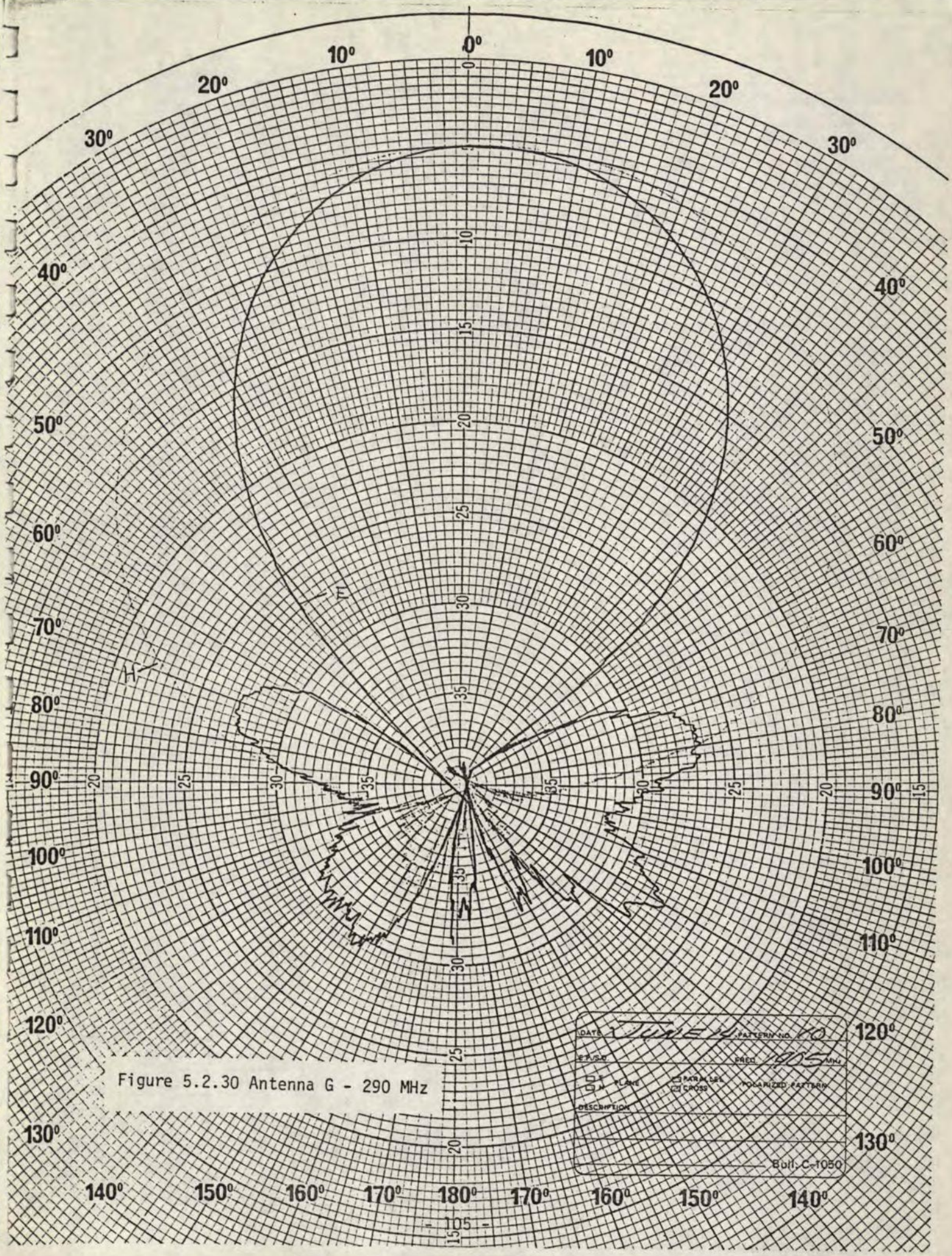

Figure 5.2.30 Antenna G - 290 MHz

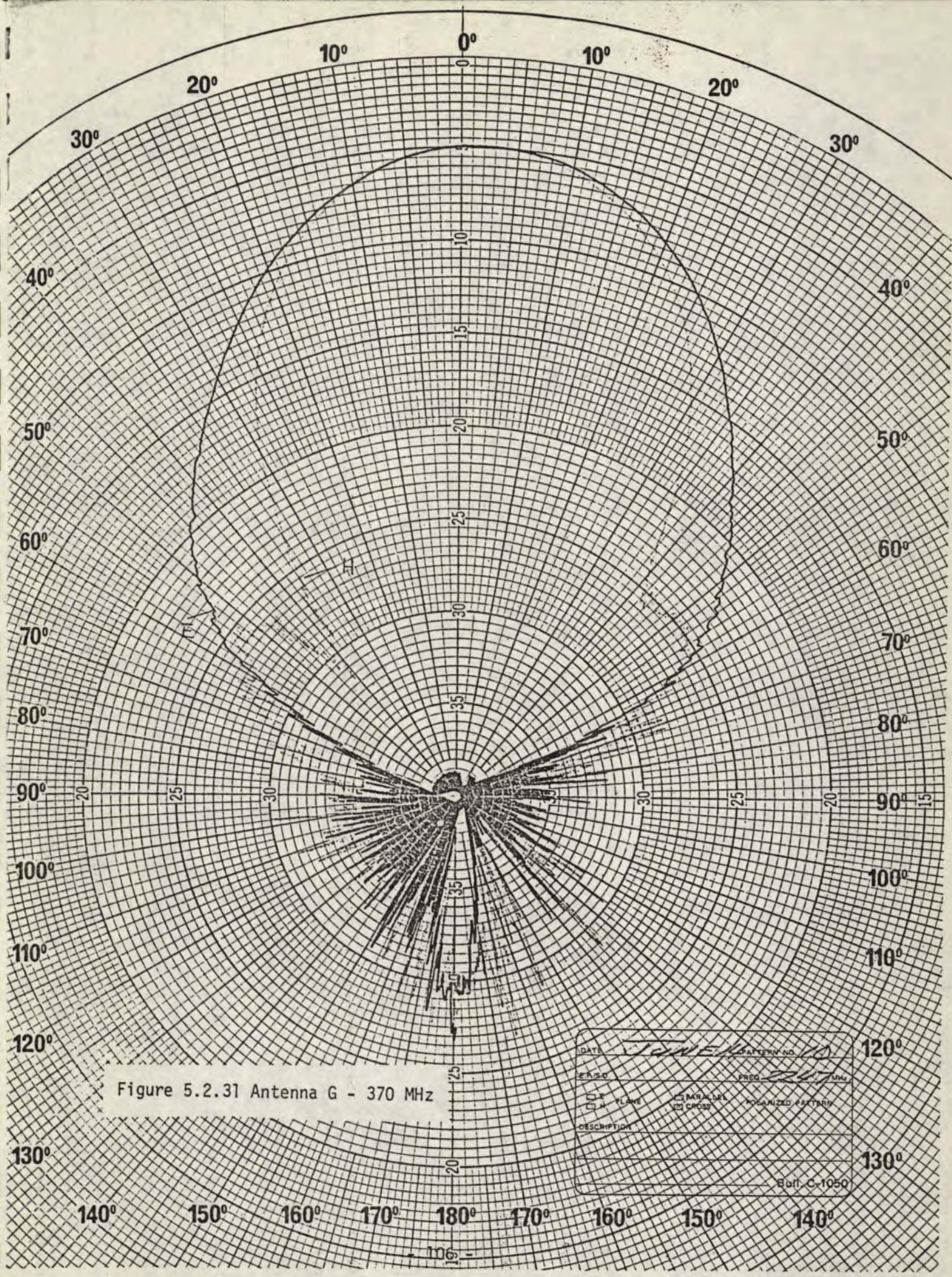

Figure 5.2.31 Antenna G - 370 MHz

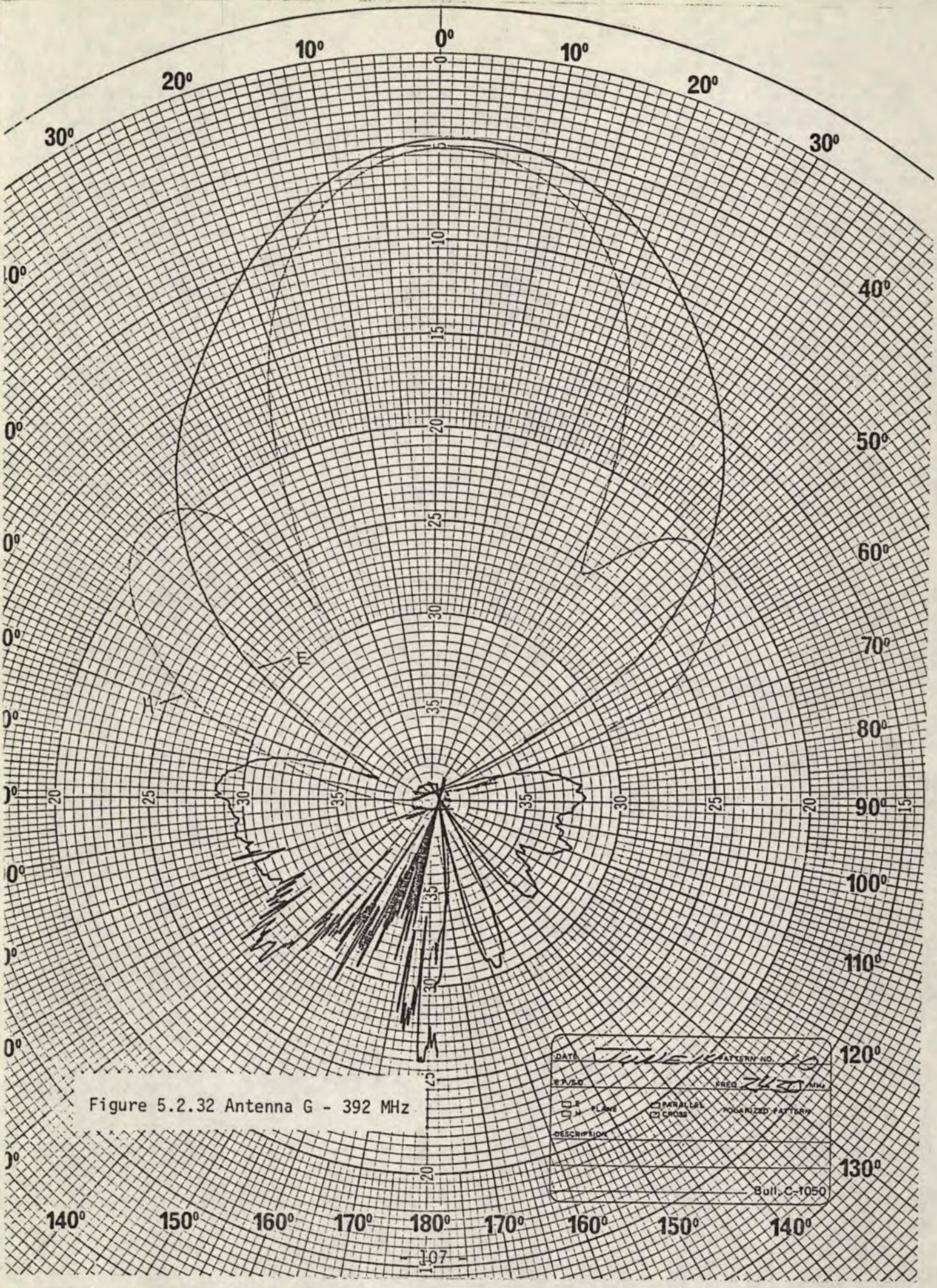

Figure 5.2.32 Antenna G - 392 MHz

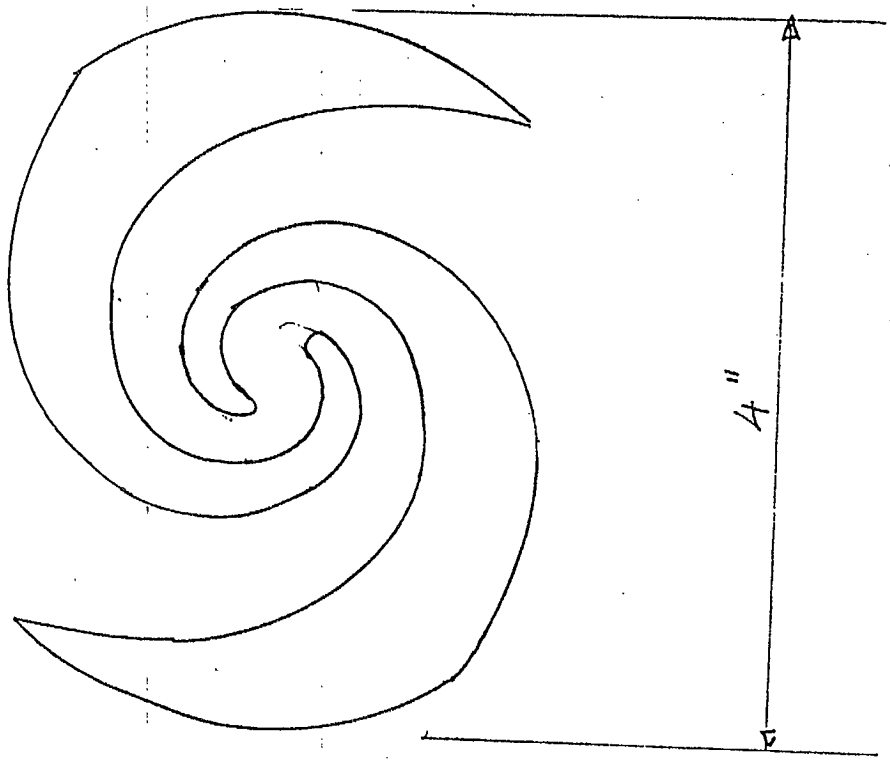

FIGURE 5.2.33 SPIRAL FEED FOR SBF ANTENNAS

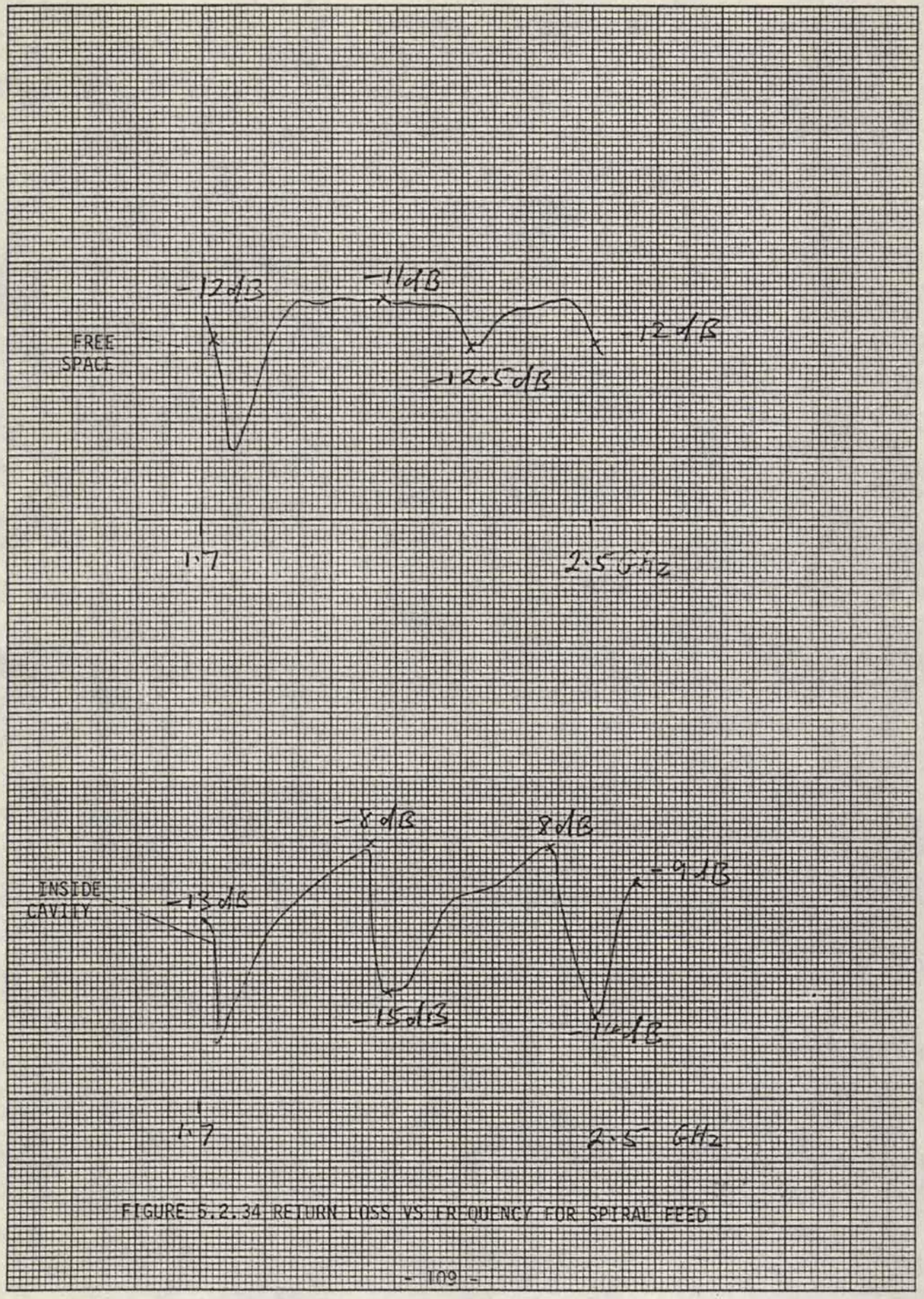

FIGURE 5.2.34 RETURN LOSS VS FREQUENCY FOR SPIRAL FEED

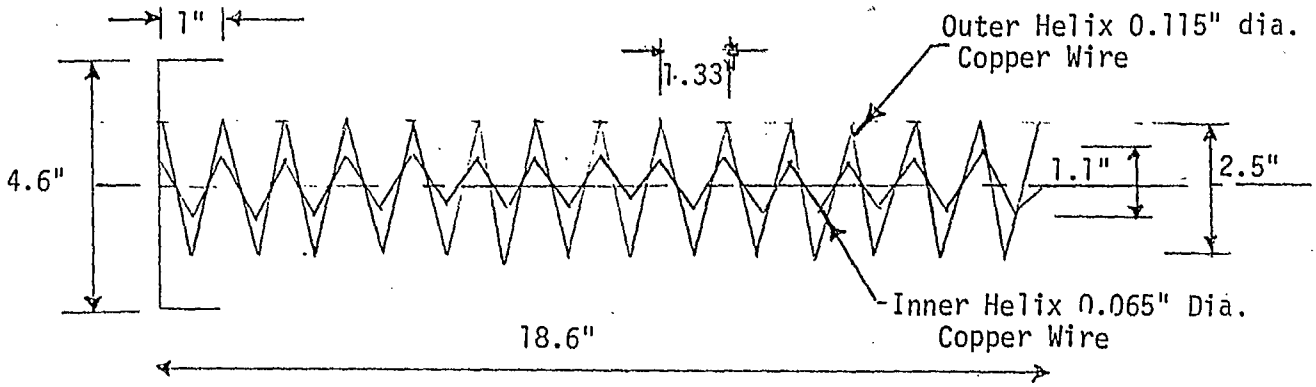

FIGURE 6.2.1 CO-AXIAL HELIX MODEL

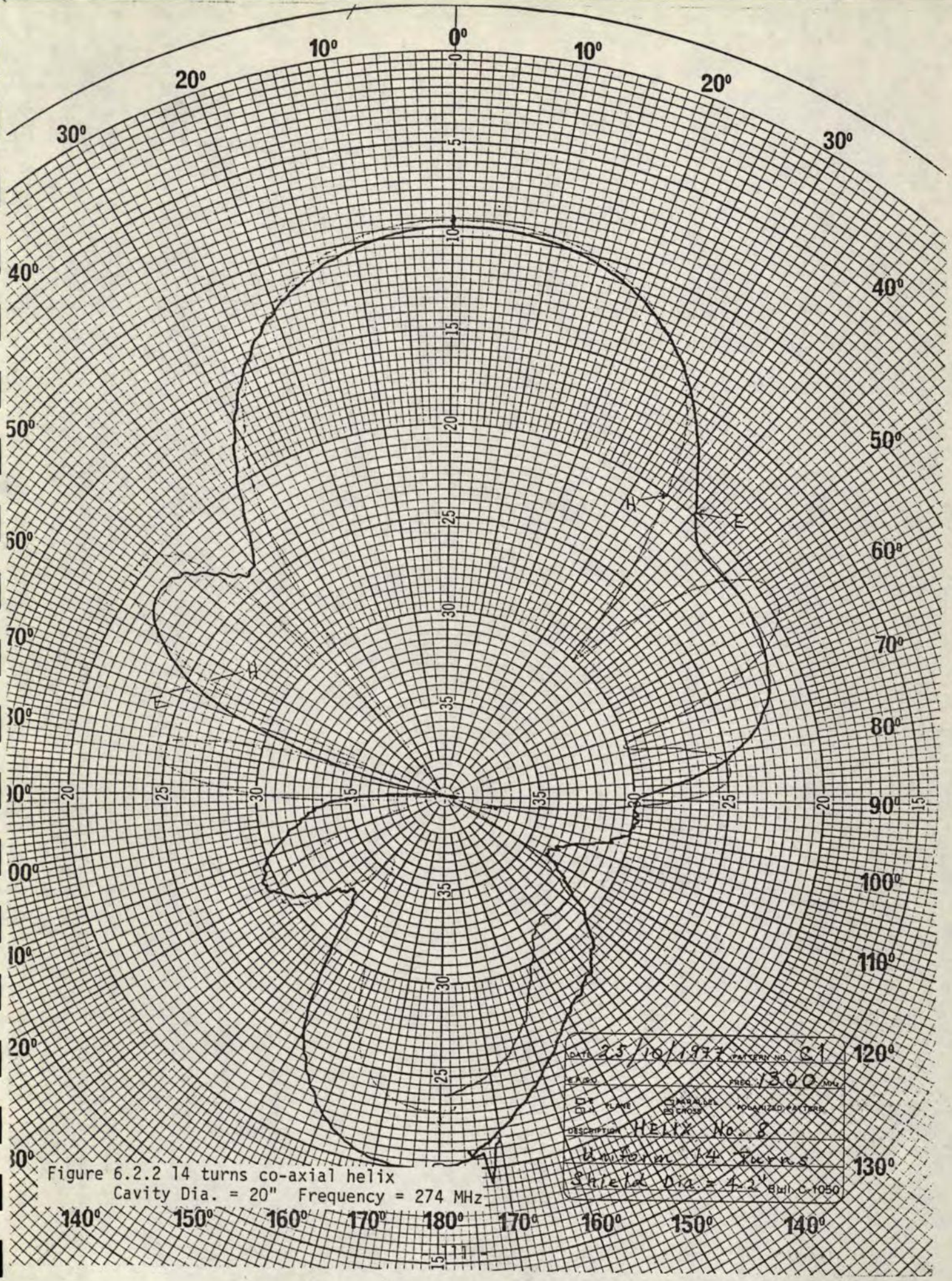

Figure 6.2.2 14 turns co-axial helix
Cavity Dia. = 20" Frequency = 274 MHz

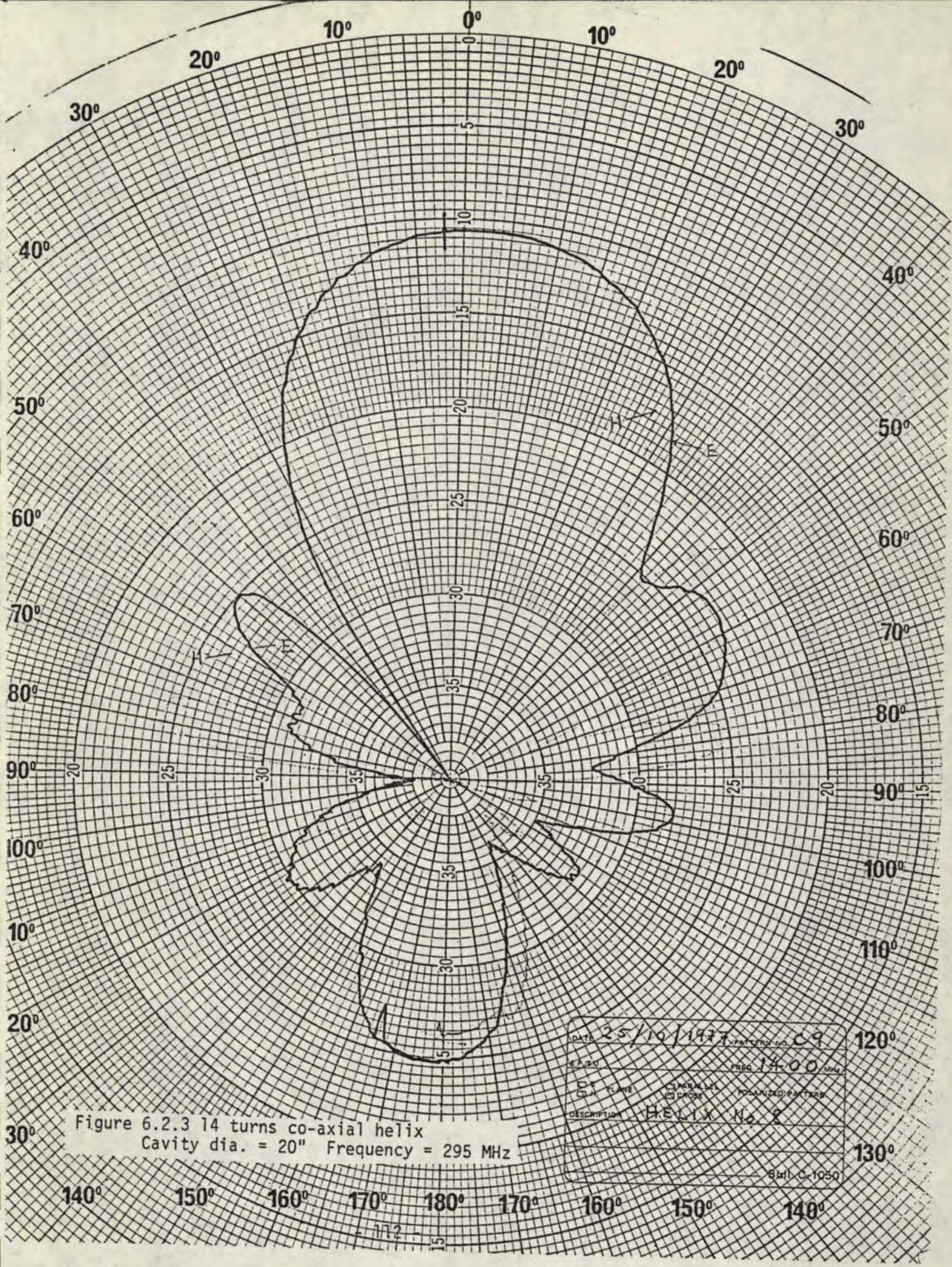

Figure 6.2.3 14 turns co-axial helix
Cavity dia. = 20" Frequency = 295 MHz

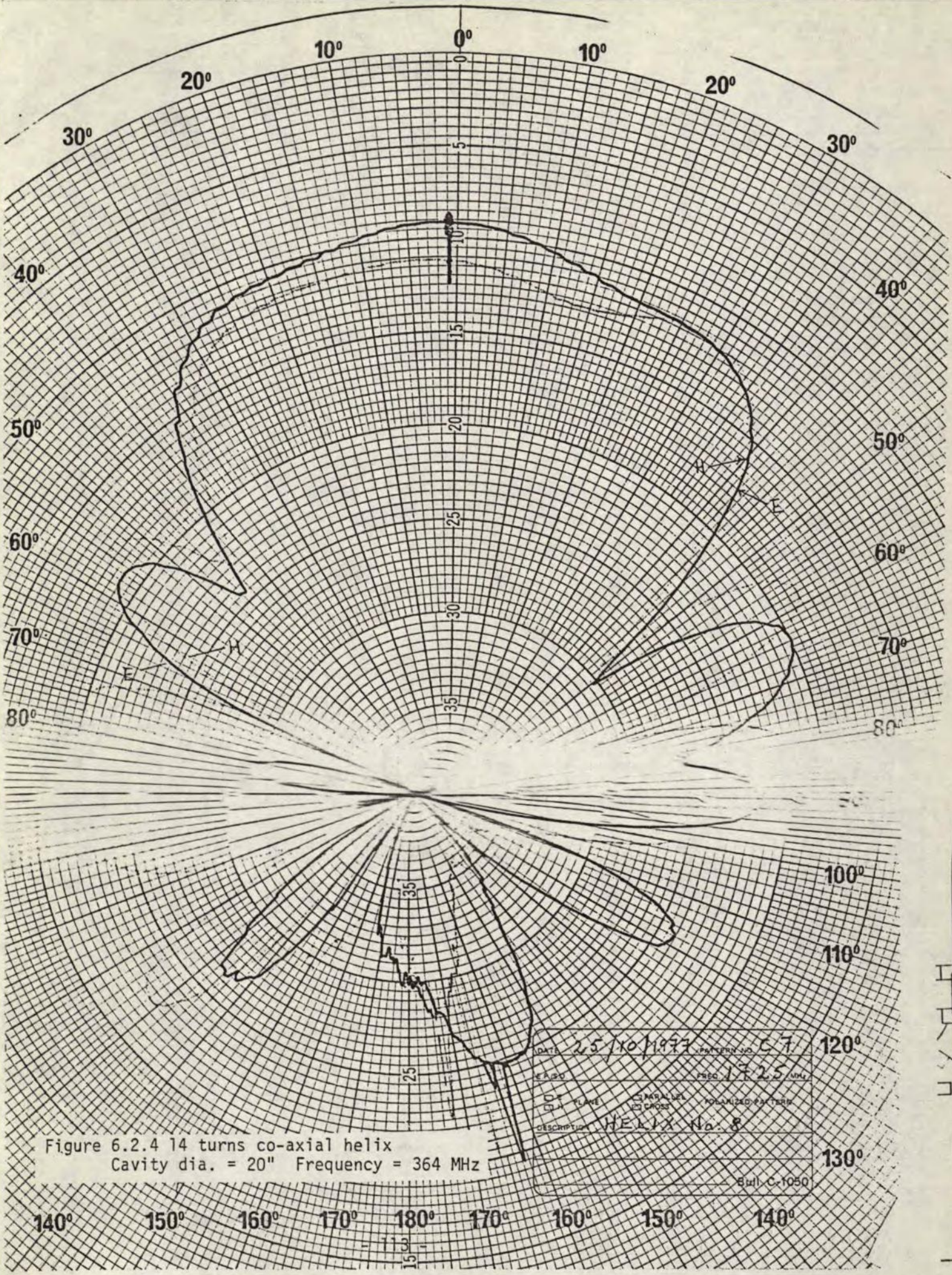

Figure 6.2.4 14 turns co-axial helix
Cavity dia. = 20" Frequency = 364 MHz

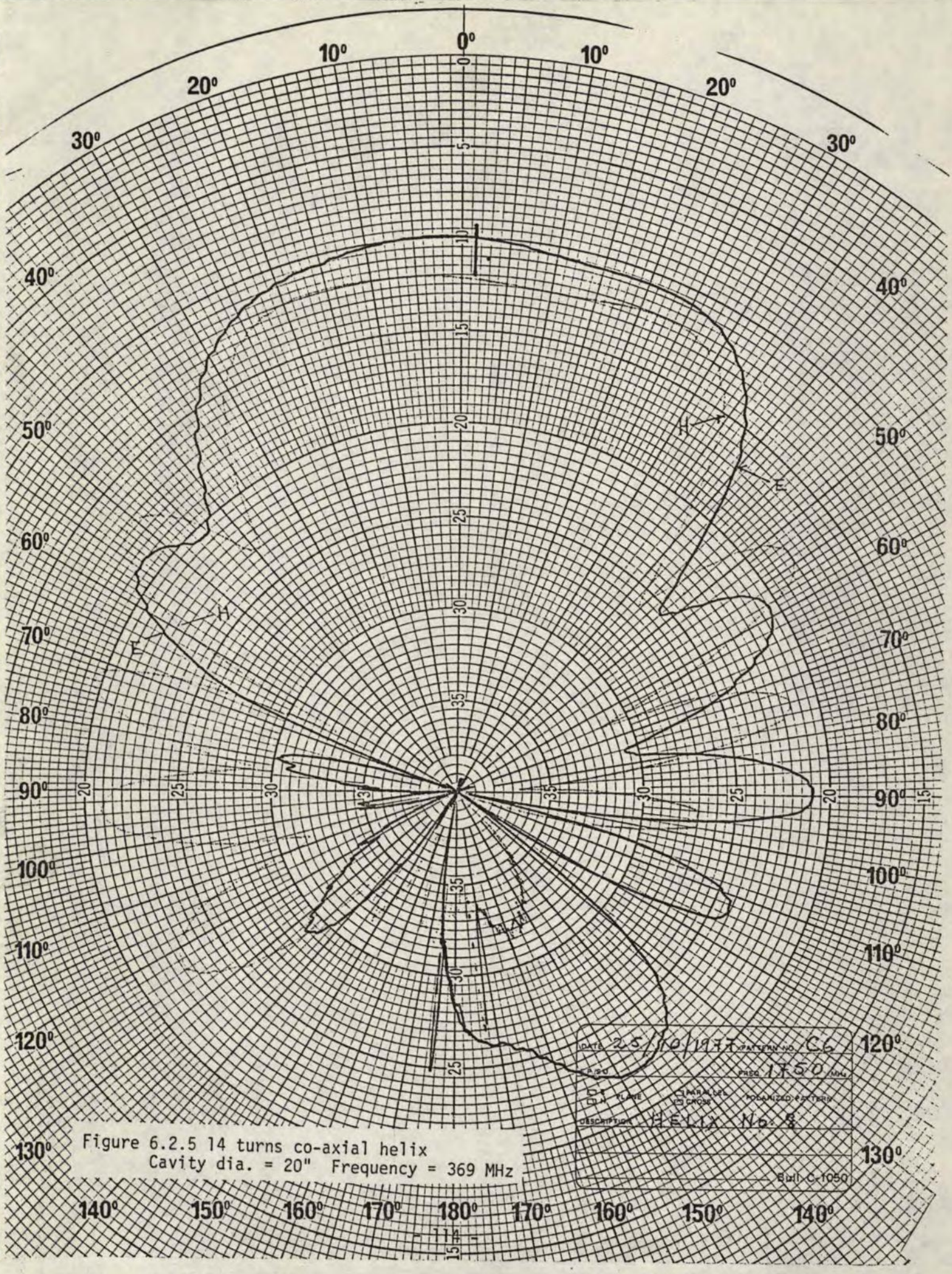

Figure 6.2.5 14 turns co-axial helix
Cavity dia. = 20" Frequency = 369 MHz

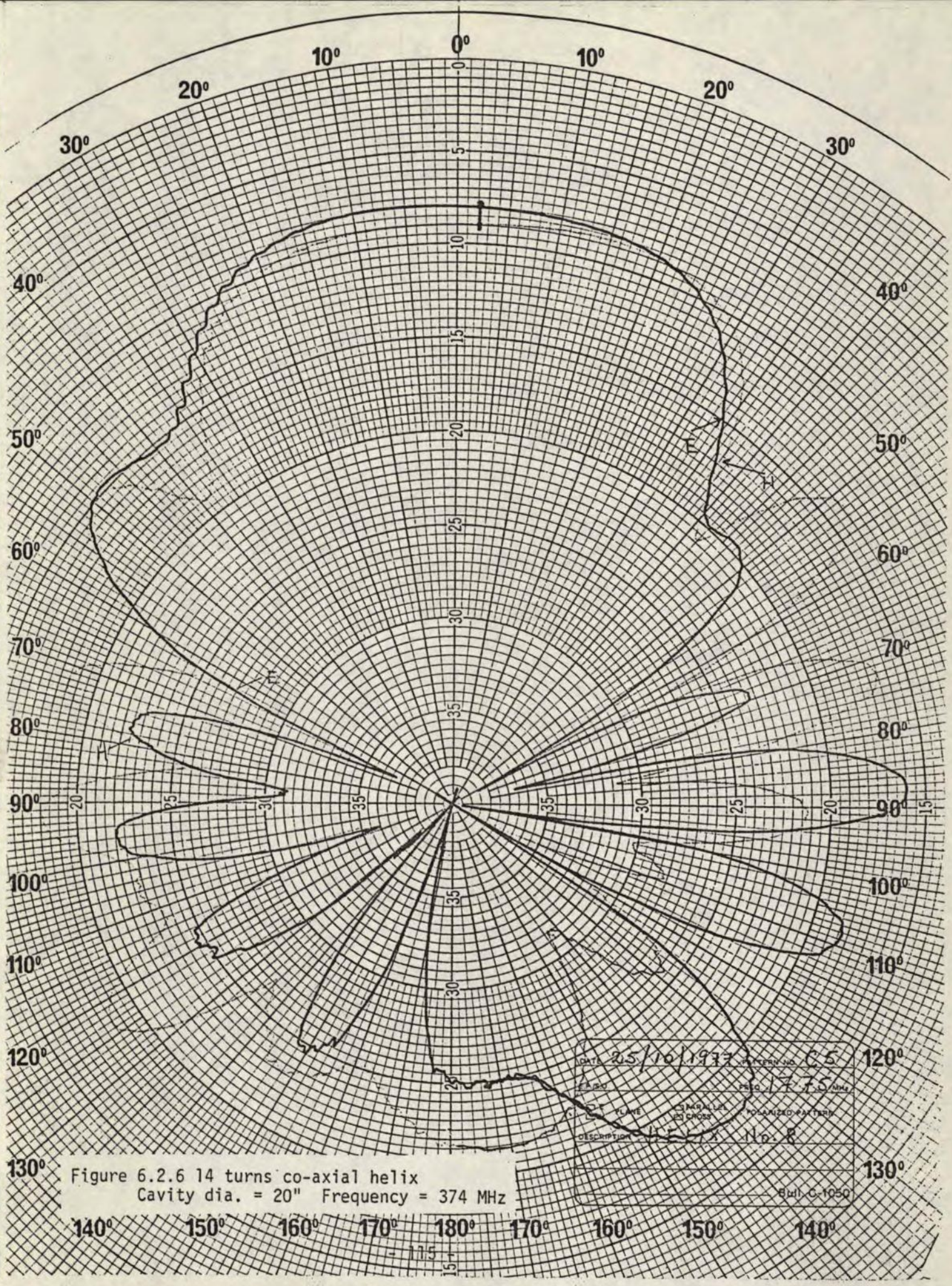

Figure 6.2.6 14 turns co-axial helix
Cavity dia. = 20" Frequency = 374 MHz

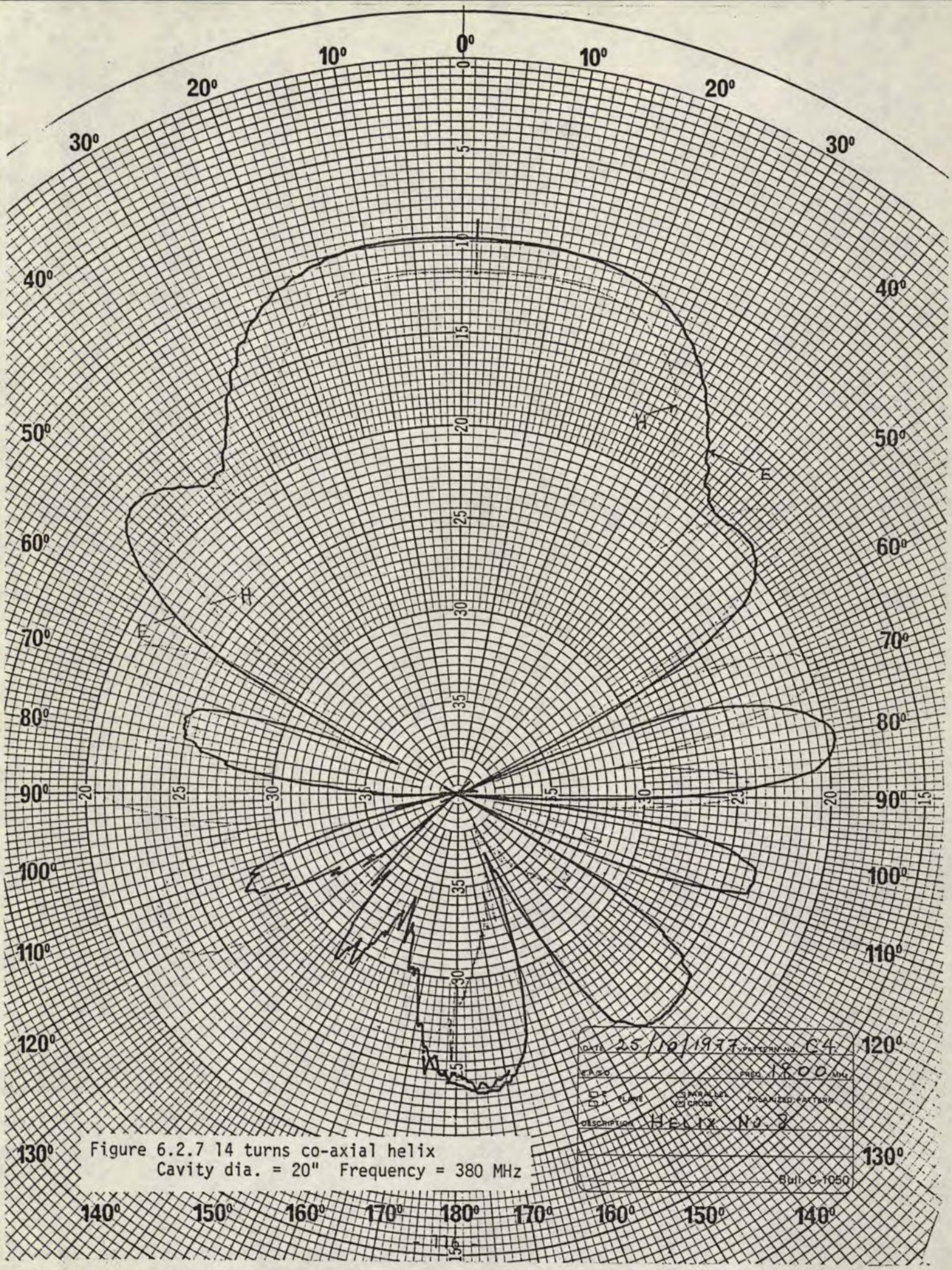

Figure 6.2.7 14 turns co-axial helix
Cavity dia. = 20" Frequency = 380 MHz

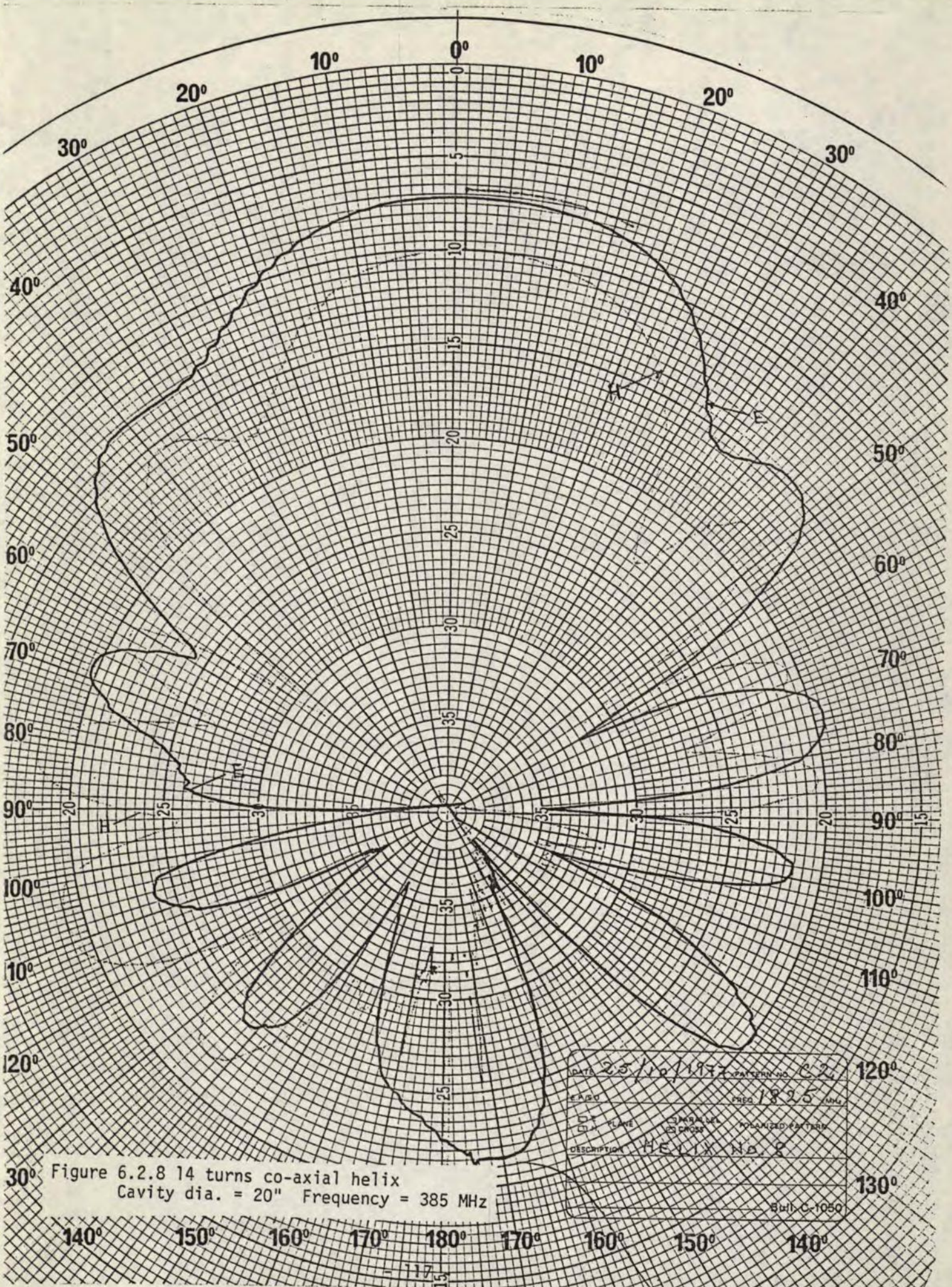

Figure 6.2.8 14 turns co-axial helix
Cavity dia. = 20" Frequency = 385 MHz

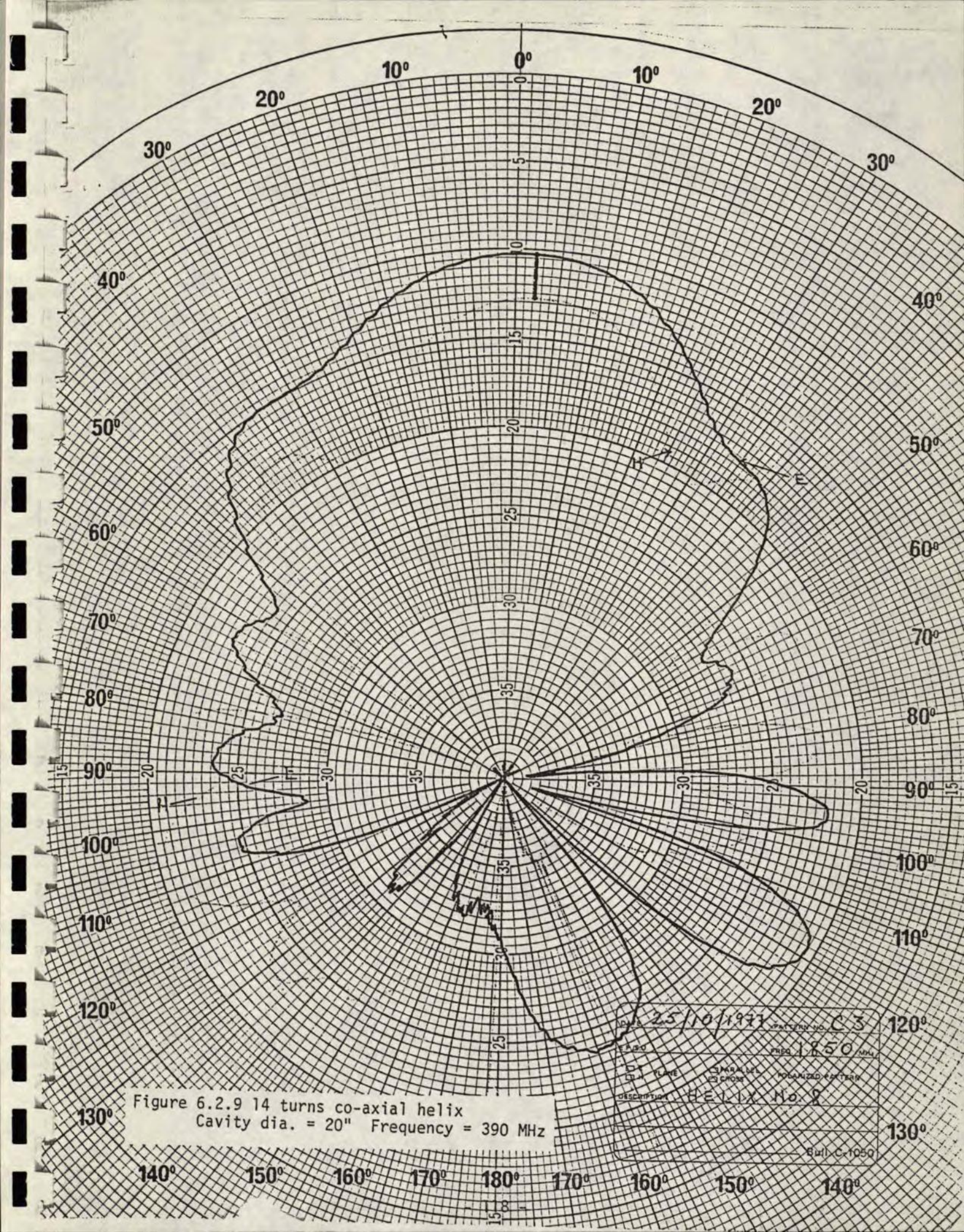

Figure 6.2.9 14 turns co-axial helix
Cavity dia. = 20" Frequency = 390 MHz

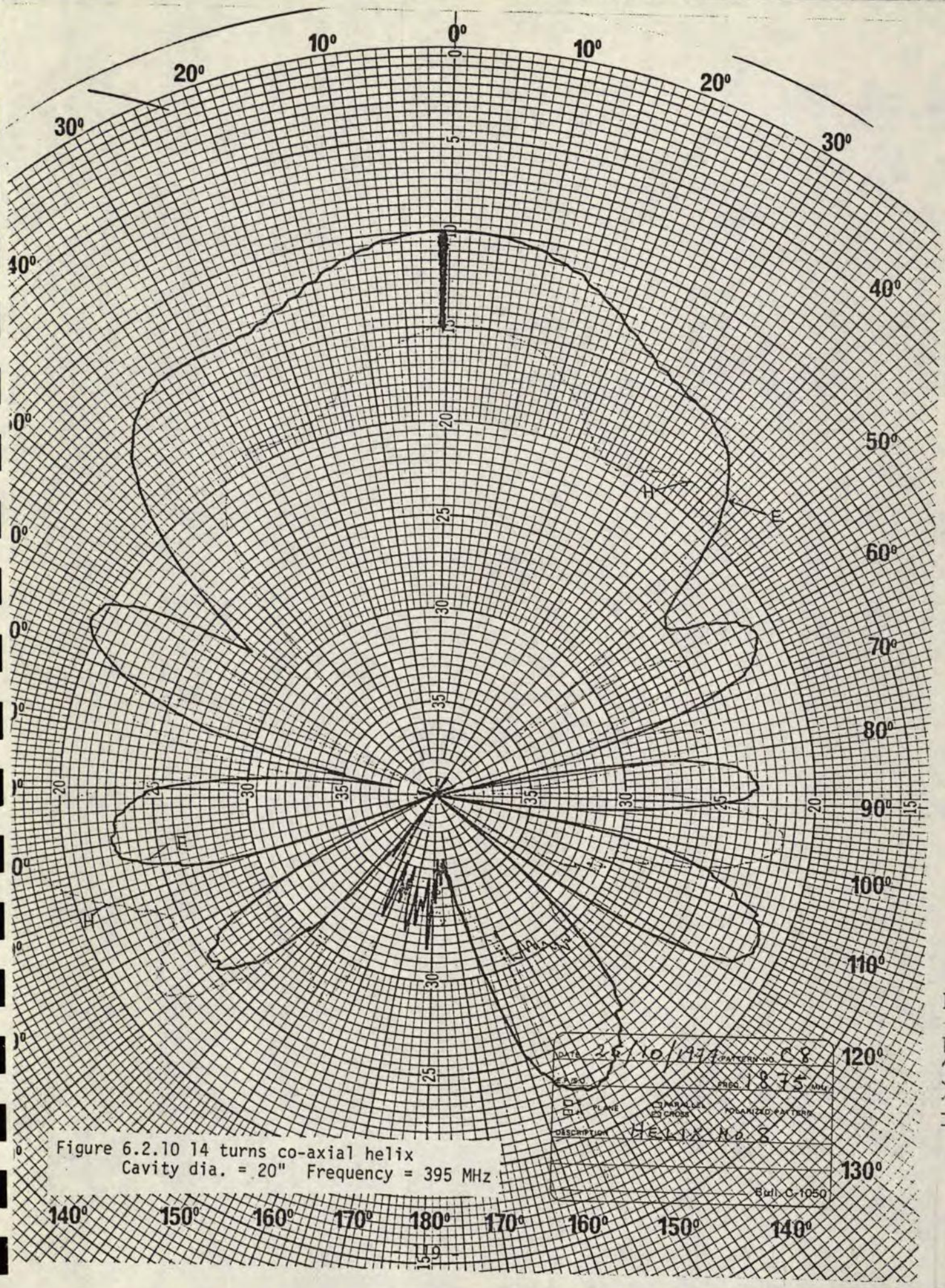

Figure 6.2.10 14 turns co-axial helix
Cavity dia. = 20" Frequency = 395 MHz

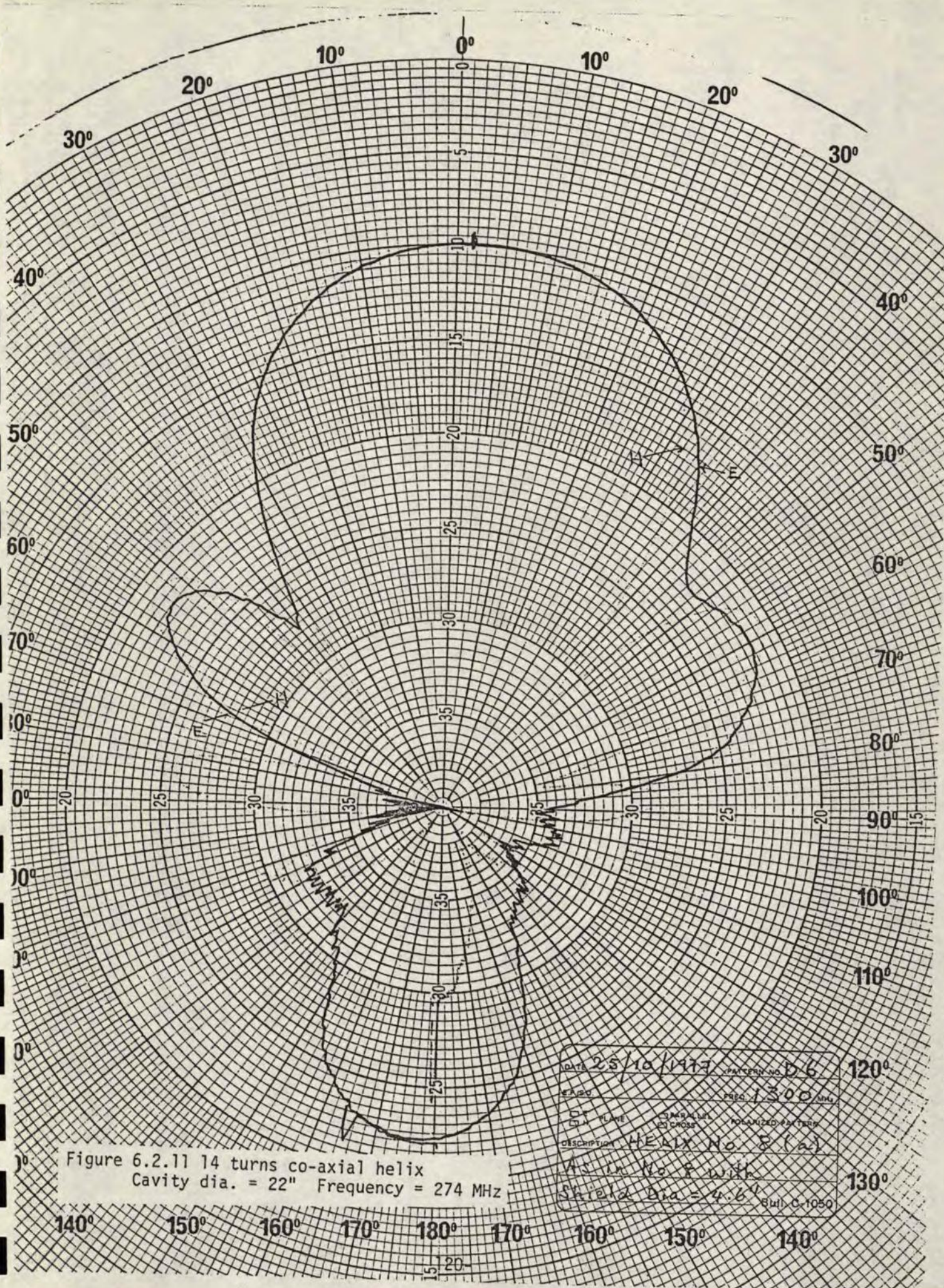

Figure 6.2.11 14 turns co-axial helix
Cavity dia. = 22" Frequency = 274 MHz

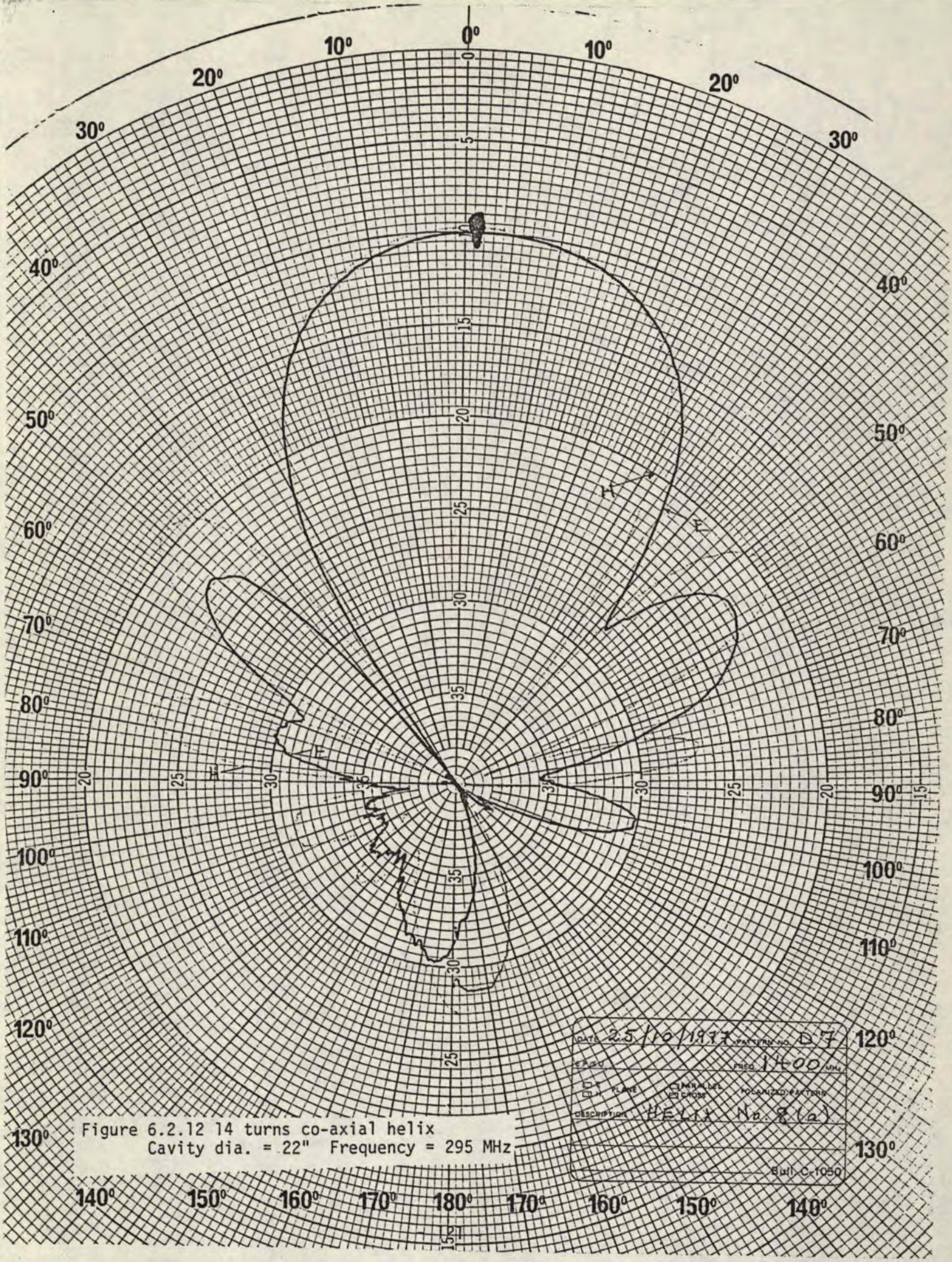

Figure 6.2.12 14 turns co-axial helix
Cavity dia. = 22" Frequency = 295 MHz

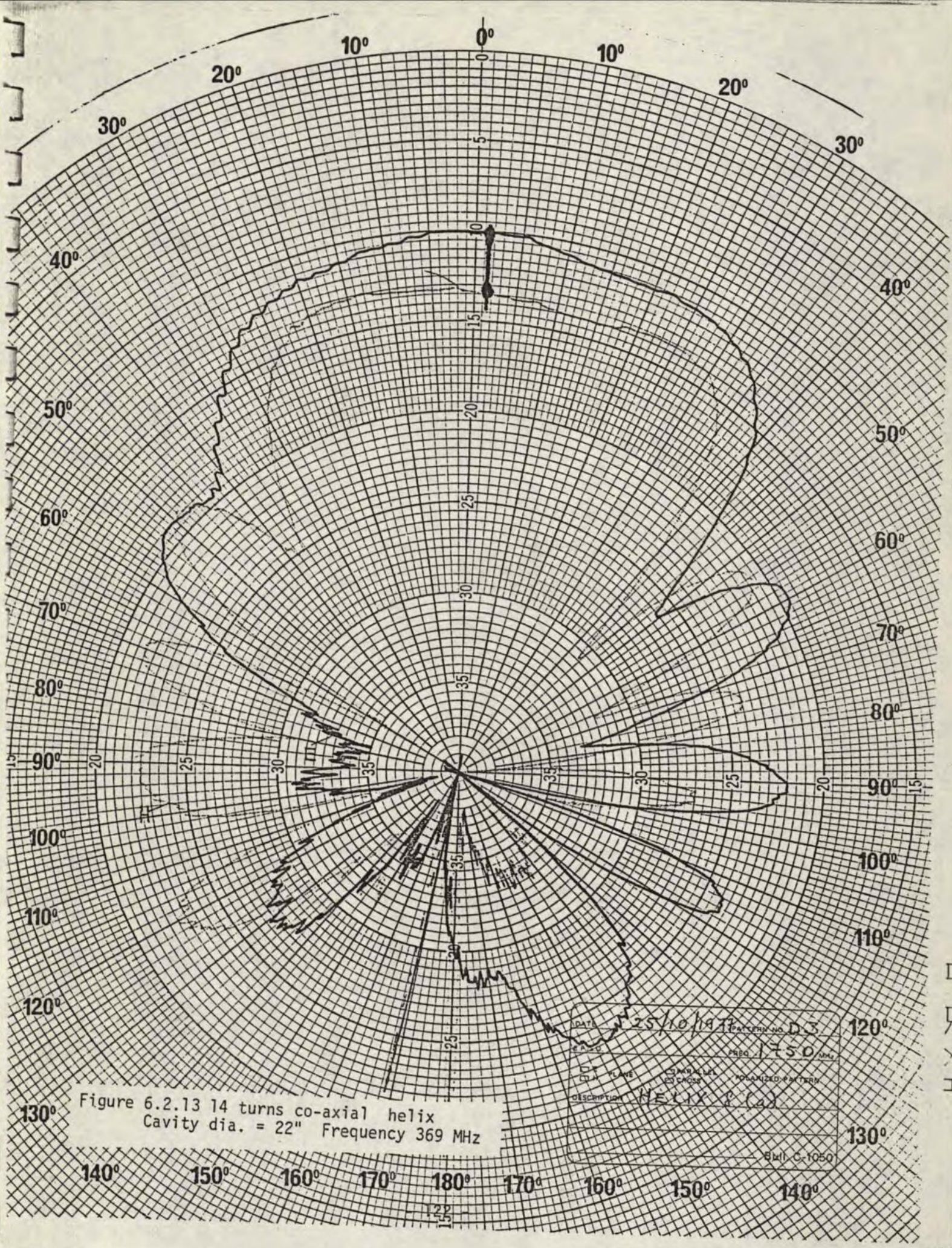

Figure 6.2.13 14 turns co-axial helix
Cavity dia. = 22" Frequency 369 MHz

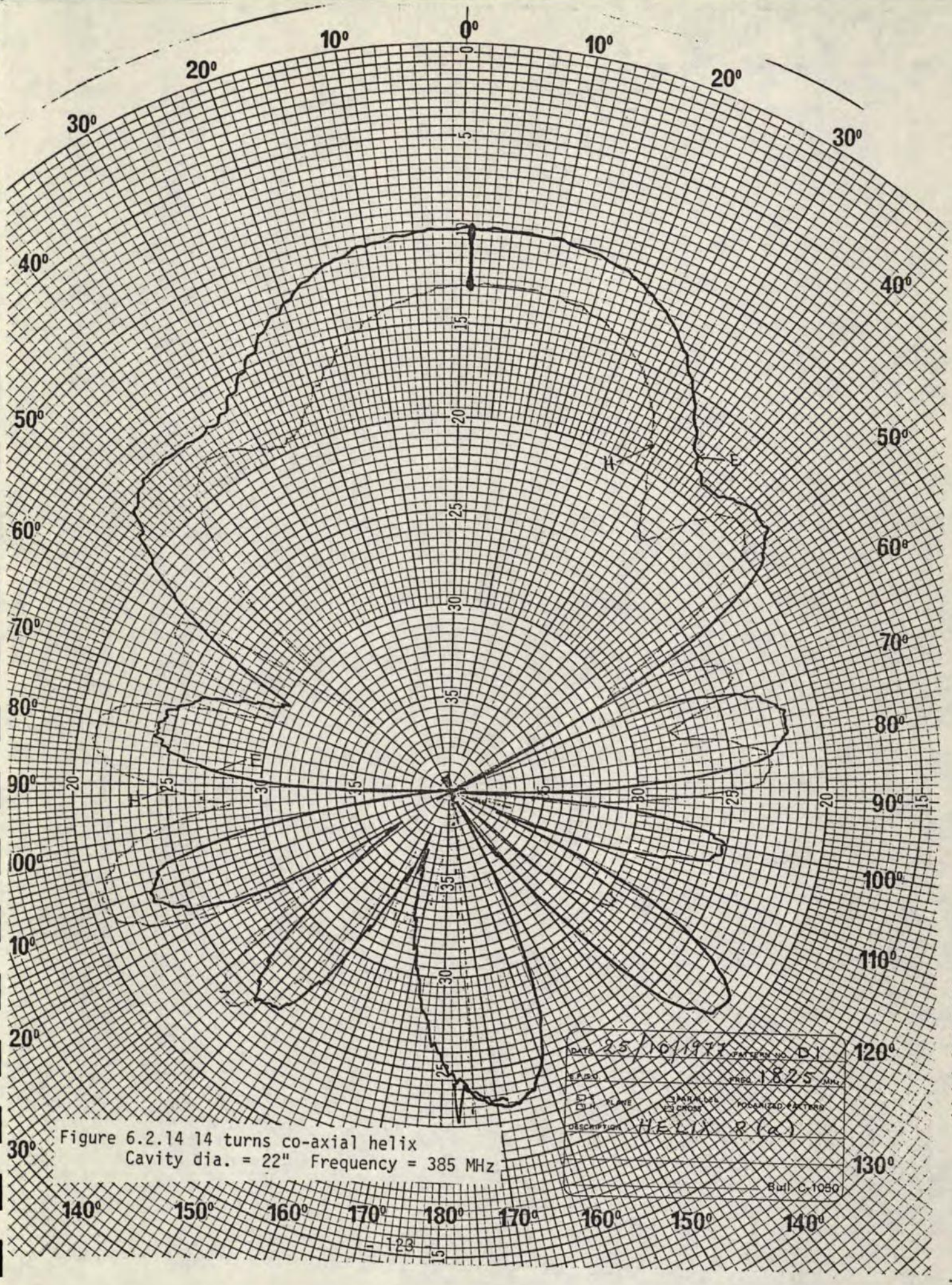

Figure 6.2.14 14 turns co-axial helix
Cavity dia. = 22" Frequency = 385 MHz

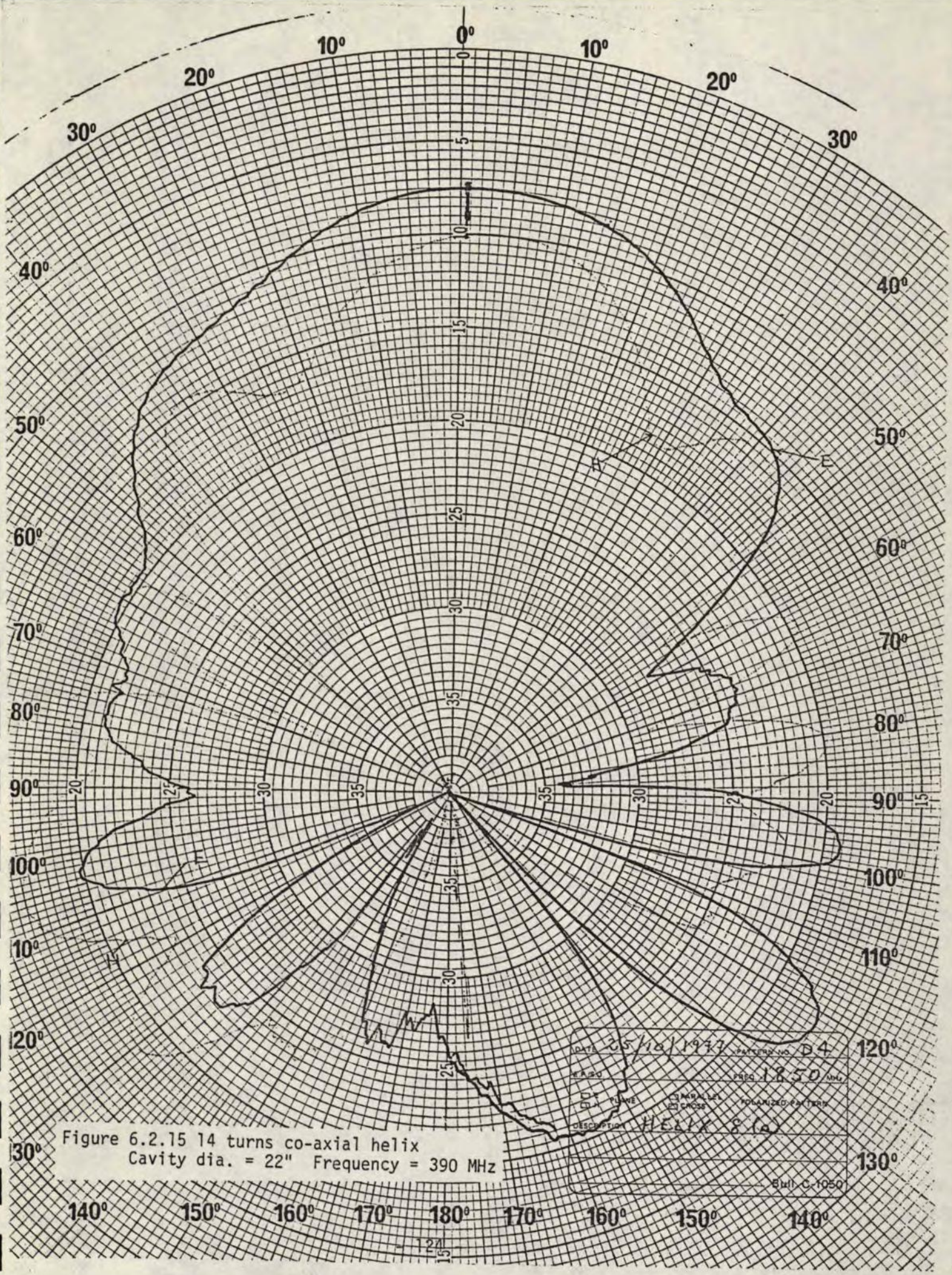

Figure 6.2.15 14 turns co-axial helix
Cavity dia. = 22" Frequency = 390 MHz

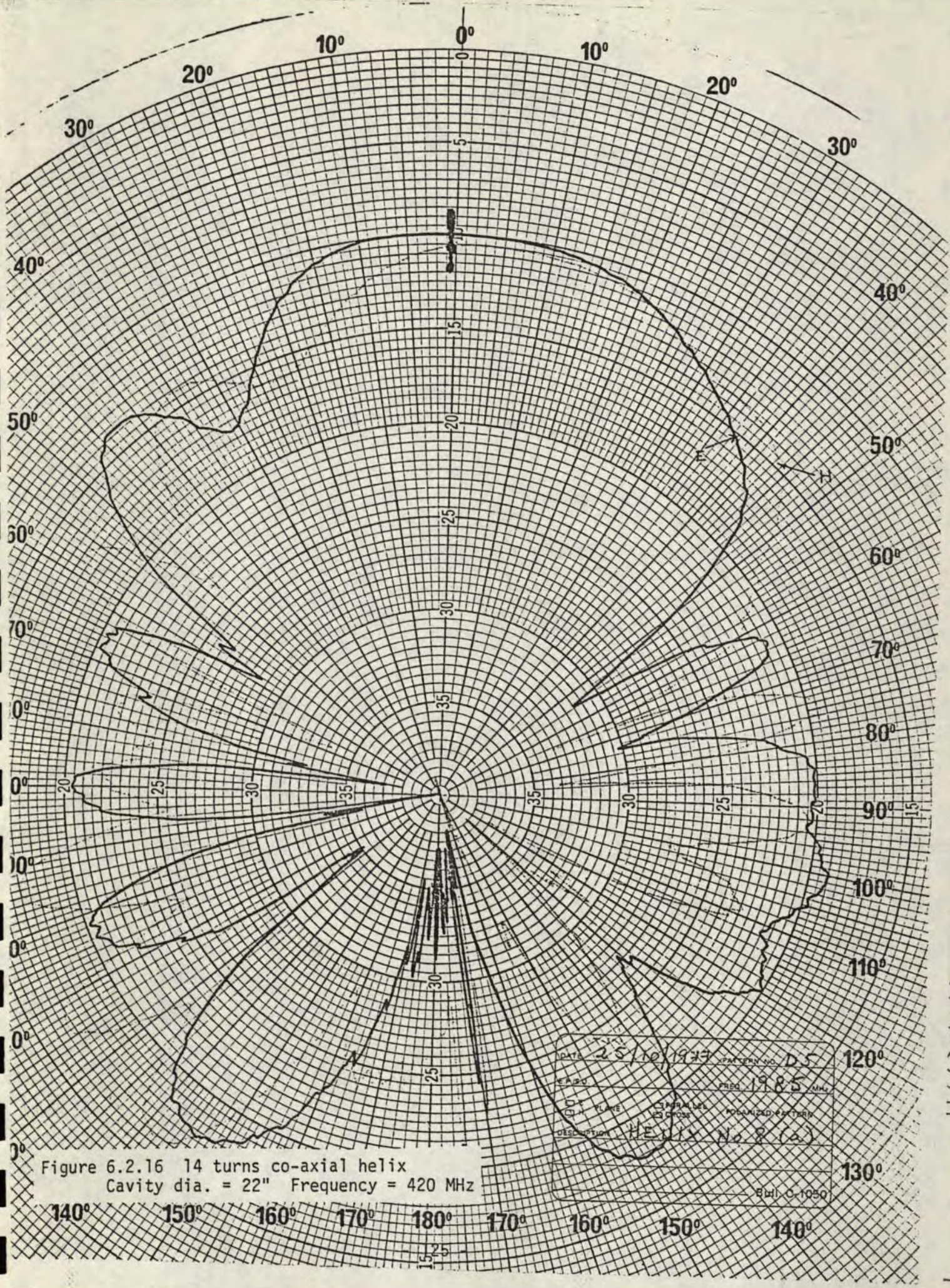

Figure 6.2.16 14 turns co-axial helix
Cavity dia. = 22" Frequency = 420 MHz

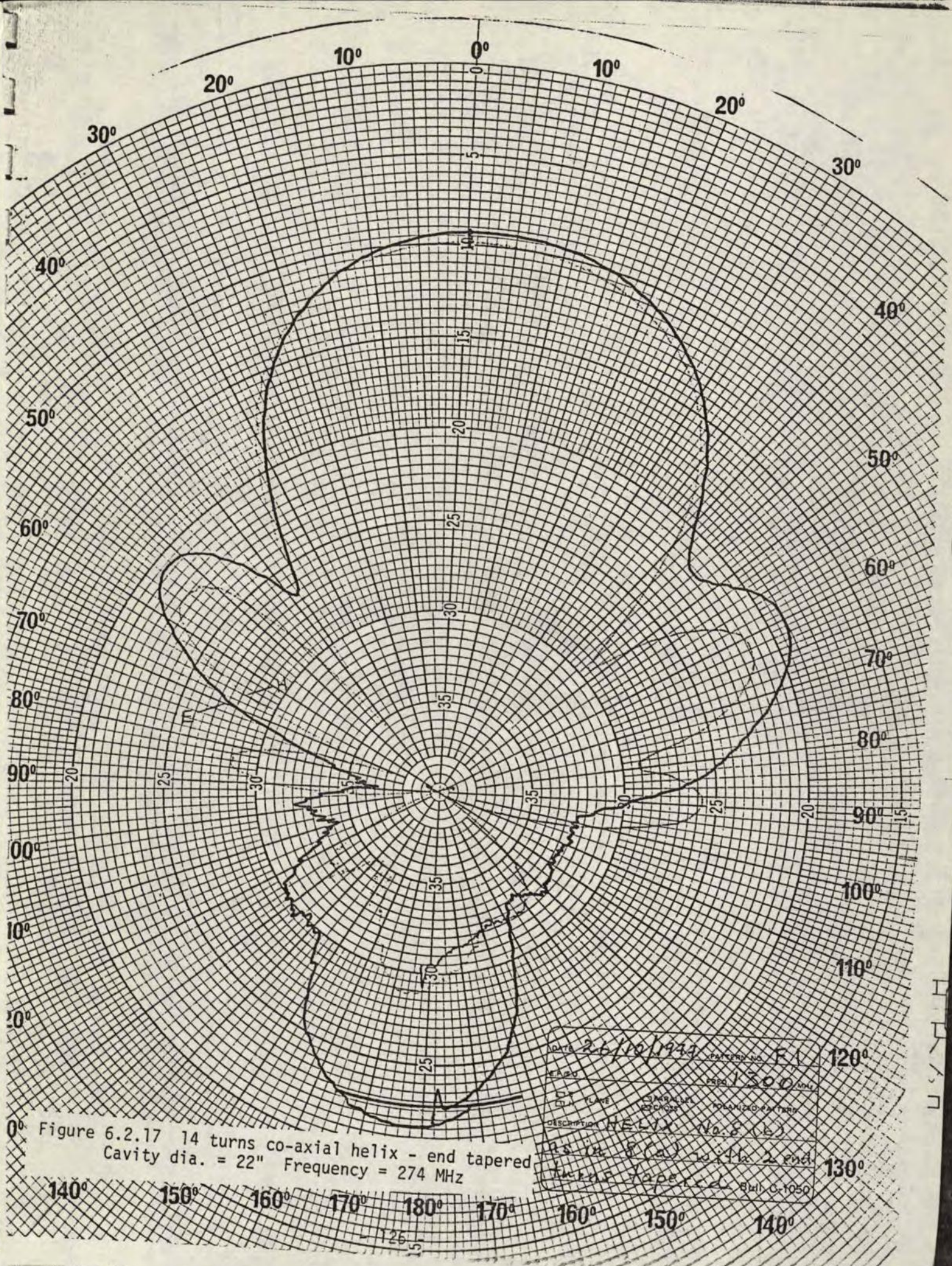

Figure 6.2.17 14 turns co-axial helix - end tapered
Cavity dia. = 22" Frequency = 274 MHz

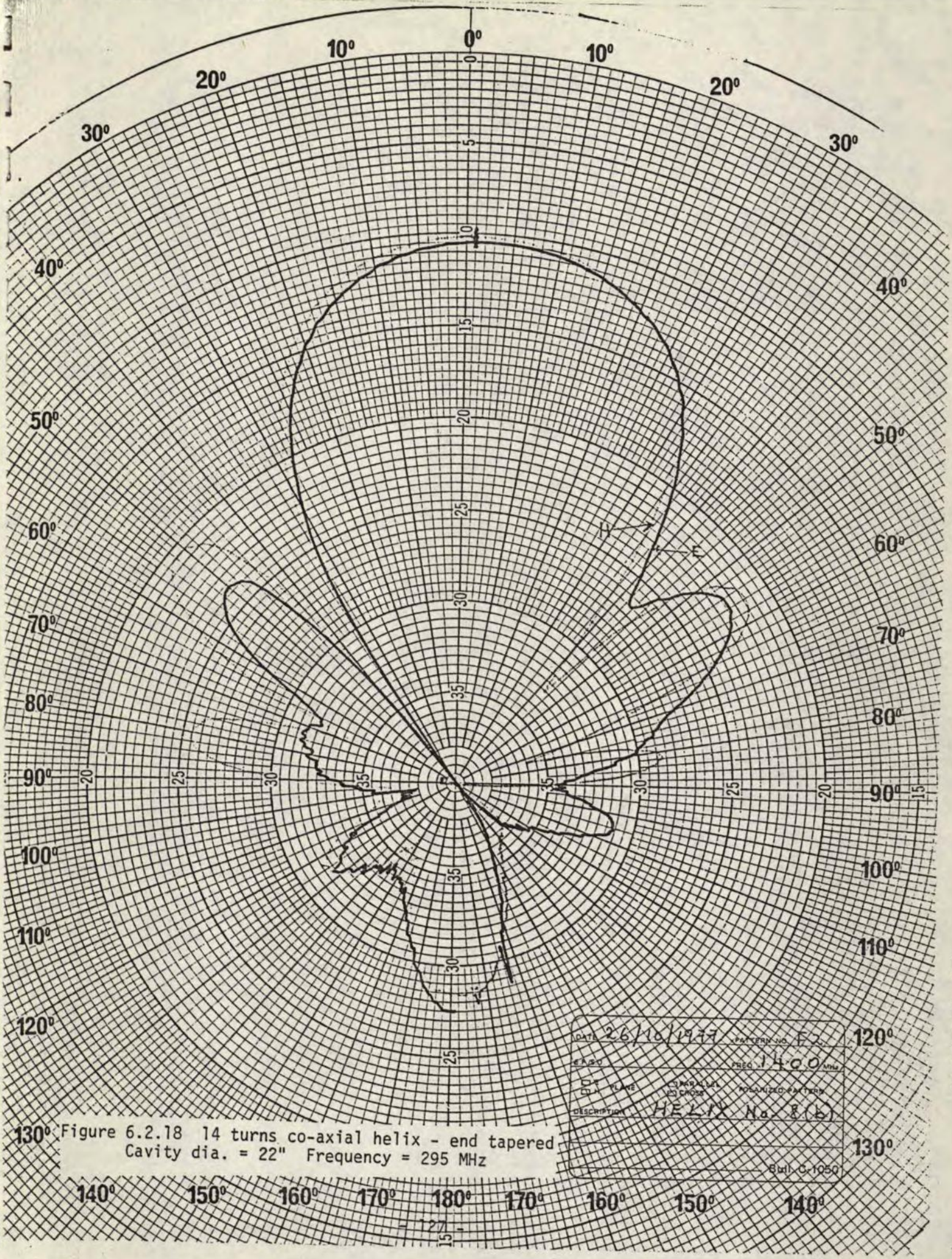

Figure 6.2.18 14 turns co-axial helix - end tapered
Cavity dia. = 22" Frequency = 295 MHz

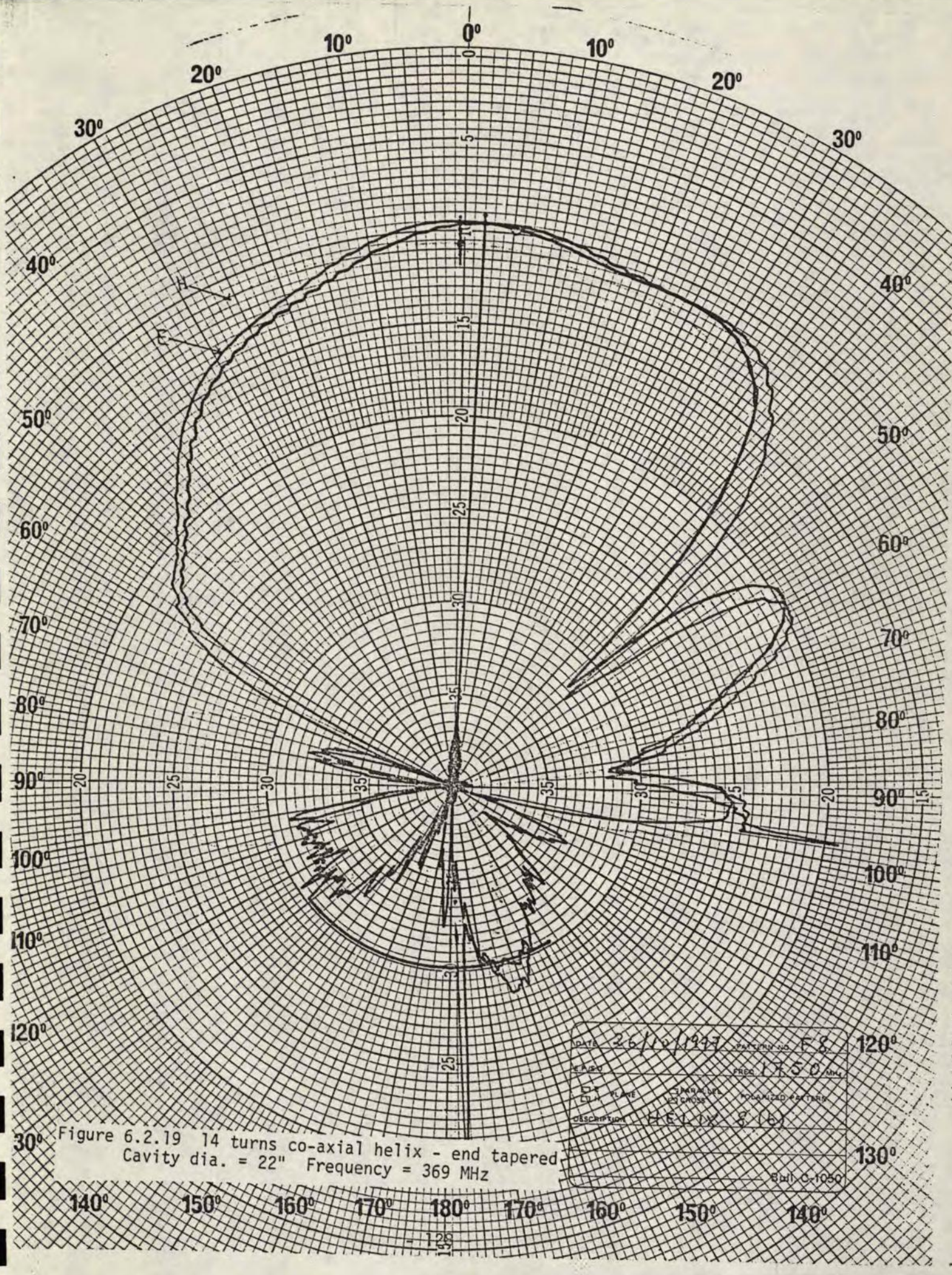

Figure 6.2.19 14 turns co-axial helix - end tapered
Cavity dia. = 22" Frequency = 369 MHz

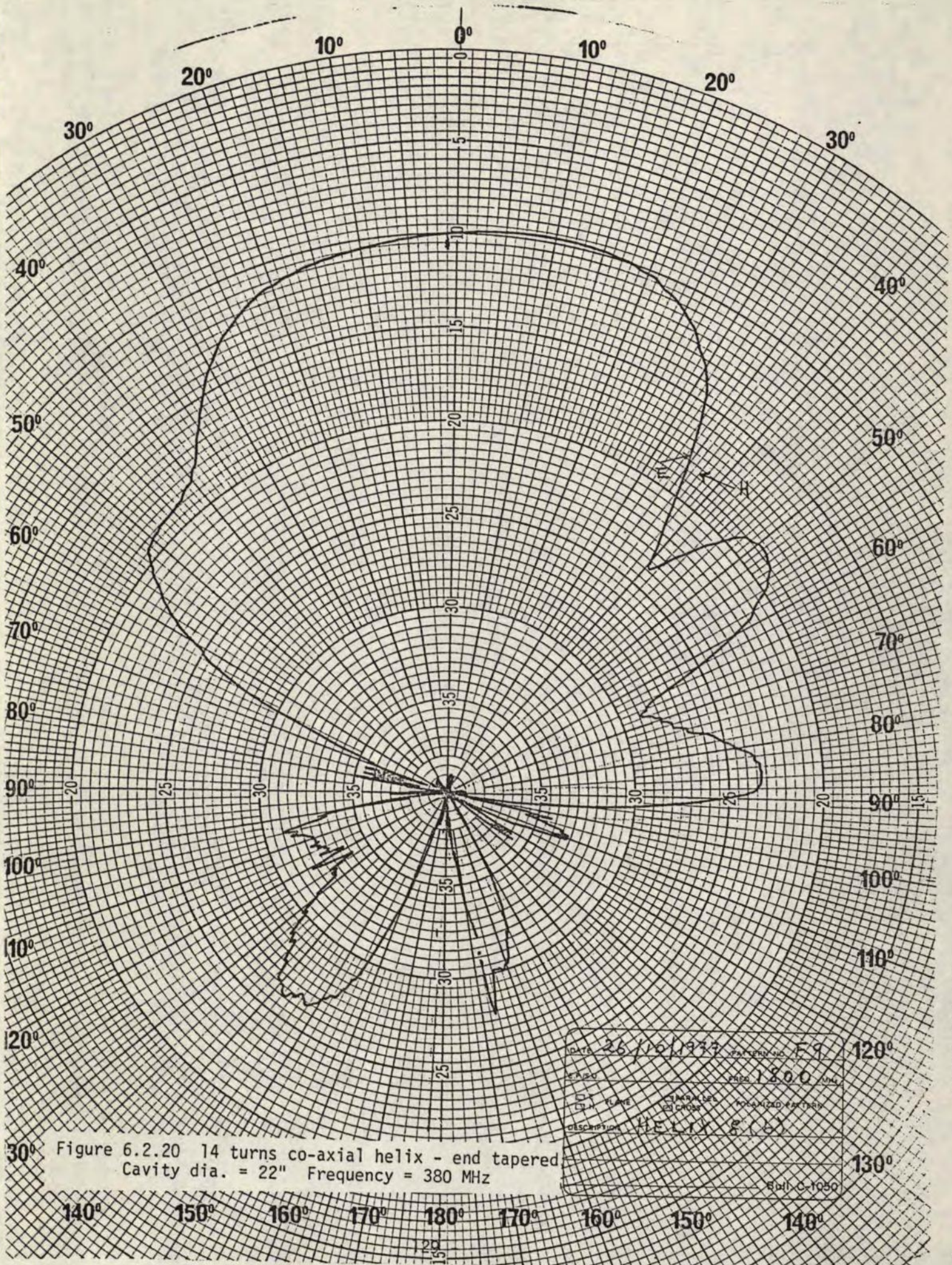

Figure 6.2.20 14 turns co-axial helix - end tapered
Cavity dia. = 22" Frequency = 380 MHz

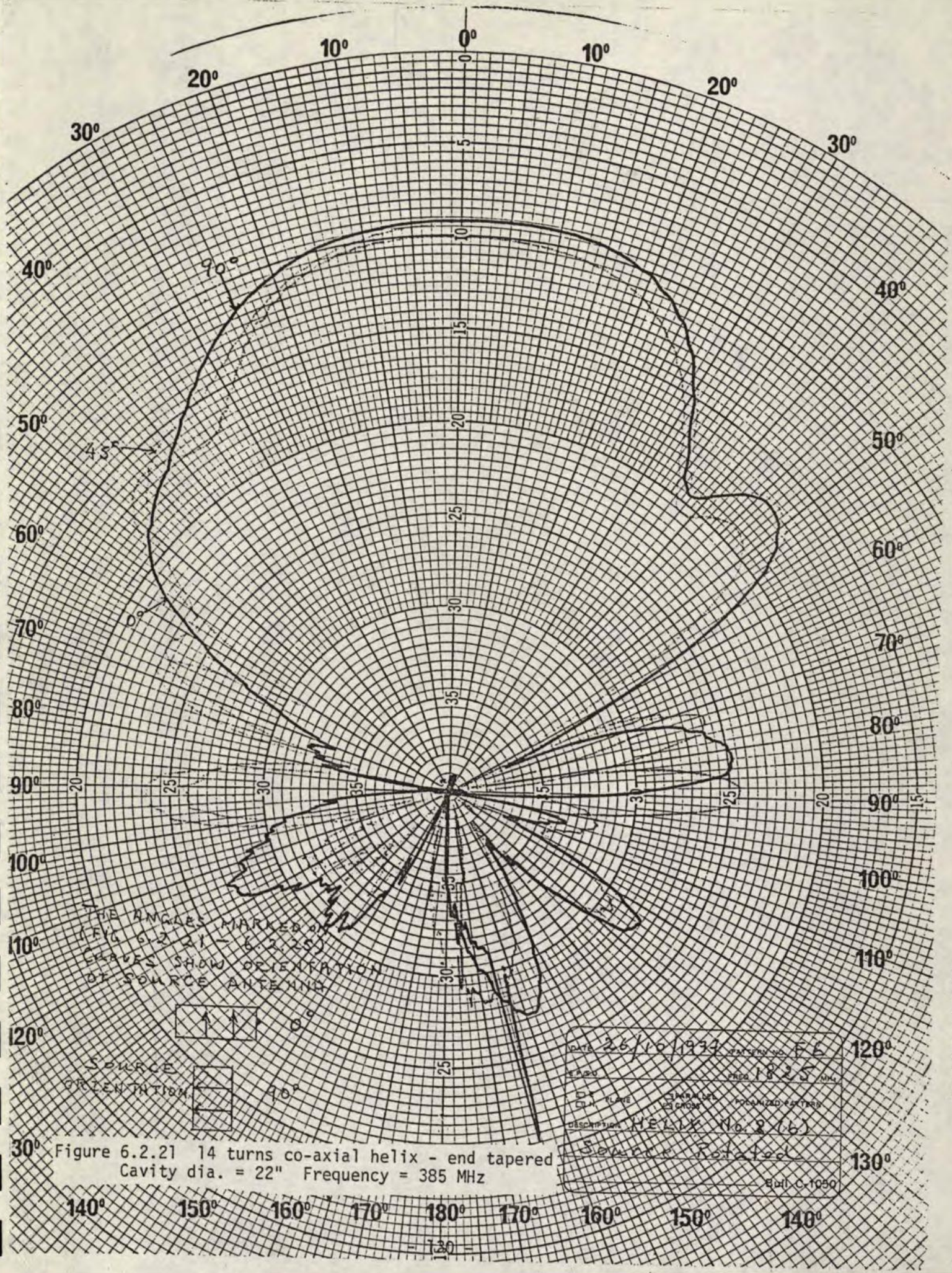

Figure 6.2.21 14 turns co-axial helix - end tapered
Cavity dia. = 22" Frequency = 385 MHz

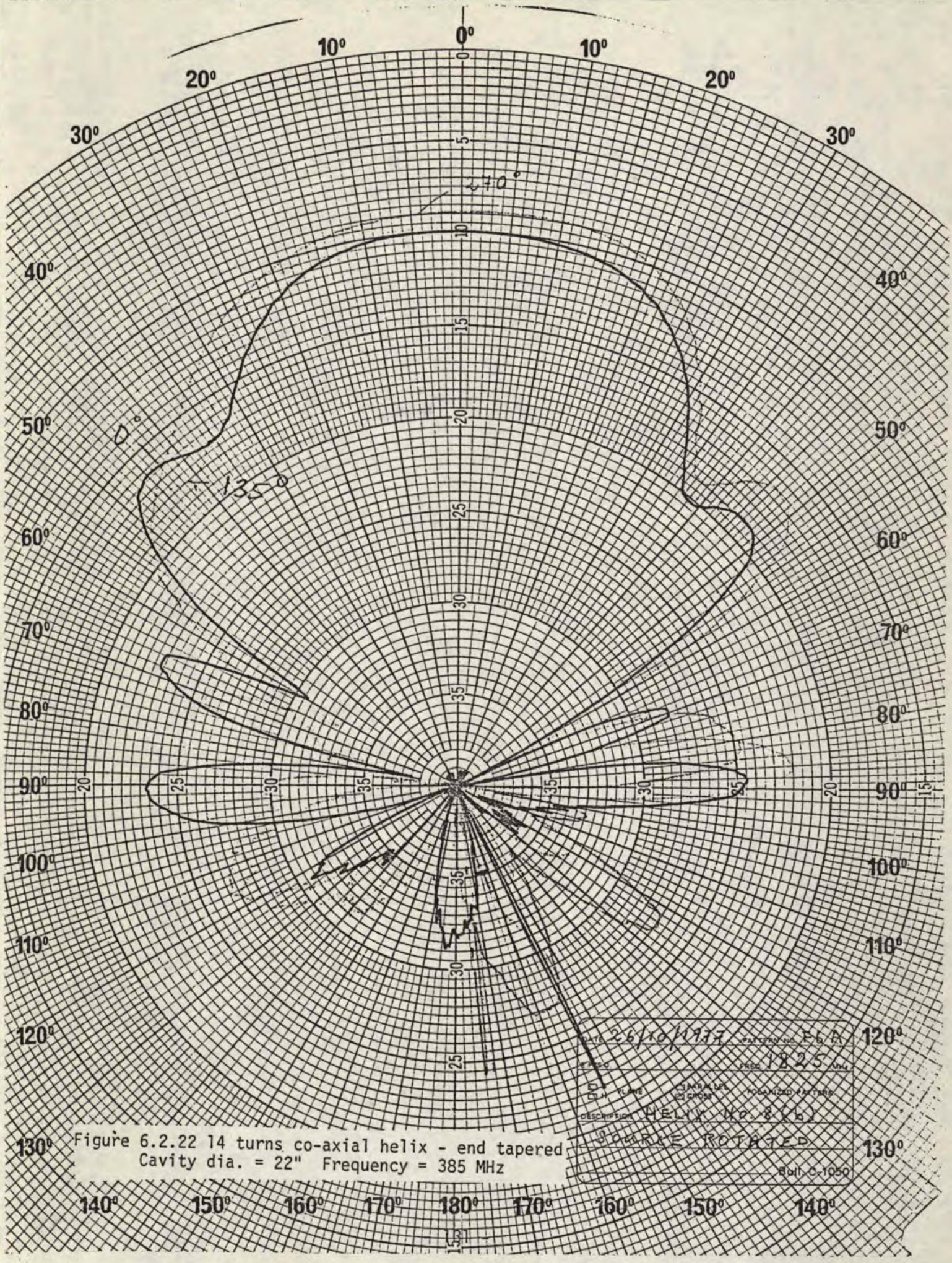

Figure 6.2.22 14 turns co-axial helix - end tapered
Cavity dia. = 22" Frequency = 385 MHz

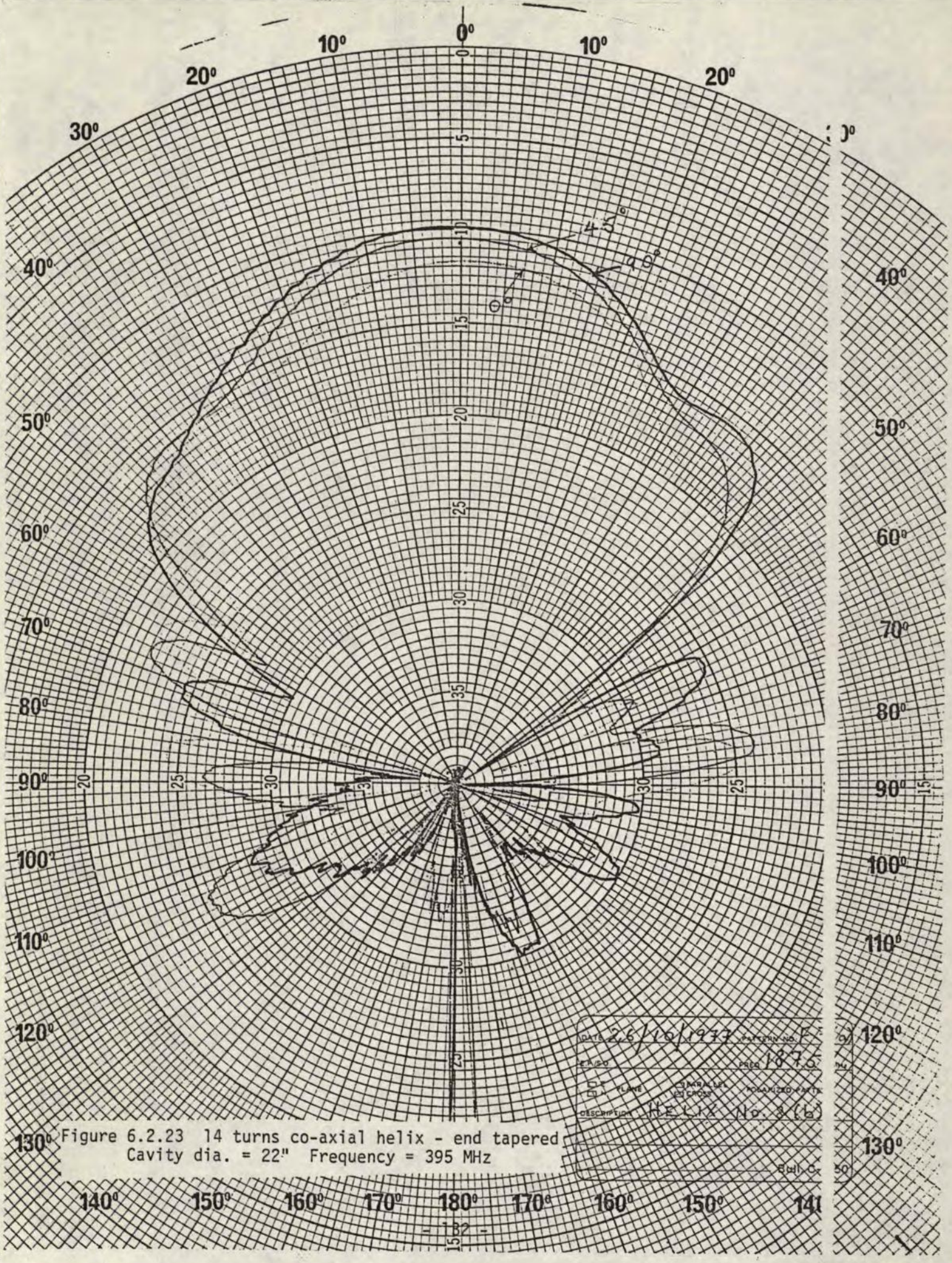

Figure 6.2.23 14 turns co-axial helix - end tapered
Cavity dia. = 22" Frequency = 395 MHz

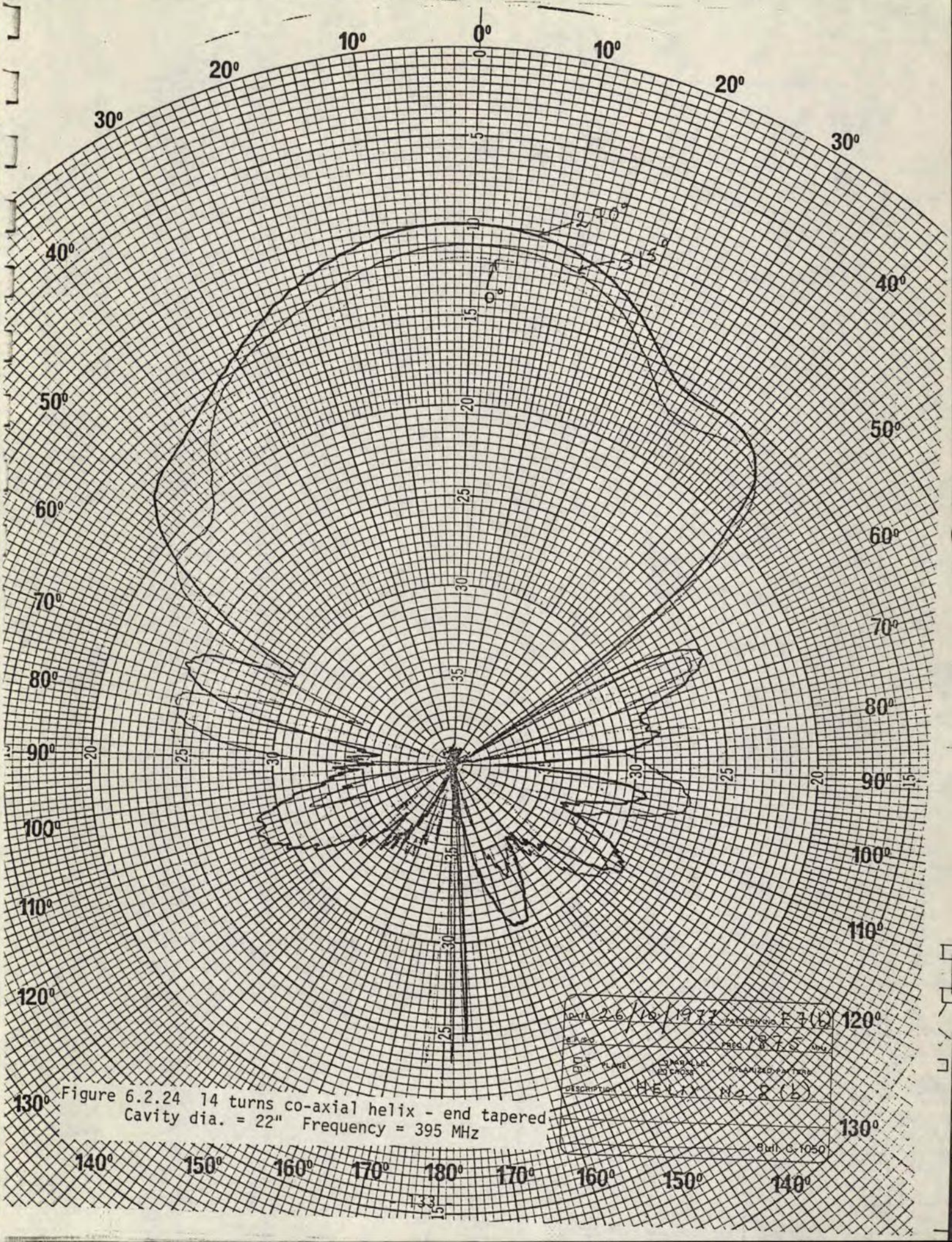

Figure 6.2.24 14 turns co-axial helix - end tapered
Cavity dia. = 22" Frequency = 395 MHz

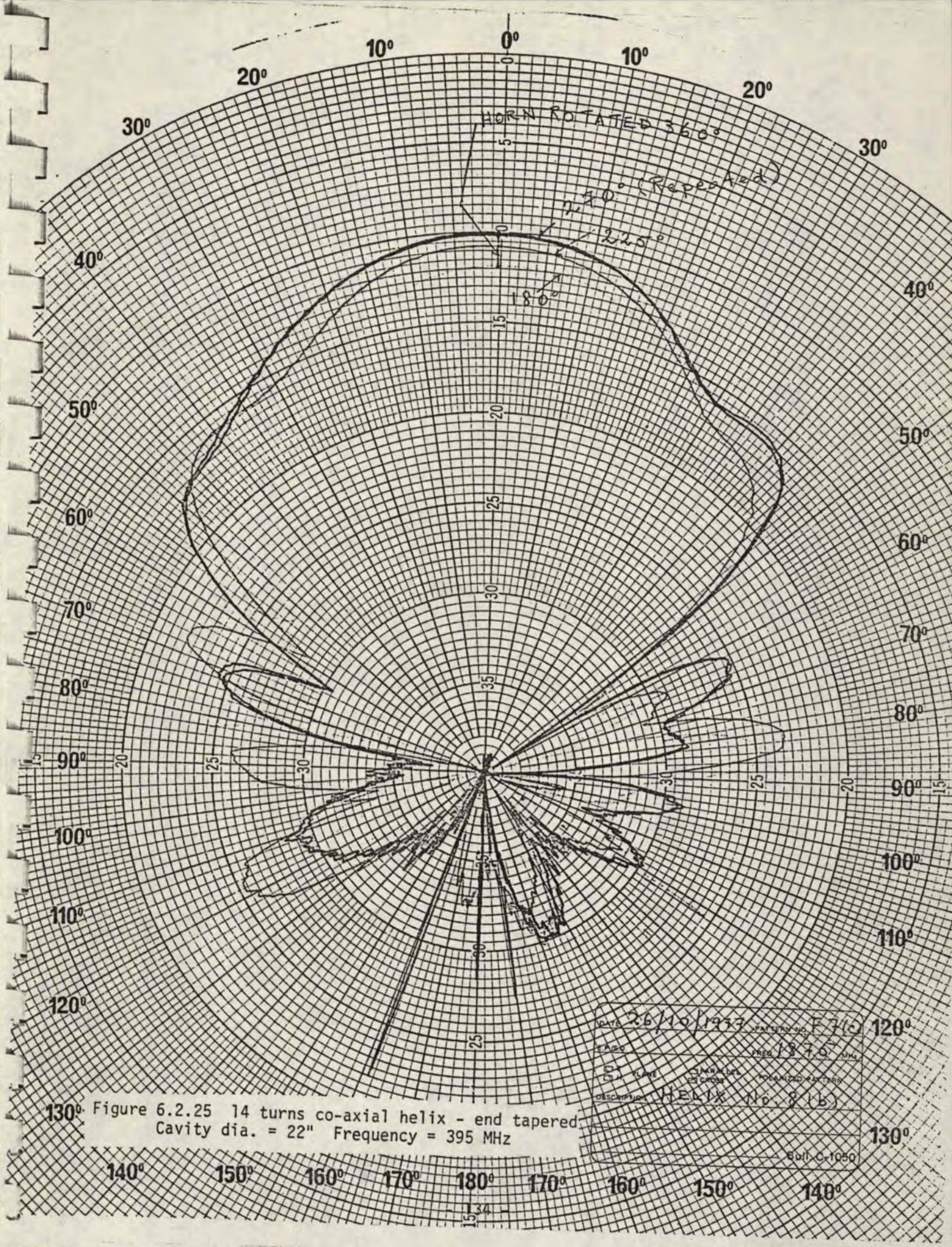

Figure 6.2.25 14 turns co-axial helix - end tapered
Cavity dia. = 22" Frequency = 395 MHz

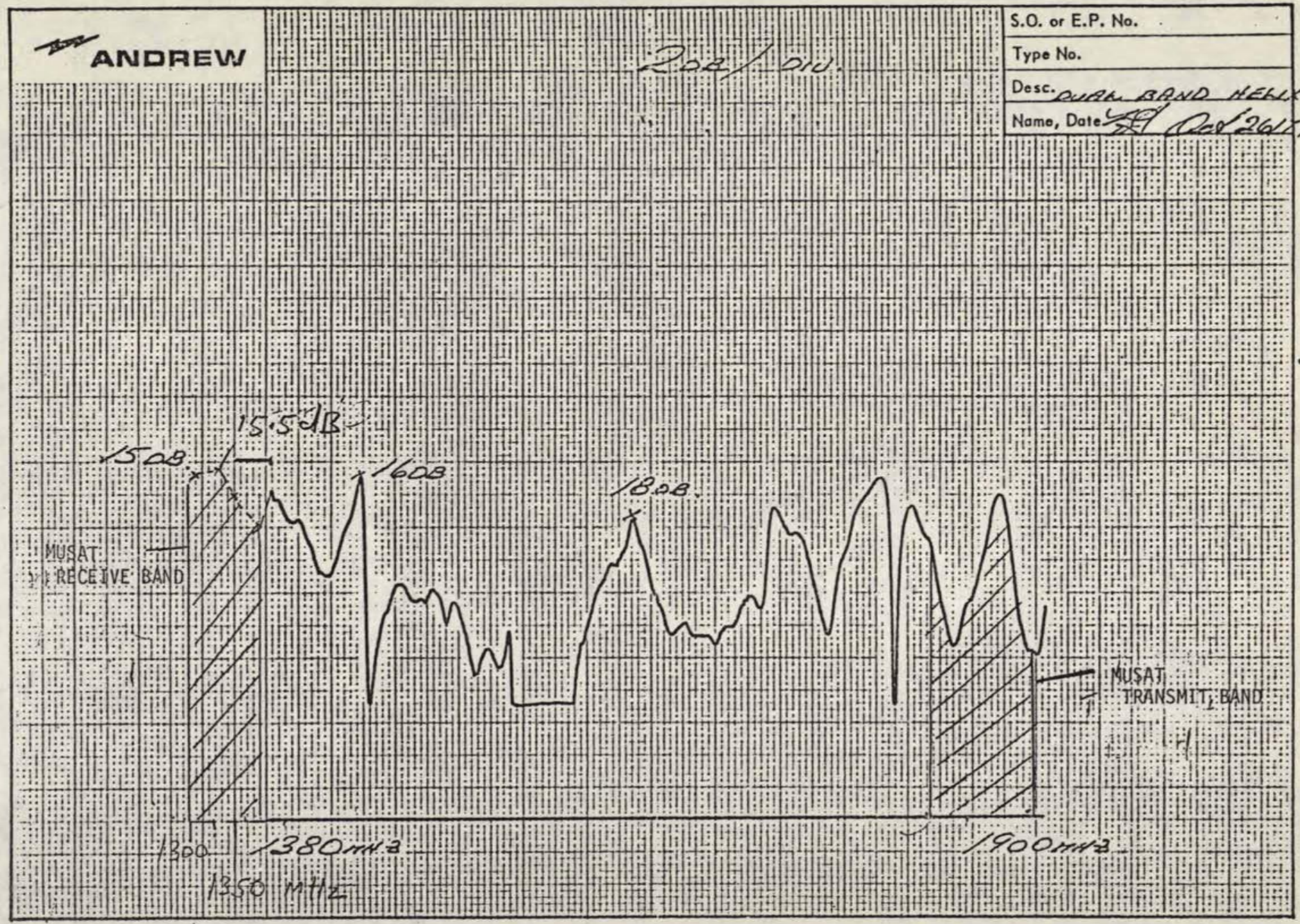

FIGURE 6.2.26 RETURN LOSS VS FREQUENCY FOR CO-AXIAL HELIX

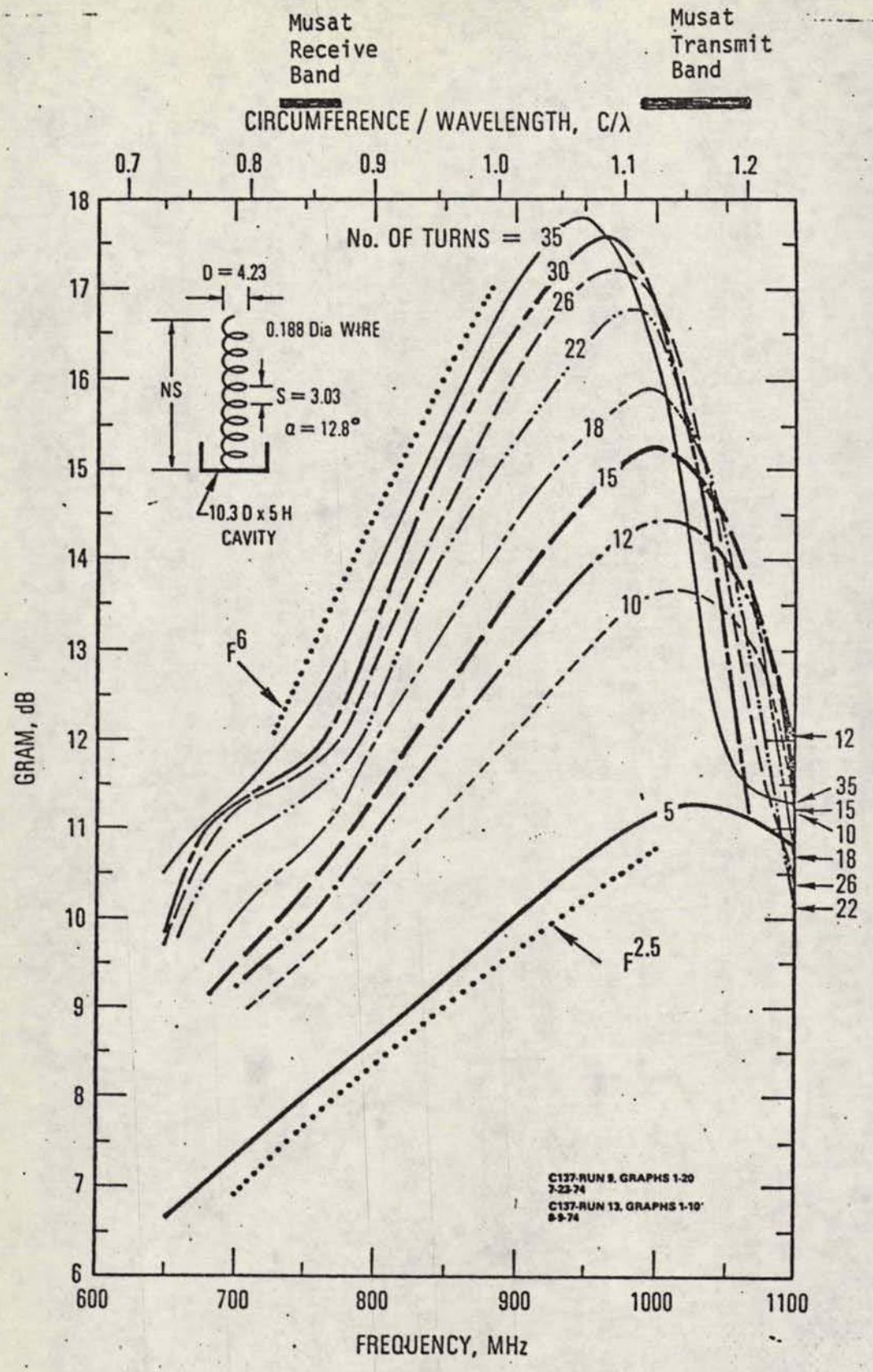

Fig.7.1.1 Antenna Gain vs Frequency for the 5 to 35 Turn Helical Antennas, 4.23-in. Diameter

(Reproduced by permission from King and Wong – "Characteristics of 5 to 35 turn helix", SAMSO-TR-77-200. Courtesy of Dr. J.L. Wong).

FIGURE 7.2.1 UNIFORM HELIX MODEL ON TEST RANGE

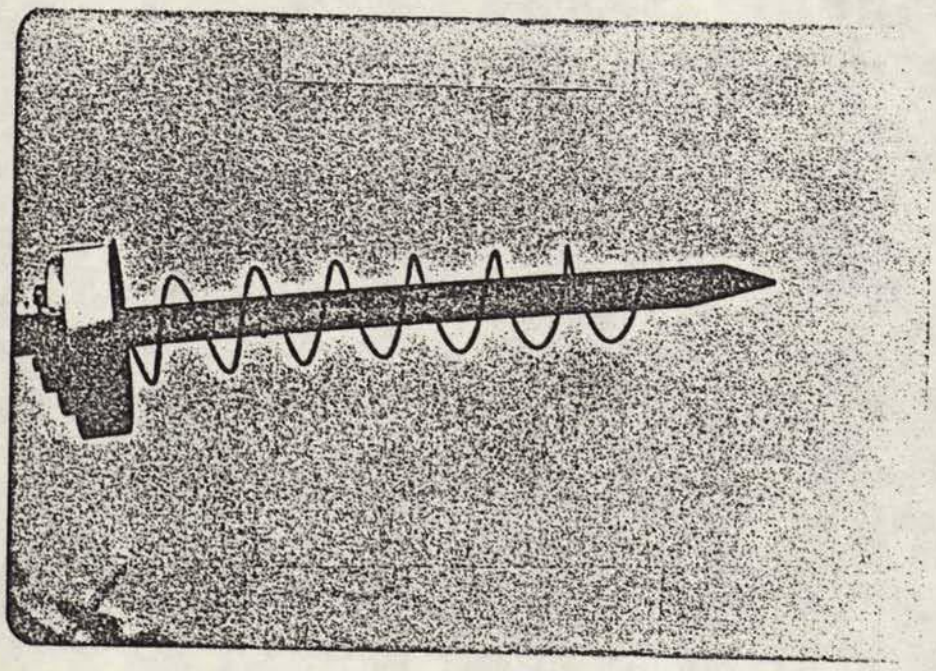

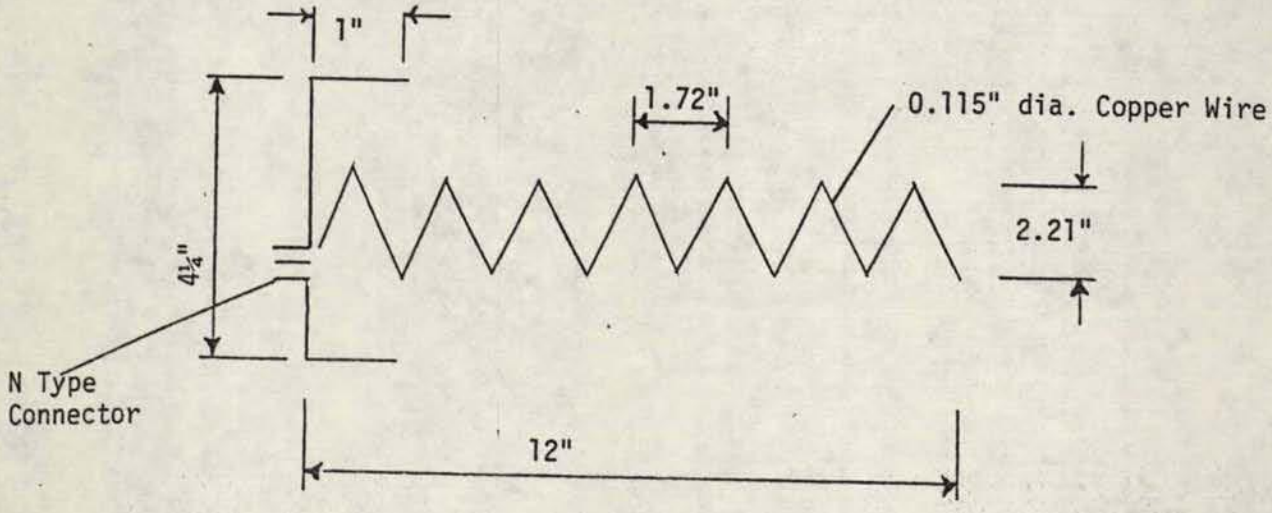

FIGURE 7.2.2 7-TURN UNIFORM HELIX MODEL

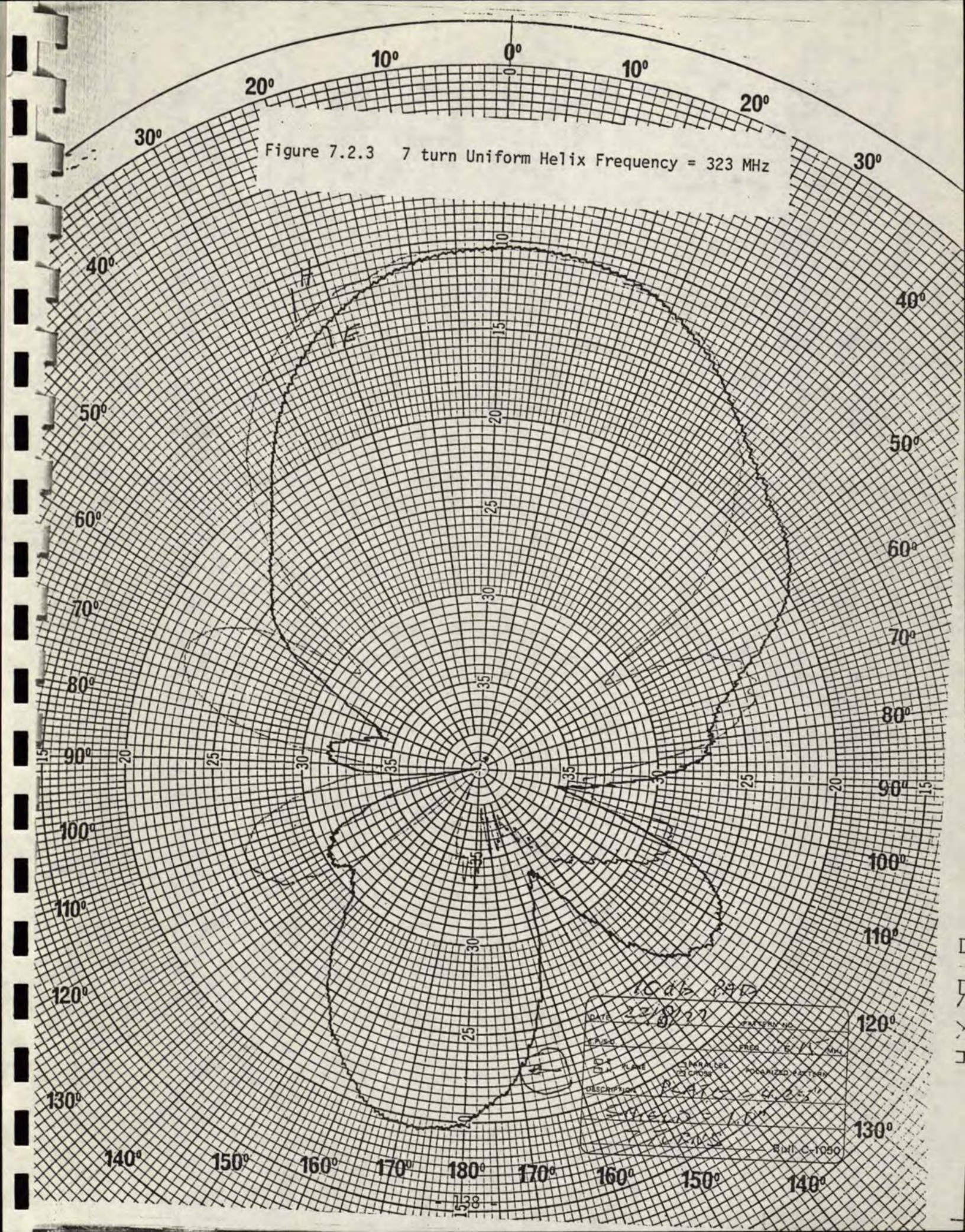

Figure 7.2.3 7 turn Uniform Helix Frequency = 323 MHz

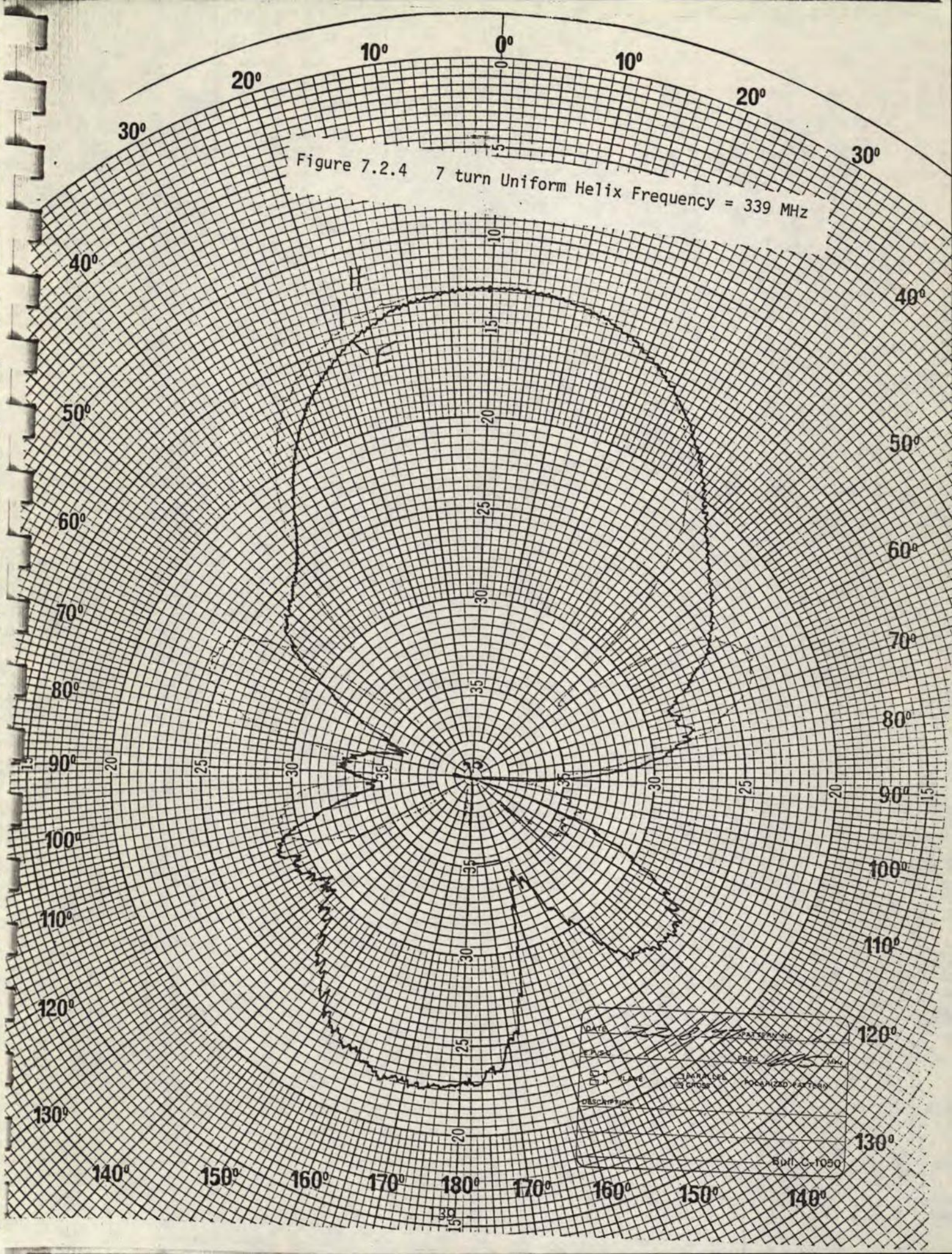

Figure 7.2.4 7 turn Uniform Helix Frequency = 339 MHz

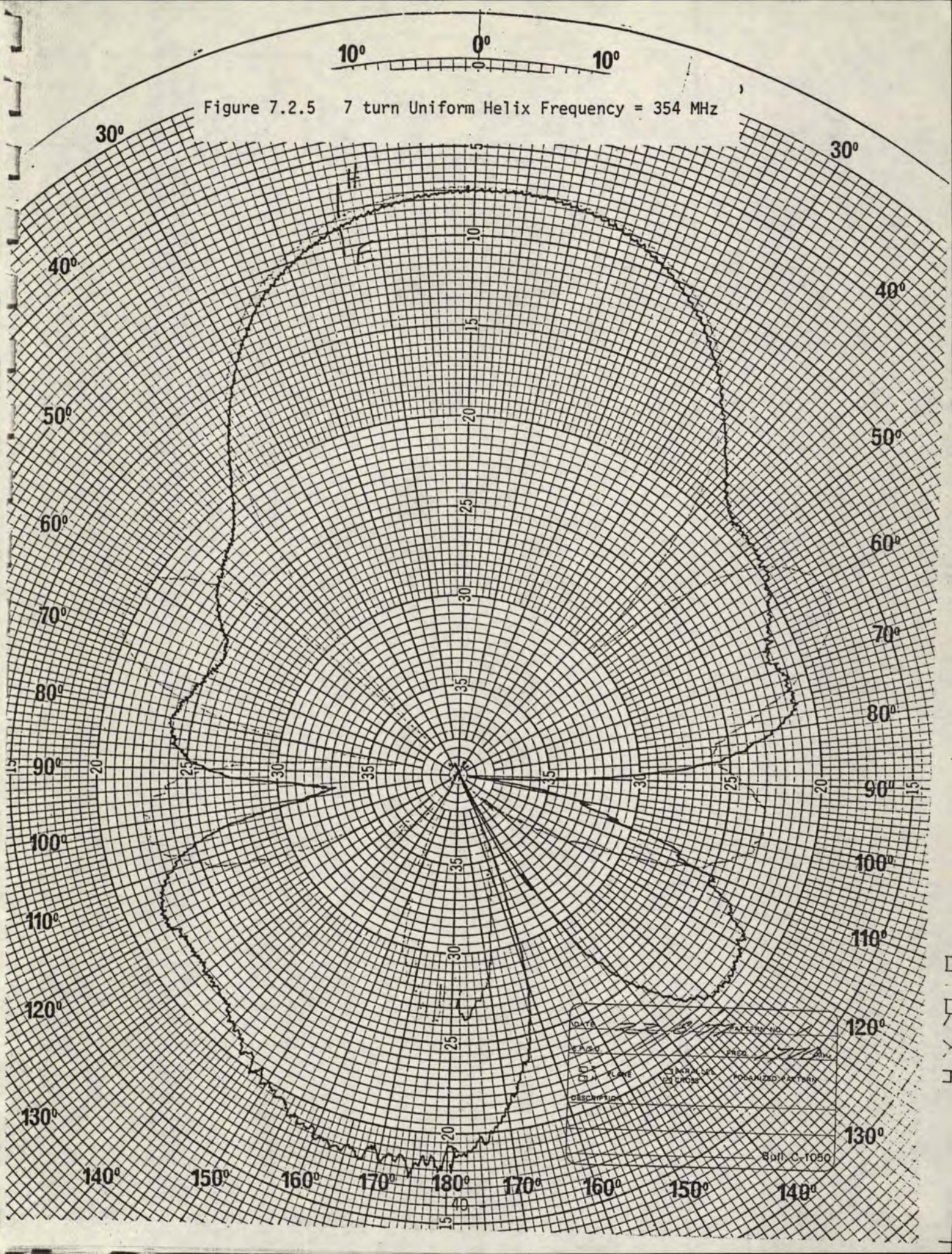

Figure 7.2.5 7 turn Uniform Helix Frequency = 354 MHz

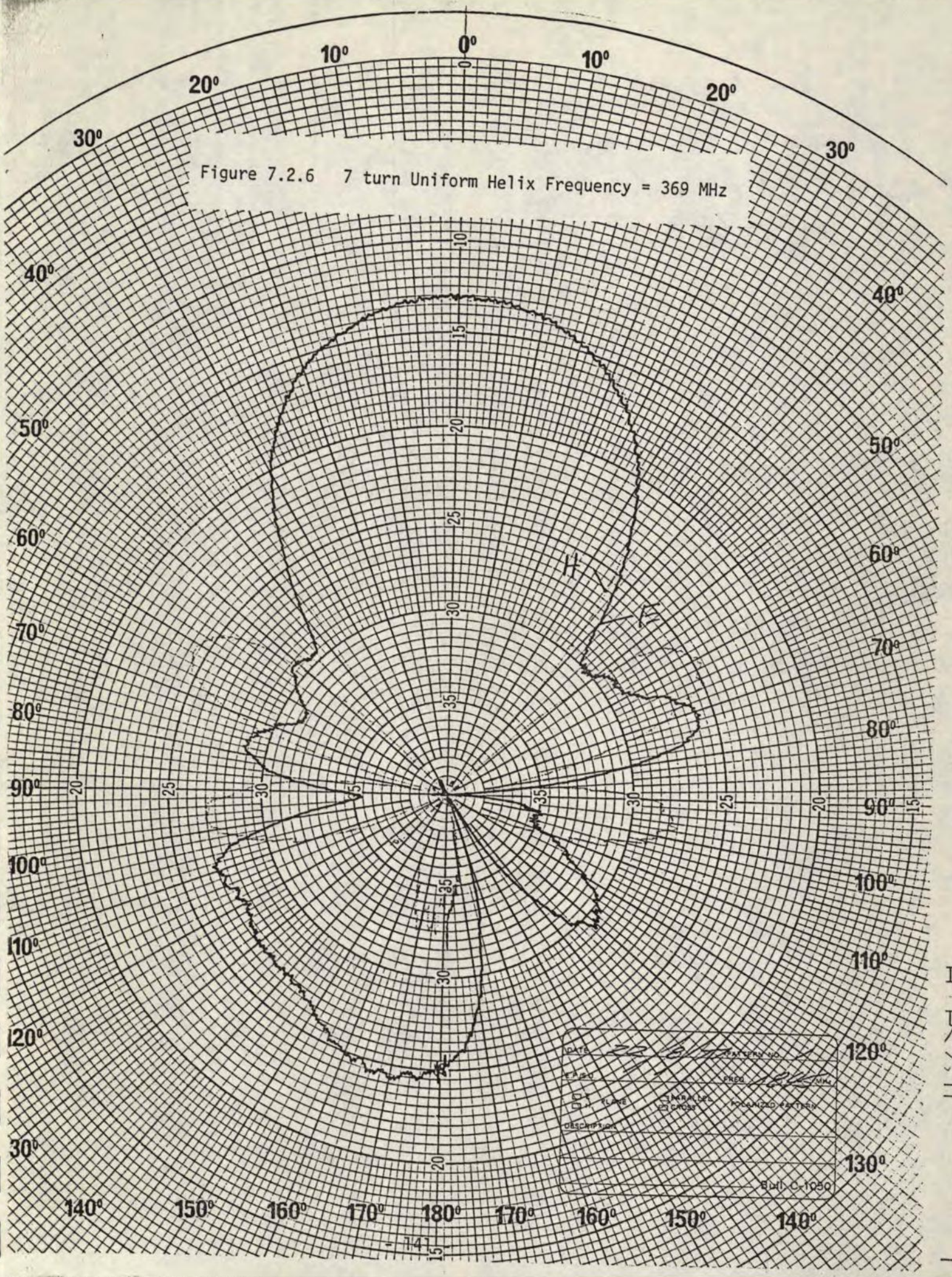

Figure 7.2.6 7 turn Uniform Helix Frequency = 369 MHz

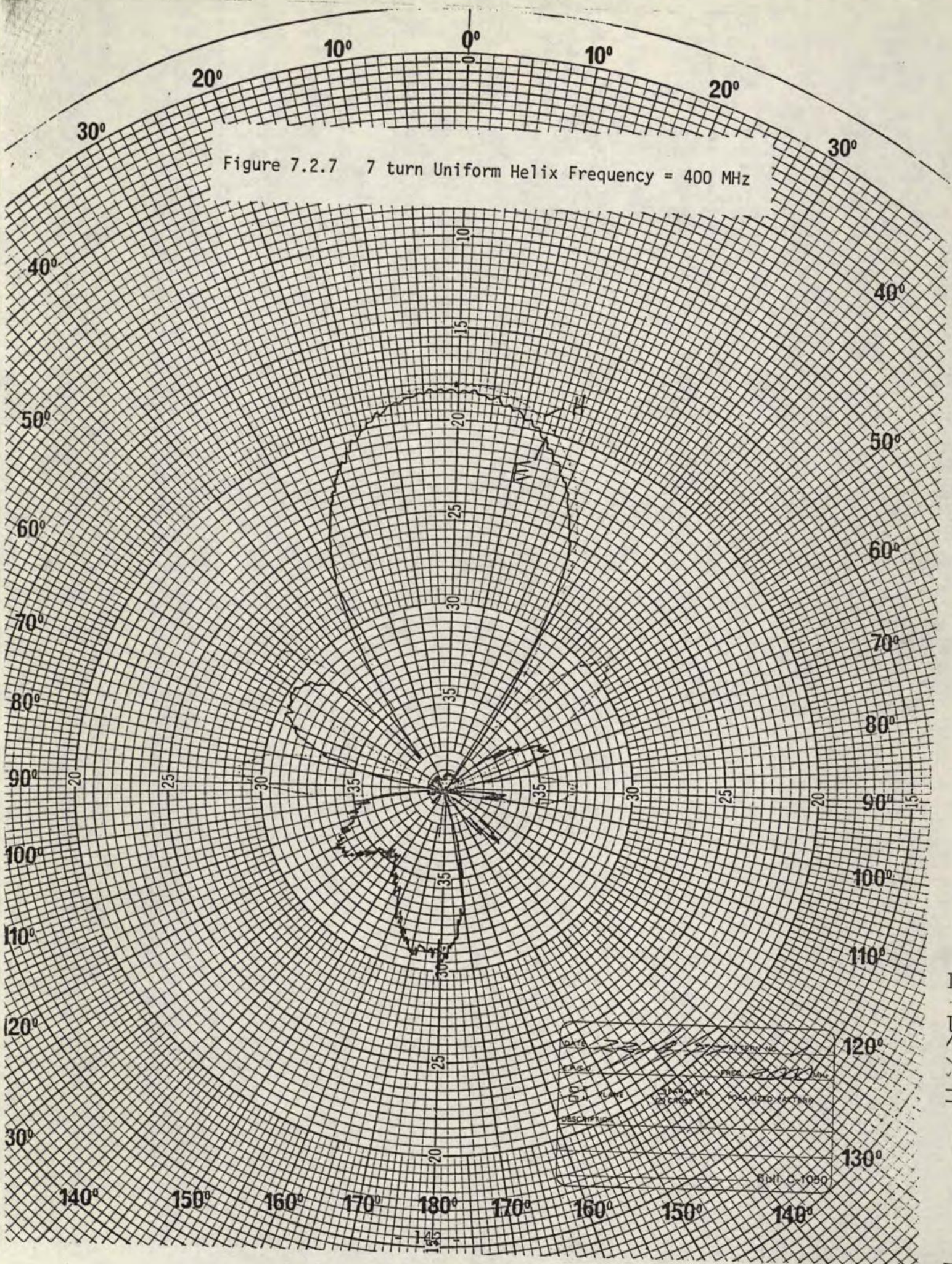

Figure 7.2.7 7 turn Uniform Helix Frequency = 400 MHz

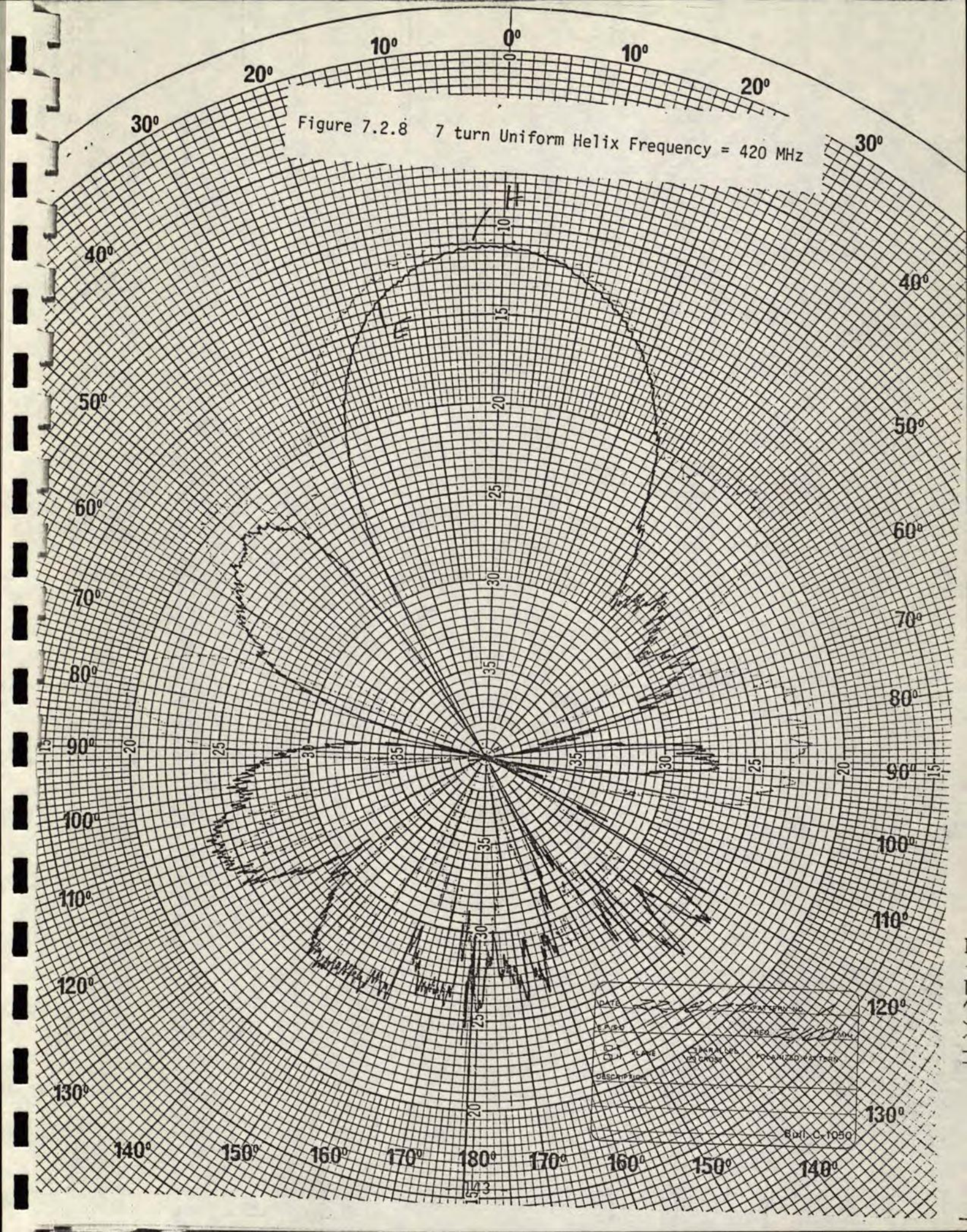

Figure 7.2.8 7 turn Uniform Helix Frequency = 420 MHz

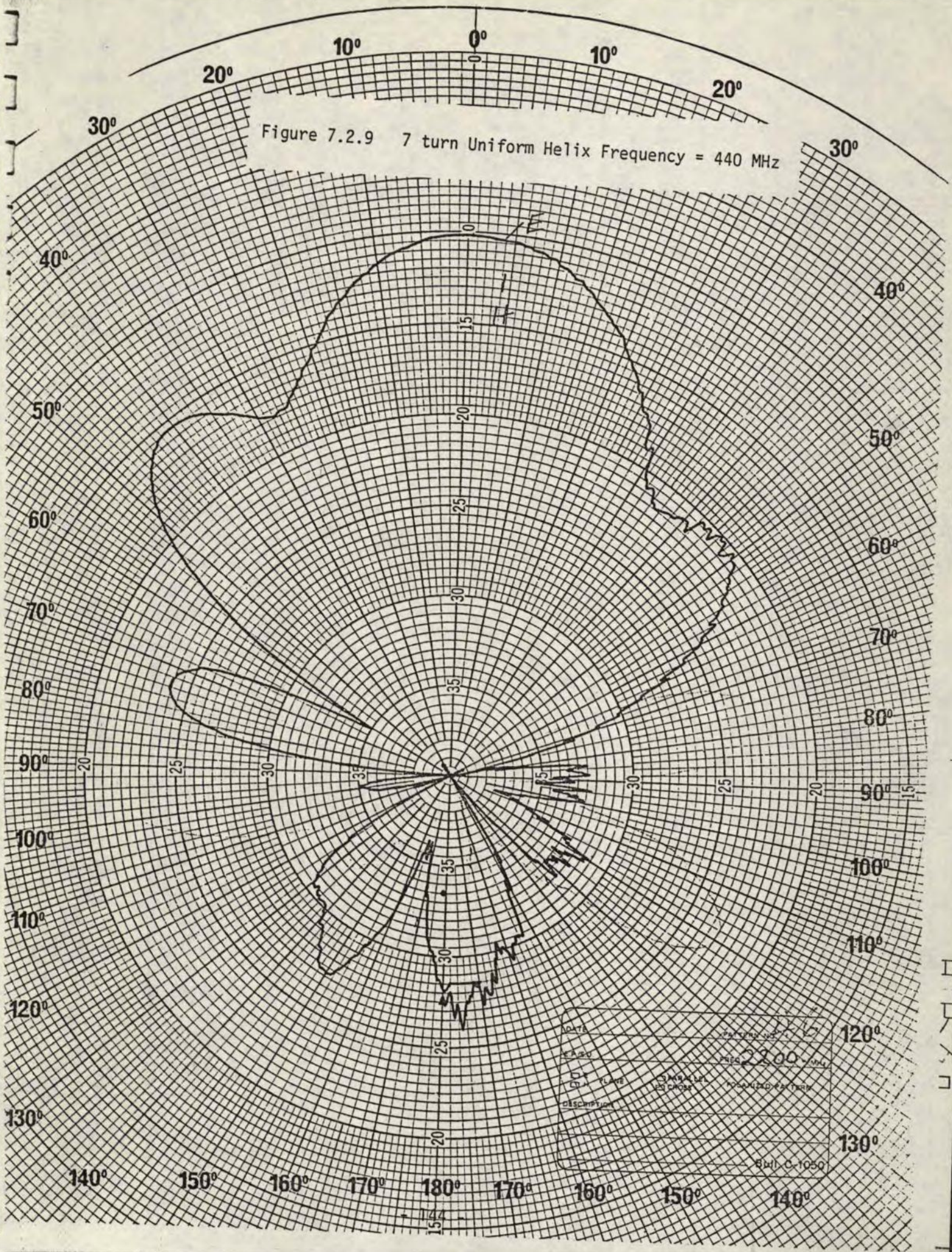

Figure 7.2.9 7 turn Uniform Helix Frequency = 440 MHz

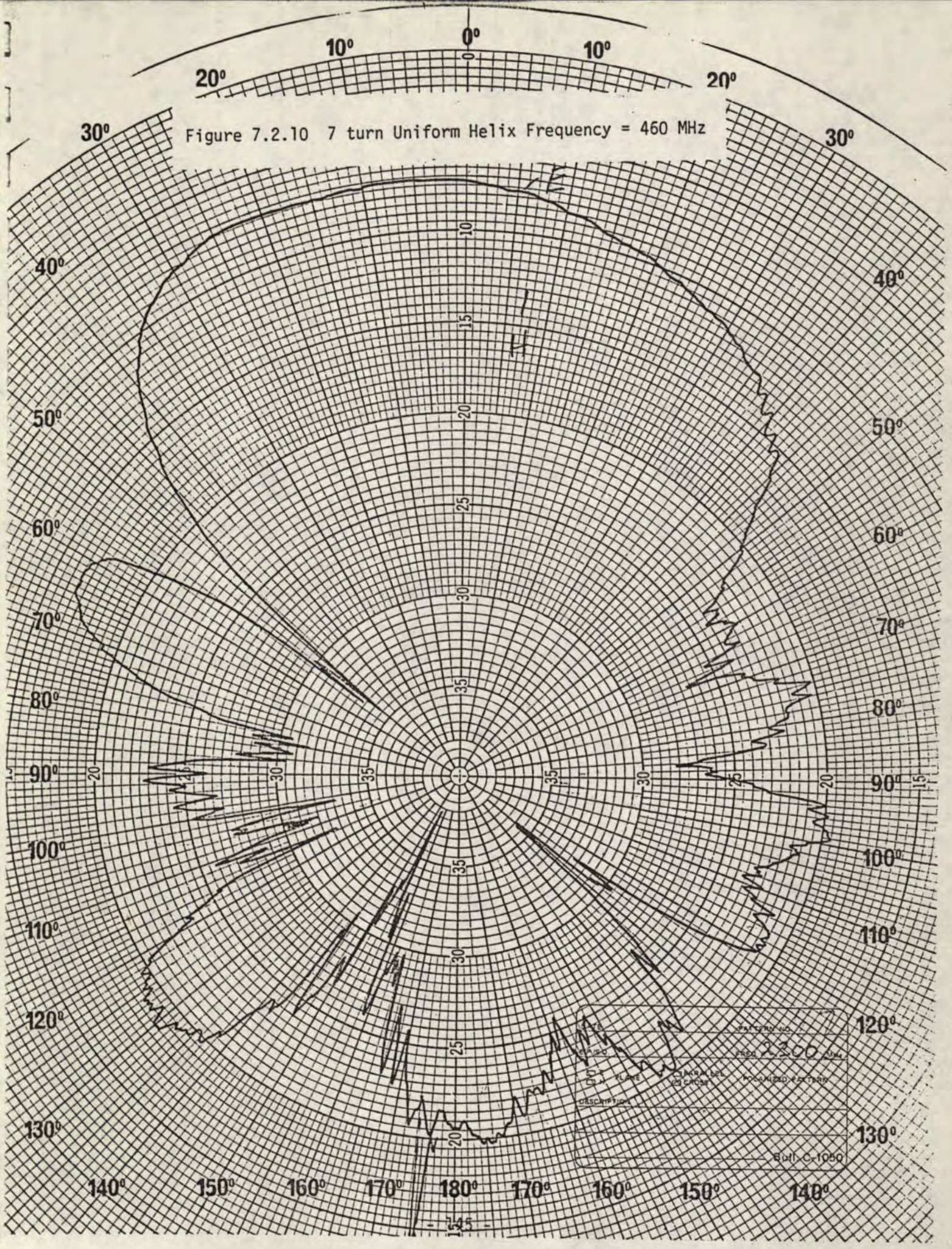

Figure 7.2.10 7 turn Uniform Helix Frequency = 460 MHz

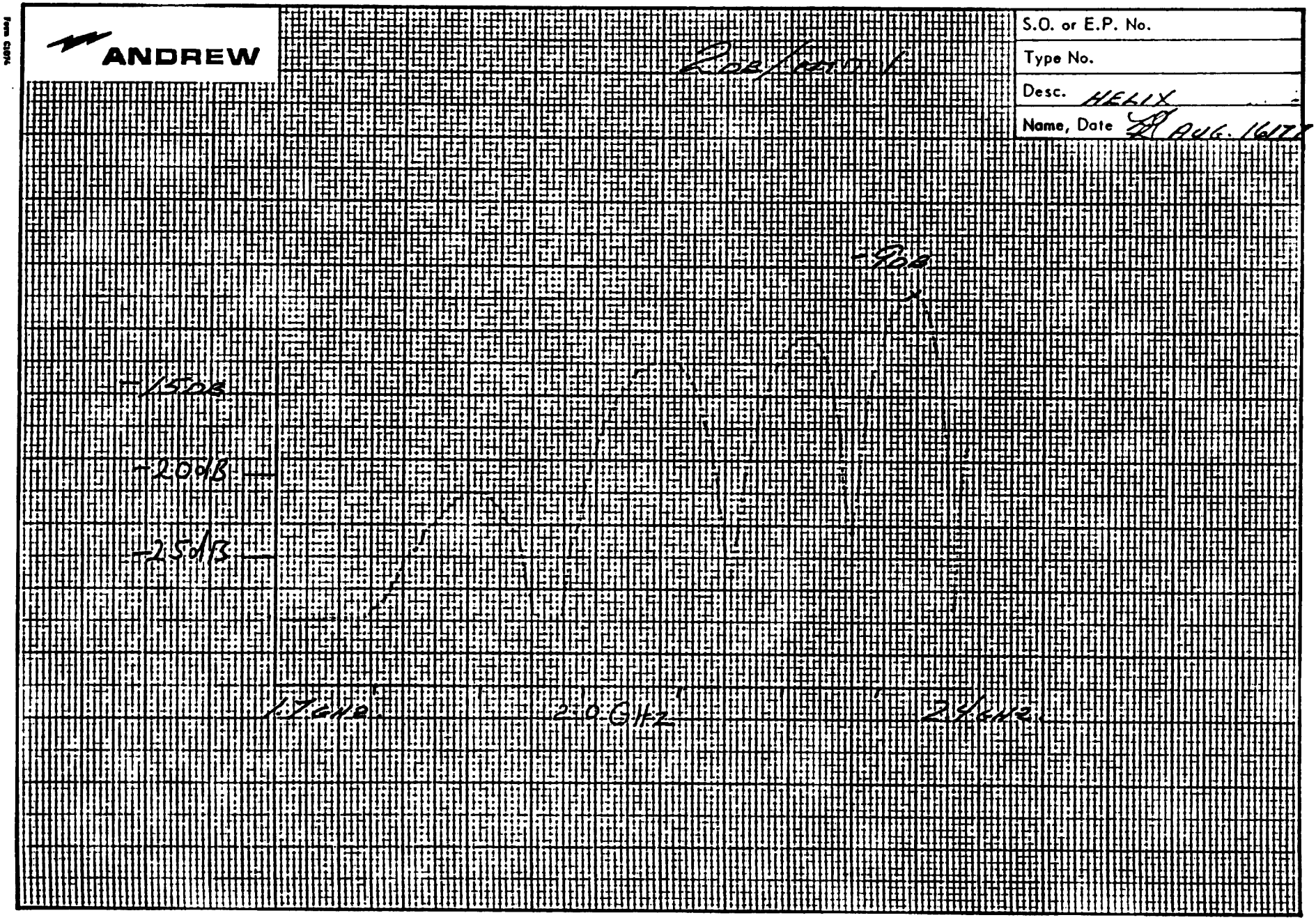

FIGURE 7.2.11 RETURN LOSS AGAINST FREQUENCY FOR 7 TURN HELIX

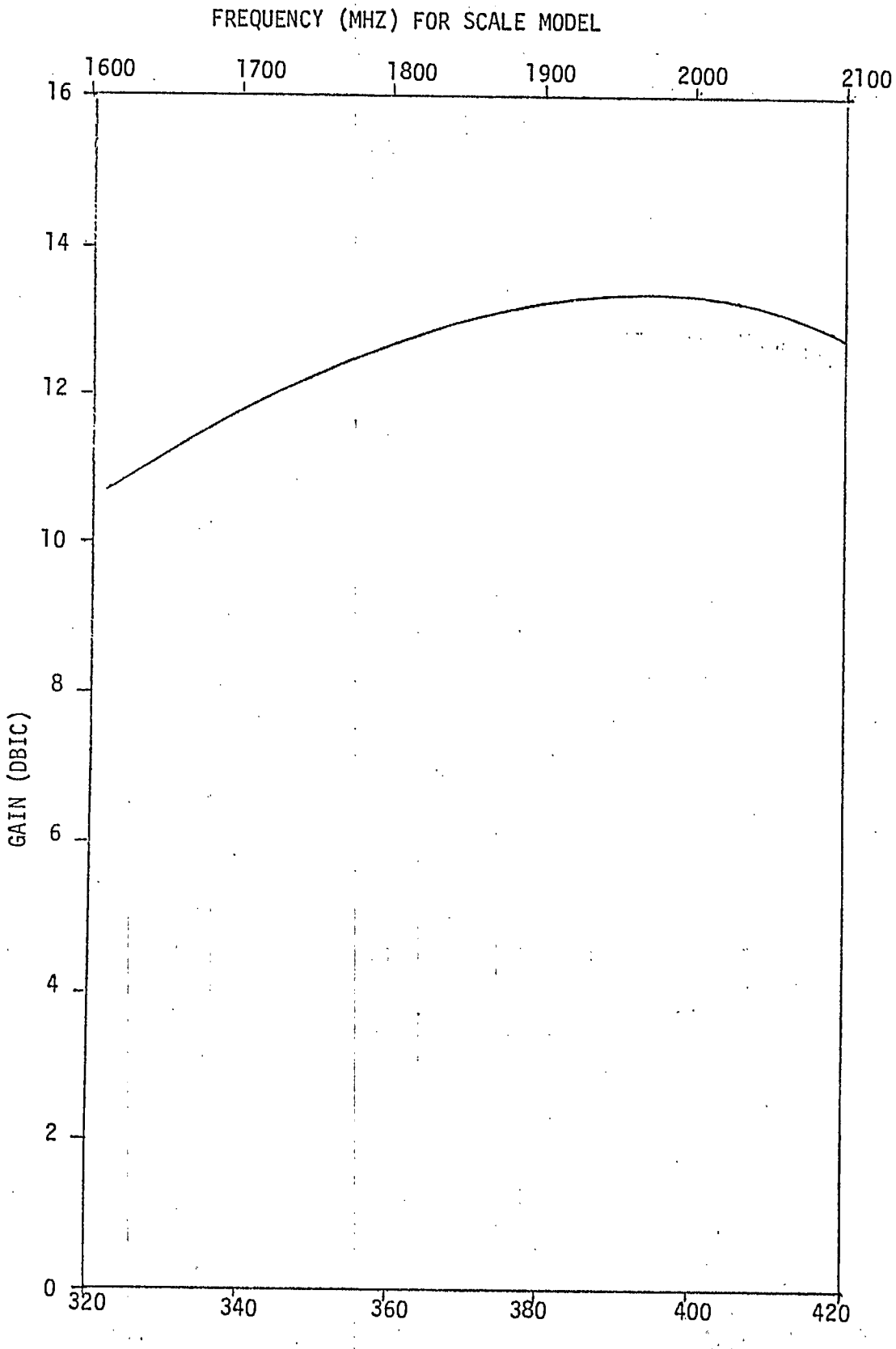

FIGURE 7.2.12 GAIN AGAINST FREQUENCY FOR 7 TURN HELIX

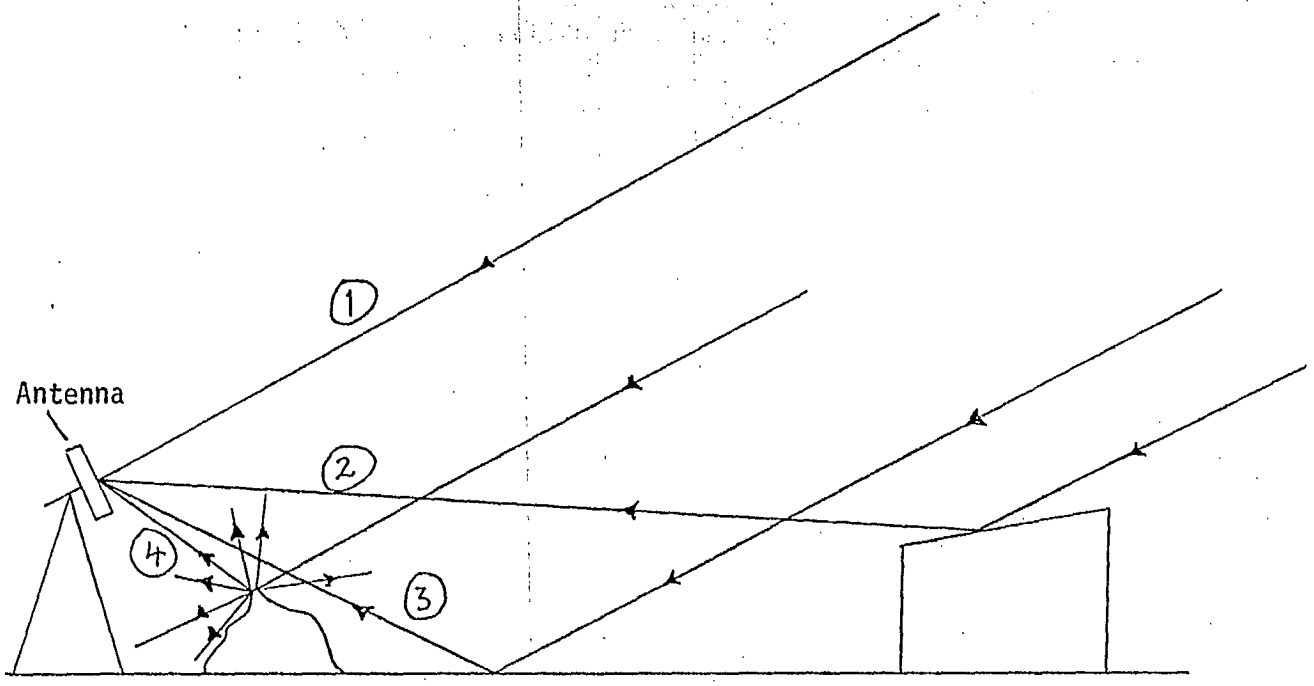

FIGURE A1.1 SOURCES OF MULTI-PATH SIGNAL

1) Direction Reflection
2) Reflectionfrom a reflecting obstruction.
3) Ground reflection.
4) Diffraction field from surrounding objects.

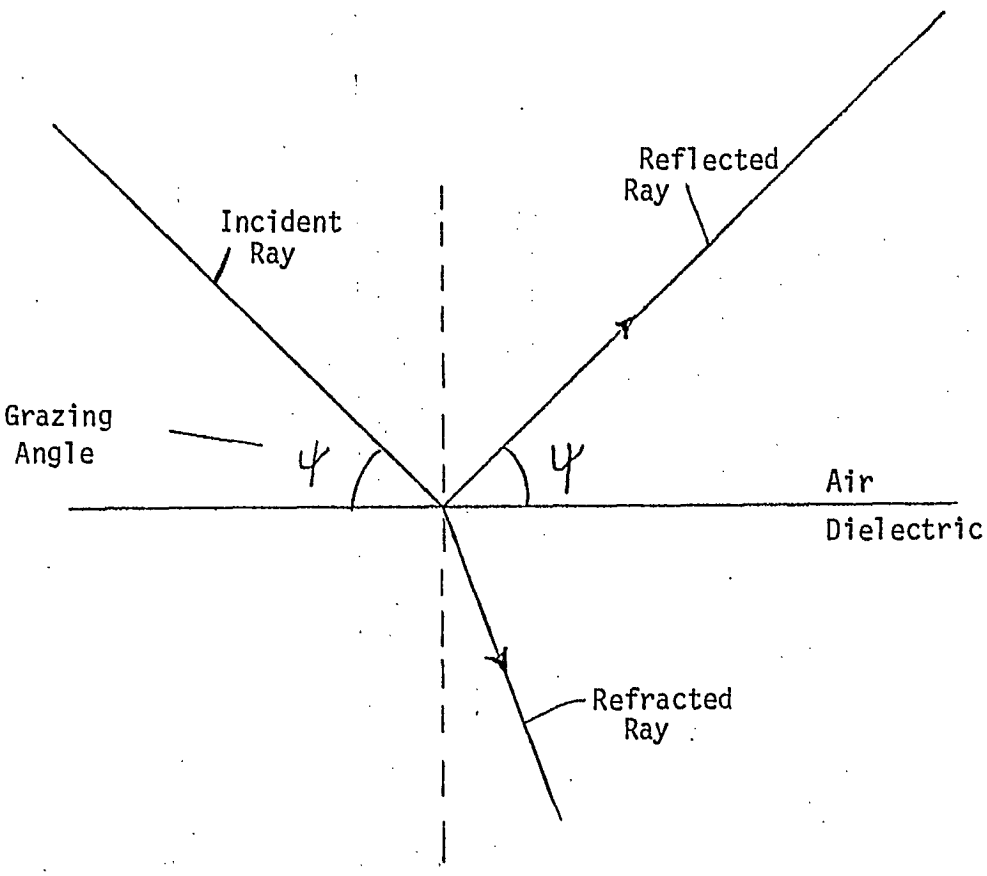
Reflected
Ray
Incident
Ray
Grazing
Angle
ψ
ψ
Air
Dielectric
Refracted
Ray

FIGURE A1.2

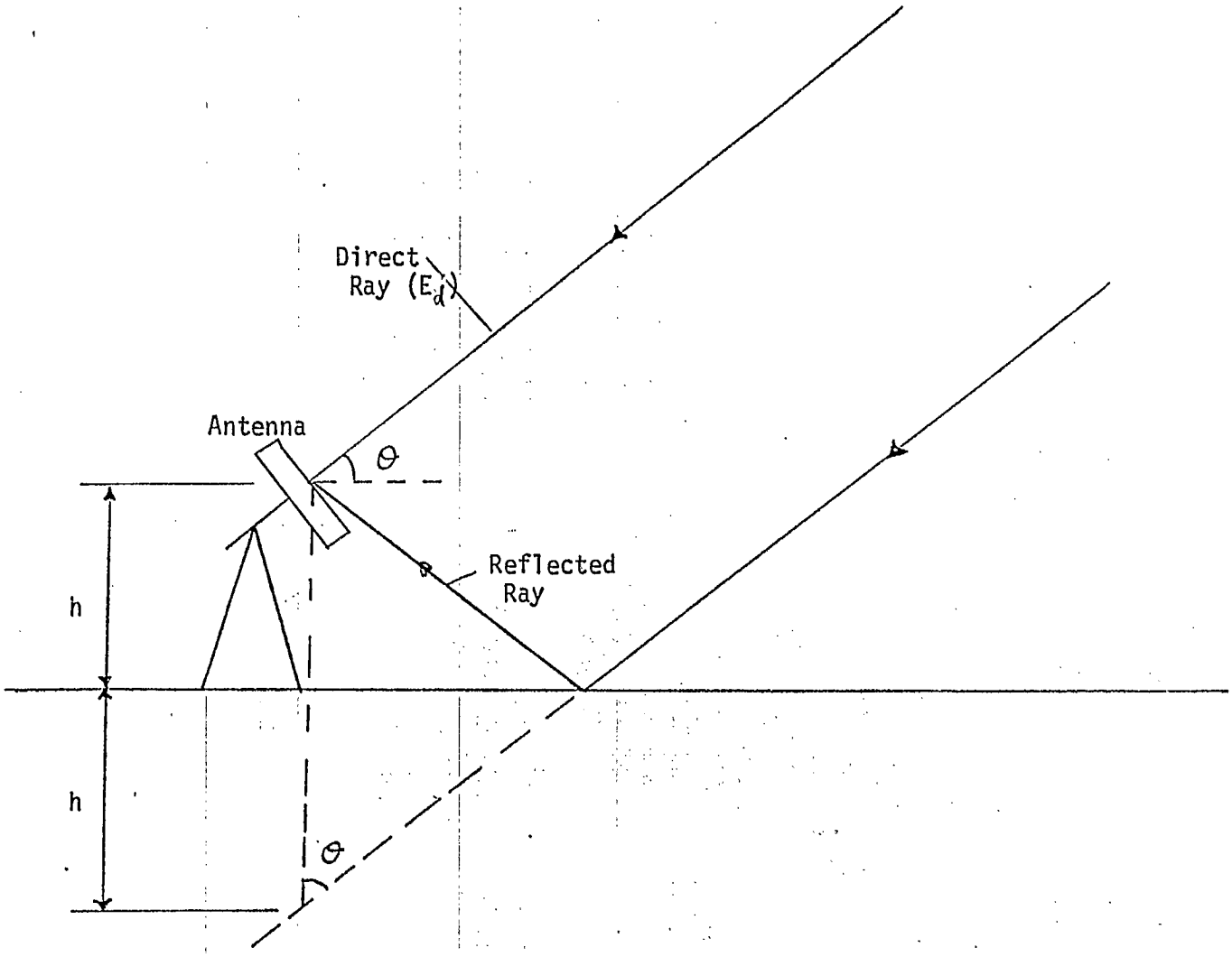

FIGURE A1.3 SIGNAL RECEPTION OF A ESA FROM A SATELLITE

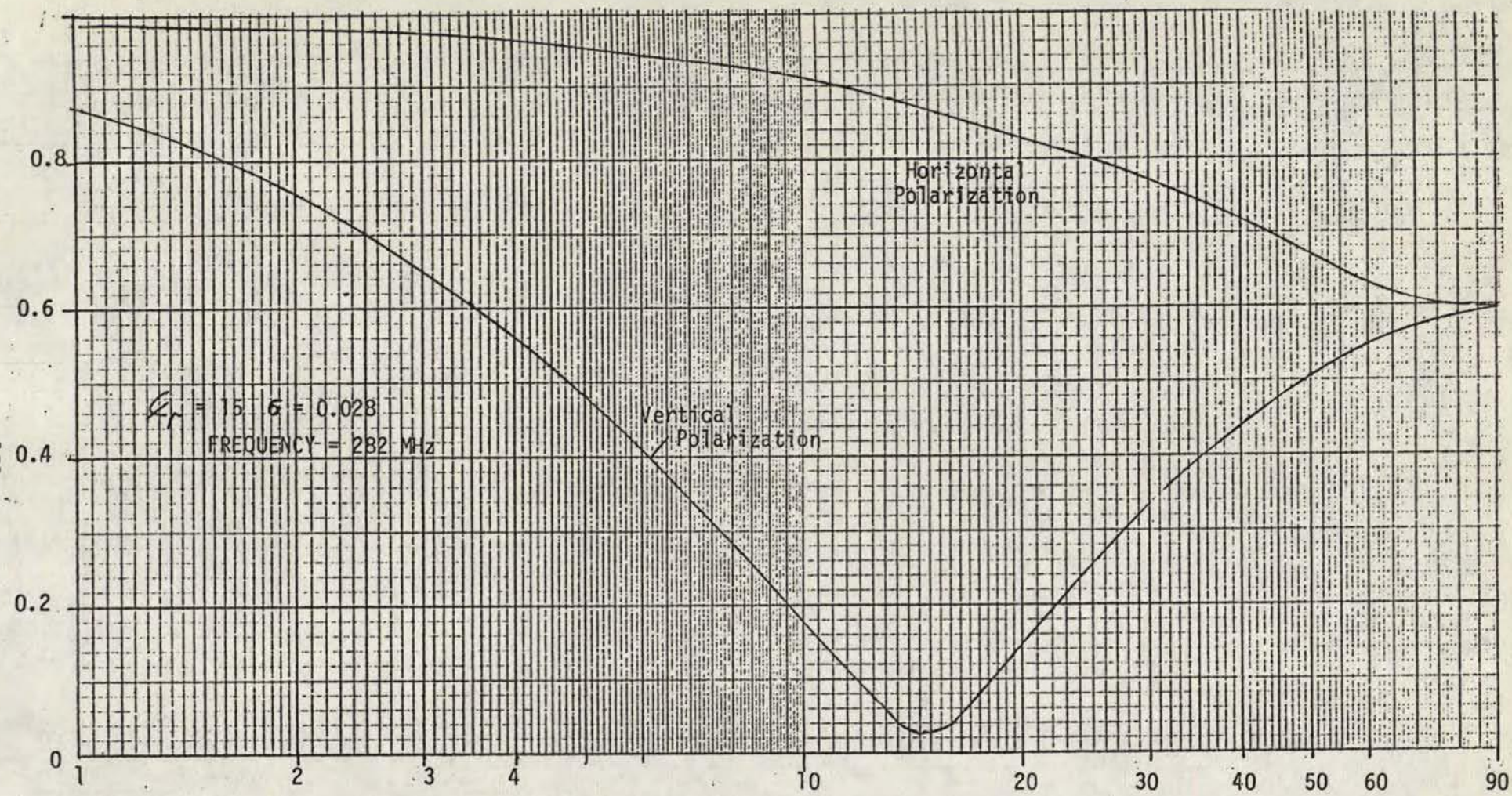

FIGURE A1.4 MAGNITUDE OF THE REFLECTION CO-EFFICIENT FOR AVERAGE LAND

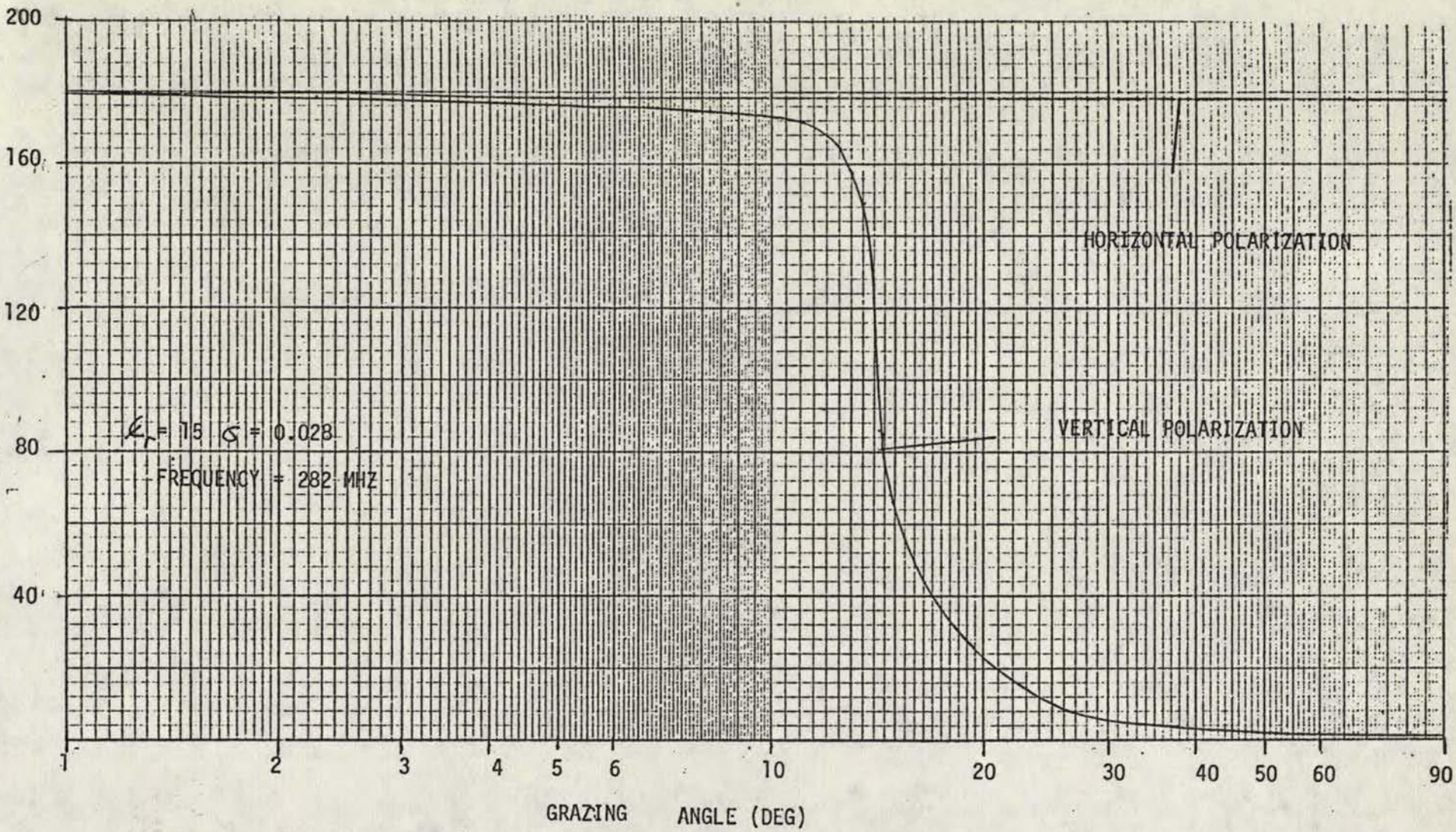

FIGURE A1.5 PHASE ANGLE OF THE REFLECTION CO-EFFICIENT FOR AVERAGE LAND

FIGURE A1.6 MINIMUM POWER RECEIVED FOR AVERAGE GROUND -282 MHZ

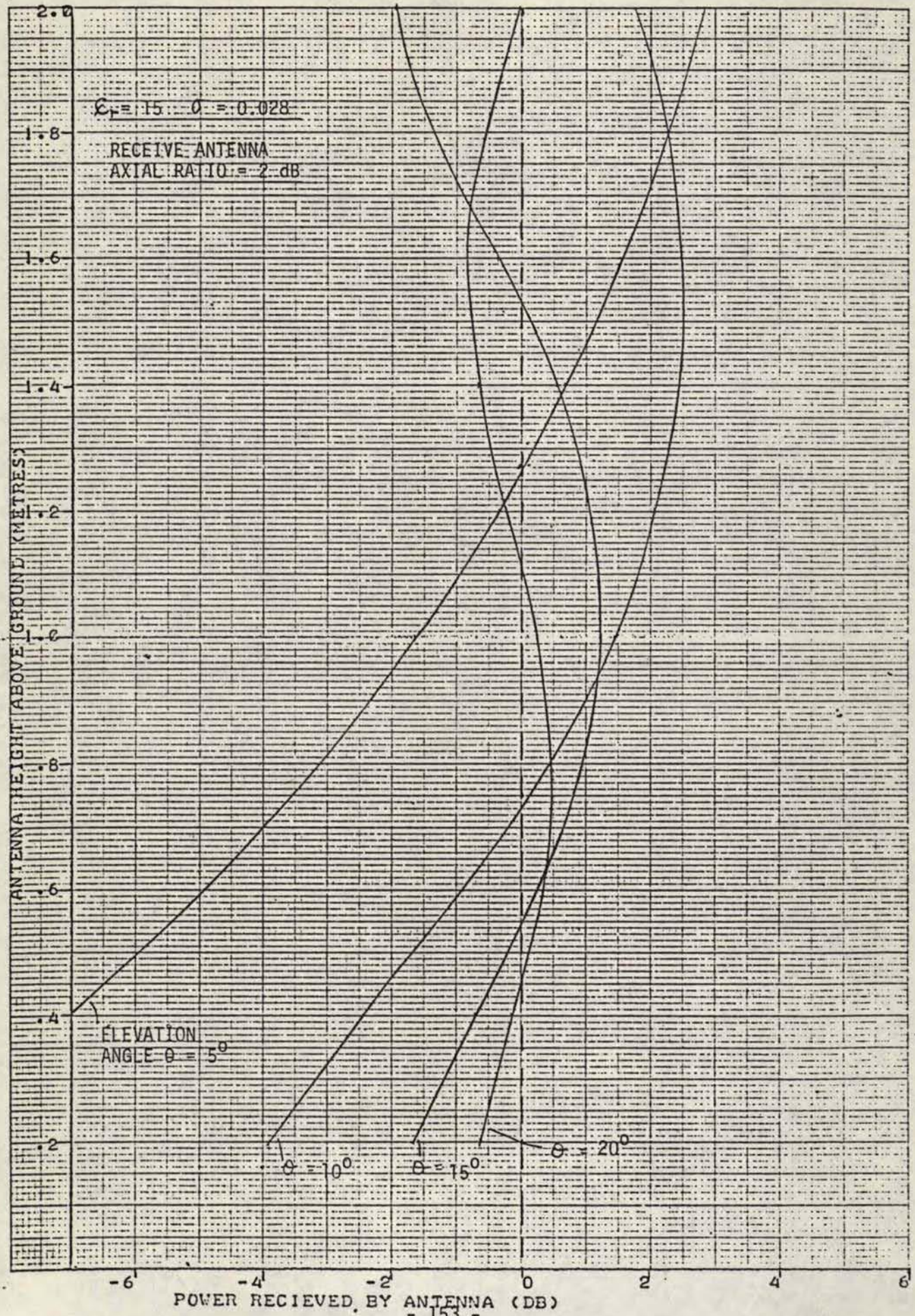

FIGURE A1.7 MINIMUM POWER RECEIVED FOR AVERAGE GROUND - 385 MHz

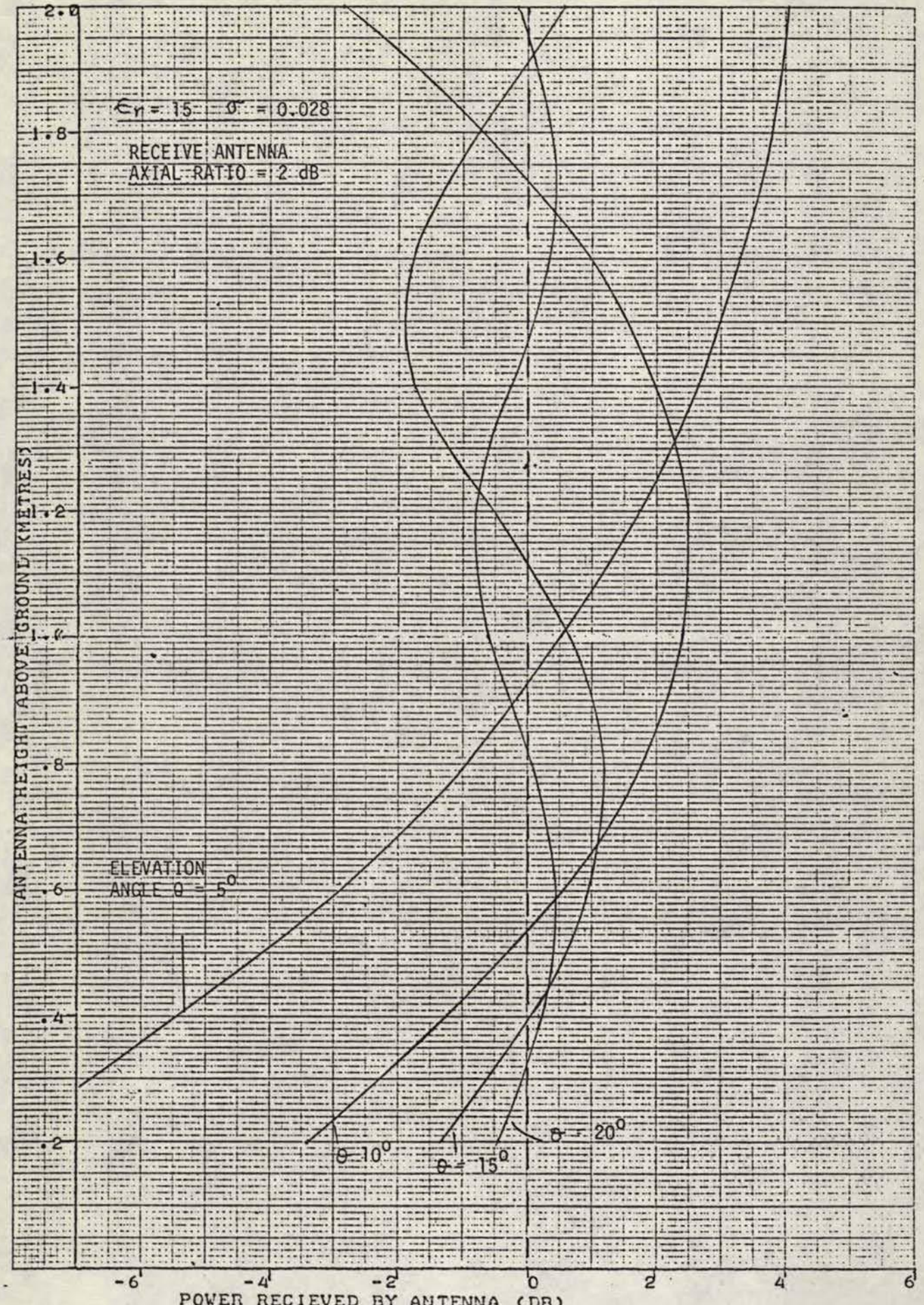

46 1323

KEUFFEL & ESSER CO. MADE IN U.S.A.

FIGURE A1.8 MINIMUM POWER RECEIVED FOR 5° ELEVATION ANGLE

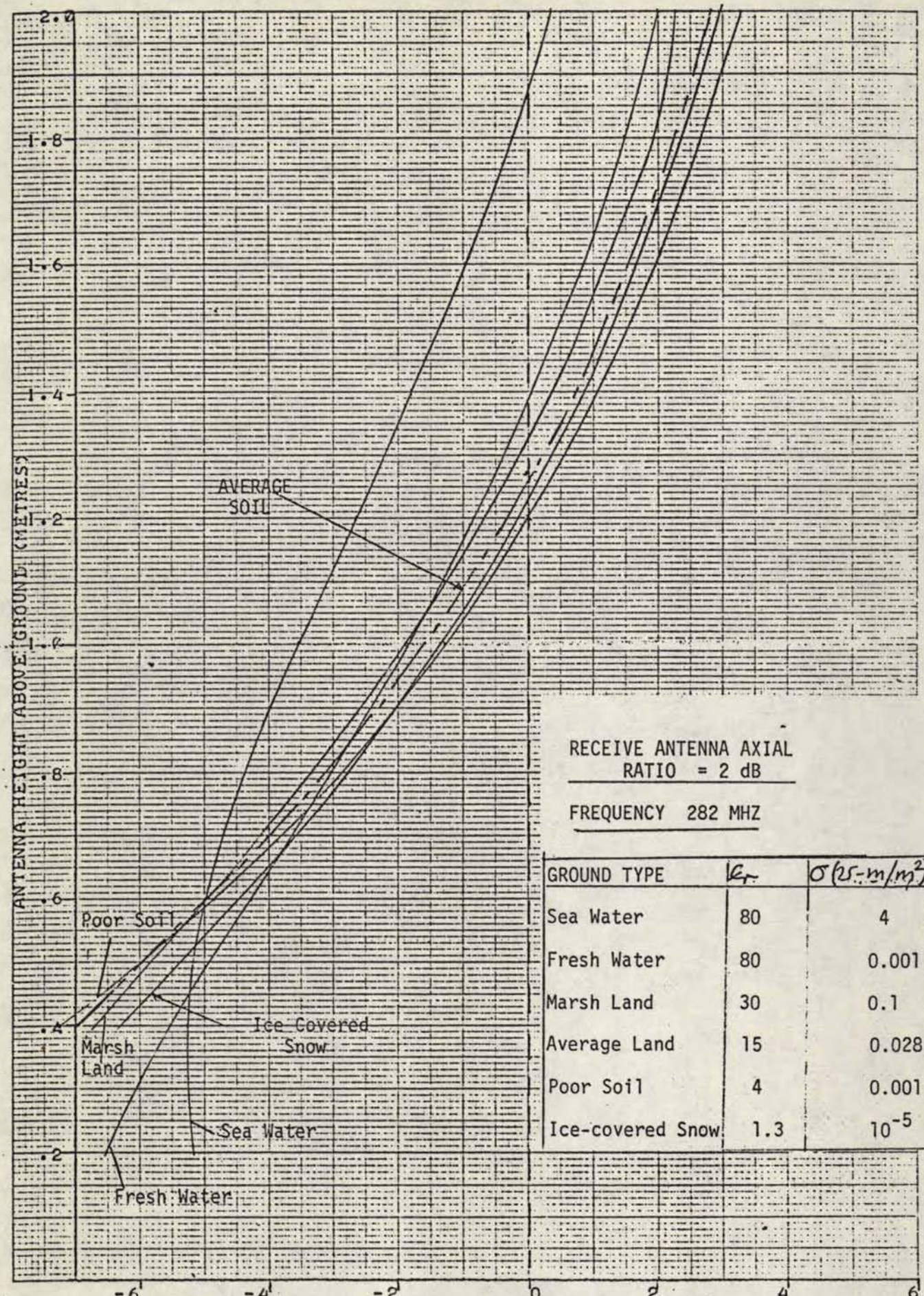

RECEIVE ANTENNA AXIAL RATIO = 2 dB

FREQUENCY 282 MHZ

GROUND TYPE	ϵ_r	σ (S-m/m^2)
Sea Water	80	4
Fresh Water	80	0.001
Marsh Land	30	0.1
Average Land	15	0.028
Poor Soil	4	0.001
Ice-covered Snow	1.3	10^{-5}

46 1323

FIGURE A1.9 MINIMUM POWER RECEIVED FOR 15° ELEVATION ANGLE

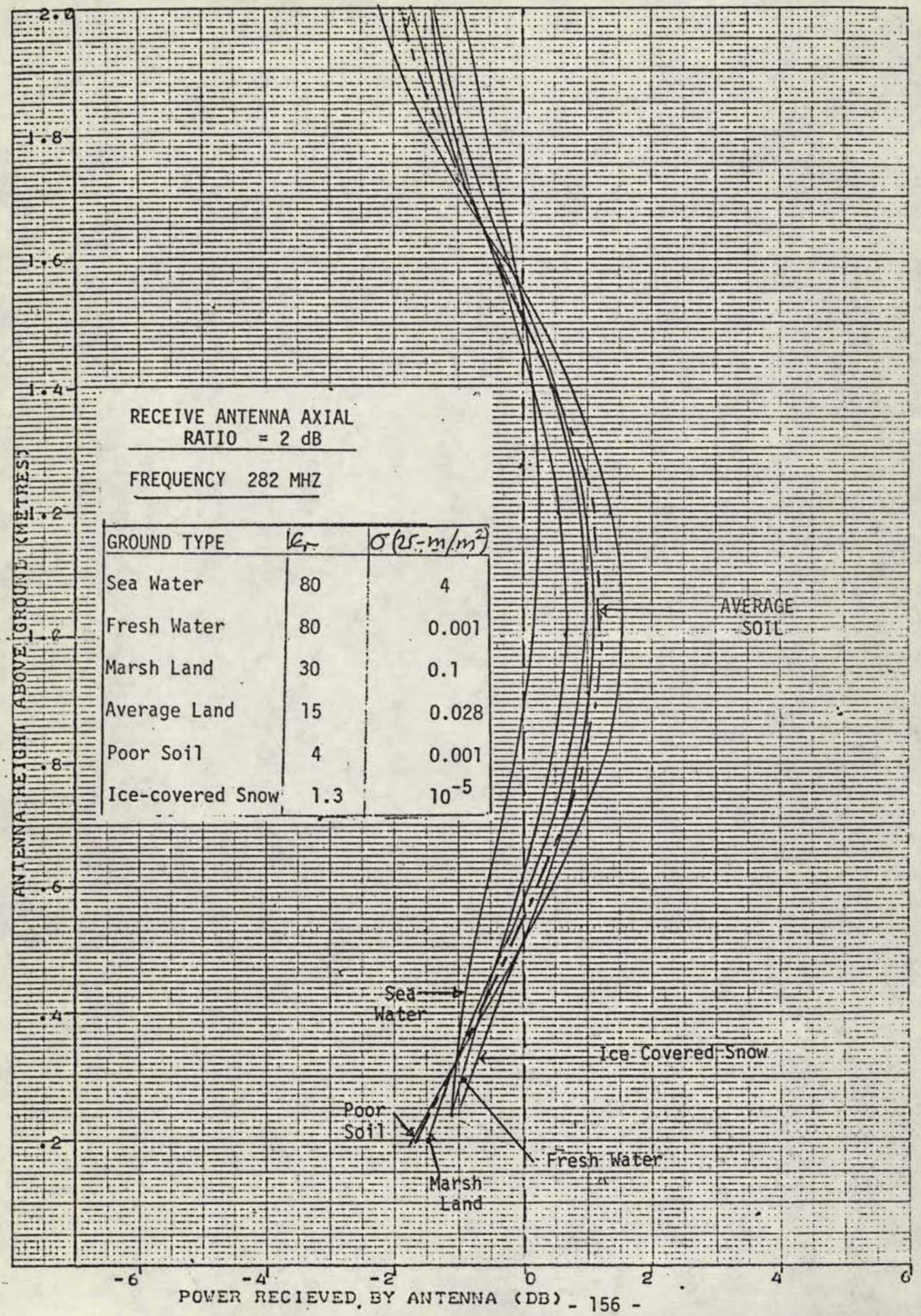

THESE DRAWINGS AND SPECIFICATIONS ARE THE PROPERTY OF ANDREW ANTENNA COMPANY LIMITED, AND MAY NOT BE REPRODUCED OR COPIED OR USED AS THE BASIS FOR THE MANUFACTURE OR SALE OF APPARATUS WITHOUT PERMISSION.

REVISIONS			
ISSUE	DESCRIPTION	DATE	APPROVED

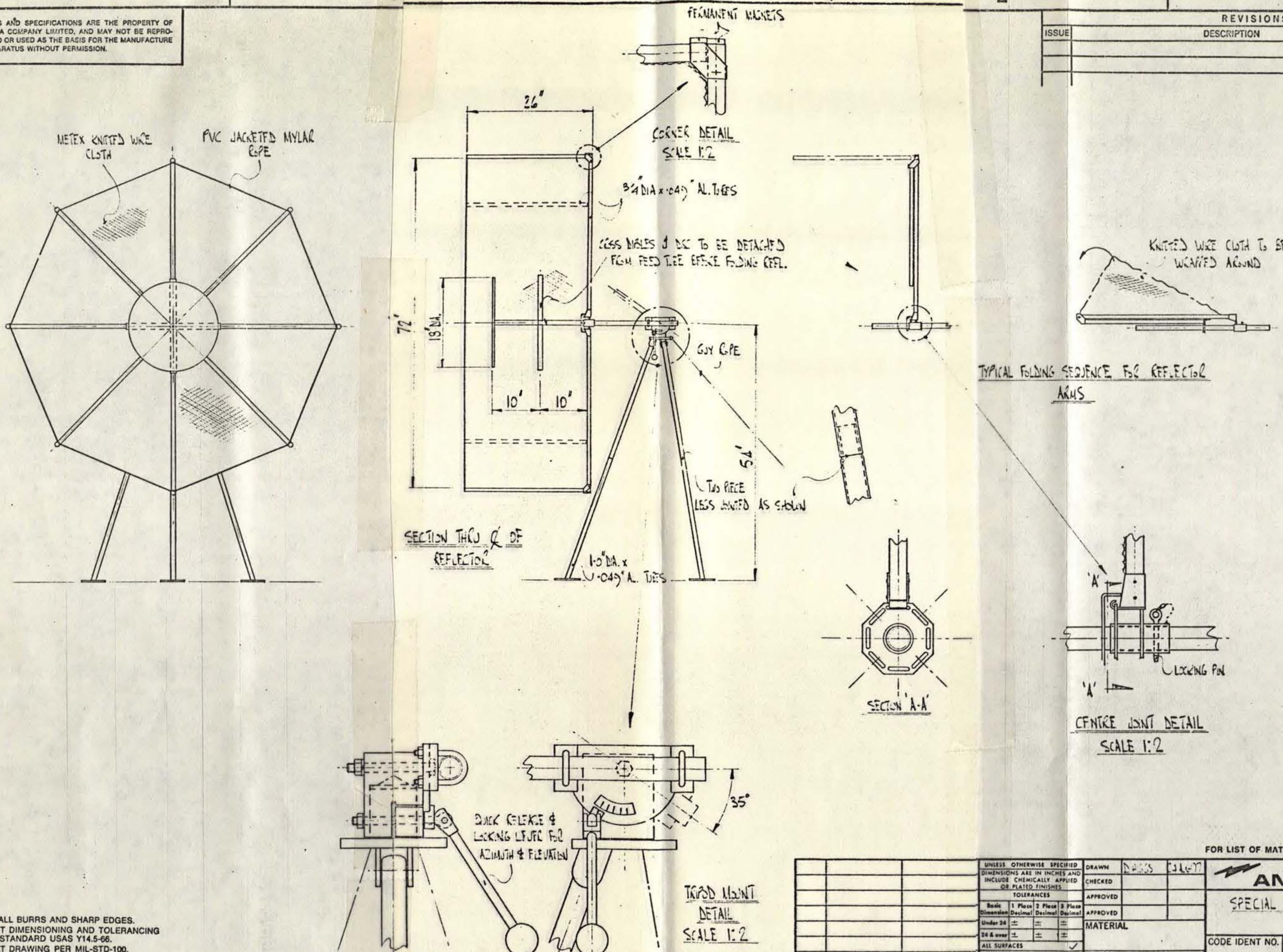

3. REMOVE ALL BURRS AND SHARP EDGES.
2. INTERPRET DIMENSIONING AND TOLERANCING PER USA STANDARD USAS Y14.5-66.
1. INTERPRET DRAWING PER MIL-STD-100.

NOTES: (UNLESS OTHERWISE SPECIFIED)

FOR LIST OF MATERIAL SEE LM

	NEXT ASSY	USED ON
DISTR	APPLICATION	

UNLESS OTHERWISE SPECIFIED DIMENSIONS ARE IN INCHES AND INCLUDE CHEMICALLY APPLIED OR PLATED FINISHES

TOLERANCES			
Basic Dimension	1 Place Decimal	2 Place Decimal	3 Place Decimal
Under 24	±	±	±
24 & over	±	±	±
ALL SURFACES ✓			
ANGLES ±			
COML TOL APPLY TO STOCK SIZES			
SUPERSEDES DWG			

DRAWN	D.H.S.S	13.1.6-77
CHECKED		
APPROVED		
APPROVED		
MATERIAL		
FINISH		

ANDREW
606 Beech Street
Whitby, Ontario, Canada

SPECIAL FOLDING TRANSPORTABLE ANTENNA

CODE IDENT NO.	SIZE D	WSK 430
SCALE 1:5 & 1:2	WEIGHT	SHEET 1 OF 1

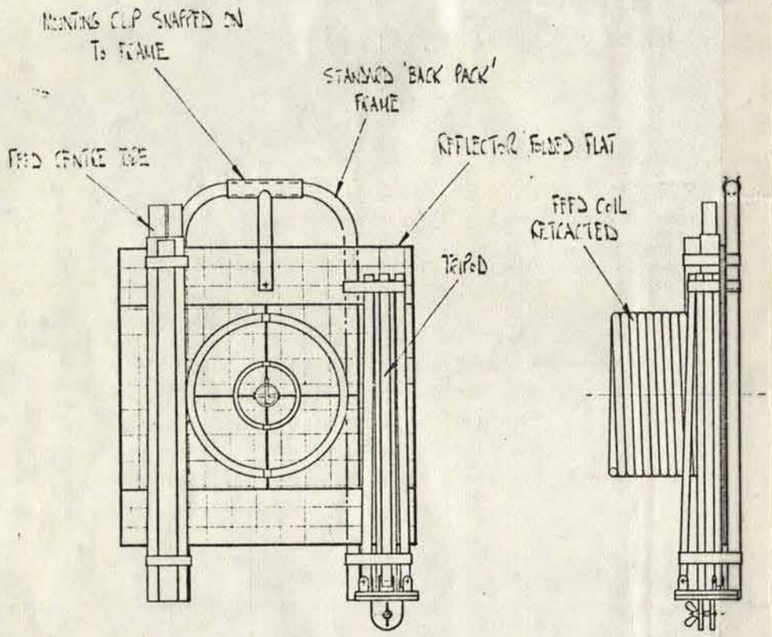

ANTENNA DISMANTLED READY FOR CARRYING

SCALE 1:6

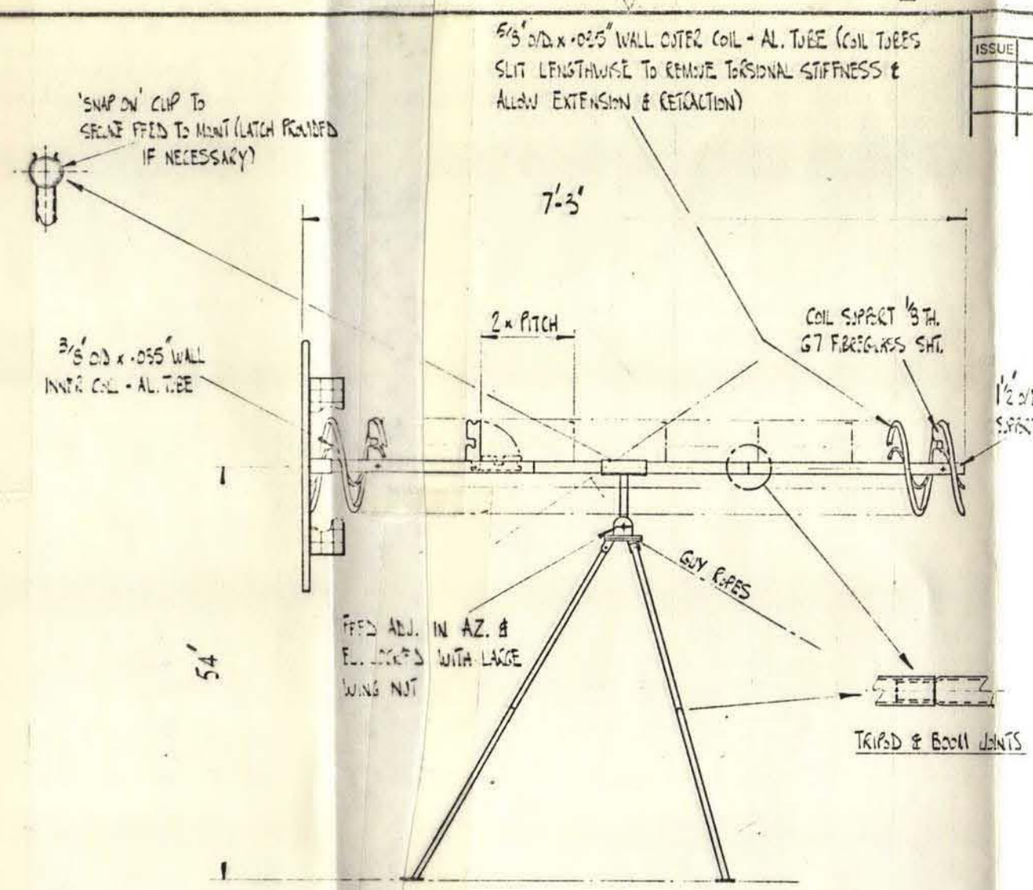

ANTENNA ASSEMBLED READY FOR USE

SCALE 1:10

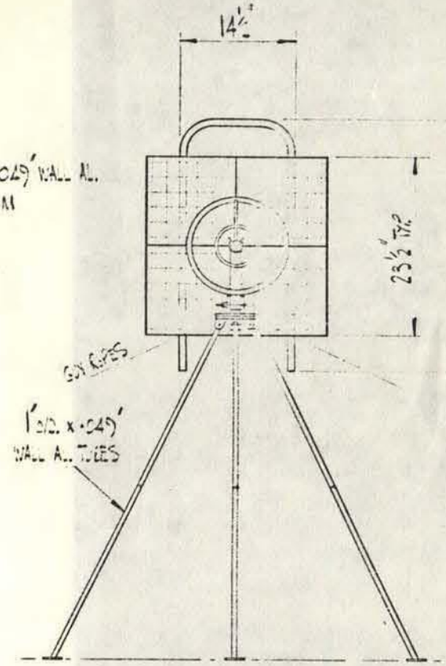

REVISIONS			
ISSUE	DESCRIPTION	DATE	APPD

3. REMOVE ALL BURRS AND SHARP EDGES.
2. INTERPRET DIMENSIONING AND TOLERANCING PER USA STANDARD USAS Y14.5-66.
1. INTERPRET DRAWING PER MIL-STD-100.

NOTES: (UNLESS OTHERWISE SPECIFIED)

FOR LIST OF MATERIAL SEE LM

NEXT ASSY	USED ON	
APPLICATION		DISTR

UNLESS OTHERWISE SPECIFIED
DIMENSIONS ARE IN INCHES AND INCLUDE CHEMICALLY APPLIED OR PLATED FINISHES
TOLERANCES

Basic Dimension	1 Place Decimal	2 Place Decimal	3 Place Decimal
Under 24	±	±	±
24 & over	±	±	±

ALL SURFACES ✓
ANGLES ±
COML TOL APPLY TO STOCK SIZES
SUPERSEDES DWG

DRAWN	D.M.S.S.	
CHECKED		
APPROVED		
APPROVED		
MATERIAL	—	
FINISH	—	

ANDREW 606 Beech Street Whitby, Ontario, Canada

SPECIAL TRANSPORTABLE ANTENNA
4FT. PARABOLIC REFLECTOR

CODE IDENT NO.	SIZE	
	D	WSC 439
SCALE 1:2	WEIGHT	SHEET 1 OF 1